Versatile regulation of autophagy by the deubiquitinase USP11

Dissertation

zur Erlangung des Doktorgrades

der Naturwissenschaften

vorgelegt beim Fachbereich14

der Johann Wolfgang Goethe – Universität

in Frankfurt am Main

von

Mila Basic

aus Zagreb

Frankfurt 2020

D 30

vom Fachbereich 14 der
Johann Wolfgang Goethe - Universität als Dissertation angenommen.

Dekan: Prof. Dr. Clemens Glaubitz

Gutachter: Prof. Dr. Volker Dötsch
              Dr. Anja Bremm

Datum der Disputation:

Table of content

I. Declaration

I herewith declare that I have not previously participated in any doctoral examination procedure in a mathematics or natural science discipline.

Frankfurt am Main, …....................

………………………………………… (Mila Basic)

II.   Author's Declaration

I herewith declare that I have produced my doctoral dissertation on the topic of

Versatile regulation of autophagy by the deubiquitinase USP11

independently and using only the tools indicated therein. In particular, all references borrowed from external sources are clearly acknowledged and identified. I confirm that I have respected the principles of good scientific practice and have not made use of the services of any commercial agency in respect of my doctorate.

Frankfurt am Main, …...................

…………………………………………….
(Mila Basic)

Except where stated otherwise by reference or acknowledgment, the work presented was generated by myself under the supervision of my advisors during my doctoral studies. All contributions from colleagues are explicitly referenced in the thesis. The material listed below was obtained in the context of collaborative research:

Figure 12: Generation of U2OS and RPE1 USP11 knockout cell lines using CRISPR/Cas9, Verena Bittl (Goethe University), Verena Bittl generated the cell lines and performed the wester blot, I initiated the generation of the cell line

Figure 17: The stable RPE1 USP11 SC2 knockout cell line expressing the GFP-LC3-RFP-LC3ΔG probe showed an increase in the autophagic flux compared to the NHT SC1 control cells assessed by live cell imaging over the course of 24 hour treatment with 250 nM Torin1, Mariana Tellechea and Alexandra Stolz (Goethe University), Mariana Tellechea performed the

experiment and calculated the fluorescent ration, I initiated the idea, did statistical analysis and made the figures

Figure 20: A knockdown of USP11 ortholog in *C. elegans*, H34C03.2, led to an increase in the basal autophagic flux compared to EV control, assessed by the GFP-LGG-1 lipidation after 6 hour BafA1 treatment, Andreas Kern and Christian Behl (Mainz University), Andreas Kern performed the experiments, I did the statistical analysis

Figure 21: A knockdown of USP11 ortholog in *C. elegans*, H34C03.2, led to an increase in the GFP-LGG1 punctae compared to EV control, assessed by confocal laser scanning microscopy after 6 hour BafA1 treatment, Andreas Kern and Christian Behl (Mainz University), Andreas Kern performed the experiments, I made the figure

Figure 22: Knockdown of USP11 ortholog, H34C03.2, led to a delayed paralysis phenotype in the *C. elegans* strain expressing the human β-amyloid protein 1-42 (hAβ42) in the muscle cells compared to EV control, Andreas Kern and Christian Behl (Mainz University), Andreas Kern performed the experiments, I did the statistical analysis

Figure 23: SILAC-based mass spectrometry approach to identify USP11 substrates after 4 hour EBSS treatment, Thomas Juretschke and Petra Beli (Mainz Universtiy), Thomas Juretschke performed the experiment and did the data analysis, I initiated the idea

Figure 24: SILAC-based mass spectrometry approach to identify the USP11 substrates after 4 hour EBSS treatment, Thomas Juretschke and Petra Beli (Mainz Universtiy), Thomas Juretschke performed the experiment and did the data analysis, I initiated the idea

Figure 25: Label-free mass spectrometry led to the identification of multiple autophagy-linked USP11 interactors and reported USP11 interactors or

substrates after 4 hour 250 nM Torin1 treatment, Florian Bonn (Goethe University), Florian did the data analysis, I did everything else

Figure 30 C, D: USP11 affects the PI3KC3 complex stability and the increased complex I formation is reflected by a higher lipid kinase activity, Alexandra Kalb (Goethe University), Alexandra Kalb did the IF experiments, and data analysis, together, we did the statistical analysis, I initiated the idea

Table 3: SILAC-based mass spectrometry approach led to identification of potential USP11 substrates based on changes in abundance of the GlyGly sites in the USP11 knockout cells after 4 hour EBSS treatment compared to the NHT control, Thomas Juretschke and Petra Beli (Mainz Universtiy), Thomas Juretschke performed the experiment and did the data analysis, I made the table out of the provided data

Table 4: SILAC-based mass spectrometry approach to identify USP11 substrates led to insights into proteome changes in USP11 knockout cells after 4 hour EBSS treatment compared to NHT control, Thomas Juretschke and Petra Beli (Mainz Universtiy), Thomas Juretschke performed the experiment and did the data analysis, I made the table out of the provided data

Table 5: Label-free mass spectrometry led to the identification of autophagy-linked USP11 interactors after 4 hour 250 nM Torin1 treatment, Florian Bonn (Goethe University), Florian Bonn did the data analysis based on which I made the table

Table 6: Label-free mass spectrometry led to the identification of reported USP11 interactors or substrates after 4 hours of Torin1 treatment, Florian Bonn (Goethe University), Florian Bonn did the data analysis based on which I made the table

Table 7: Label-free mass spectrometry led to the identification of multiple autophagy-related proteins after 4 hours of Torin1 treatment, Florian Bonn

(Goethe University), Florian did the data analysis based on which I made the table

5

Frankfurt am Main, …....................

 ………………………………………

(Mila Basic)

III.   List of abbreviations

A	Alanine
AB	Antibody
ABC	Ammonium bicarbonate
ACN	Acetonitrile
AMBRA1	Activating molecule in Beclin-1 regulated autophagy 1
AMPK	5' AMP-activated protein kinase
APS	Ammonium persulfate
ATG	Autophagy-related genes/proteins
ATG14	Autophagy-related protein 14
ATP	Adenosine triphosphate
BafA1	Bafilomycin A1
Beclin-1	Coiled-coil myosin-like BCL2-interacting protein
bp	Base pairs
BSA	Bovine serum albumin
C18	Octadecyl-bonded silica
CAA	Chloroacetamide
cDNA	Complementary DNA
CHX	Cycloheximide
CMA	Chaperone-mediated autophagy
co-IP	Co-immunoprecipitation
CQ	Chloroquine
CRISPR	Clustered regularly inteterspaced palindromic repeats
c-terminal	Carboxy-terminal
ddH$_2$O	Double distilled water
DMEM	Dulbecco's Modified Eagle Medium
DMSO	Dimethyl sulfoxide
DNA	Deoxyribonucleic acid
dNTP	Deoxynucleoside triphosphate
DTT	Dithiotreitol
DUB	Deubiquitinase
EBSS	Earle's Balanced Salt Solution
EDTA	Ethylenediaminetetraacetic acid
ER	Endoplasmatic reticulum
EV	Empty vector
FACS	Fluorescence activated cell sorting
FBS	Fetal bovine serum
FDA	Food and Drug Administration
FDR	False discovery rate
FIP200	FAK family kinase-interacting protein of 200 kDa
FLAG tag	DYKDDDDK-peptide
G (Gly)	Glycine
g	Acceleration of gravity
GAPDH	Glyceraldehyde 3-phosphate dehydrogenase
GFP	Green fluorescent protein
GlyGly	diGlycine remnant
gRNA	Guide ribonucleic acid
h	Hour
HA tag	Human influenza hemagglutinin
Hek293 cells	Human embryonic kidney cell line 293
HEPES	4-(2-hydroxyethyl)-1-piperazineethanesulfonic acid

HOPS	Homotypic fusion and protein sorting
Hsc70	Heat shock cognate protein 70
HUWE1	HECT, UBA and WWE domain-containing protein 1
IF	Immunofluorescence
IP	Immunoprecipitation
K	Lysine
k	Kilo
kDa	Kilo Dalton
KO	Knockout
LAMP-2A	Lysosome-associated membrane protein 2
LB-medium	Luria-Bertani medum
LC-MS/MS	Liquid chromatography-tandem mass spectrometry
LC3-I / LC3-II	Unlipidated LC3 / 7apidated LC3
LDS	Lithium dodecyl sulfate
LGG-1	LC3, GABARAP and GATE-16 family protein
Lys	Lysine
LysC	Lysyl endopeptidase
M	Molar
m	Mili
mA	Mili Amper
min	Minute
MOPS	3-(N-morpholino)propanesulfonic acid
MS	Mass spectrometry
mTOR	Mammalian/mechanistic target of rapamycin
MTX	Mitoxantrone
Myc tag	EQKLISEEDL-peptide
N	Number of experimental replicates
ng	Nano gram
NHT	Non-human targeting
NRBF2	Nuclear receptor-binding factor 2
N-terminal	Amino-terminal
o/n	Overnight
P	Phosphorylation
PA-ubi	Propargylated ubiquitin
PBS	Phosphate buffered saline
PCR	Polymerase chain reaction
PE	Phosphatydiletanolamine
PEI	Polyethylenimine
PFA	Paraformaldehyde
PI(3)P	Phosphatidylinositol 3-phosphate
PTM	Post-translational modification
qPCR	Quantitative real time PCR
RAPTOR	Regulatory-associated protein of mTOR
RFP	Red fluorescent protein
RNA	Ribonucleic acid
RPE1 cells	Retinal pigment epithelial cell line 1
PTM	Post-translational modification
PVDF	Polyvinylidene fluoride
R	Arginine
RNF2	E3 ubiquitin-protein ligase RING2
RPE1	Retinal pigment epithelial cell line
rpm	Rotation per minute

RT	Room temperature
RUBICON	Beclin-1 associated RUN domain containing protein
S	Serine
s	Second
SC	Single clone
SDB-RPS	Polystyrene-divinylbenzen copolymer partially modified with sulphonic acid
SDS	Sodium dodecyl sulphate
SDS-PAGE	Sodium dodecyl sulphate-polyacrylamide gel electrophoresis
SENP	Sentrin-specific protease (SUMO-specific protease)
SILAC	Stabile isotope labeling with amino acids in cell culture
siRNA	Small interfering RNA
SUMO	Small ubiquitin-related modifier
TAE buffer	Tris-acetate buffer
TBS	Tris-buffered saline
TCEP	Tris(2-carboxyethyl)phosphine
TEMED	Tetramethylethylenediamine
TF	Transcription factor
TFA	Trifluoroacetic acid
TFEB	Transcription factor EB
tN	Number of technical replicates in an experiment
TOR	Target of rapamycin
TRAF6	Tumor necrosis factor receptor (TNFR)-associated factor 6
U	Unit
U2OS cells	Human osteosarcoma cell line
ub	Ubiquitin
ULK1	Unc-51 like autophagy activating kinase 1
UPS	Ubiquitin-proteasome system
USP	Ubiquitin-specific protease
USP11	Ubiquitin-specific protease 11
UVRAG	UV Radiation Resistance Associated Gene Protein
V	Volt
VPS15	Serine/threonine protein kinase VPS15
VPS34	Phosphatidylinositol 3-kinase
w/o	Without
WIPI	WD repeat domain phosphoinositide-interacting protein
WT	Wild type
ZNF598	Zinc Finger Protein 598

IV. List of figures

V.   List of tables

VI. Zusammenfassung

Die Aufrechterhaltung der Zellhomöostase ist entscheidend für das Überleben der Zellen. Verschiedene Qualitätskontrollmechanismen stellen unter anderem sicher, dass fehlgefaltete Proteine, Proteinaggregate oder beschädigte Organellen entsorgt, und intrazelluläre Pathogene eliminiert werden. Zwei Hauptwege der zellulären Qualitätskontrolle sind das Ubiquitin-Proteasom-System (UPS) und die Autophagie.

Das UPS beruht auf der Konjugation des kleinen, globulären Proteins Ubiquitin an ein Zielprotein, wodurch dieses für den Abbau durch das Proteasom markiert wird. Die schnelle Beseitigung fehlgefalteter Proteine ist entscheidend, um deren Akkumulation und Aggregation zuvorzukommen, und somit schwerwiegende Störungen zellulärer Prozesse zu verhindern.

Es werden drei Arten von Autophagie unterschieden: Chaperon-vermittelte Autophagie (CMA), Mikroautophagie und Makroautophagie. Bei der CMA werden Proteine mit einem spezifischen KFERQ- oder KFERQ-ähnlichen Motiv unter anderem vom Hitzeschockprotein Hsc70 erkannt und als Proteinkomplex zum Lysosom geführt, wo sie durch LAMP-2A ins Lysosom gelangen und abgebaut werden. Die Mikroautophagie bezeichnet die direkte Aufnahme eines Teils des Zytoplasmas und deren Komponenten ins Lysosom durch einstülpen der lysosomalen Membran. Die Makroautophagie (im Folgenden: Autophagie) ist ein energetisch anspruchsvoller, streng regulierter Prozess, an dem mehrere Proteinkomplexe beteiligt sind, die in hierarchischer Reihenfolge ein neuartiges Doppelmembranvesikel bilden, das aus dem endoplasmatischen Retikulum (ER) stammt. Diese Membran dehnt sich durch die Wirkung der Autophagie-Maschinerie aus, umfasst das abzubauende Zellmaterial und schließt sich. Das gebildete Autophagosom wird anschließend entlang des Aktin-Zytoskeletts transportiert, bis es sich unter Membranfusion an ein Lysosom bindet und sein Inhalt durch lysosomale saure Hydrolasen abgebaut wird. Substrate für den Abbau durch Autophagie können selektiv oder nicht selektiv ausgewählt werden. Eine basale, nicht selektive Autophagie tritt in allen Zellen auf. Autophagie kann jedoch auch spezifisch durch Stress induziert werden. Stress kann in diesem Zusammenhang als das Auftreten von Proteinaggregation, beschädigten

Organellen, intrazellulären Pathogenen usw. definiert werden. In diesem Fall werden die zu entsorgenden Strukturen ubiquitiniert, anschließend von Autophagie-Rezeptoren erkannt und selektiv dem Abbau in Autophagosomen zugeführt. Nährstoffmangel, Glukose- oder Aminosäuremangel fallen ebenfalls in die Kategorie der Stressfaktoren, die Autophagie auslösen. Hier werden keine spezifischen Proteine oder Organellen abgebaut, sondern es wird ein Teil des Zytoplasmas zufällig nach dem „Bystander-Prinzip" von Autophagosomen aufgenommen und abgebaut, was zur Freisetzung von Nährstoffen führt, die zur Überwindung der Hungerperiode beitragen sollen. Autophagie wird durch das Zusammenspiel der drei Proteinkinase mTOR, AMPK und ULK1 kontrolliert induziert. Insbesondere ULK1 übernimmt eine Schlüsselrolle und aktiviert eine Vielzahl von Komponenten der Autophagie-Maschinerie. Neben Phosphorylierung sind auch weitere posttranslationale Modifikationen wie Ubiquitinierung, SUMOylierung und Acetylierung an der korrekten Initiation von Autophagie beteiligt. Zusammen führen sie zum Aufbau des pro-autophagischen PI3KC3-Komplexes I, der die Lipidkinase VPS34, VPS15, Beclin-1, NRBF2 und die pro-autophagische Untereinheit ATG14 umfasst. ATG14 ist für die Translokation des Komplexes zum ER, dem Ort der Autophagosomenbildung verantwortlich. VPS34 phosphoryliert Lipide des ER und produziert Phosphatidylinositol-3-phosphate (PI(3)Ps), die für die autophagosomale Membran charakteristisch sind. Die Funktion des PI(3)Ps besteht darin, nachgeschaltete Effektorproteine wie WIPI2 zu rekrutieren. WIPI2 rekrutiert wiederum ATG16L, Mitglied des ATG5-12-16L-Komplexes. ATG5-12-16L ist die E3 Ligase für die Ubiquitin-ähnliche Konjugationsmaschinerie, die LC3 auf beiden Seiten der autophagosomalen Membran an Phosphatidylethanolamin (PE) konjugiert. Autophagie-Rezeptoren binden einerseits das LIR (LC3-interagierende Region) Motiv in LC3, erkennen und binden aber gleichzeitig ubiquitinierte Autophagie-Substrate und transportieren diese spezifisch zum Autophagosom für den Abbau. Der Prozess der Autophagie wird durch verschiedene posttranslationale Modifikationen streng reguliert, wodurch eine korrekte Initiation, Dauer und Terminierung sichergestellt wird. Protein-Ubiquitinierung spielt hier eine entscheidende Rolle indem es den proteasomalen Abbau von einzelnen Komponenten der Autophagie-Maschinerie vermittelt, aber auch

Komposition und Stabilität von Proteinkomplexen durch nicht-proteolytische Ubiquitin-Signale reguliert.

Im Rahmen der vorliegenden Arbeit konnte gezeigt werden, dass die Ubiquitin-spezifische Protease 11 (USP11) an der Regulation der Autophagie beteiligt ist. Die gesammelten Daten deuten darauf hin, dass USP11 mit mehreren Komponenten der Autophagie-Maschinerie interagiert und so in den Verlauf der Autophagie eingreift. Ein transienter oder permanenter Verlust von USP11, vermittelt durch RNA Interferenz oder CRISPR/Cas Technologie, resultierte in einen erhöhten Autophagie-Flux. Diese Beobachtung konnte im Modellorganismus *Caenorhabditis elegans* bestätigt werden, was wiederum die Rolle von USP11 in der Autophagie-Regulation stärkt und eine Konservierung des Mechanismus vermuten lässt. Um die molekularen Details der USP11-abhängigen Regulation aufzuklären, wurden potenzielle Substrate und Interaktionspartner von USP11 mittels Massenspektrometrie identifizieren. Es zeigte sich, dass USP11 mit mehreren Proteinen und Komplexen der Autophagie-Maschinerie interagiert, unter anderem mit VPS15, einer Komponente des PI3KC3 Komplexes. Im Nachfolgenden konzentrierten sich die Untersuchungen hauptsächlich darauf, ob und wie USP11 Assemblierung und Aktivität des PI3KC3 Komplexes reguliert. Interaktionsstudien zeigten, dass USP11 neben VPS15 auch VPS34, Beclin-1, ATG14 und NRBF2 co-immunopräzipitiert. Diese Interaktionen fanden gleichermaßen unter physiologischen Wachstumsbedingungen als auch nach Autophagie-Induktion statt. Einen ersten Hinweis darauf, dass der PI3KC3 Komplex USP11-regulierte Ubiquitin-Signale trägt, lieferten co-Immunopräzipitations-experimente von katalytisch inaktivem USP11 (C318S). Die abschließenden Western blot Analysen identifizierten potentiell modifizierte Spezies von NRBF2, VPS15, VPS34 und Beclin-1 in Form zusätzlicher bzw. „verschmierter" Banden. Das Auftreten dieser Banden in Gegenwart von USP11 (C318S) deutet darauf hin, dass eine Monoubiquitinierung (einzelne Bande) bzw. Polyubiquitinierung (mehrere Banden) der PI3KC3-Komplexkomponenten vorliegt, und dass diese Modifikationen durch die Bindung von inaktivem USP11 (C318S) stabilisiert und von einer Deubiquitinierung durch aktives USP11 abgeschirmt wird. Mit Ausnahme von NRBF2 sind die Protein-Expressionslevel aller PI3KC3

Komplexkomponenten in Kontroll- und USP11 knockout Zellen unverändert. Dies deutet auf eine Modifikation mit nicht-proteolytischen Ubiquitin-Signalen hin. NRBF2 Level sind in Abwesenheit von USP11 erhöht, insbesondere nach Initiation von Autophagie durch Aminosäure-Depletion. Für diese Beobachtung gibt es zwei mögliche Erklärungen. Entweder reguliert USP11 einer E3 Ubiquitin-Ligase die wiederum NRBF2 Stabilität kontrolliert; oder USP11 editiert ein Ubiquitin-Signal, dass die Inkorporation von NRBF2 in den PI3KC3 Komplex I beeinflusst und potentiell vor einem Abbau nach Autophagie-Induktion schützt. Erhöhte NRBF2 Level nach Aminosäure-Depletion konnten auch in Proteomanalysen von USP11 knockout Zellen bestätigt werden. NRBF2 liegt als Homodimer vor und führt durch seine Interaktion mit zwei PI3KC3 Kernkomplexen (Heterotetramere bestehend aus VPS34, VPS14, Beclin-1 und ATG14) zu einer Dimerisierung dieser Heterotetramere, was wiederum zu einer Verstärkung der Lipidkinase-Aktivität der PI3KC3 Komplexe führt. Um zu testen, ob erhöhte NRBF2-Level, verursacht durch eine USP11 Depletion, einen Einfluss auf die PI3KC3 Komplexbildung hat, wurde eine Immunpräzipitation von endogenem ATG14 durchgeführt. Diese zeigte, dass in USP11 knockout Zellen, verglichen zu Kontrollzellen, ATG14 verstärkt mit anderen PI3KC3 Komplexkomponenten interagiert. Bemerkenswerterweise wurde in Zellen, die exogenes USP11 überexprimieren, ein gegenteiliger Effekt beobachtet. In diesem Fall war fast keine NRBF2 Bindung an ATG14 nachweisbar. Weiter wurde untersucht, ob sich die Änderungen in der PI3KC3 Komplexbildung in einer erhöhten VPS34-Aktivität widerspiegeln. Zu diesem Zweck wurde die Rekrutierung des Effektorproteins WIPI2 mittels Immunfluoreszenzmikroskopie quantifiziert. Die Bildung von WIPI2-Punkten korreliert mit der Menge an produziertem PI(3)P durch VPS34 und ist somit ein indirekter Nachweis für die Lipidkinaseaktivität des PI3KC3 Komplexes. Wie vermutet wurden mehr WIPI2-Punkte in USP11 knockout Zellen detektiert, was zusätzlich für eine höhere PI3KC3-Komplexaktivität spricht.

Während der genaue Mechanismus der USP11-abhängigen Regulation des PI3KC3-Komplexes nicht vollständig geklärt ist, konnte festgestellt werden, dass ein Fehlen von USP11 zu einer erhöhten VPS34 Aktivität und erhöhten NRBF2 Level führt. Überexpression von USP11 inhibiert den Autophagie-Flux

und reduziert die Wechselwirkung von NRBF2 mit endogenem ATG14, was darauf hindeutet, dass USP11 ein nicht-proteolytisches Signal an NRBF2 reguliert. In Abwesenheit von USP11 scheint mehr pro-autophagischer PI3KC3 Komplex I gebildet zu werden, wodurch NRBF2 potentiell vor einer Extraktion aus dem Komplex und einem nachfolgenden Abbau geschützt wird. Der proteolytische Umsatz von NRBF2 Protein, der durch Zugabe des Translationshemmers Cycloheximid untersucht wurde, zeigte, dass NRBF2 Proteinlevel nach Initiation von Autophagie abnehmen. Diese Daten lassen vermuten, dass eine unbekannte E3 Ligase vorhanden ist, die, in einer möglichen negativen Rückkopplungsschleife, NRBF2 zum Abbau markiert und so den Autophagie-Flux einzuschränken. Es muss noch vollständig geklärt werden, ob die Stabilisierung von NRBF2 in USP11 knockout Zellen darauf zurückzuführen ist, dass USP11 eine E3-Ligase direkt reguliert, oder ob USP11 ein Ubiquitin-Signal an NRBF2 entfernt, dass zu einer verstärkten Inkorporation von NRBF2 in den PI3KC3 Komplex führt und so ein Abbau von NRBF2 erschwert wird. Auf Grundlage der präsentierten Daten sind beide Optionen möglich. Neben der Wechselwirkung mit dem PI3KC3 Komplexe konnte im Rahmen der vorliegenden Arbeit ebenfalls beobachtet werden, dass mTOR, eine Schlüsselkinase des Zellstoffwechsels und der Autophagie, mit USP11 interagiert und USP11-abhängig ubiquitiniert ist. In USP11 knockout Zellen sind mTOR Proteinlevel reduziert, was darauf hinweist, dass USP11 den proteolytischen Abbau von mTOR kontrolliert. Diese Daten zeigen, dass USP11 den Prozess der Autophagie auf verschiedenen Ebenen negativ reguliert und mehrere Komponenten der Autophagie-Maschinerie deubiquitiniert.

Zusammenfassend lässt sich sagen, dass die vorliegende Arbeit zur Identifizierung von USP11 als ein neuartiger, negativer Regulators der Autophagie führte. Es konnte gezeigt werden, dass USP11 mit dem PI3KC3-Lipidkinasekomplex interagiert, der entscheidend zur Bildung von Autophagosomen beiträgt, und dass die DUB-Aktivität von USP11 den posttranslationalen Status seiner Komponenten beeinflusst, was wiederum die Komposition und die Aktivität des Komplexes zu bestimmen scheint. Zusätzlich deuten die gewonnen Daten darauf hin, dass USP11 die

Autophagie auch über mTOR beeinflusst, indem USP11 mTOR deubiquitiniert und so vor einem Abbau durch das Proteasom schützt.

VII.   Summary

Maintaining cell homeostasis is crucial for cell survival. This involves multiple quality control mechanisms designated to clear misfolded proteins, remove protein aggregates or damaged organelles, clear intracellular pathogens, etc. Two main cellular quality control pathways are the ubiquitin-proteasome system (UPS) and autophagy.

The former relies on the conjugation of a small, globular protein ubiquitin to a target protein thereby "flagging" it for degradation by the proteasome. Prompt clearance of misfolded proteins is crucial for avoiding their accumulation that will eventually lead to their aggregation and interfere with cellular processes.

The latter, autophagy, encompasses three pathways: chaperone-mediated autophagy (CMA), microautophagy and macroautophagy. CMA relies on recognition of a specific KFERQ, or KFERQ-like motif on proteins by the hsc70 and co-chaperones, its delivery to the lysosome, followed by the target protein unfolding and direct translocation to the lumen of the lysosome via LAMP-2A where the target is degraded. Microautophagy involves direct uptake of a portion of the cytoplasm by the lysosome, and this process can be selective and non-selective. Macroautophagy (hereafter autophagy) is an energetically demanding, tightly regulated process involving multiple protein complexes, acting in a hierarchical order to create a novel, double-membrane vesicle stemming from the endoplasmatic reticulum (ER). This membrane expands through the action of the autophagy machinery, engulfing the cargo, ultimately closing and fusing with the lysosome leading to cargo degradation and release of its building blocks. The cargo for autophagy degradation can be targeted selectively, or non-selectively. Basal, non-selective autophagy occurs in all cells, however, autophagy can also be specifically induced by stress. Stress in this context can be defined as occurrence of protein aggregation, damaged organelles, intracellular pathogens etc. In this case, we are referring to selective autophagy, wherein the cargo is ubiquitinated, recognized by autophagy receptors, and selectively targeted for autophagic degradation. Nutrient deprivation, glucose or amino acid starvation, also fall in the category of stressors inducing autophagy. Here, no cargo is targeted for degradation, rather a portion of the cytoplasm is randomly engulfed by the

"bystander principle", leading to degradation and the release of nutrients aimed to help overcome the starvation period. In any of the above cases, through cross talk of three key kinases mTOR, AMPK, and ULK1, autophagy is induced in a timely manner. ULK1, the key kinase involved in induction and downstream of the induction ensuring progression, is responsible for activation of many of the autophagy machinery. In addition to phosphorylation, ubiquitination, SUMOylation, and acetylation have all been shown to be involved in autophagy regulation. Together, they lead to assembly of pro-autophagic PI3KC3 complex I comprising VPS34, the lipid kinase, VPS15, Beclin-1, NRBF2 and distinct pro-autophagic subunit ATG14. The latter is responsible for translocation of the complex to the ER, to site of autophagosome formation. VPS34 phosphorylates the lipids of the ER producing phosphatidylinositol 3-phosphates (PI(3)Ps) characteristic for the autophagosomal membrane. The function of the PI(3)Ps is to recruit the downstream effector proteins, such as WIPI2. WIPI2 in turn recruits ATG16L, of the ATG5-12-16L complex. ATG5-12-16L, itself assembled in an ubiquitin-like conjugation manner, is the E3 for the second ubiquitin-like conjugation machinery, one that conjugates LC3 to phosphatidylethanolamine (PE) on both sides of the autophagosomal membrane. One of the roles of LC3 is to be bound by autophagy receptors via their LC3-interacting region motif, while simultaneously binding to ubiquitinated cargo in the case of aforementioned selective autophagy. In the final stage, the autophagosome closes and fuses with the lysosome, leading to cargo degradation and nutrient release.

The process of autophagy is tightly regulated by post-translational modifications, ensuring induction, adequate duration, and termination. Ubiquitination has been well described playing a crucial role. Besides mediating the proteolytical signal of target proteins to the proteasome, it is also playing important non-proteolytical roles, such as stabilizing protein complexes.

We have found that ubiquitin-specific protease 11, USP11, is involved in regulation of autophagy, likely through regulation of multiple complexes. We found that transient or stable loss of USP11 leads to an increase in autophagic flux based on LC3 lipidation, using multiple methods. Excitingly, we found this phenotype is conserved in model organism *Caenorhabditis*

elegans (*C. elegans*), suggesting USP11-dependent autophagy regulation is highly important. Our approach to identify potential substrates and USP11 interactors that would elucidate the molecular mechanism of this regulation, led to the discovery of multiple autophagy-related proteins and complexes. Our interactome analysis revealed multiple hits revolving around the PI3KC3 complex, including the core subunit VPS15 itself. This thesis mostly focused on the PI3KC3 complex, its assembly, and activity regulation. We found that USP11 can co-immunoprecipitate all members of the complex. Moreover, we found that catalytic inactive USP11 (C318S) co-imunnoprecipitates modified species of NRBF2, VPS15, VPS34 and Beclin-1. The appearance of these bands on a western blot is distinct between the complexes. Whereas for VPS34 and Beclin-1 we observed a distinct additional band, for NRBF2 and VPS15 we observed smeared bands typical for poly-ubiquitination. In all mentioned cases, we observed no difference between physiological conditions and autophagy induction, the only factor accounting for the modifications is USP11 activity. Importantly, for none of the complex components did we observe a modulation of protein levels, indicating they are non-proteolytical signals, except for NRBF2. However, we observed NRBF2 is stabilized in the absence of USP11, suggesting USP11 is not rescuing NRBF2 from the proteasome-mediated degradation, as the opposite would be expected. This finding was confirmed in the proteome analysis of USP11 knockout cells upon 4 hour EBSS treatment where we identified increased levels of NRBF2. NRBF2 is a core subunit of the complex that forms a homodimer via its coiled-coil domain, thereby able to dimerize the complex enhancing its activity. To test if increased levels of NRBF2 in USP11 knockout cells are reflected on tighter complex formation or higher complex activity, we performed endogenous immunoprecipitation of pro-autophagic ATG14, and observed more complex components interacting with ATG14 in the USP11 knockout cells, compared to control cells, in agreement with our hypothesis. Strikingly, when we overexpressed USP11, we found the opposite effect, almost no NRBF2 co-immunoprecipitating with ATG14. Further, we investigated if tighter complex is reflected in increased VPS34 activity, and we did find that to be the case. Based on WIPI2 punctae quantification, formation of which is based on PI(3)P produced by the kinase,

that the PI3KC3 complex is more active in USP11 knockout cells compared to control cells. Whereas the exact mechanism of USP11-dependent PI3KC3 complex regulation remains elusive, we found that the absence of USP11 results in increased VPS34 activity and increased NRBF2 levels. When USP11 was overexpressed, we found the autophagic flux to be impaired based on LC3 lipidation and western blot readout and almost no NRBF2 interacting with the endogenous ATG14, suggesting USP11 is regulating a non-proteolytical signal on NRBF2. In the absence of USP11, the complex is tightly assembled, therefore likely protecting NRBF2 from extraction from the complex and subsequent degradation, whereas when USP11 is overexpressed, we observed no significant difference in NRBF2 protein levels, however, it is only weakly interacting with the complex. The turnover of NRBF2, investigated by a cycloheximide chase, revealed NRBF2 levels are reducing over time during the course of autophagy, indicating that there is likely an unknown E3 ligase targeting NRBF2 for degradation, likely as a negative feedback loop to restrict autophagic flux. It remains to be fully elucidated if the stabilization of NRBF2 in USP11 knockout cells is a result of USP11 regulating directly the E3 ligase, or the complex being tightly assembled, thereby protecting extraction of NRBF2 and subsequent degradation. Based on our data, it is likely both, however this remains to be proven.

Moreover, we found that mTOR, one of the key kinases regulating cell metabolism, is interacting with USP11. We also found that mTOR is ubiquitinated in an USP11-dependent way and that the levels of mTOR are reduced in USP11 knockout cells indicating that USP11 is regulating mTOR turnover. The preliminary, yet strong data further emphasize the importance of identifying USP11 substrates. Although we have not addressed if mTOR level reduction is reflected in autophagy induction or termination regulation, reduced mTOR levels in absence of USP11 further support the finding that USP11 is a negative regulator of autophagy.

Taken together, our work led to identification of a novel, negative regulator of autophagy. We found that USP11 interacts with PI3KC3 complex, a crucial complex for autophagosome nucleation, and that the activity of USP11 affects post-translational status of its components. Significant efforts have paved the

way of understanding many ways in which the complex is formed and activated, and this work has added another regulator to the list. Importantly, our data indicates USP11 is overall a negative regulator of autophagy. Moreover, we found that USP11 regulates mTOR stability, a key kinase in the regulation of cellular metabolism, autophagy included. Further work will demonstrate if this observation is contributing to autophagy phenotype we have established, or if this knowledge can be used to modulate mTOR stability to impact other pathways.

1 Introduction

1.1 The ubiquitin system

Ubiquitin is a small, 76-amino acid protein with a globular fold that gets covalently attached to (usually) lysines of other proteins via its C-terminal glycine (Vijay-Kumar, Bugg, and Cook 1987). Another ubiquitin can get attached via its C-terminal glycine to a lysine residue of the ubiquitin proximal to the substrate thereby forming a chain (Komander and Rape 2012; Yau and Rape 2016; Swatek and Komander 2016).

One of the first reports on ubiquitin described it as a polypeptide with lymphocyte-differentiating properties isolated from the thymus and immediately recognized as a highly conserved protein between organisms then named UBIP, for "ubiquitous immunopoietic polypeptide" (Goldstein et al. 1975).

Soon after, a report on ubiquitin identified it being covalently attached to histone 2A branching of lysine 119 (Lys119/K119), but no function was described (Goldknopf et al. 1977; Goldknopf and Busch 1977).

One of the first detailed functional observations and one scientists associate the name "ubiquitin" to most was that ATP-dependent ubiquitin attachment to substrate proteins "flags" them for degradation by the proteasome, hence the original name APF-1, for "ATP-dependent proteolysis factor 1" (Ciehanover, Hod, and Hershko 1978; Hershko et al. 1980; A. Ciechanover et al. 1980; Hershko and Ciechanover 1982; Ciechanover, Finley, and Varshavsky 1984). Finally, in 1980 it was recognized as the same protein, one we today call "ubiquitin" (Wilkinson, Urban, and Haas 1980).

To this date, multiple roles of ubiquitination as a post-translational modification (PTM) have been described. Besides mediating protein turnover, ubiquitination can affect a protein's interactome, localization, activity etc. As the name suggests, ubiquitin is ubiquitously expressed and conserved among eukaryotes regulating all cellular pathways from inflammation, DNA damage response, immune response etc. (Oh, Akopian, and Rape 2018). The ubiquitin system, comprising of enzymes attaching ubiquitin to substrates, proteins "reading the code", and enzymes reversing the signal, is a highly

sophisticated, incredibly diverse and well represented in the proteome, ensuring that the signal mediated by ubiquitin exerts its necessary function, and elicits an appropriate cellular response.

1.1.1 Ubiquitin conjugation to substrates

Ubiquitin is synthesized as an inactive precursor and then processed to reveal its C-terminal glycine (G/Gly) that can be utilized by the ubiquitin machinery (Lund et al. 1985; Wiborg et al. 1985). In mammalian cells there are four different precursors; UBA52 and UBA80, mostly processed post-translationally, and two polyubiquitin precursors, UBB and UBC, processed both co- and post-translationally (Pickart and Rose 1985; Falquet et al. 1995; Larsen, Krantz, and Wilkinson 1998; Grou et al. 2015).

Covalent attachment of ubiquitin to a substrate or to another ubiquitin is a multi-step process involving a cascade of reactions. First, ubiquitin is activated by an E1 activating enzyme in an ATP-dependent manner by covalently attaching C-terminal glycine of ubiquitin to its catalytic cysteine (C/Cys) (Schulman and Harper 2009). In the next step, ubiquitin is transferred to the catalytic cysteine of an E2 conjugating enzyme (E2~ubiquitin) (Ye and Rape 2009). Finally, with the help of an E3 ligating enzyme bringing the E2~ubiquitin conjugate and the substrate together, ubiquitin is transferred onto a lysine of the substrate via its C-terminal glycine either directly, or via a short E3~ubiquitin intermediate (Figure 1 A) (Deshaies and Joazeiro 2009; Rotin and Kumar 2009; Berndsen and Wolberger 2014).

There are two major families of E3 ligases based on their domain structure: RING (Really interesting new gene) E3 ligases and HECT (Homologous to E6AP C-terminus) ligases. Whereas the former facilitates direct transfer of ubiquitin to the substrate, the latter forms an E3~ubiquitin intermediate. To this date, there are E3 ligases known deviating from the two major classes, like the RBR (Ring between ring) E3 ligases which are a RING-HECT hybrid (Deshaies and Joazeiro 2009; Rotin and Kumar 2009; Berndsen and Wolberger 2014; Smit and Sixma 2014).

As mentioned, ubiquitin can not only be transferred to a lysine of a substrate (monoubiquitination, or multi-monoubiquitination), it can be transferred to a lysine of another ubiquitin moiety (polyubiquitination). Ubiquitin has seven lysine residues to which another ubiquitin can be transferred onto (K6, K11, K27, K29, K33, K48, and K63) (Figure 1 B) (Swatek and Komander 2016). Moreover, ubiquitin can form linear chains, where the C-terminal glycine is attached to the N-terminal methionine of the following ubiquitin (Kirisako et al. 2006). Importantly, using mass spectrometry approaches, all the eight chain types have been identified in eukaryotic cells from yeast (*Saccharomyces cerevisiae*) to human cells (Peng et al. 2003; Wagner et al. 2011; Kim et al. 2011; Swatek and Komander 2016).

The ubiquitin chains can branch, adding layers of complexity to how the ubiquitin signal can be read and interpreted (Yau and Rape 2016). With respect to the chain specificity and the mechanism of ubiquitin transfer to the substrate or another ubiquitin: in HECT E3 ligases, the E3 enzyme achieves specificity, whereas for the RING E3 ligases, it is conferred by the E2 enzyme.

The ubiquitin code is read by various proteins containing the ubiquitin-binding domains, and the signal is relayed onto appropriate effectors or serves its purpose per se, as enhancing an interaction between proteins etc.

Increasing complexity of the ubiquitin system is reflected upon representation of E1, E2, and E3 enzymes in the proteome; there are two known E1 enzymes, around 40 E2, and more than 600 E3 (>95 % are RING E3 ligases).
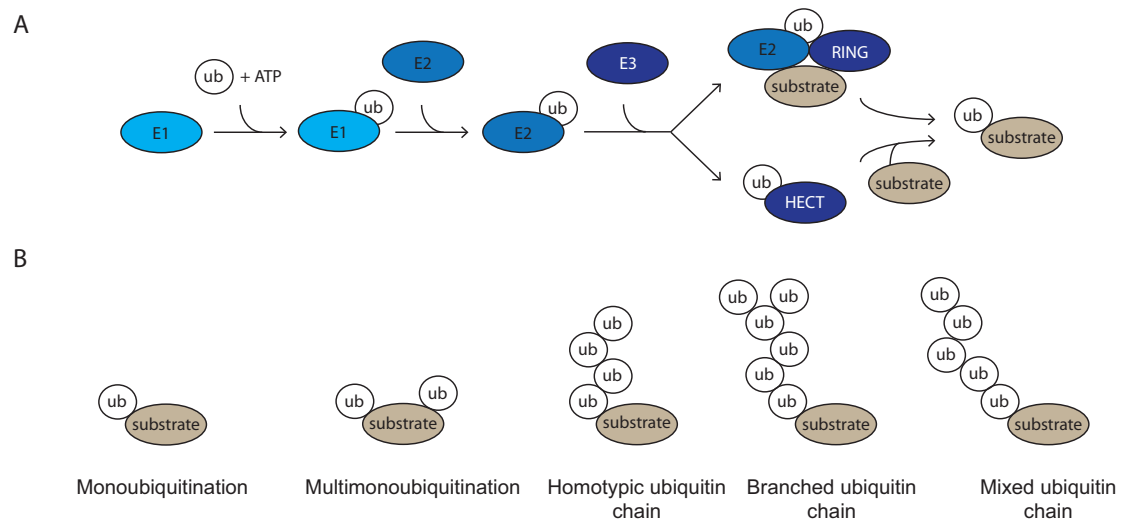
Figure 1: Simplified schematic depiction of ubiquitin conjugation reaction and types of ubiquitin modification. A Ubiquitin (ub) is conjugated to a substrate in a 3-step cascade reaction. Depending on the type of the E3 ligase, the specificity of the ubiquitin chain is determined by the E2 (RING E3 ligases), or by the E3 itself (HECT E3 ligases). **B** Substrates can be modified by ubiquitin in multiple ways.

1.1.2 Deubiquitinating enzymes

One of the most important features of the ubiquitin signal is reversibility. Ubiquitin is removed from substrates, chains are trimmed, or cleaved from substrates en bloc or step-wise by deubiquitinating enzymes (DUBs) (Figure 2 A) (Clague et al. 2013; Yau and Rape 2016; Oh, Akopian, and Rape 2018). To this date, there are around 100 DUBs identified, divided in seven classes, mechanistically either cysteine proteases or metalloproteases (Mevissen and Komander 2017; Haahr et al. 2018; Hermanns et al. 2018; Kwasna et al. 2018; Clague, Urbé, and Komander 2019). The former accounts for the following families: the ubiquitin-specific proteases (USPs), the ovarian tumor proteases (OTUs), the ubiquitin C-terminal hydrolases (UCHs), the Josephin family, the motif interacting with ubiquitin (MIU)-containing DUB family (MINDYs), and latest addition, the Zinc finger-containing ubiquitin peptidase 1 (ZUFSP/ZUP1) (Figure 2 B). The latter accounts for only one class, the family of Zn^{2+}-dependent JAB1/MPN/MOV34 metalloproteases (JAMMs, also known as MPN+).
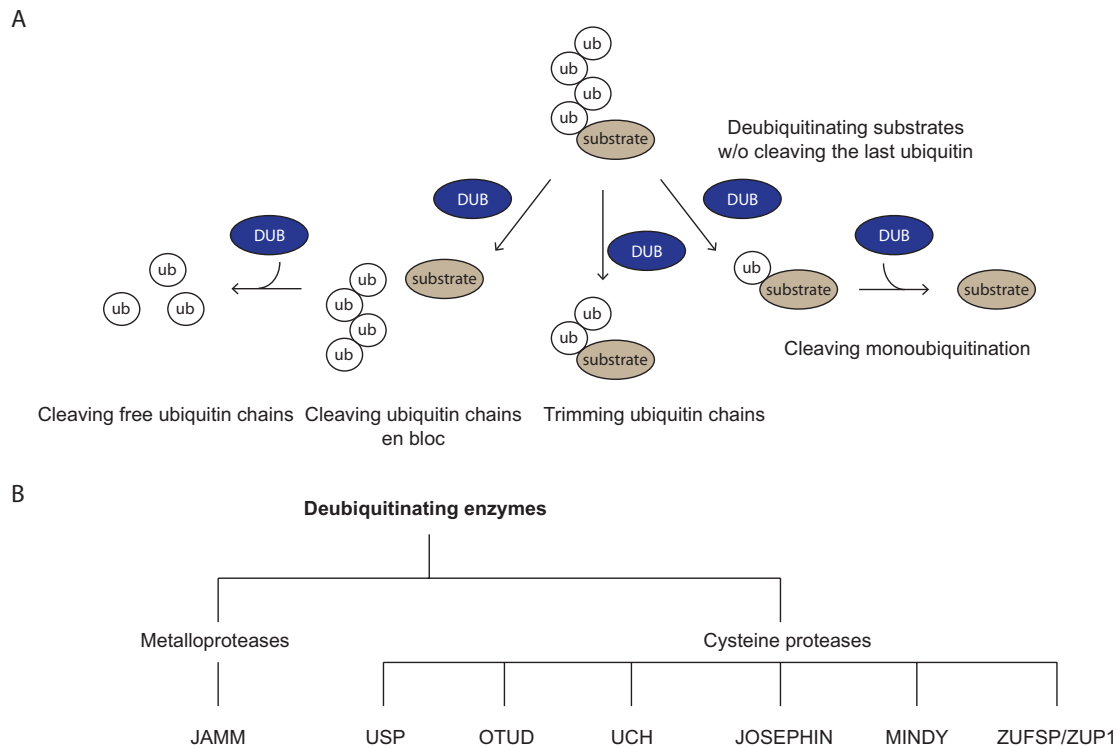
Figure 2: Simplified schematic depiction of ubiquitin (ub) deconjugation by deubiquitinating enzymes (DUBs) and their classification. A Ubiquitin can be removed from a substrate, or the chain can be edited in multiple ways. **B** To this date, deubiquitinating enzymes are divided in 2 major classes depending on the catalytic mechanism, and a family of 7 subclasses.

The largest class of DUBs are the USPs with just above 50 members (Mevissen and Komander 2017; Clague, Urbé, and Komander 2019). The catalytic domain shared among the members, the USP papain-like domain, resembles a palm, a thumb, and fingers of a hand, where the catalytic cysteine is situated between the palm and the thumb (Hu et al. 2002; Komander, Clague, and Urbé 2009). Any preference towards a chain type, or binding specific proteins is conferred by the modular composition of accessory domains, like the UBL domains, B-box domain, DUSP domains etc. (Clague et al. 2013). Kinetic analysis of 12 members of the USP family, including USP11, revealed little ubiquitin linkage specificity (tested *in vitro* using di-ubiquitin substrates), although none of them seemed to cleave the linear di-ubiquitin (Faesen et al. 2011).

As important the function of the DUBs is in modulating the ubiquitin signal, as important it is that they themselves are tightly regulated. This is achieved in multiple ways, for example by PTMs, by their interaction partners, by binding their substrates (Sahtoe and Sixma 2015).

1.1.3 Ubiquitin specific protease 11 (USP11)

The deubiquitinating enzyme USP11 was first discovered, and cloned in 1996 (Swanson et al. 1996). Then, it was named UHX1 for "ubiquitin hydrolase on the X chromosome". Interestingly, it was reported expressed in all tissues with specifically high levels in the retina, suggesting it could be involved in X-linked retina disorders. Since then, multiple nuclear and cytoplasmic roles for USP11 have been described, and to this date, none associating USP11 and autophagy.

Functionally, USP11 was first described in 2002 by Ishigatsubo and colleagues as an interactor of, and deubiquitinase for RanBPM (Ideguchi et al. 2002), a protein responsible for the correct nucleation of microtubules. USP11 was able to reverse RanBPM ubiquitination *in vitro*, however, it remained unclear if this was a proteolytic, or non-proteolytic ubiquitin signal. Importantly, overexpressed USP11 was described to predominantly localize in the nucleus. Over a decade later, Baek and colleagues reported that USP11 deubiquitinates and regulates protein turnover of Mgl-1, a tumor suppressor (Lim et al. 2016). Mgl-1 interacts with and is stabilized by interacting with RanBPM, a USP11 substrate (Ideguchi et al. 2002). This work elegantly described USP11-RanBPM-Mgl-1 axis and its tumor suppressor role.

In 2007, a study investigated USP11 involvement in NF-κB signaling. USP11 was found to regulate levels of IκB kinase α (IKKα), interestingly, on a transcriptional level, not post-translational (Yamaguchi et al. 2007). Two important things were established; knockdown of USP11 results in enhanced response to TNFα-mediated NF-κB signaling via an unknown mechanism, and that USP11 mediates IKKα translocation to the nucleus where it mediates

p53-dependant gene expression is response to TNFα which is impaired in case of USP11 knockdown. Similarly, positive effect on NF-κB signaling upon loss of USP11 was found by another group (Sun et al. 2010). Here, USP11 was identified in a proteome approach as an interactor of IκBα. But in contrast to the previous findings (Yamaguchi et al. 2007), USP11 was found to directly deubiquitinate and stabilize IκBα in response to TNFα-mediated NF-κB signaling. Interestingly, here, reintroducing USP11 catalytic mutant in USP11-depleted cells partially rescued the phenotype, suggesting an additional, scaffolding role of USP11 in NF-κB signaling. In summary, both reports identify USP11 as a negative regulator of NF-κB signaling via multiple mechanisms that remain elusive.

USP11 was also identified as BRCA2 interactor (Schoenfeld et al. 2004), protein involved in DNA damage response. Overexpressed USP11 was again shown residing in the nucleus and exhibiting BRCA2-dependant pro-survival role, however, likely not via regulating BRCA2 stability. Importantly, siRNA-mediated knockdown of USP11 had negative effect on cell growth in a colony forming unit experiment. Together, USP11 is exhibiting a pro-survival role by interacting with BRCA2. USP11 was linked again to DNA damage response in a study where USP11 was shown to deubiquitinate XPC (xeroderma pigmentosum complementation group C), a protein involved in nucleotide excision repair (NER), preventing its premature dissociation from DNA damage sites upon UV irradiation (Shah et al. 2017). Deubiquitination by USP11 was shown to counteract premature VCP/p-97 dependent XPC removal. Furthermore, USP11 levels were shown decreased in chronically irradiated skin tumors in both mice and human samples. Interestingly, USP7 was also shown to deubiquitinate XPC and rescue it from VCP/p-97-mediated degradation, and yet it does seem to be an interchangeable role with USP11 (He et al. 2014; Shah et al. 2017). In the context of skin cancer, USP11 appears to exhibit a tumor suppressor role. Further link between USP7 and USP11 was established when in 2014 USP11 was added to list of p53 stability regulators (Ke et al. 2014). USP7 was previously shown to positively regulate levels of p53 by regulating both p53 and Mdm2, an E3 ligase ubiquitinating p53 and targeting it for proteasomal degradation (Li et al. 2002; 2004; Cummins et al. 2004). Here, USP11 was shown to interact with p53

and regulate p53 levels in a dose dependent manner rescuing it from proteasomal degradation. USP11 had no effect on p53 mRNA levels, and its ability to stabilize p53 was dependant on USP11 activity. One of the genes under p53 expression regulation is p21 (Linke et al. 1996). USP11 was shown to regulate p21 stability in the nucleus, hence, regulates cell-cycle progression and DNA damage-induced G2 arrest (Deng et al. 2018). In contrast to previous finding (Ke et al. 2014), USP11 overexpression had no effect on p53 levels. Loss of USP11 led to p21-dependant increase proliferation in both colon and lung cancer cells, as well as *in vivo*. By regulating p21 level, USP11 is regulating apoptosis induction acting as a tumor suppressor.

USP11 was identified in a RNAi screen in combination with PARP inhibitor AZD2281 in a viability screen causing synthetic lethality phenotype (Wiltshire et al. 2010). This again suggested a role of USP11 in DNA damage response. Furthermore, USP11 depleted cells were found to be hypersensitive to any genotoxic stress. Importantly, this phenotype could be rescued by reintroducing WT USP11 but not catalytic inactive USP11, indicating dependence on USP11 catalytic activity.

As USP11 was shown to give promising results in combination with PARP inhibitor AZD2281 in sensitizing cells to death, it was investigated in more detail in context of pancreatic ductal adenocarcinoma (PDA) (Burkhart et al. 2013). In PDA, PARP inhibitors showed promising results; therefore inhibiting USP11 might be of therapeutic interest in this context. Here, mitoxantrone (MTX) was identified in a high throughput screening of 2,000 FDA-approved compounds as a USP11 inhibitor. Previously, MTX was described as DNA intercalating agent and type II topoisomerase inhibitor used in context of leukemia and breast cancer (Crespi et al. 1986; Bhalla et al. 1993; Bellosillo et al. 1998). Here, the activity of MTX on USP11 was shown in an *in vitro* DUB activity assay. Moreover, MTX performance exceeded previously used drug gemcitabine (previously used drug in PDA) in terms of inducing cell death in a PDA cell line. However, when used in cells defective in Fanconi anemia pathway, BRCA2, or in a combination with a range of PARP inhibitors, MTX did not exhibit synthetic lethality phenotype. This suggested either MTX is potent due to its USP11-independent activity or that MTX-

dependent USP11 inhibition in PDA was not efficient. Interestingly, USP11 knockdown sensitized the cells to gemcitabine treatment. Nonetheless, the same phenotype achieved by USP11 knockdown could not be reproduced with MTX. This research suggests USP11 depletion, or inhibition is a promising therapeutic strategy in PDA, but requires further identification, or development of inhibitors.

USP11 was shown to deubiquitinate and stabilize cellular inhibitor of apoptosis 2 (cIAP2) rescuing it from proteasome-mediated degradation in a screen identifying DUBs rendering cells resistant to Smac mimetics induced apoptosis as a therapeutic strategy (Lee et al. 2015). Indeed, USP11 knockdown reduced levels of cIAP2 and sensitized the cells to induction of BV6- or birinapant-induced apoptosis. Moreover, mitoxantrone (MTX), identified earlier as a USP11 inhibitor (Burkhart et al. 2013), had a negative effect on cell viability. MTX was shown to exhibit other functions too, like inhibiting topoisomerase II (Crespi et al. 1986; Bellosillo et al. 1998), so this has to be taken into consideration. Consistent with two previous reports describing USP11 as a negative regulator of NF-κB signaling, loss of USP11 induced a slight increase in signaling in response to TNFα, however, eventually it led to apoptotic death. The physiological importance of these findings was tested in colon cancer and melanoma cells, which were shown to have USP11 overexpressed. Finally, it was shown that USP11 is regulated on transcriptional level in a JNK-dependent manner as a response to TNFα. Hence, inhibition of JNK or USP11, leading to downregulation of cIAP2, sensitizes the cells to TNFα-induced apoptosis.

Moreover, USP11 was identified in a DUB library screen for factors promoting mammary glad tumorigenesis (Zhou et al. 2017). Overexpression of USP11 correlated with poor patient prognosis. Upon identification of USP11 as a candidate, mass spectrometry approach linked USP11 and XIAP. XIAP is another member of the inhibitor of apoptosis (IAP) family. Whereas depletion, or MTX inhibition of WT USP11 resulted in decreased level of XIAP, overexpression of USP11 stabilized it. Catalytic inactive USP11 showed no effect; again suggesting DUB activity of USP11 is crucial for the XIAP stability. Overexpression of USP11, leading to increased XIAP levels, inhibited apoptosis induction thus promoting tumorigenesis. As inhibition of

XIAP by an inhibitor sensitized breast cancer cells to cisplatin, inhibition of USP11 might be a novel way to induce apoptosis in breast cancer by inducing destabilization of XIAP, similarly what was shown for cIAP2 (Lee et al. 2015).

Additionally, USP11 was shown to regulate TGFβ signaling by deubiquitylating TGFβ RI receptor (ALK5) (Al-Salihi et al. 2012). Identified as an interactor of SMAD7, a negative regulator of TGFβ signaling (Nakao et al. 1997) via mass spectrometry, overexpression of USP11 enhanced TGFβ-induced SMAD2 phosphorylation, translocation to the nucleus and enhanced the TGFβ-induced reporter activity. In agreement with these findings, knockdown of USP11 attenuated TGFβ signaling. Finally, USP11 was shown to interact with ALK5. USP11 could partially reduce ALK5 deubiquitination in a proteasome-dependent manner opposing SMAD7-dependant E3 ligase recruitment and proteasomal targeting of ALK5 in not yet fully understood manner, thereby resulting in enhanced TGFβ-dependent signaling.

Another report linked USP11 to positive TGFβ signaling regulation, however, via deubiquitination and stabilization of TGFβ RII receptor (Jacko et al. 2016). Whereas inhibition with MTX attenuated TGFβ signaling, overexpression of WT USP11 reduced TGFβ RII ubiquitination and increased stabilization, thereby led to SMAD2/3 phosphorylation and pathway activation. It is important to note that these experiments were performed in pulmonary fibroblasts, whereas the report on USP11 ALK5 deubiquitination was mostly done using human embryonic kidney cells (Hek) (Al-Salihi et al. 2012), so the variation in reported substrates may be cell line-dependent. In 2018, USP11 was also shown to deubiquitination and stabilization of TGFβ RII receptor, however in human breast cancer cells (Garcia et al. 2018). Here, USP11 was identified as an upregulated member of ubiquitin-proteasome system upon induction of epithelial mechenshimal transition (EMT), as well as upon TGFβ treatment in human breast cancer. Here, too, high USP11 levels correlated with poor patient outcome in patients with epithelial tumor origin. Overexpression of WT USP11, but not catalytically inactive USP11, was required for EMT and resulted in more sphere formation in a mammoshpere assay. Similarly, overexpression of WT USP11, but not catalytically inactive USP11, resulted in faster wound healing, and increased migration.

USP11 was identified in another siRNA screen, as a modulator of promyelocytic leukaemia (PML) protein stability in a proteasome-dependent manner (Wu et al. 2014). Here, USP11 was shown to counteract both SUMO-dependent RNF4 and SUMO-independent Roc1–Cul3–KLHL20-mediated PML ubiquitination. Interestingly, USP11-dependent PML stabilization was shown to suppress multiple malignant traits of glioblastoma multiforme (GBM). Furthermore, it was uncovered that USP11 is transcriptionally repressed in a Notch1-dependent way in a cohort of GBM patient material and this correlated with lower PML levels, and higher malignancy. Interestingly, whereas this report suggested that lower levels of USP11 correlate with higher malignancy of GBM, this was not the case in PDA (Burkhart et al. 2013), where inhibition of USP11 appeared to be linked with inhibition of cancer growth. It is therefore important to keep in mind that whether USP11 acts as a tumor suppressor or an oncogene is highly context dependent, as well that it is important to dissect if USP11 presence in cells or its catalytically activity is responsible for distinct observations. Another report linking USP11 and RNF4 identified USP11-dependent regulation of PML stability (Hendriks et al. 2015). Here, USP11 was identified as an RNF4 interactor via mass spectrometry approach. Both proteins, transiently overexpressed, were found to colocalize in the nucleus, although USP11 was found throughout the cell. Interestingly, *in vitro* both WT and catalytically dead USP11 could bind hybrid SUMO-2-ubiquitin chains, and WT USP11 was able to deubiquitinate them. Functionally, USP11 knockdown led to a decrease in PML bodies, like previously reported. As expected, knockdown of RNF4 led to a significant increase. However, co-depletion of both led to an intermediate phenotype suggesting USP11 counterbalances RNF4-mediated PML ubiquitination. Together, these reports suggest an important role of USP11 in mediating PML degradation by counteracting RNF4 activity.

USP11 was shown to deubiquitinate and stabilize eIF4B (eukaryotic initiation factor 4B). Diffuse large B-cell lymphoma (DLBCL) cells are highly lipid dependent. Inhibiting lipid synthesis *de nov*o, by inhibiting fatty acid synthase (FASN), would be a good therapeutic strategy to inhibit tumor growth (Kapadia et al. 2018). Interestingly, depleting or inhibiting FASN abrogateed *de novo* protein synthesis, inhibited cell proliferation, and led to a reduction in

eIF4B levels, strictly on protein level. Conversely, depleting eIF4B led to a reduction of FASN on both mRNA and protein levels, and increased expression of some tumor suppressors. To elucidate what is the cause for reduction of eIF4B protein levels, DUBs were looked at next and USP11 was shown to stabilize eIF4B levels. Importantly, *in vitro*, USP11, but not USP7 was shown to directly deubiquitinate eIF4B. By regulating eIF4B, USP11 was shown to regulate downstream oncogenic properties of eIF4B. Consistent with findings comparing the effect of WT, or catalytically inactive USP11, MTX-mediated USP11 inhibition was shown to mimic USP11 depletion phenotype. Interestingly, FASN-dependent USP11 regulation was only observed in ABC- but not in GC-DLBCLs (FASN resistant), however, depletion of PI3K signaling pathway, sensitized cells to treatments with inhibitors. The observed difference was reflected in the difference in phosphorylation of p70-RSK reduced in ABC- DLBCLs. This suggested PI3K signaling is involved in FASN-USP11-eIF4B signaling triad. Moreover, they found USP11 interacts with S6Kinase (S6K) and can be modified by it *in vitro*. USP11 has AGC-substrate motif (RxRxxS/T) at serine 453 (S453) and overexpression of the phospho-mimetic aspartic acid mutant had the same effect as overexpressing WT USP11 on increased translation, and increased levels of oncogenes. Conversely, overexpression of the phospho-deficient mutant USP11 (S453A) showed none of these phenotypes, and remarkably, was not able to deubiquitinate eIF4B, implying S6K-dependent phosphorylation is required for USP11 and eIF4B interaction and USP11-dependent eIF4B deubiquitination. FASN-p70-S6K-USP11-eIF4B is a novel oncogenic driver in lipid-dependent DLBCL.

An interesting tumor suppressor role of USP11 was found when it was shown that USP11 deubiquitinates and stabilizes PTEN (phosphatase and tensin homolog) in the nucleus (Park et al. 2019). PTEN is a lipid phosphatase and a negative regulator of highly oncogenic PI3K/AKT pathway. PTEN was described to be regulated by a number of E3 ligases (including XIAP, USP11 substrate) and DUBs (including USP7, close interactor of USP11). USP11 was identified as a negative regulator of PTEN by a DUB screen based on AKT phosphorylation, cellular levels of both phosphatidylinositol (3,4,5)-trisphosphate, and PTEN protein levels. USP11 was shown to stabilize PTEN

levels and this was activity-dependent. Excitingly, USP11 was shown to remove poly-ubiquitin chain from PTEN, whereas USP7 was able to remove the monoubiquitin previously shown to enable its nuclear export. Importantly, *in vitro* assays showed loss of USP11 induced cell growth, mobility, and led to increased metabolic rate (higher rates of glucose uptake, lactate production, and glutamine consumption). This publication was also the first to report *Usp11⁻* mice. They were viable, and born at expected Mendelian frequency. Male mice were shown to be increasingly susceptible to prostate cancer, similarly what was reported for PTEN-depleted mice, suggesting an important X-linked role of USP11 in prostate cancer. When prostate and breast cancer samples were investigated, it was found that low USP11 level correlated with low PTEN activity and higher malignancy. Furthermore, when investigating mRNA and protein levels in cell culture dishes of various confluency, it was reported that mRNA levels of USP11 were far higher in dense cells than in sparse cell. Similarly, PTEN levels were also elevated in dense cells, however, the mRNA was stable regardless of cell density. Sparse cells also showed a faster turnover of PTEN. This led to an interesting hypothesis that cell density regulates USP11 on the mRNA level, hence leading to an increase in protein level that makes USP11 more potent at regulating PTEN stability. This hypothesis was confirmed by identifying USP11 promoter to be under regulation of FOXO proteins, and modulation of FOXO proteins could reproduce all observed PTEN observed phenotypes. Conversely, loss of PTEN also regulated USP11 expression. This work elucidated an important, tumor suppressor FOXO-PTEN-USP11 feed-forward regulatory mechanism showing again that USP11 has distinct roles in distinct cell compartments. Comprehensive list of published data on USP11 can be found in Table 1.

Table 1: Summary of published data on USP11 with emphasis on the most important information, such as identified substrates and tumor suppressor/oncogenic role. USP11 has many described roles and substrates, and its role in tumor promotion, or suppression is highly context dependent.

Year	Substrate	Function	Localization/ Cell context	Growth
Ideguchi et al. 2002	RanBPM *in vitro*	Unclear	Nucleus	

Lim et al. 2016	Mgl-1 (interactor of RanBPM)	USP11 deubiquitinates and stabilized Mgl-1 in RanBPM-dependent manner	Nucleus/ Lung, kidney	USP11 tumor suppressor; loss of USP11 increased oncogenesis (increased migration) = EMT
Yamaguchi et al. 2007	IKKα	Transcriptional regulation, IKKα translocates to the nucleus and regulates p53-dependent gene expression		Negative regulator of NF-κB signaling
Sun et al. 2010	IκBα	Deubiquitinates and stabilizes IκBα. Catalytic inactive partially rescues the phenotype		Negative regulator of NF-κB signaling
Al-Salihi et al. 2012	ALK5 = TGFβ RI	Deubiquitinates the receptor	Cytosol/ Mostly Hek cells	Positive regulator of TGFβ signaling; growth
Jacko et al. 2016	TGFβ RII	Deubiquitinates the receptor	Cytosol/ Pulmonary diseases, lung epithelial cells	Positive regulator of TGFβ signaling; growth
Garcia et al. 2018	TGFβ RII	Deubiquitinates the receptor	Cytosol/ Breast cancer cells	Positive regulator of TGFβ signaling, promotes EMT
Zhao et al. 2016	LPA1 (Lysophosphatidic acid receptor 1)	Deubiquitinates the receptor, counteracts Nedd4 ubiquitination	-/ Lung	MTX inhibits USP11, destabilized the receptor, reduces LPA1-dependent inflammation
Xu et al. 2016	Correlation	Increased levels of caspase-3, Fas, Fas ligand, active caspase 8	-/ Brain	Increased apoptosis induction after intracerebral hemorrhage
Istomine et al. 2019		Unregulated USP11 in a subset of T cells	-/ T cells	Positive regulator of TGFβ signaling, promotes growth and differentiation
Wang et al. 2019	Snail	Deubiquitinates and stabilizes Snail, TF	-/ Ovarian cancer	Promotes EMT by stabilizing Snail
Zhang et al. 2016	VGLL4	Deubiquitinates and stabilizes the transcription repressor	Nucleus/ Kidney cells	Tumor suppressor; loss of USP11, loss of transcription repressor; induced YAP-dependent

				growth
Schoenfeld et al. 2004	BRCA2	Interaction	Nucleus	USP11 is pro-survival
Shah et al. 2017	XPC (xeroderma pigmentosum complementation group C)	XPC is needed for NER; deubiquitination needed to remain at DNA damage site. Additionally USP7 deubiquitinates XPC	Nucleus/ Skin cancer	USP11 tumor suppressor
Maertens et al. 2010	PRC1	Deubiquitinates PRC1, no effect on H2A ubiquitination in contrast to (Yu et al. 2016; Ting et al. 2019)	Function in the nucleaus, associated to chromatin	Loss of USP11 led to senescence-like proliferative arrest
Ting et al. 2019	H2A K119 and H2B K120 deubiquitination through interaction with the NuRD complex	Chromatin remodeling, NHEJ and HR	Nucleus	USP11 is a guardian of the genomic stability and promotes cell survival
Yu et al. 2016	γH2AX	USP11 deubiquitylates γH2AX, not the canonical H2A K119 and H2B K120	Nucleus	Loss of USP11 misregulates proteins at DSB foci (e.g. 53BP1), and hypersensitises cells to γ-irradiation
Lee et al. 2015	cIAP2	Deubiquitinates and stabilizes cIAP2	-/ Colon cancer, melanoma cells	Inhibition of JNK (that regulates USP11 expression) or USP11 leads to sensitizing cells to apopotosis
Zhou et al. 2017	XIAP	Deubiquitinates and stabilizes XIAP		Inhibition of USP11 leads to sensitizing cells to apopotosis
Lin et al. 2008	E7 from HPV-16E7	Deubiquitinates and stabilizes E7 (a growth inducing protein)	-/ Viral replication	Tumor promoter; promoting cell growth, pro-survival
Wu et al. 2014	PML	Counteracts RNF4 and	Nucleus/ Glioblastoma	Tumor suppressor

		KLHL20–Cul3 (Cullin 3)–Roc1 ubiquitination and stabilizes PML	multiforme (GBM); USP11 transcriptional ly repressed in glioma – low PML levels	
Hendriks et al. 2015	PML	Ineracts with RNF4 and Counteracts RNF4 ubiquitination of PML; can cleave SUMO-ubi chains	Nucleus	Tumor suppressor
Ke et al. 2014	P53	Deubiquitinates and stabilizes p53, previously shown for USP7		Tumor suppressor; stabilizes p53
Deng et al. 2018	p21	Deubiquitinates and stabilized p21 (p53 is regulating expression of p21). USP11 did not regulate p53 levels in contrast to (Ke et al. 2014)	Nucleus/ Lung and colon cancer cells	Tumor suppressor; p21 is needed to ensure DNA damage is repaired. Loss of USP11 induced tumorigenesis
Stockum et al. 2018	RAE1	USP11 deubiquitinates RAE1 and likely modulate its interactome	Spindle/ Nothing specific, U2OS	USP11 KD reduced cell proliferation (produced incorrectly spindle nucleated cells)
Wang et al. 2017	E2F1	Down regulation of USP11 – downregulation of E2F1 – downregulation of Peg10 mRNA – less proliferation	Nucleus/ Lung	Downregulation of USP11 supresses cell repair and wound healing
Kapadia et al. 2018	eIF4B eukaryotic initiation factor 4B	USP11 deubiquitinates and stabilizes eIF4B on protein level (dependent on S6K phosphorylation of USP11)	Cytosol/ Diffuse large B-cell lymphoma (DLBCL)	Oncogene; FASN-S6K-USP11-P-deubiquitnates eIF4B and drives oncogene translation up
Zhang et al.	Correlation		Cytoplasmic	Oncogene;

			expression was higher, and nuclear lower in in non-cancerous tissue/ Hepatocellular carcinoma (HCC)	Correlated with vascular invasion, differentiation tumor number, and recurrence, and shorter overall patient survival
2018				
Yang et al. 2017	EZH2 (enhancer of zeste 2)	Deubiquitinates and stabilizes EZH2	-/ Breast cancer	Stabliziation of EZH2 in part could explain USP11-dependent malignancy, cell proliferation, and poor patient prognosis
Sun et al. 2019	PPP1CA (protein phosphatase 1)	USP11 positively regulates the ERK/MAPK signaling pathways in a PPP1CA-dependent manner	-/ Colorectal cancer	Oncogene; USP11 promotes cell proliferation, migration, and invasion
Park et al. 2019	PTEN (phosphatase and tensin homolog)	USP11 stabilizes PTEN, tumor suppressor, but PTEN also regulates USP11 expression that is under FOXO regulation. mRNA and protein levels of USP11 are higher in dense cells	USP11 stabilizes PTEN both in nucleus and cytosol, but opposed to other DUBs that regulate it, more in the nucleus (together with USP7 removing mono ubiquitination on PTEN)/ Prostate, breast cancer, HAP1	Tumor suppressor; Loss of USP11 led to increase in cell proliferation, mobility and increased cell metabolism. First USP11 mouse.
Luo et al. 2020	ARID1A	USP11 deubiquitinates and stabilizes ARID1A, TRIM32 ubiquitinates it and targets for degradation	Nucleus/ Prostate, breast cancer, HAP1	Tumor suppressor; ARID1A is too

1.2 Autophagy

1.2.1 Overview of autophagy

Autophagy is a well-studied, catabolic process crucial for maintenance of cell homeostasis involving degradation of intracellular material via the lysosome. Together with the ubiquitin-proteasome system (UPS), autophagy is the main cellular quality control mechanism (Sun et al. 2019). There are several kinds of autophagy: chaperone mediated autophagy, microautophagy, and macroautophagy (Table 2). Chaperone-mediated autophagy (CMA) is based on recognition of a specific KFERQ, or KFERQ-like motif on proteins by hsc70 (Heat Shock Cognate protein 70) and co-chaperones, its delivery to the lysosome, followed by the target protein unfolding and direct translocation to the lumen of the lysosome via LAMP-2A (Lysosome-associated membrane protein 2) where the target is degraded (Cuervo and Wong 2014). Several features are important for CMA: it is selective, it does not involve generation of a new membrane (vesicle-free), and it involves direct cargo delivery to the lysosomal lumen via LAMP-2A translocation without membrane perturbation. The latter is a key feature of microautophagy that entails direct engulfment of cytoplasmic material by the lysosome either via membrane invagination, or via an "arm-like" extension to the cytoplasm leading to sequestering of a part of the cytoplasm and generation of a vesicle inside of the lysosome (Mijaljica, Prescott, and Devenish 2011). Finally, there is macroautophagy (hereafter referred to as autophagy) that involves multiple protein complexes working in a hierarchical order (Koyama-Honda et al. 2013) to initiate generation of a novel double-lipid bilayer vesicle at the endoplasmatic reticulum (ER) (Axe et al. 2008; Sanchez-Wandelmer, Ktistakis, and Reggiori 2015) that expands and matures engulfing cytoplasmic material and finally closes and fuses with the lysosome resulting in cargo degradation (Xie and Klionsky 2007; Mizushima 2007). Cargo designated for autophagic degradation can be specifically selected or degraded by the bystander principle, in which case it is termed selective or non-selective autophagy, respectively (Johansen and Lamark 2011; Stolz, Ernst, and Dikic 2014). Importantly, autophagy can be induced by stress such

a hypoxia, glucose or amino acid starvation, as well as by damaged mitochondria etc., as a pro-survival mechanism. Considering the process results in degradation, hence recycling of cell's building blocks, it provides a temporary source of nutrients to overcome the period of stress (Rabinowitz and White 2010). The name itself is derived from this fact, as autophagy is derived from Greek words meaning "self-eating".

Table 2: Overview of the different types of autophagy and their distinct features.

	Chaperone mediated autophagy	Microautophagy	Macroautophagy
Cargo selection	Selective	Non-selective or selective	Non-selective or selective
Membrane source	Vesicle-free	Vesicle-free	ER: generation of a novel double-lipid bilayer vesicle
Machinery	hsc70 and co-chaperones, intake via LAMP-2A translocation	Direct uptake by the lysosome	Multiple protein complexes and sophisticated regulation

Autophagy machinery was originally discovered and described in yeast by seminal work of Yoshinori Ohsumi for which he was awarded the Nobel Prize in 2016. In the landmark publication, 15 APG (autophagy) genes were identified that failed to accumulate autophagy bodies and degrade proteins under nitrogen starvation, which resulted in reduced yeast viability used as the screen readout (Tsukada and Ohsumi 1993). Today, the field accepted a unified nomenclature for these proteins; ATG as "autophagy-related genes" (Klionsky et al. 2003). Importantly, autophagy is a highly conserved process from yeast to mammals, and its sophisticated machinery is tightly regulated for a controlled execution, and any deviation has implications in diseases from neurodegeneration to cancer (Shintani and Klionsky 2004; Itakura et al. 2008; Levine and Kroemer 2008; Choi, Ryter, and Levine 2013).

1.2.2 Autophagy machinery

1.2.2.1 Kinases involved in autophagy initiation

Serine/threonine-protein kinase ULK1 (yeast Atg1) plays a central role in autophagy induction. In yeast, Atg1 complex consists of Atg1, Atg13, Atg17, Atg31, and Atg29 (Noda and Fujioka 2015). In mammalian cells, ULK1 forms a complex with FIP200 (RB1CC1), mATG13, and ATG101 (Noda and Fujioka 2015). In nutrient rich times it is associating with mTOR, a negative regulator of autophagy (Noda and Ohsumi 1998), that phosphorylates it at S757 and inhibits its activity (Figure 3 A) (Jung et al. 2009; Kim et al. 2011; Egan et al. 2011). The mTOR kinase also phosphorylates another member of the complex, mATG13 (Figure 3 A) (Hosokawa et al. 2009; Jung et al. 2009). Phosphorylation on S757 site by mTOR on ULK1 prevents its association with AMPK, the energy sensing kinase (Kim et al. 2011; Egan et al. 2011). Upon glucose starvation, AMPK is activated; it phosphorylates TSC2 (Inoki et al. 2002; Inoki, Zhu, and Guan 2003) and RAPTOR (Hara et al. 2002; Gwinn et al. 2008; Lee et al. 2010) leading to mTOR inhibition (Figure 3 B). Subsequently, this leads to the loss of mTOR-mediated inhibiting phosphorylation at S757 on ULK1 and ULK1 activation. In addition, AMPK activates ULK1 directly by phosphorylating it at several sites including S317, S777, and S555 (Figure 3 B) (Kim et al. 2011; Egan et al. 2011). In parallel to ULK1 phosphorylation, AMPK phosphorylates GNB2L1 (RACK1) at T50 in hepatocytes and it serves as an adaptor for PI3KC3 complex assembly by interacting with VPS15, Beclin-1, and ATG14 (Figure 3 B) (Zhao et al. 2015), that will be discussed in more detail in the following section. Interestingly, activated ULK1 was found to phosphorylate AMPK in turn, leading to decreased AMPK activity based on the T172 phospho-site on AMPK as a readout, likely as a negative feedback loop to restrict autophagy induction (Löffler et al. 2011). Exact chronology remains unclear; this phosphorylation may lead to loss of T172 AMPK phospho-site or it can sterically prevent deposition of novel phosphorylation by upstream kinases like LKB1/TAK1 or CaMKK2 (Löffler et al. 2011; Jeon 2016). Upon amino acid starvation activation of AMPK is not necessary (Yuan, Russell, and Guan 2013); rather, ULK1 is directly activated by mTOR inhibition in not yet fully understood way. One way this is achieved is through direct mTOR regulation of AMBRA1

(Activating molecule in Beclin-1 regulated autophagy 1), an E3 ligase. mTOR phosphorylates AMBRA1 at S52 (Nazio et al. 2013). This modification disappears when autophagy is induced and coincides with increased AMBRA1-TRAF6 ULK1 K63-linked ubiquitination that leads to increased ULK1 stability, self-association, and activity (Figure 3 C) (Nazio et al. 2013). Additionally, mTOR inactivation upon nutrient depletion is crucial for transcription factor TFEB translocation to the nucleus where it activates expression of lysosome biogenesis genes and autophagy-related genes (Roczniak-Ferguson et al. 2012; Martina et al. 2012; Settembre et al. 2011; 2012). In nutrient rich conditions, TFEB associates with mTOR at the lysosome where it is phosphorylated by mTOR at several sites, including S211 and S142. This results in TFEB sequestration in the cytosol through interaction with 14-3-3 proteins and exclusion from the nucleus (Roczniak-Ferguson et al. 2012; Martina et al. 2012; Settembre et al. 2011; 2012). Upon mTOR inhibition and loss of inhibiting phospho-sites, TFEB translocates to the nucleus, thereby serving as an immediate signal transducer to the nucleus promptly after mTOR is inactivated due to lack of nutrients (Figure 3 C). mTOR itself is localized to the lysosome by interacting with Rag proteins—a family of four related small guanosine triphosphatases (GTPases): RagAB and RagCD (Sancak et al. 2008). Interaction with Rag proteins mediated by RAPTOR does not have a direct effect on the activity of mTOR, only localization, unlike its interaction with Rheb that alosterically activates mTOR (Roccio, Bos, and Zwartkruis 2006; Smith et al. 2005; Long et al. 2005). However, both proteins are essential for amino acid sensing (Sancak et al. 2008; 2010). Rag proteins are localized to the lysosomes by interacting with the Ragulator complex consisting of LAMTOR1-5 and this is necessary for amino acid sensing (Sancak et al. 2010). Once activated via interplay of mTOR and AMPK, ULK1 phosphorylates itself, as well as its complex components mATG13 and FIP200, further increasing its activity (Jung et al. 2009), as well as multiple downstream autophagy-related substrates necessary for initiation of autophagosome formation. One crucial step is ULK1 phosphorylation of AMBRA1 that releases AMBRA1 and PI3KC3 complex from dynein allowing it to translocate to ER for autophagosome biogenesis induction (Di Bartolomeo et al. 2010).
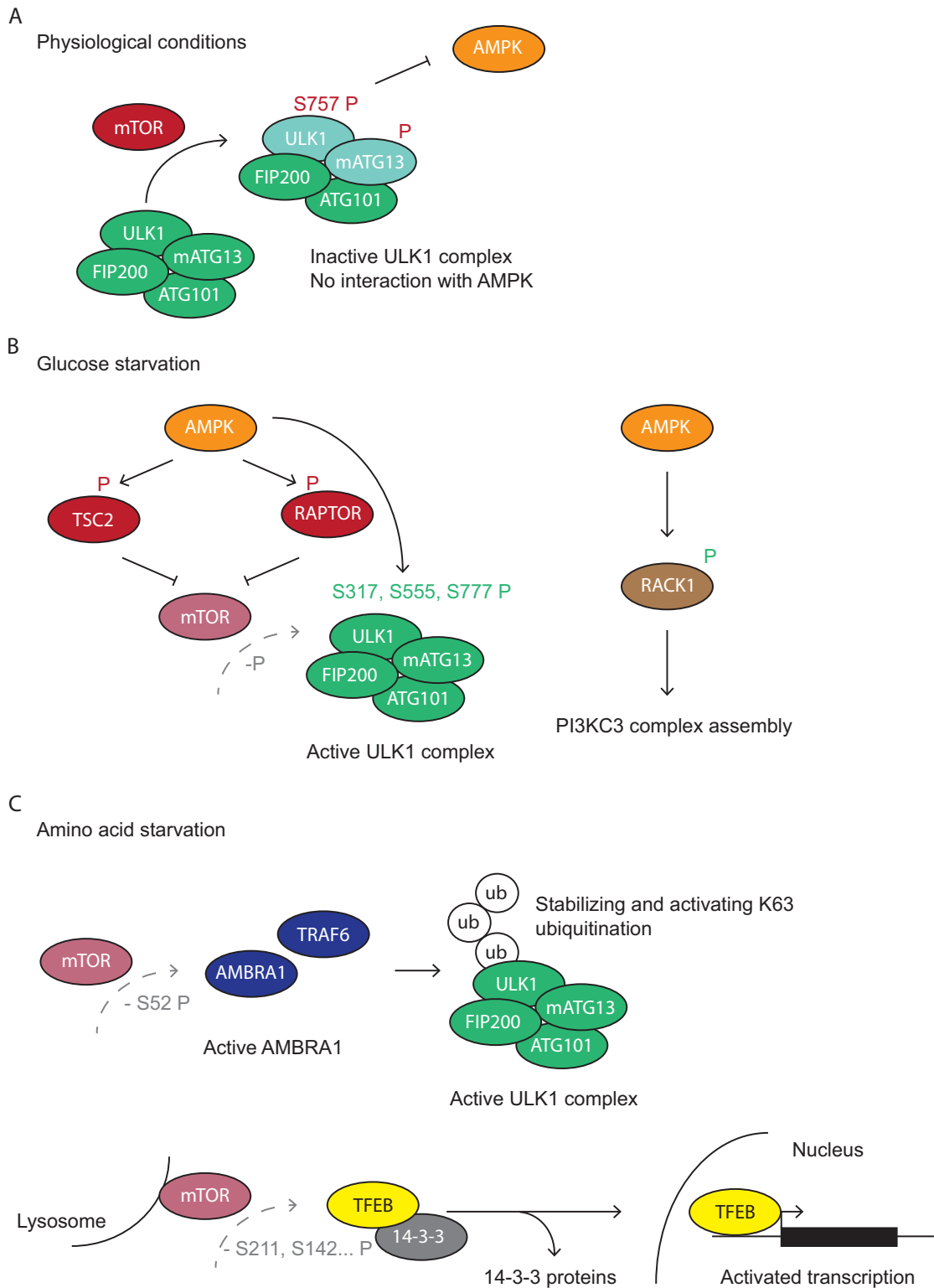
Figure 3: Schematic depiction of kinases involved in autophagy induction. A Under physiological conditions, mTOR is actively suppressing autophagy induction by phosphorylating ULK1 complex; ULK1 and mATG13. This phosphorylation prevents AMPK and ULK1 interaction. **B** Upon glucose starvation, AMPK gets activated, phosphorylates TSC2 and RAPTOR leading to mTOR inhibition, and loss of mTOR-mediated inhibiting

phosphorylation on ULK1 and mATG13. AMPK also directly phosphorylates and activates ULK1. AMPK phosphorylates RACK1, leading to the assembly of downstream PI3KC3 complex. **C** Upon amino acid starvation, mTOR inactivation leads to loss of inhibiting phosphorylation on AMBRA1, and AMBRA1- and TRAF6-mediated K63 ubiquitination of ULK1 enabling ULK1 activation. In parallel, inactivation of mTOR leads to loss of inhibiting phosphorylation on TFEB, loss of interaction with 14-3-3 proteins, and translocation to the nucleus activating lysosome- and autophagy-related gene transcription.

1.2.2.2 PI3KC3 complex architecture and composition

VPS34, a class III phosphatidylinositol 3-OH kinase (PI3K), generates phosphatidylinositol-phosphates (PI(3)Ps) that are crucial for autophagosome nucleation at the ER (Herman and Emr 1990; Hiles et al. 1992; Yu, Long, and Shen 2015; Backer 2016). VPS34 uses phosphoinositol as a substrate and phosphorylates the 3'-position of the inositol ring resulting in PI(3)Ps. VPS34 forms a complex with regulatory, pseudokinase VPS15 (Stack et al. 1993; Yan et al. 2009), Beclin-1 (yeast Apg6/Vps30p (Liang et al. 1999), and a fourth subunit that defines the complex function. There are two distinct complexes conserved from yeast to humans. BARKOR/ATG14 is specific for the pro-autophagic PI3KC3 complex, named complex I (Kametaka et al. 1998; Kihara et al. 2001; Sun et al. 2008; Itakura et al. 2008). ATG14 is the subunit responsible for PI3KC3 complex targeting to the ER nucleation site via its N-terminal CXXC motifs, as well as C-terminal BATS domain (Barkor/Atg14L autophagosome targeting sequence) upon autophagy induction (Sun et al. 2008; Matsunaga et al. 2010; Fan, Nassiri, and Zhong 2011). ATG14 is replaced by UVRAG (UV radiation resistance-associated gene) in the autophagosome maturation step, as well as endosomal trafficking-specific PI3KC3 complex II (Kihara et al. 2001; Sun et al. 2008; Itakura et al. 2008). RUBICON (Beclin-1 associated RUN domain containing protein) is another subunit of the complex that can interact with both ATG14-associating and UVRAG-associating Beclin-1 and downregulates autophagy when in complex I at a later, autophagosome maturation stage (Matsunaga et al. 2009; Yun Zhong et al. 2009). There are several other noteworthy complex components and accessory proteins, most important of which is the above-mentioned E3 ligase AMBRA1 that will be

discussed in later chapters (Fimia et al. 2007; Antonioli et al. 2014). Another one is Bif-1 (Endophilin B1), a positive regulator of the complex via its interaction with UVRAG and Beclin-1 (Takahashi et al. 2007). The last identified "core" subunit is NRBF2 (Nuclear receptor-binding factor 2, yeast Atg38) (Araki et al. 2013; Cao et al. 2014; Zhong et al. 2014; Lu et al. 2014), as strictly complex I-specific, with one publication additionally reporting a weak interaction with UVRAG (Lu et al. 2014). Although one report indicates negative effect of NRBF2 on autophagy (Zhong et al. 2014), strong evidence favors a positive role for NRFB2 in autophagy (Araki et al. 2013; Lu et al. 2014; Cao et al. 2014). Despite the fact that NRBF2 knockout mice seem without obvious defects, only with a late developing liver necrosis phenotype, VPS34 from knockout mice is found co-immunoprecipitating with less ATG14, VPS15, and Beclin-1, and in general producing less PI(3)Ps, implying reduced autophagy rate, while UVRAG-VPS34 interaction remains unchanged (Lu et al. 2014). Similar data is found both in yeast (Araki et al. 2013) and human cell culture (Cao et al. 2014). Thanks to structural insights into complex architecture, it is now known that NRBF2 is indeed a positive regulator of autophagy. The complex is V, or Y shaped, with the left arm consisting of Beclin-1 and ATG14 in complex I (UVRAG instead of ATG14 in complex II), and the right arm consisting of VPS15 and VPS34 (Figure 4 A) (Baskaran et al. 2014; Rostislavleva et al. 2015; M. Ma et al. 2017). The base of the complex is the homodimer of NRBF2 formed via its Coiled Coil Domain (CCD) domain, thus leading to dimerization of the complex in mammalian PI3KC3 complex, enhancing VPS34 lipid kinase activity at the membrane (Araki et al. 2013; Lu et al. 2014; Zhong et al. 2014; Young et al. 2016). NRBF2 interacts directly with the PI3KC3 complex via ATG14 and Beclin-1 (Araki et al. 2013; Lu et al. 2014; Zhong et al. 2014; Young et al. 2016), in VPS15-dependent manner (Lu et al. 2014; Cao et al. 2014). The N-terminal part of NRBF2 that protrudes into the core of the complex, the MIT (Microtubule Interacting and Trafficking) domain, is sufficient to allosterically enhance complex activity *in vitro* (Young et al. 2016). Interestingly, although in the mammalian complex I, NRBF2 can dimerise the PI3KC3 complex, yeast Atg38 does not (Ohashi et al. 2016).
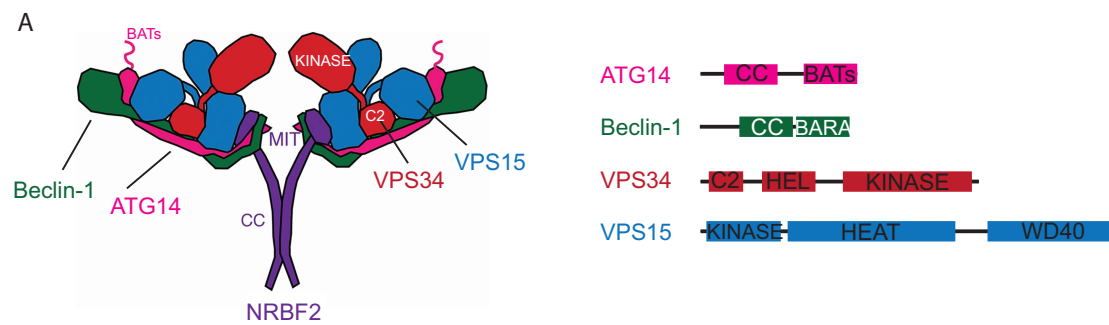
Figure 4: Schematic depiction of the PI3KC3 complex I. A Schematic representation of the PI3KC3 complex I (adapted from (Young et al. 2016)), and the individual components' domain structure (based on (Baskaran et al. 2014), CC (coiled coil), HEL (helical), BATs (Barkor/ATG14(L) autophagosome-targeting sequence). ATG14 BATs domain binds the lipids of the ER membrane, and VPS34 kinase domain is also optimally positioned towards the lipid substrates.

1.2.2.3 Phosphatidylinositol 3-phosphate (PI(3)P) effector proteins and ATG9 vesicles

The role of the PI3KC3 complex I is to phosphorylate the lipids of the ER generating PI(3)Ps, thereby forming the omegasome, precursor of the autophagosome (Axe et al. 2008; Hayashi-Nishino et al. 2009). The molecular function of PI(3)Ps is to recruit downstream effectors, such as WIPI1 and WIPI2 proteins (WD-repeat protein interacting with phosphoinositide) (Polson et al. 2010), orthologs of yeast Atg18 (Obara et al. 2008), enabling recruitment of autophagosome elongation machinery (Figure 5 A). There are four WIPI proteins, of which WIPI2 has the most well described role in autophagy (Polson et al. 2010; Proikas-Cezanne et al. 2015). WIPI2 recruits ATG16L1 of the ATG12-5-16L1 ubiquitin-like LC3 conjugation machinery to the autophagosome for its expansion, cargo recruitment, and closure (Dooley et al. 2014).

A

ER
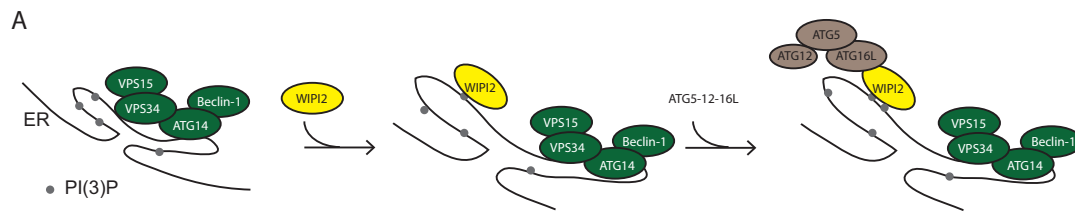
PI(3)P

Figure 5: Schematic depiction of the WIPI2 recruitment through activity of PI3KC3 complex I. A Schematic representation of the PI3KC3 complex PI(3)P production that recruits WIPI2. WIPI2 in turn recruits downstream ATG12-5-16L protein complex, important for LC3 lipidation.

Interestingly, FIP200 of the ULK1 complex interacts with ATG16L1 (Fujita et al. 2013; Gammoh et al. 2013; Nishimura et al. 2013), however, WIPI2-ATG16L interaction does not depend on FIP200 and is not required for WIPI2-driven LC3 lipidation (Dooley et al. 2014). This suggests distinct roles for ULK1 complex at the phagophore, at different stages of autophagy. Considering WIPI proteins bind to PI(3)Ps produced by VPS34, their recruitment to the phagophore can be used as a readout for the kinase activity using immunofluorescence for distinct WIPI punctae quantification (Proikas-Cezanne et al. 2007). There are other PI(3)P effector proteins that can be used in the similar fashion, such as DFCP1, the role of which in autophagy is not yet clear (Axe et al. 2008). Yeast Atg18 was found to interact with Atg2, and this interaction is independent of Atg18 binding to PI(3)P, however, it is required for their localization at the phagophore assembly site (Obara et al. 2008). Whereas in yeast, Atg2 is involved in autophagy, Cvt pathway (Cytoplasm to vacuole), and Atg9 trafficking/retrieval (Wang et al. 2001; Reggiori et al. 2004; Obara et al. 2008; Gómez-Sánchez et al. 2018), the role in mammalian cells is not investigated in detail. ATG9, the only transmembrane protein essential for autophagy, is only transiently associating with the autophagosome in mammalian cells and its role in autophagy is not clear (Young et al. 2006; Orsi et al. 2012; Koyama-Honda et al. 2013; Karanasios et al. 2016). In yeast, Atg9-containing vesicles are proposed to deliver membrane components to the phagophore assembly site indicating a role early in the process (Reggiori et al. 2004; Yamamoto et al. 2012; Karanasios et al. 2016). Recently, however, it was described using

48

mass spectrometry that ATG9 vesicles are enriched in arfaptins and phosphoinositide-metabolizing enzymes, namely PI4-kinase PI4KIIIβ (Judith et al. 2019). PI4KIIIβ products, PI(4)P, are also found in the autophagosomes partially colocalizing with the ATG13 of ULK1 complex, as well as LC3B, albeit to a lesser extent. PI(4)Ps were therefore found to also be important in autophagosome biogenesis, importantly, independently of PI(3)P production, and potentially even more upstream (Judith et al. 2019).

1.2.2.4 ATG12-5-16L1 ubiquitin-like conjugation machinery

Through interaction with WIPI2, recruited to the autophagosome by binding PI(3)P, ATG16L1 is recruited next. ATG12-5-16L1 conjugation machinery was originally described in yeast following the seminal work of Yoshinori Ohsumi (Tsukada and Ohsumi 1993). Then termed Apg, it was described that Apg12 is conjugated to K149 of Apg5 in ATP-dependent manner and this conjugation was dependent on Apg7 and Apg10, the E1-, and E2-like enzymes, respectively (Figure 6 A) (Mizushima et al. 1998; Tanida et al. 1999; Kim et al. 1999; Shintani et al. 1999; Mizushima, Yoshimori, and Ohsumi 2002; Nemoto et al. 2003). Only a year later, the same group discovered that the Apg12-5 conjugate interacts with Apg16, and that Apg16 is indispensible for the Apg12-5 role in autophagy (Figure 6 A) (Mizushima, Noda, and Ohsumi 1999). Investigation of the autophagosome formation in Apg5-deficient mouse embryonic stem cells revealed that Apg12 conjugation to Apg5 is not essential for its membrane targeting, but is required for its function in membrane expansion (Mizushima et al. 2001). Furthermore, same publication revealed Apg12-5 conjugate is localized on the outer side of the membrane and dissociates from the autophagosme before its closure. Structural analysis of the ATG16L1 complex revealed ATG16L1 forms a dimer, and together with the ATG12-5 conjugate, a 2:2 heterotetramer (Fujioka et al. 2010). ATG16 acts as a scaffold for LC3 lipidation downstream, thereby specifying the LC3 conjugation site (Mizushima et al. 2003), as ATG16 artificially targeted to the plasma membrane exerts its function there

(Fujita, Itoh, et al. 2008). This indicated that upstream signaling is necessary for correct targeting and ATG16-dependent autophagosome expansion. Discovering WIPI2 binding to PI(3)Ps and recruiting ATG16L1 explained this observation. Moreover, the yeast Atg16 complex is able to tether vesicles *in vitro*, partially in an Atg12-independent way, suggesting an additional role in autophagy (Walczak and Martens 2013).
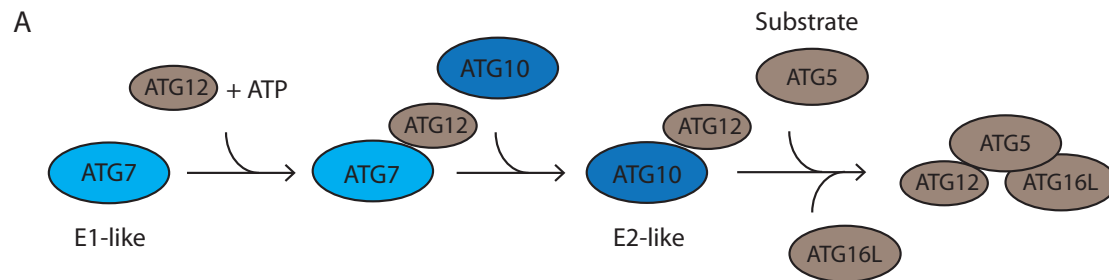
Figure 6: Schematic depiction of the ubiquitin-like ATG12-5-16L complex assembly. A The ATG12-5-16L complex is assembled in an ubiquitin-like manner, wherein ATG7 is the E1-like, and ATG10 the E2-like enzyme. ATG16 forms a complex with the ATG12-5 conjugate.

1.2.2.5 LC3 ubiquitin-like conjugation machinery

Identification of yeast Atg8, unsurprisingly, also stemmed from the landmark publication of Ohsumi (Tsukada and Ohsumi 1993). Atg8 is processed by the protease Atg4, called Apg4/Aut2, exposing the C-terminal glycine conjugated to the membrane, in E1-like enzyme Atg7-dependent manner (Figure 7 A) (Kirisako et al. 2000). The exact mechanism of membrane conjugation was discovered soon after; Apg8 is covalently conjugated to phosphatidylethanolamine through an amide bond between the C-terminal glycine and the amino group of phosphatidylethanolamine (PE) (Figure 7 A) (Ichimura et al. 2000). The same publication identified Atg3 as the E2-like enzyme for Atg8 conjugation and showed conjugation of Atg8 to PE is essential for autophagy (Ichimura et al. 2000). The above described Atg16 complex is the E3-like enzyme for Atg8 (Figure 6 A) (Hanada et al. 2007). In mammals, there are at least six homologs divided in two subfamilies: LC3 (LC3A, LC3B, LC3C) and GABARAP (GABARAP, GABARAP-L1 and L2, also

known as GATE-16) (Kabeya 2000; Wang et al. 1999; Sagiv et al. 2000; Legesse-Miller et al. 2000). LC3 is found on both sides of the membrane (Kabeya 2000), which allows it to act in selective autophagy. As mentioned earlier, autophagic cargo can be selected specifically or unspecifically, and in the case of the former, we are talking abut selective autophagy. In process of selective autophagy, cargo is polyubiquitinated and recognized by a group of proteins called autophagy receptors (Kirkin et al. 2009; Johansen and Lamark 2011). Autophagy receptors have two important features: ubiquitin-binding domain to bind the cargo and LC3-interacting region (LIR) motif that binds to LC3 conjugated to the membrane (Noda, Ohsumi, and Inagaki 2010; Birgisdottir, Lamark, and Johansen 2013). This allows a tight expansion of the membrane specifically around the cargo. To this date, multiple autophagy receptors have been identified, such as p62, NBR1, Nix1 etc. (Komatsu et al. 2007; Waters et al. 2009; Novak et al. 2010). Unlipidated, cytoplasmic LC3 is referred to as LC3-I, and lipidated LC3 as LC3-II. The two species can be separated by SDS-PAGE and visualized by western blot as LC3-II migrates faster than LC3-I (Klionsky et al. 2016). This can be taken advantage of to evaluate autophagic flux in cells.
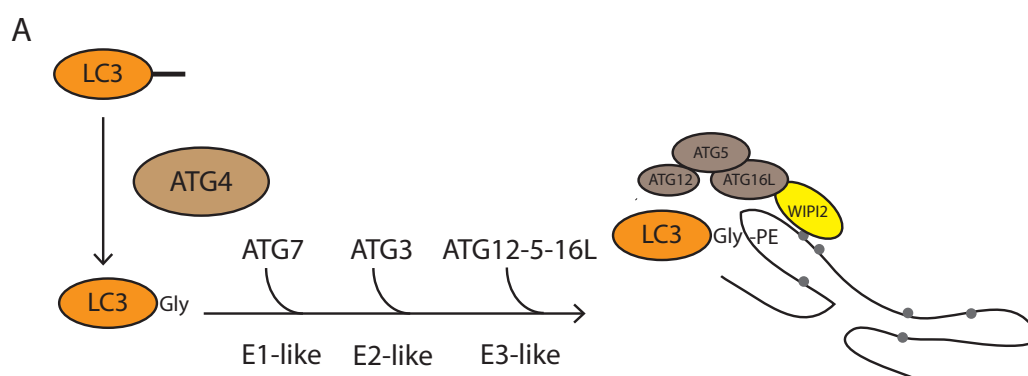
Figure 7: Schematic depiction of the ubiquitin-like LC3 conjugation machinery. A LC3 lipidation is crucial for autophagosome expansion and closure. LC3 is first processed by ATG4 protease, followed by conjugation by the E1-, E2- and E3-like enzymes, ATG7, ATG3, and ATG12-5-16L, respectively. LC3 is conjugated via its C-terminal glycine to PE on both sides of the growing autophagosome.

1.2.2.6 Autophagosome closure and autophagosome-lysosome fusion

Many things remain unclear about the final stages of autophagosome closure, and autophagosome-lysosome fusion. It has been shown that ATG4 plays a crucial role in autophagosome maturation, likely due to its activity in deconjugating randomly membrane-inserted LC3, thereby increasing the cytoplasmic pool needed specifically for growth of the autophagosome (Nakatogawa et al. 2012). Moreover, others have shown that overexpression of catalytically inactive ATG4 leads to sequestering of LC3 and paralogues and results in unclosed autophagosomes (Fujita, Hayashi-Nishino, et al. 2008). In context of mitophagy, it was reported than Atg8 homologs are specifically required for the fusion, but not for the formation of the autophagosome (Nguyen et al. 2016). Importantly, the activity of the ATG4 protease is under ULK1 regulation, as it has been shown that ULK1 phosphorylates ATG4 at S316 leading to inhibition of its catalytic activity and this phosphorylation can be reversed by the phosphatase PP2A-PP2R3B (Pengo et al. 2017), once again emphasizing the ubiquitous role of ULK1 in all stages of autophagy. The autophagosome-lysosome fusion is largely unexplored and the current knowledge relies on general findings about the endocytic pathway, vesicle tethering and fusion (Nakamura and Yoshimori 2017; Reggiori and Ungermann 2017).

1.2.3 Regulation of PI3KC3 complex by post-translational modifications

1.2.3.1 Regulation of PI3KC3 complex by phosphorylation and acetylation

The dynamics of the PI3KC3 complex assembly, as well as its activity, is regulated by post-translational modifications (PTMs).

AMPK was shown to be a master regulator of VPS34 interactions under glucose starvation by phosphorylating VPS34 at T163 and S165 to inhibit the non-autophagic complex II and phosphorylate Beclin-1 at S91 and S94 to support the formation of the pro-autophagic complex I (Figure 8 A) (Kim et al.

2013). Moreover, AMPK-dependent VPS34 regulation depends on ATG14 as it promotes pro-autophagic, ATG14-associated Beclin-1 phosphorylation. Importantly, this publication emphasizes the dynamic nature of complex stoichiometry and how the function and activity of VPS34 is directly connected to proteins it preferentially binds as a result of a particular stimuli at a given time. Interestingly, mTOR is also phosphorylating, thereby regulating, the PI3KC3 complex itself. Whereas it was shown that it does not affect the composition of any of the complexes, it phosphorylates ATG14 directly at multiple sites and inhibits the ATG14-bound VPS34 lipid kinase activity both *in vivo* and *in vitro* (Figure 8 B) (Yuan, Russell, and Guan 2013). Similarly, the NRBF2 autophagy-regulating role was found to be under mTOR control, as NRBF2 was identified as an mTOR substrate (X. Ma et al. 2017). The mTOR-dependent phosphorylation at S113 and S120 is a molecular switch between phosphorylated NRBF2 preferentially binding VPS34/VPS15 and unphosphorylated NRBF2 shifting preference to binding pro-autophagic ATG14/Beclin-1, as well as the ULK1 complex, thereby increasing autophagic flux (Figure 8 C) (X. Ma et al. 2017). This corresponds to activity of mTOR under nutrient rich conditions and inactivation of mTOR upon autophagy induction, respectively. mTOR also inhibits late stages of autophagy by phosphorylating UVRAG and increasing its association with RUBICON, thus preventing its association with the HOPS (homotypic fusion and protein sorting) complex and inhibiting conversion of endosomes into lysosomes (Figure 8 B) (Kim et al. 2015). ULK1 phosphorylates ATG14 at S29 in Beclin-1-, FIP200-, and ATG13-dependant way (Figure 8 D) (Park et al. 2016). This phosphorylation is downstream of mTOR inactivation by nutrient depletion and upstream from lipid kinase activity, as wortmannin did not have an effect on S29 phosphorylation (Park et al. 2016). However, phosphorylation at S29 enhanced lipid kinase activity and was important for autophagosome formation, but was not important for autophagosome maturation (Park et al. 2016). Moreover, ULK1 phosphorylates ATG14-associated Beclin-1 at S14, enhances its activity, and is required for full autophagic flux following amino acid starvation (Figure 8 D) (Russell et al. 2013). ATG14 is mediating the interaction between ULK1 and Beclin-1, as CCD domain mutant unable to bind Beclin-1 results in absence of phosphorylated Beclin-1 (Russell et al.

2013). Interestingly, ATG14-free, UVRAG-associated Beclin-1 is also phosphorylated by ULK1, suggesting an additional role for this site in autophagosome maturation (Russell et al. 2013). Remarkably, S14 phosphorylation is conserved in *C. elegans,* but is not found in yeast ortholog ATG6 (Russell et al. 2013). More ULK1-dependent phosphorylation sites were identified using an ULK1 inhibitor SBI-0206965 combined with mass spectrometry, even for known substrates like Beclin-1 (Egan et al. 2015). Here, it was shown that among substrates there is also AMBRA1 and VPS34, for which phenotypes have not been investigated further. Additionally, Beclin-1 was shown to be phosphorylated by death-associated protein kinase (DAPk) resulting in autophagy activation by reducing Beclin-1 interactions with Bcl-2 and Bcl-XL (Figure 8 E) (Zalckvar et al. 2009).
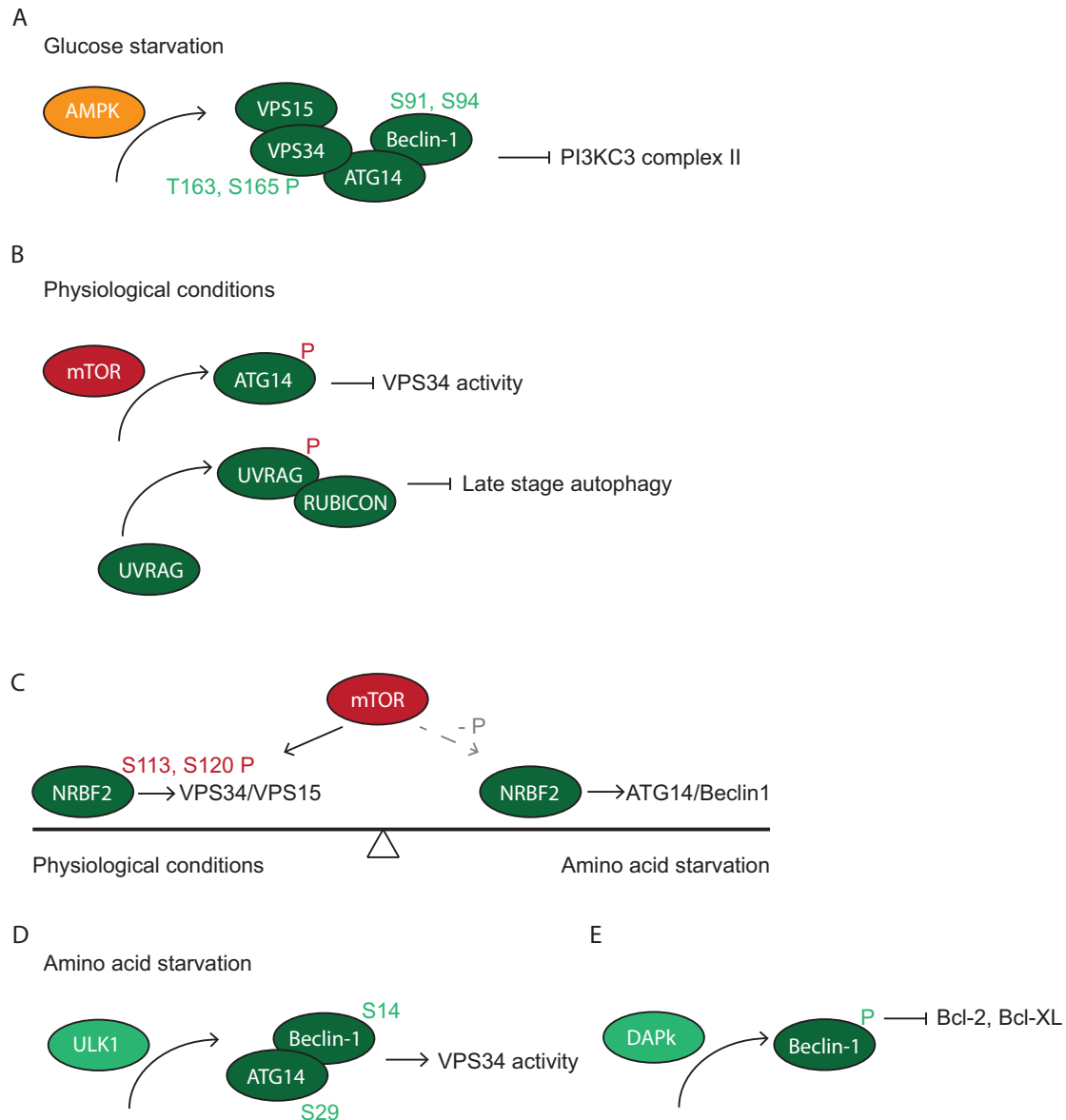
Figure 8: Schematic depiction of PI3KC3 complex regulation by autophagy-activating phosphorylation (P). A AMPK phosphorylates both VPS34 and Beclin-1, thereby favoring pro-autophagic complex I formation. **B** mTOR phosphorylates ATG14 and UVRAG, inhibiting VPS34 activity, and interaction with the HOPS complex, respectively. **C** mTOR phosphorylates NRBF2 under physiological conditions, favoring association with VPS34 and VPS15. Upon amino acid starvation and loss of inhibiting phosphorylation, NRBF2 preferentially forms a complex with pro-autophagic ATG14 and Beclin-1. **D** ULK1 phosphorylates both ATG14 and Beclin-1, leading to increased VPS34 activity. **E** Beclin-1 is phosphorylated by DAPk leading to decreased association with autophagy-inhibiting Bcl-2 and Bcl-XL.

Beclin-1 phosphorylation is also mediated by epidermal growth factor receptor (EGFR) at multiple tyrosines leading to a decreased Beclin-1-

dependent VPS34 activity by increasing interaction with autophagy inhibitors: Bcl-2 and RUBICON (Figure 9 A) (Wei et al. 2013). Beclin-1 is a reported substrate of Akt; another negative phosphorylation event resulting in increased Beclin-1 association with 14-3-3 and vimentin, thereby autophagy inhibition (Figure 9 B) (Wang et al. 2012). Importantly, EGFR and Beclin-1, as well as Akt and Beclin-1 link, directly connect tumor progression and autophagy. VPS34 is phosphorylated by Cdk1/Cdk5 at T159/T668 and these sites were shown to decrease the interaction with Beclin-1 during mitosis, and reduce autophagy by a decreased lipid kinase activity, respectively (Figure 9 C) (Furuya et al. 2010).
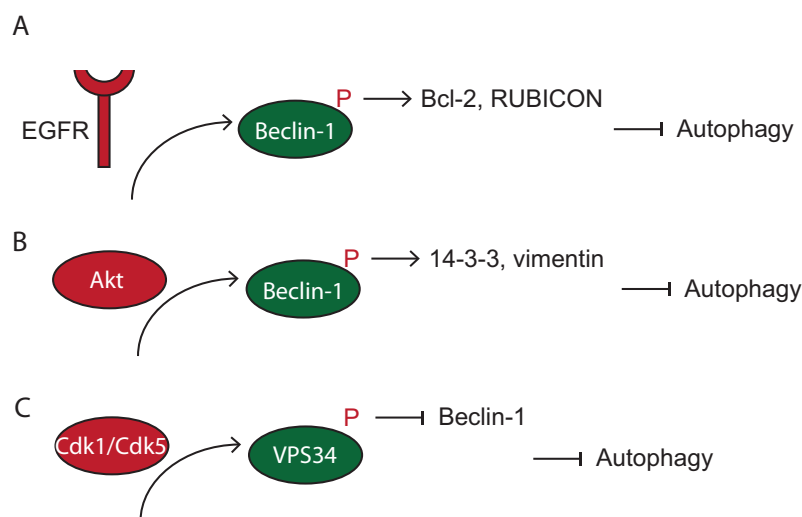
Figure 9: Schematic depiction of PI3KC3 complex regulation by autophagy-inhibiting phosphorylation (P). A EGFR phosphorylates Beclin-1, thereby favoring interaction with autophagy-inhibiting Bcl-2 and RUBICON. **B** Akt phosphorylates Beclin-1, thereby favoring interaction with autophagy-inhibiting 14-3-3 proteins and vimentin. **C** VPS34 is phosphorylated by Cdk1/Cdk5 leading to decreased interaction with Beclin-1 and inhibiting autophagy.

Phosphorylation is intertwined with acetylation in autophagy regulation. Upon mTOR inactivation by hypoxia or glutamine starvation, acetyltransferase ARD1 loses mTOR-mediated inhibiting phosphorylation at S288 (Qian et al. 2017). Subsequently, ARD1 and PGK1 (Phosphoglycerate kinase 1) associate; ARD1 acetylates PGK1 at K388 that in turn phosphorylates Beclin-1 at S30 to induce autophagy (Figure 10 A) (Qian et al. 2017). Furthermore,

VPS34 is directly acetylated by acetyltransferase p300 at K29, K771, K781, and potentially at two more sites. Whereas K29 deacetylation enhances interaction with ATG14 in Beclin-1-dependent way for autophagy induction, K29 inhibits VPS34 lipid kinase activity by increasing interaction with RUBICON. K771 and adjacent K781 site disrupt interaction with lipid kinase substrates, thereby inhibiting VPS34 activity (Figure 10 B). Taken together, deacetylation of VPS34 is required for canonical and non-canonical autophagy (bypasses upstream kinases).
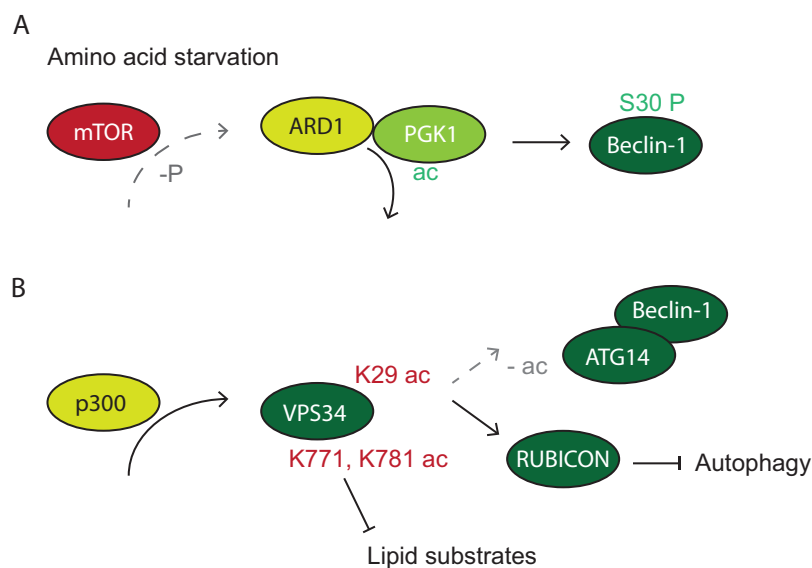
Figure 10: Schematic depiction of PI3KC3 complex regulation by acetylation (ac). A Amino acid starvation leads to mTOR inhibition thereby loss of mTOR-mediated ARD1 phosphorylation. ARD1 associates with PGK1 and acetylates it. Activated PGK1 then phosphorylates Beclin-1 enhancing autophagy. **B** p300 acetylates VPS34 at multiple sites. K29 acetylation leads to association with RUBICON and autophagy inhibition. Deacetylation at K29 is needed for association with ATG14 and Beclin-1. In parallel, acetylation at two adjacent sites K771 and K781 prevents association with VPS34 lipid substrates, thereby inhibiting autophagy.

1.2.3.2 Regulation of PI3KC3 complex by ubiquitin and ubiquitin-like proteins

PI3KC3 complex is regulated by ubiquitination and SUMOylation, in addition to phosphorylation and acetylation discussed in the previous section. Most well described complex component in this context is Beclin-1. Beclin-1 was

shown to be ubiquitinated at K117 by TRAF6 (tumor necrosis factor receptor (TNFR)-associated factor 6) in macrophages as a response to Toll-like receptor 4 (TLR4) stimulation with lipopolysaccharide and this K63 polyubiquitination is reversed by deubiquitinating enzyme A20 (Figure 11 A) (Shi and Kehrl 2010). Interestingly, this ubiquitination likely promotes Beclin-1 oligomerisation, as Beclin-1 has ubiquitin binding domains preferentially binding K63-linked ubiquitin chains, and leads to increase in VPS34 lipid kinase activity, thereby amplifies autophagy stimulation which is counteracted by A20 deubiquitination (Shi and Kehrl 2010). TRAF6 and A20 activity in context of Beclin-1 is analogous to their role in NF-κB signaling. Additionally, E3 ligase TRIM59 negatively regulates Beclin-1 levels on transcriptional level through negative regulation of NF-κB pathway (Figure 11 B) (Han et al. 2018). Interestingly, it also regulates K63-linked ubiquitination status of Beclin-1 by promoting K48-linked ubiquitination of TRAF6 leading to its degradation (Figure 11 B) (Han et al. 2018). Together, loss of TRIM59 leads to less TRAF6 targeting and more TRAF6-mediated Beclin-1 ubiquitination, therefore autophagy stimulation. USP19 is another DUB found to link the immune response and autophagy by removing K11-linked ubiquitin chains from K437 on Beclin-1 leading to its stabilization, therefore positively regulating autophagy, but negatively regulating type I interferon (IFN) signaling (Figure 11 C) (Jin et al. 2016; Cui, Jin, and Wang 2016). Contradictory, another report found that K63-linked polyubiquitin is attached to K437 of Beclin-1, and that this ubiquitin signal does not lead to destabilization of Beclin-1, but is required for autophagy induction (Xia et al. 2013). K63-linked ubiquitinated of Beclin-1 K437 is found to enhance VPS34 activity and it is mediated by E3 ligase AMBRA1, but inhibited by competitive binding of WASH (Wiskott-Aldrich syndrome protein (WASP) and SCAR homologue) and Beclin-1 (Figure 11 C) (Xia et al. 2013). Interestingly, majority of experiments in both papers were conducted in HeLa cells, hence cell line specificity in an unlikely explanation. E3 ligase RNF216 was shown to attach K48-linked ubiquitin chains on Beclin-1 that promote proteasomal degradation and inhibit autophagy in macrophages (Figure 11 D) (Xu et al. 2014). Furthermore, E3 ligase Nedd4 (neural-precursor-cell-expressed developmentally down-regulated protein 4) mediates K11- and K63-linked

ubiquitination of Beclin-1, wherein K11-linked chains regulates Beclin-1 stability (Figure 11 E) (Platta et al. 2012). Nedd4 was further found to regulate VPS34 stability by reversing K48 degradation signal on K419 of VPS34 by recruiting USP13 to cleave it, leading to VPS34 stabilization and autophagy induction (Figure 11 F) (Xie, Jin, and Cui 2020). Two more DUBs were linked to regulation of autophagy via stabilizing Beclin-1: USP10 and aforementioned USP13 by identifying a small-molecule inhibitor spautin-1 (specific and potent autophagy inhibitor-) (Figure 11 G) (Liu et al. 2011). Unexpectedly, in turn, VPS34 and Beclin-1 also regulate the stability of USP10 and USP13 (Liu et al. 2011). Considering USP10 regulates p53, and is regulated itself by USP13, this paper establishes the link between USP10 and USP13 inhibition, PI3KC3 complex, and p53 stabilization (Liu et al. 2011).
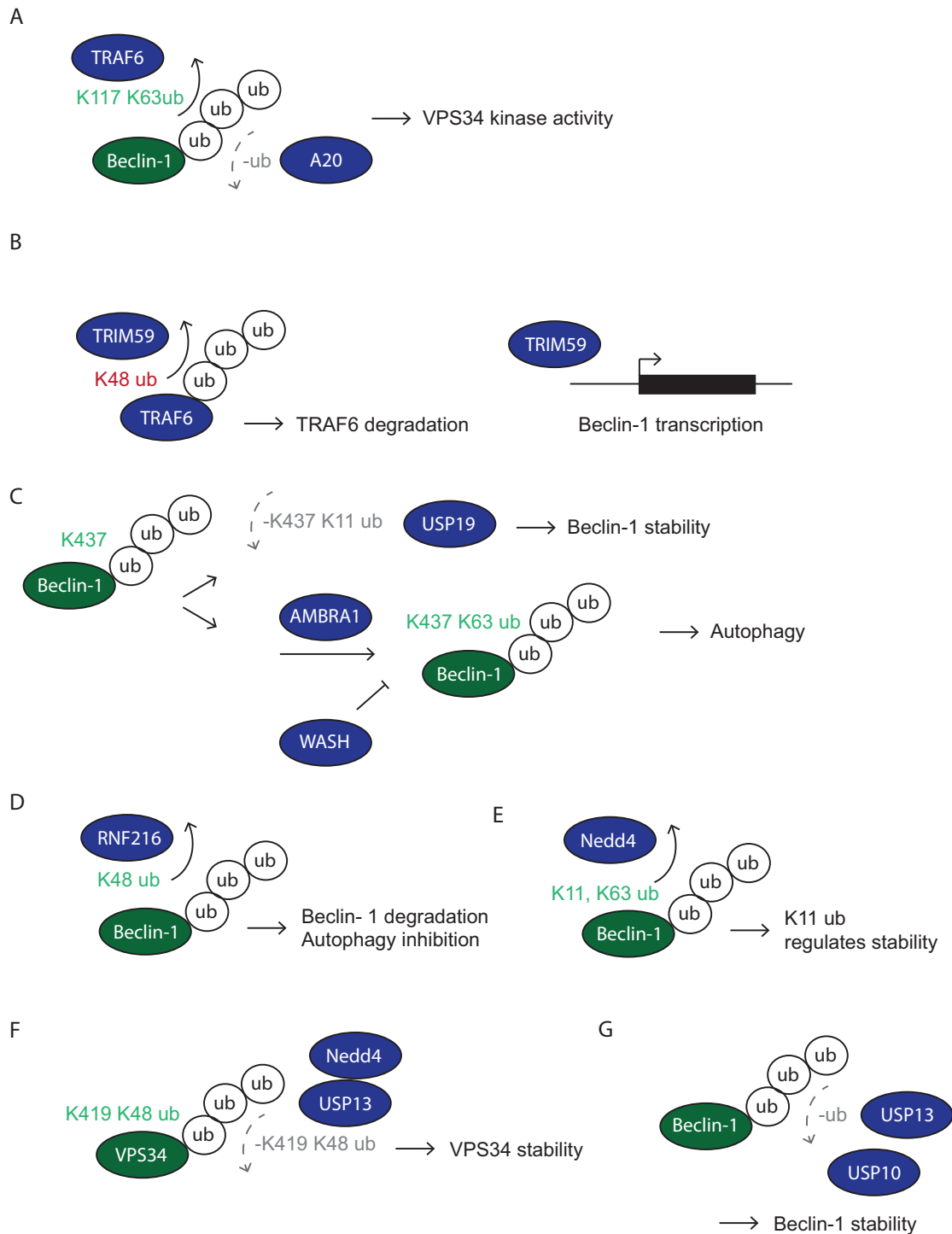
Figure 11: Schematic depiction of PI3KC3 complex regulation by ubiquitination. A TRAF6-mediated K63 ubiquitination is counteracted by deubiquitinase A20. K117 K63 ubiquitination stimulates VPS34 activity. **B** TRIM59 regulates Beclin-1 in two ways: in regulates Beclin-1 transcription, and regulates TRAF6 stability, thereby modulating K63 ubiquitination of Beclin-1. **C** K437 site on Beclin-1 was shown to be the site of both K11 and K63 ubiquitination. Whereas K11 removal by USP19 leads to Beclin-1 stabilization, K63 ubiquitin chain deposition by AMBRA1 was shown to have a positive effect on autophagy. **D** E3 ligase RNF216 targets Beclin-1 for degradation via K48 ubiquitination. **E** E3 ligase Nedd4

regulates Beclin-1 stability via K11 chains. **F** Nedd4 recruits USP13 to deubiquitinate VPS34 leading to VPS34 stability. **G** USP10 and USP13 both regulate stability of Beclin-1.

One complex component of more transient nature is aforementioned E3 ligase AMBRA1. Besides noted roles in positive ULK1 regulation and release of PI3KC3 complex from the dynein (Nazio et al. 2013; Di Bartolomeo et al. 2010), AMBRA1 plays a role in regulation of autophagy duration (Antonioli et al. 2014). Under physiological conditions, DDB1/Cul4 (DNA damage-binding protein 1/Culin-4) interacts with AMBRA1 and restricts its protein levels. Under autophagy induction Cul4 dissociates from AMBRA1, AMBRA1 associates with ElonginB/Cul5 (Culin-5) leading to Cul5-dependent DEPTOR stabilization, thereby inhibiting mTOR for autophagy induction (Antonioli et al. 2014). Dissociation of Cul4 and AMBRA1 is only transient, with their re-association and AMBRA1 level restriction reestablished, autophagy is terminated (Antonioli et al. 2014). Additionally, this paper is a source of information of AMBRA1-interacting Cullins, adaptors and substrate receptors identified by mass spectrometry, many of which have reported roles in autophagy discussed elsewhere. Cul4 is not the only E3 ligase reported to regulate AMBRA1 levels. RNF2 (also called RING1B) associates with PI3KC3 complex during autophagy and targets AMBRA1 for proteasomal degradation by catalyzing K48 chains at K45 of AMBRA1 (Xia et al. 2014). Moreover, they reported it is WASH that recruits RNF2 to target AMBRA1 for degradation (Xia et al. 2014). It their previous study, they showed WASH inhibits AMBRA-mediated Beclin-1 K63 ubiquitination shown to enhance autophagy, meaning negative regulation of autophagy by WASH is double layered; inhibiting Beclin-1 non-proteolytical ubiquitination and targeting AMBRA1 for degradation (Xia et al. 2013; 2014). Cul4 and Cul5 are not the only Cullins regulating autophagy duration. KLHL20/Cul3 ubiquitinates and targets ULK1 for degradation after ULK1 activation by auto-phosphorylation, thereby limiting positive ULK1 effect on autophagy induction, additionally enhanced by destabilizing ATG13 (Liu et al. 2016). Furthermore, KLHL20/Cul3 also regulate stability of the PI3KC3 complex adding another regulatory layer of autophagy termination (Liu et al. 2016). KLHL20 directly

interacts with Beclin-1 and VPS34 upon prolonged starvation at the phagophore and leads to downregulation of their protein levels. ATG14 levels were accordingly reduced as well, however, it was an secondary effect (Liu et al. 2016).

In addition to ubiquitination as both proteolytical and non-proteolytical signal mediating stability of complex components or association and interaction, respectively, SUMOylation also plays a role in PI3KC3 complex. KAP1 (KRAB-ZFP-associated protein 1) mediates SUMOylation on K840 of VPS34, thereby increasing its activity (Yang et al. 2013). Interestingly, this SUMOylation event is mediated by acetylated hsp70 (heat shock protein 70) that also interacts with VPS34 and Beclin-1, once again implying important role of acetylation in autophagy induction (Yang et al. 2013).

1.3 Aims of the study

Aim of this project was to investigate how autophagy is regulated by the ubiquitin system. Ubiquitination plays a critical role both through regulating the stability of upstream regulators or components of the autophagic machinery, and via facilitating the recruitment of cargo to autophagy receptors. As such, modulators of ubiquitin signaling can influence autophagy, and several deubiquitinating enzymes (DUBs) have already been shown to control the dynamics of autophagic substrate degradation. The presented work aimed to further study DUBs in this context, the project was hypothesis driven, proteomics data suggested a role for USP11 (and thus USP11-regulated ubiquitin signals) in autophagy regulation based on identifying USP11 at multiple points within the autophagy interaction network. Objectives were: confirm that USP11 controls autophagy flux, investigate how conserved its role in autophagy is (by using a model organism), reveal its molecular mechanism of action by identifying relevant USP11 substrates to ultimately pinpoint the autophagy-relevant ubiquitin signal that USP11 regulates, terminates, or edits.

2 Results

2.1 Establishing the tools to study USP11 effect on autophagy

2.1.1 Targeting USP11 by CRISPR/Cas9 and RNA interference

In order to investigate the effect USP11 has on autophagy, various cell lines were generated. First, CRISPR/Cas9 technology was employed to generate USP11 knockout (KO) cell lines in collaboration with Verena Bittl (Goethe University). Two parental cell lines were used: hTERT-immortalized retinal pigment epithelial (RPE1) and human bone osteosarcoma epithelial (U2OS) cell lines. As a control, non-human targeting (NHT) sequence was used in RPE1 cells. For technical reasons, only parental cells were used as a control in U2OS cells. Details are outlaid in the "Materials and Methods" section. A USP11-specific antibody was used to verify the knockout efficacy in each cell line (Figure 12 A). In addition, the western blot confirmed specificity of the USP11 antibody as no additional bands were detected. Moreover, the absence of a band at the expected height of USP11 (≈110 kDa) in both knockout cell lines was an additional proof of antibody specificity. Sufficient knockout, and appropriate NHT control supported usage of polyclonal RPE1 cell lines in further experiments.
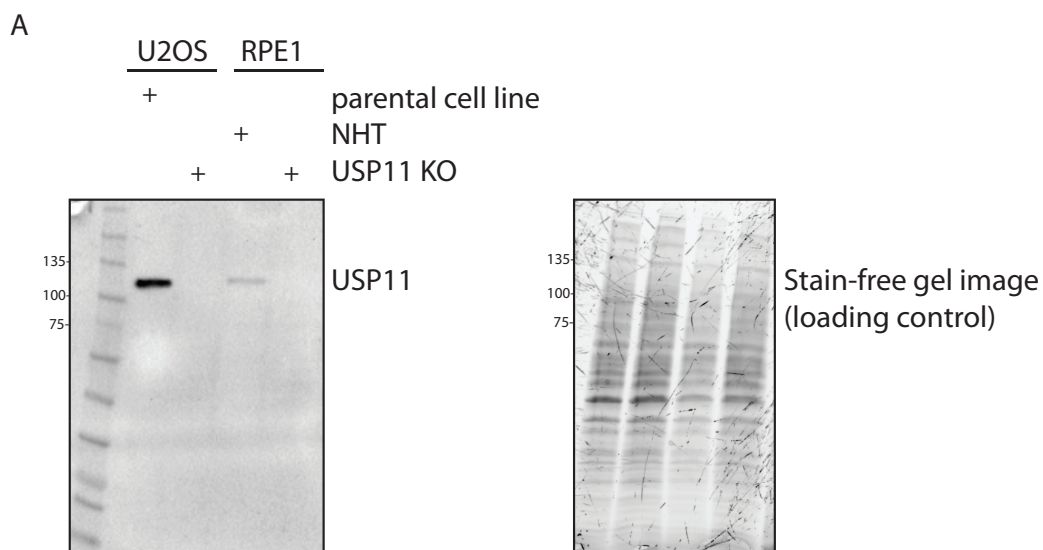
Figure 12: Generation of U2OS and RPE1 USP11 knockout cell lines using CRISPR/Cas9. A Western blot confirming USP11 knockout efficacy using a USP11-specific antibody.

The constitutive knockout cell lines have obvious advantages. To name a few: no additional transfection reagents are needed, experiments are conducted more efficiently, it is easy to scale up experiments etc. However, a major disadvantage is that cells can adapt to a depleted protein over time by having other proteins functionally compensating for the absent one. Therefore, it is necessary to use additional, short-term approaches to silence a gene.   As a complementary approach to having constitutive USP11 knockout cell lines, transient transfection of small interfering RNA (siRNA) was used. Four USP11 sequence-specific siRNAs were tested in U2OS cells (siUSP11#5-8), and compared to control siRNA (siCtrl). USP11 depletion was evaluated by western blot (Figure 13 A). For further experiments, siUSP11#6 and siUSP11#8 were used, based on their knockdown efficacy, and reproducibility.
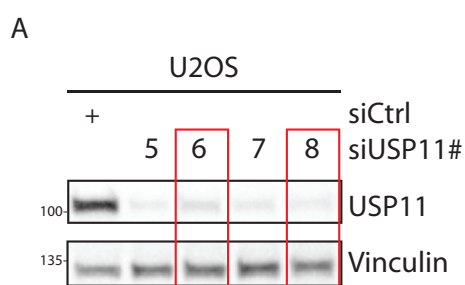
Figure 13: Verification of four USP11-sequence specific siRNAs in U2OS cells. A Western blot confirming siRNA-mediated USP11 knockdown efficacy using a USP11 specific antibody. Marked in red are siUSP11 sequences that were used for further experiments

2.1.2 Studying USP11 in context of autophagy

LC3 lipidation is commonly monitored by western blot to evaluate autophagic flux. It is possible to resolve unlipidated and lipidated LC3 species (LC3-I and LC3-II, respectively) by SDS-PAGE followed by a western blot as LC3-II runs

at a lower molecular weight (Klionsky et al. 2016). This conversion corresponds to autophagosome formation and can be further enriched by supplementation of cell medium with bafilomycin A1 (BafA1). BafA1 is a drug inhibiting the vacuolar-type H(+)-ATPase leading to the inhibition of lysosomal acidification and subsequent degradation of the content, LC3 and cargo, therefore leading to their accumulation (Yoshimori et al. 1991). Importantly, when evaluating the effect of a protein depletion on the autophagic flux, lower LC3-II levels can correspond to less autophagy induction, or on the contrary, faster autophagic flux leading to a faster clearance of LC3-II. Therefore, to differentiate between the two, a BafA1-treated sample is necessary. If addition of BafA1 has no effect on increasing the LC3-II levels, the defect is in the early stages of autophagy induction, whereas if it results in a significant increase, the lower levels of LC3-II were a result of a faster flux. The disadvantage of using LC3-II lipidation as the autophagic flux readout is that it is an accumulation of the total LC3 levels from the whole cell population which is often heterogeneous. Meaning, it is not possible to conclude if the levels observed on a western blot are a result of an equal contribution of all cells, or if it is reflecting a minor cell population contributing to a significant phenotype, masking a mild phenotype of the majority. Hence, flow cytometry-based approaches are often used. Flow cytometry provides readout for each cell of a population giving an insight in the behavior of the entire cell population. For this, cell lines harboring fluorescently tagged LC3 can be used. Precisely, two different LC3 probes were used: the GFP-LC3-RFP and the GFP-LC3-RFP-LC3ΔG (Kaizuka et al. 2016). Both probes are processed by the endogenous protease ATG4, the same way as the endogenous LC3 (Kirisako et al. 2000), resulting in 1:1 ratios of GFP-LC3 and RFP, or GFP-LC3 and RFP-LC3ΔG, respectively. GFP-LC3 can be lipidated and incorporated in the autophagosomal membrane and degraded (or recycled), identically to the endogenous LC3. In parallel, RFP or RFP-LC3ΔG stays in the cytoplasm and serves as an internal control. Without the C-terminal glycine, RFP-LC3ΔG cannot be lipidated and embedded in the autophagosomal membrane. Upon autophagy induction, loss of GFP fluorescence due to utilization by the autophagy machinery can be monitored as a direct readout of autophagic flux, and compared to RFP fluorescence

that stays constant. The higher the flux, the lower GFP/RFP ratio is expected. Conversely, the lower the flux, the higher GFP/RFP ratio is expected. With this in mind, RPE1 NHT control and constitutive USP11 knockout cells were virally transduced with GFP-LC3-RFP-LC3ΔG probe. Subsequently, single clones were selected for each cell line using fluorescent-assisted cell sorting (FACS). Four single clones (SC) were tested for NHT and five for USP11 knockout cell line (Figure 14 A, B). SC1 of the NHT and SC2 of the USP11 knockout cells were selected for further experiments based on the three following criteria: verification that they were indeed single clones, the physical properties of each cell population evaluated by the forward and side scatter were highly similar, and the ratio of GFP/RFP under basal conditions was the same for both cell lines, approximating to 1. Additionally, to be able to use siRNA as a complementary method to deplete USP11, RPE1 SC cell line expressing the GFP-LC3-RFP probe was kindly provided by Paolo Grumati (former Goethe University, current The Telethon Institute of Genetics and Medicine).
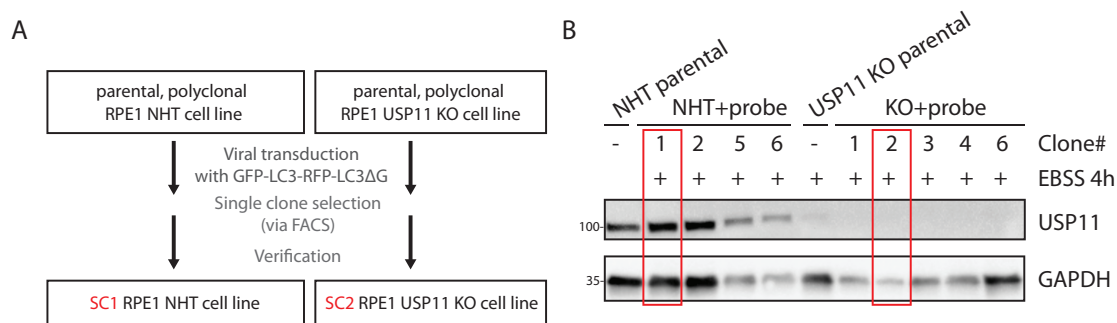
Figure 14: Flow cytometry approach to study autophagy requires generation of cell lines harboring fluorescently labeled LC3. A Strategy depicting the generation of the NHT and the USP11 KO single clone cell lines containing the GFP-LC3-RFP-LC3ΔG probe. **B** Western blot showing USP11 levels in the single clone selection process. Marked in red are SC1 of the NHT control, and SC2 of the USP11 KO cell line, that were used for further experiments.

2.2   USP11 negatively regulates the autophagic flux in human cells

To establish whether USP11 has an effect on the autophagic flux, two flow cytometry-based approaches were utilized using cell lines harboring fluorescently labeled LC3 introduced in the previous section. Autophagy was induced by amino acid starvation using Earle's Balanced Salt Solution (EBSS) for 4 hours and fluorescence ratio of GFP/RFP was monitored and quantified (Figure 15 A). Measured GFP/RFP ratio in the USP11 constitutive knockout SC2 cell line revealed an average 2.06 fold increase in the autophagic flux after 4 hours of EBSS treatment compared to the NHT SC1 control (Figure 15 B) (p-value < 0.001, 2way ANOVA, and Bonferroni posttest).
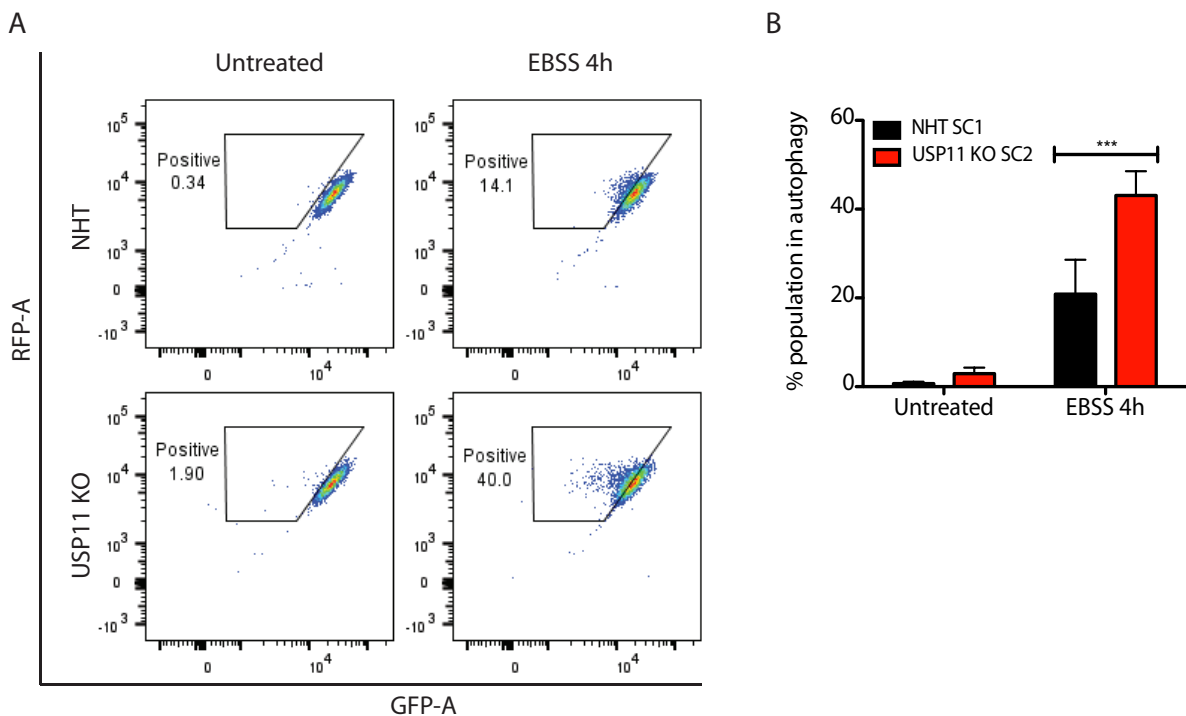
Figure 15: The RPE1 USP11 knockout cells expressing the GFP-LC3-RFP-LC3ΔG probe showed an increase in the autophagic flux compared to the NHT control cells expressing the same probe after 4 hours of EBSS treatment based on GFP/RFP ratio. A Scatter plots depicting the NHT SC1 control, and the USP11 SC2 knockout cell populations under physiological, as well as under 4 hour EBSS treatment. The cells with stably depleted USP11 exhibit striking decrease in GFP/RFP ratio upon starvation, indicative of a higher autophagic flux. **B** Quantification of the autophagy-positive cells based on the gates shown in figure A revealed statistically significant increase in the USP11 knockout cells compared to the NHT control cells (p-value < 0.001, 2way ANOVA, and Bonferroni posttest, N=3).

To verify the effect by a complementary USP11 depletion method, transient transfection of siRNA was used in the RPE1 SC cell line stably expressing the GFP-LC3-RFP probe (Figure 16 A). Loss of USP11 mediated by two distinct siRNAs (siRNA#6 and siRNA#8) compared to the control siRNA (siCtrl) led to an average of 1.23, and 1.27 fold increase, respectively, after 4 hours of EBSS treatment (Figure 16 B) (p-value < 0.01 for siRNA#6, p-value < 0.001 for siRNA#8, 2way ANOVA, and Bonferroni posttest). USP11 depletion was verified after each experiment by the cell lysis of leftover cells, SDS-PAGE, followed by a western blot (Figure 16 C). The reason for the difference in autophagic capacity, and the smaller fold increases between two experimental approaches likely resides in the fact that transient transfection of cells with siRNA is itself a stress-inducing treatment (p-value < 0.05 for untreated condition, and p-value < 0.001 for EBSS 4 h, 2way ANOVA, and Bonferroni posttest). This is reflected in the increased values for autophagy-positive cells observed already under basal conditions, hence further stress induced by starvation potentially limits the capacity of cells to respond (Figure 16 D).
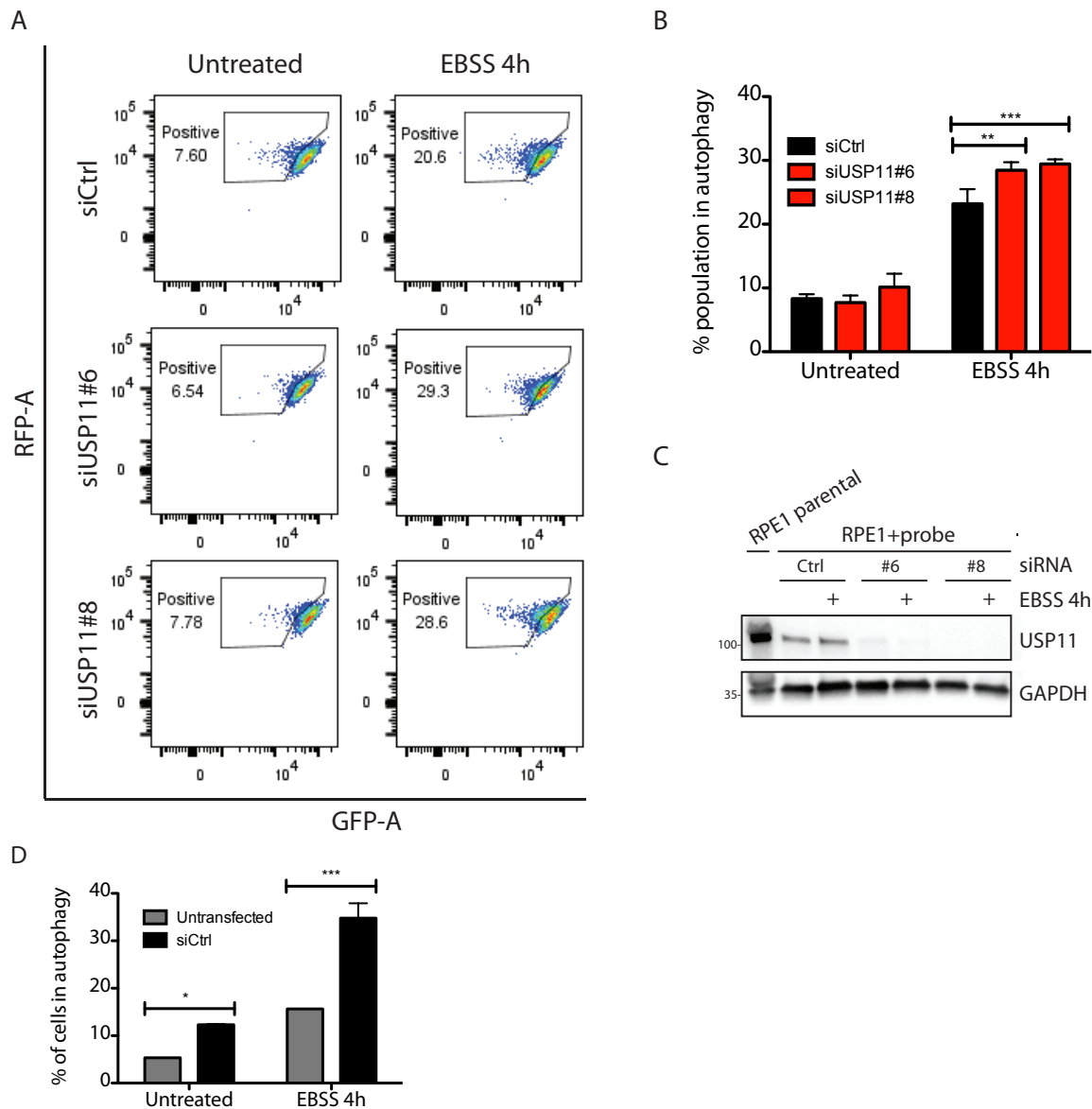
Figure 16: The siRNA-mediated USP11 knockdown led to an increase in the autophagic flux in the RPE1 cells expressing the GFP-LC3-RFP probe compared to the control siRNA after 4 hour EBSS treatment based on the GFP/RFP ratio. A Scatter plots depicting the control siRNA, and the siUSP11#6 and siUSP11#8 knockdown cell populations under physiological, as well as under 4 hour EBSS treatment. Transient loss of USP11 led to a notable decrease in GFP/RFP ratio, indicative of higher autophagic flux. **B** Quantification of the autophagy-positive cells based on the gates shown in A revealed statistically significant increase in the USP11 knockdown cells compared to the control siRNA cells (p-value < 0.01 for siRNA#6, p-value < 0.001 for siRNA#8, 2way ANOVA, and Bonferroni posttest, N=3). **C** A representative western blot validating USP11 depletion in the samples used for flow cytometry. **D** Quantification of the autophagy-positive RPE1 cells expressing the GFP-LC3-RFP probe transfected with the control siRNA compared to the same, but untransfected cell line, revealed a striking increase in the autophagic flux in the transfected cells. This suggested that the transfection is a stress- and autophagy-inducing process (p-value < 0.05 for untreated condition, and p-value < 0.001 for EBSS 4h, 2way ANOVA, and Bonferroni posttest, N=2).

In order to increase temporal resolution of USP11-dependent autophagy phenotype, time course flux analyses were performed. In the first approach, live-cell imaging system IncuCyte® was used, which automatically acquires images over a defined period of time. For this, the autophagy probe-expressing cells were used in an experiment performed together with Mariana Tellechea and Alexandra Stolz (Goethe University). From obtained images, the average GFP/RFP ratio is calculated for each time point (Figure 17 A). As previously described, GFP/RFP ratio is a direct readout of the autophagic flux. To this end, triplicate wells containing either the NHT SC1 or the USP11 knockout SC2 (both expressing the GFP-LC3-RFP-LC3ΔG probe) or the RPE1 SC cell line (stably expressing the GFP-LC3-RFP probe) were seeded. Autophagy was induced for 24 hours using 250 nM Torin1, an mTOR inhibitor (Liu et al. 2010). To enable comparison, initial values were normalized to 1 at time point 1 hour for each cell line. Importantly, no statistically significant difference was observed between the RPE1 NHT SC1 cells and the RPE1 SC cell line stably expressing the LC3 probe at any time point (2way ANOVA, and Bonferroni posttest), justifying their use as the control cell line for the USP11 knockout cell line. As expected, comparing the autophagic flux in the RPE1 NHT SC1 control and the USP11 KO SC2 revealed statistically significant difference for time points 13 to 24 (Figure 17 B) (p-value < 0.01 for time points 18 and 21, p-value < 0.05 for all others, 2way ANOVA, and Bonferroni posttest).
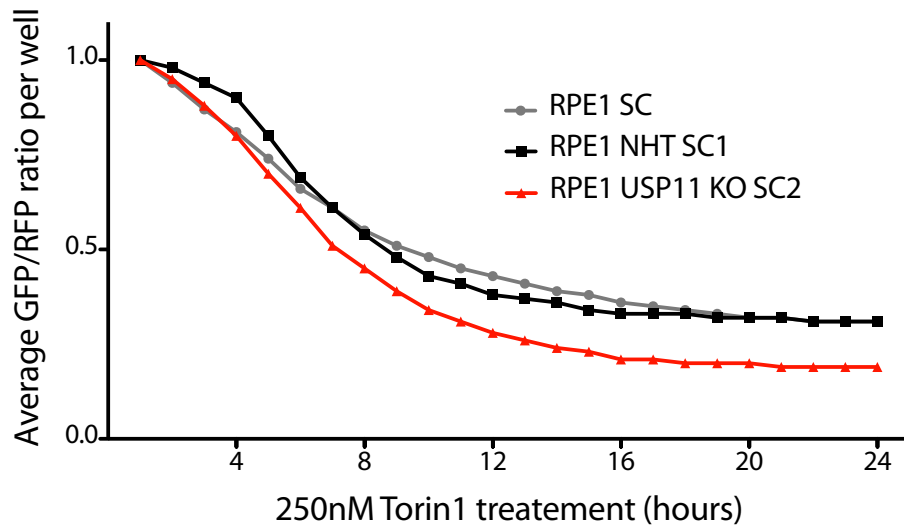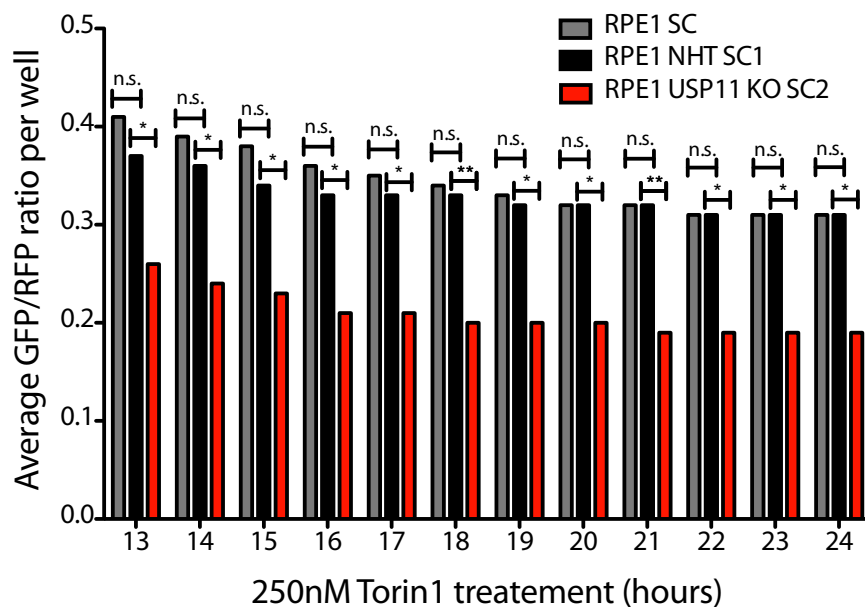
Figure 17: The stable RPE1 USP11 SC2 knockout cell line expressing the GFP-LC3-RFP-LC3ΔG probe showed an increase in the autophagic flux compared to the NHT SC1 control cells assessed by live cell imaging over the course of 24 hour treatment with 250 nM Torin1. A Average GFP/RFP ratio plotted over time (in hours) of 250 nM Torin1 treatment, in triplicate wells, revealed long-term increase in the autophagic flux upon loss of USP11. **B** Quantification of time points 13 to 24 h based on the GFP/RFP ratio revealed statistical significance between the RPE1 NHT SC1 and the USP11 KO SC2 cells (p-value < 0.01 for time points 18 and 21, p-value < 0.05 for all others, 2way ANOVA, and Bonferroni posttest, tN=3), and no statistically significant difference between the RPE1 NHT control SC1 cells and the RPE1 SC cells expressing the LC3 probe, as expected (2way ANOVA, and Bonferroni posttest).

In the second approach to establish the effect loss of USP11 has in cell culture with increased temporal resolution, LC3 lipidation was monitored. Here, autophagy was induced in the RPE1 NHT and the USP11 knockout cells with EBSS for 2, 4, and 6 hours, with an additional 6 hour time point supplementation with BafA1, or Mg132. Mg132 inhibits proteasomal degradation and served as a negative control for the LC3-II accumulation. Given that the aim of the experiment was to address the effect of USP11 depletion on the autophagic flux, and not on potential transcriptional or translational regulation, EBSS medium was supplemented with cycloheximide (CHX). Addition of CHX enables avoidance of the potential contribution of newly synthesized LC3, thereby limiting the cells to utilize only their current, intracellular LC3 pool. Protein p53, a well-studied, short-lived protein served as a control for the CHX efficacy (Vousden and Lane 2007). As expected, the LC3-II levels were significantly enriched in the USP11 knockout cells compared to the NHT control after 6 hours of autophagy induction and BafA1-induced autophagosome accumulation (Figure 18 A). Complementary, a qPCR analysis of the LC3B mRNA normalized to GAPDH mRNA level showed that USP11 does not regulate LC3B transcription under basal conditions, nor after 4 hours of EBSS-induced autophagy (Figure 18 B) (2way ANOVA, and Bonferroni posttest).
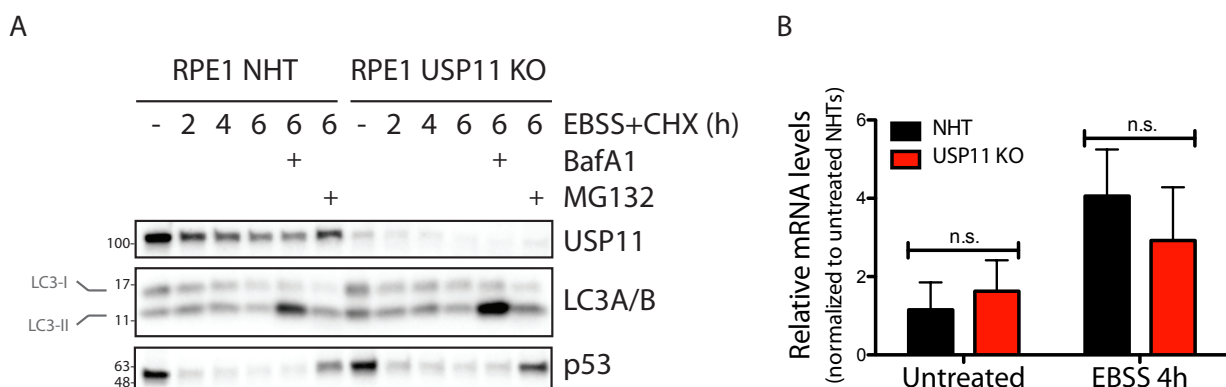
Figure 18: The RPE1 USP11 knockout cells displayed an increase in the autophagic flux compared to the NHT control cells, assessed by LC3-II levels after 6 hour EBSS and BafA1 treatment. A Western blot showing a time course analysis of EBSS-induced autophagy and CHX-mediated translational inhibition in the constitutive USP11 knockout cell

line compared to the NHT control. The LC3-II levels were significantly increased in the USP11 knockout cells compared to the control cells after 6 hour EBSS and BafA1 treatment. Protein p53 served as a CHX control, and Mg132 treatment served as a negative control for the LC3-II accumulation (N=3). **B** Quantification of the LC3B mRNA levels obtained by qPCR normalized to GAPDH revealed no significant difference between the NHT and the USP11 knockout cell lines (2way ANOVA, and Bonferroni posttest, tN=2, N=2).

Considering that the loss of USP11 led to an increase in the autophagic flux, the next question was if the overexpression of USP11 led to a decrease in the flux. To test this, GFP-tagged USP11 was transiently overexpressed in U2OS cells and the LC3 lipidation was monitored by western blot. Two controls were used: the untransfected control and the GFP only control. The untransfected control served to elucidate the contribution of transfection as a stress- and autophagy-inducing treatment and the GFP control served to demonstrate that the tag alone had no effect on autophagy. Autophagy was induced with EBSS for 1 to 4 hours and LC3 accumulation was induced with autophagosome-lysosome fusion inhibitor chloroquine (CQ) (Mauthe et al. 2018), instead of BafA1. Importantly, the overexpression of USP11 led to a decrease in the autophagic flux assessed by the LC3-II accumulation compared to both the untransfected and the GFP control (Figure 19 A). This experiment provided an additional confirmation that the transfection itself requires a control for a comprehensible understanding of an autophagy-related phenotype judging by a significant reduction in the LC3-II in the GFP control sample compared to the untransfected control indicating that autophagy was induced by transfection alone. In general, the interpretation of overexpression data calls for caution given that the transient transfection can yield a heterogeneous cell population and this can easily be overlooked when analyzing western blots. Here, an overall reduction in the LC3-II levels is a strong indication that the observed phenotype is reflecting the whole population and is not an artifact. If the population was heterogeneous, reduction in the LC3-II levels would be masked by the high LC3-II levels of the untransfected cells and there would be no real difference visible on a western blot, which is not the case here. Comparing all three cell populations emphasizes the need for multiple controls, however, what is important is that

USP11 overexpression has a clearly negative effect on the LC3 lipidation regardless to which control it is compared to.

A
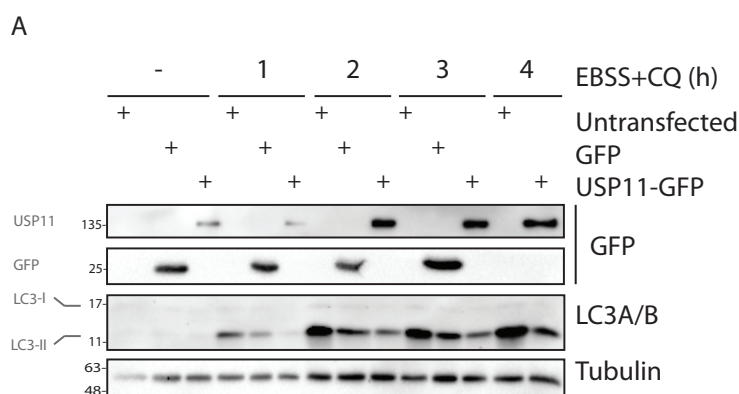
Figure 19: Transient overexpression of USP11 led to a decrease in the autophagic flux in U2OS cells compared to untransfected and GFP only control assessed by LC3-II accumulation. A Western blot showing a time course analysis of EBSS-induced autophagy for 1 to 4 hours and CQ-induced autophagosome accumulation in the untransfected cells, the GFP, and the USP11-GFP overexpressed cells. The overexpression of USP11 had the opposite effect on the LC3 lipidation compared to USP11 depletion, based on less accumulated LC3-II compared to both control samples. Interestingly, the transfection of the GFP control led to less LC3-II accumulation compared to the untransfected control indicating that the GFP transfection itself induced autophagy.

Taken together, data obtained by using distinct USP11 depletion methods, USP11 overexpression, different readout methods, and various time points, demonstrated that USP11 negatively impacts the autophagic flux in human cells.

2.3   Loss of USP11 leads to an increase in the autophagic flux in *Caenorhabditis elegans*

In order to establish whether the USP11-dependent autophagy regulation is evolutionary conserved, the autophagic flux was investigated in the model organism *Caenorhabditis elegans (C. elegans)* in collaboration with Andreas Kern and Christian Behl (Mainz University). With this aim, *C. elegans* USP11 ortholog, H34C03.2, was depleted using siRNA in worm strain expressing

GFP-tagged LGG-1 (GFP::LGG-1). Empty vector (EV) was used as a knockdown control. After a control DMSO or a BafA1 treatment for 6 hours, the worms were lysed and the proteins resolved by SDS-PAGE and analyzed by western blot (Figure 20 A). As for human LC3 and GABARAP proteins, lipidation of *C. elegans* ortholog, the LGG-1, can be analyzed in the same manner. Loss of H34C03.2 resulted in significantly increased LGG-1 lipidation as per western blot quantification compared to the EV control, suggesting an increased basal autophagic flux (Figure 20 B) (p-value < 0.005, one sample t-test). H34C03.2 depletion efficacy was assessed using qPCR and revealed an average of 2.88 fold relative reduction, or an average of 65,3 % less mRNA levels normalized to the empty vector control (Figure 20 C) (p-value < 0.005, one sample t-test).
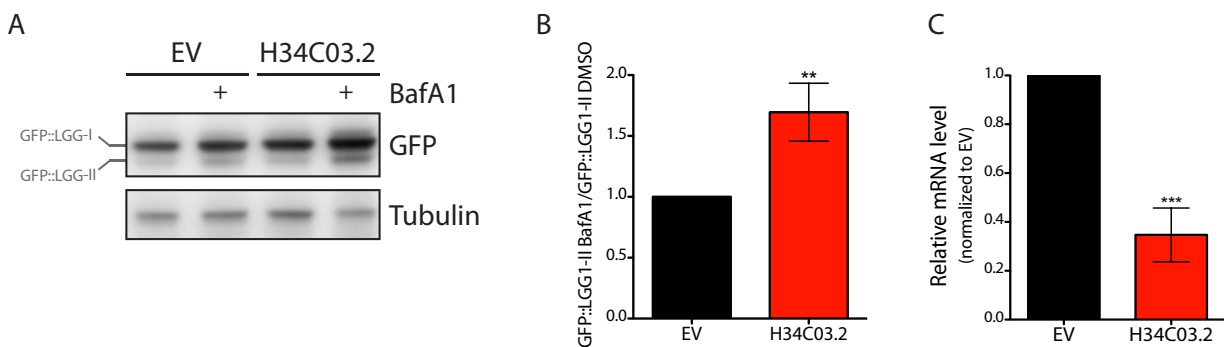
Figure 20: Knockdown of USP11 ortholog in *C. elegans*, H34C03.2, led to an increase in the basal autophagic flux compared to EV control, assessed by the GFP-LGG-1 lipidation after 6 hour BafA1 treatment. A Western blot showing an increase in the lipidated LGG-1 levels in H34C03.2 knockdown worms compared to EV control. **B** Quantification of the western blots revealed the increase is significant (p-value < 0.005, one sample t-test, N=5). **C** Depletion of H34C03.2 was assessed by qPCR. The quantification demonstrated statistically significant decrease in the H34C03.2 mRNA levels compared to the EV control (p-value < 0.005, one sample t-test, N=4).

As a complementary approach to evaluate the autophagic flux, the same treatments (DMSO control or BafA1 treatment for 6 hours) were used to analyze the worms expressing the GFP-tagged LGG-1 using confocal fluorescence microscopy. Image analysis revealed significantly more GFP-positive punctae in the H34C03.2 depleted worms compared to the EV control, indicating a higher autophagosome number (Figure 21 A).
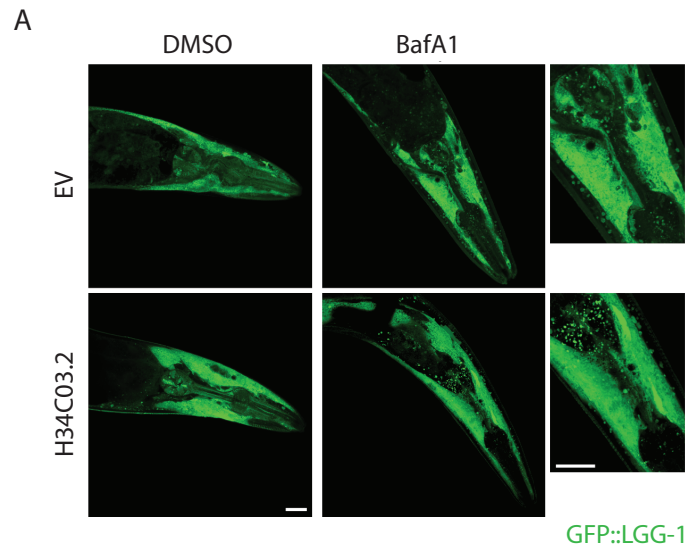
Figure 21: Knockdown of USP11 ortholog in *C. elegans*, H34C03.2, led to an increase in the GFP-LGG1 punctae compared to EV control, assessed by confocal laser scanning microscopy after 6 hour BafA1 treatment. A Microscopy images demonstrated an increase in the GFP-LGG1 punctae indicative of a higher autophagosome number in H34C03.2 knockdown worms compared to EV control (scale bar 50µm).

Importantly, to test if these findings translate to a physiologically relevant advantage, a *C. elegans* paralysis test was performed. For this purpose, the *C. elegans* CL2006 strain expressing the human β-amyloid protein 1-42 (hAβ42) under a muscle cell-specific promoter was used (Dostal and Link 2010). These worms develop a paralysis during the course of their adulthood as the accumulating aggregates overwhelm the proteasomal and autophagic quality control mechanisms in the muscle cells where the protein expresses. This phenotype can be monitored and quantified. Strikingly, H34C03.2 depletion led to a significantly delayed paralysis phenotype compared to the EV control at days 8 to 12 of adulthood pointing to a more productive autophagic process alleviating aggregation-induced paralysis (Figure 22 A, B) (p-value < 0.01 for day 8, p-value < 0.001 for days 9-12, 2way ANOVA, and Bonferroni posttest).
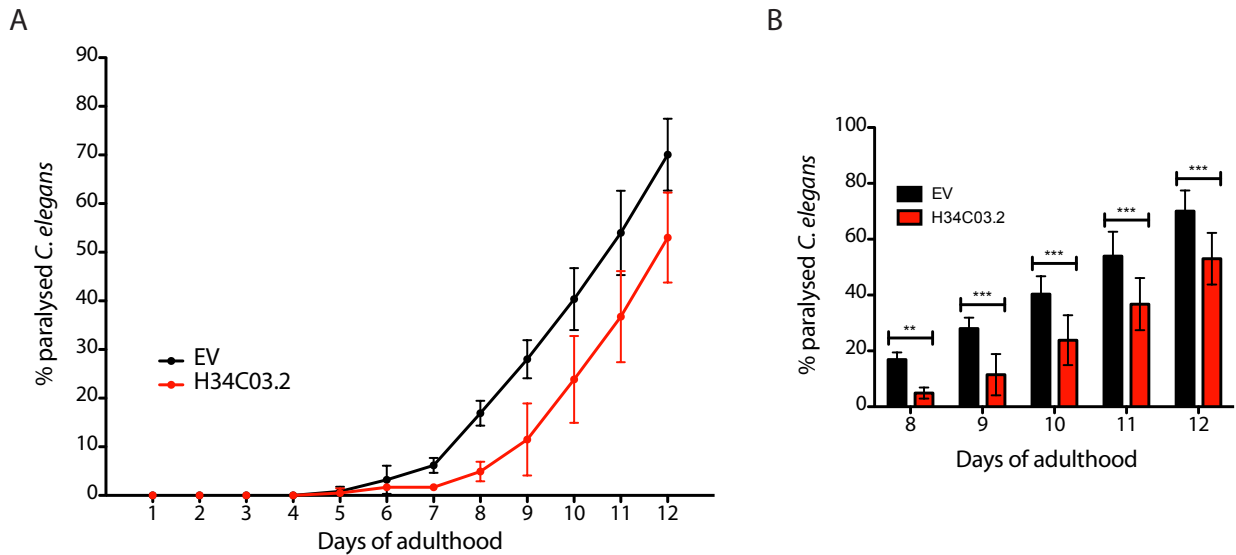
Figure 22: Knockdown of USP11 ortholog, H34C03.2, led to a delayed paralysis phenotype in the *C. elegans* strain expressing the human β-amyloid protein 1-42 (hAβ42) in the muscle cells compared to the EV control. A A paralysis test demonstrated a physiological advantage in the H34C03.2 knockdown worms compared to the EV control, pointing to a higher autophagic flux mitigating the toxicity induced by the increased protein aggregation. **B** Quantification of the days 8 to 12 of adulthood revealed the significance of the observed phenotype (p-value < 0.01 for day 8, p-value < 0.001 for days 9-12, 2way ANOVA, and Bonferroni posttest).

In summary, USP11-mediated autophagy regulation is mechanistically evolutionary conserved based on the reproducibility of the autophagy phenotype observed in human cell culture and *C. elegans*, underscoring the importance of USP11 as a novel autophagy regulator.

2.4 USP11 substrate identification and interactome determination points to multiple regulatory pathways

Understanding the mechanism of USP11-dependant autophagy regulation required substrate identification by a proteome-wide, unbiased experimental approach. To determine USP11 substrates, Stable Isotope Labeling with Amino acids in Cell culture (SILAC)-based mass spectrometry approach was used in collaboration with Thomas Juretschke and Petra Beli (Mainz University). In the SILAC approach, cells were grown in the medium

supplemented with non-radioactively labeled lysines and arginines (L and R, respectively). These amino acids are incorporated in proteins giving them a unique spectral signature enabling relative abundance quantification between different samples. Another feature of the SILAC approach is that the metabolic labeling allows early sample combining and minimizes the issues that arise from different sample handling. Here, the RPE1 NHT control cells were light labeled (K0, R0) and the USP11 knockout cells were heavy labeled (K8, R10) (incorporation test >95 %). On the day of the experiment, both cell lines were treated with EBSS for 4 hours prior to lysis. Cell lysates were combined and digested with LysC and trypsin leaving ubiquitinated proteins with a Gly-Gly remnant on lysine side chains that can be enriched with a Lys-ε-Gly-Gly (K-ε-GG) specific antibody (PTM Scan ubiquitin branch motif IAP beads). Detailed protocol can be found in "Materials and Methods" section and a schematic overview in Figure 23. Importantly, input samples are taken directly after the lysis. This allows the analysis of the whole cell proteome and allows quantification of the Gly-Gly enriched peptides in relative abundance between the cell lines, as well as normalized to the proteome of respective cell lines.

The results of the GlyGly site enrichment revealed few potential (direct) substrates (Figure 23 A), and similar was observed for the total cell proteome changes (Figure 24 A). None of the potential sites were of known USP11 substrates, nor substrates with known links to autophagy (Table 3). Similarly, the proteome analysis revealed almost no changes between the NHT control and the USP11 knockout after 4 hours of autophagy induction, however, one significant hit was found to have mildly increased levels in the USP11 knockouts; NRBF2 (Nuclear receptor-binding factor 2) (Figure 24 A, Table 4). NRBF2 is a subunit of the lipid kinase PI3KC3 complex that will be discussed in more detail in the further sections.
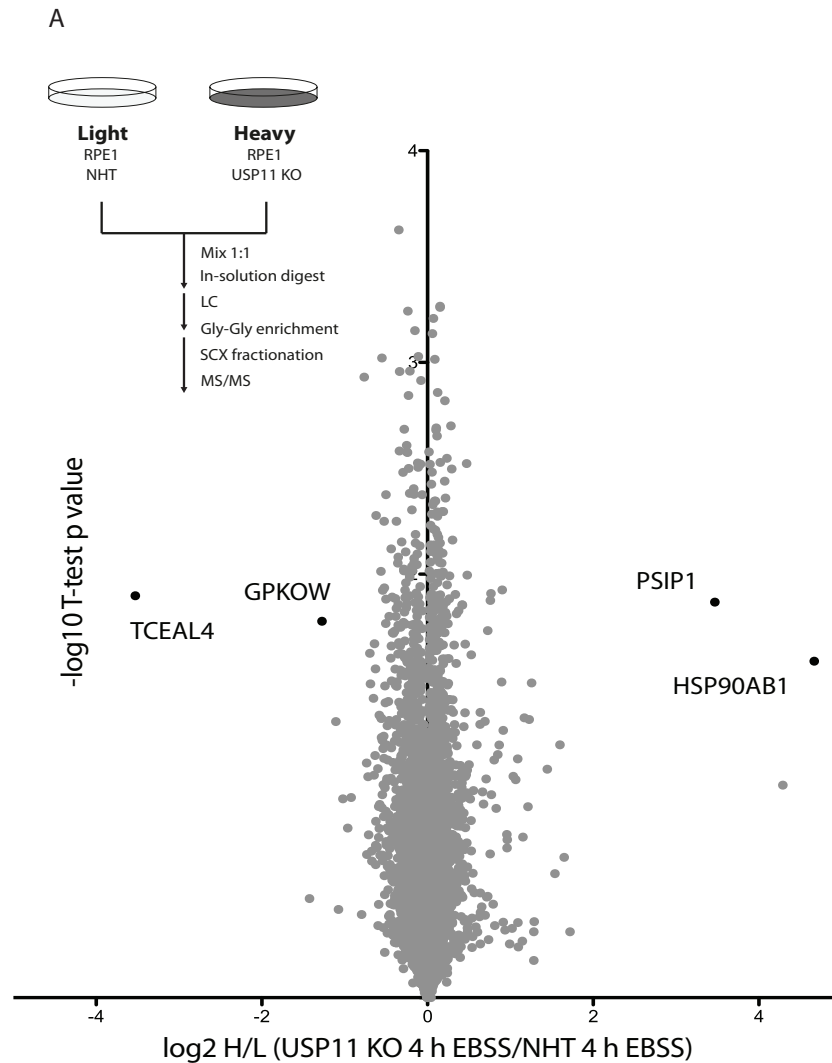
Figure 23: SILAC-based mass spectrometry approach to identify USP11 substrates after 4 hour EBSS treatment. A Volcano plot showing GlyGly site enrichment. On the left side are the sites that werere more abundant in the NHT control, and on the right, the ones more enriched in the USP11 knockouts (potential substrates). Schematic representation of the workflow is included in the figure.

Table 3: SILAC-based mass spectrometry approach led to identification of potential USP11 substrates based on changes in abundance of the GlyGly sites in the USP11 knockout cells after 4 hour EBSS treatment compared to the NHT control. A List of the most downregulated GlyGly sites in the USP11 knockout cells compared to the NHT control after 4 hour EBSS treatment. All labeled hits are significant (FDR<5 %). **B** List of most upregulated GlyGly sites in the USP11 knockout cells compared to the NHT control after 4 hour EBSS treatment, indicating they are potential substrates. All labeled hits are significant (FDR<5 %).

A

Most downregulated GlyGly peptides in USP11 knockout cells after 4 h EBSS treatment

TCEAL4	Transcription elongation factor A protein-like 4
GPKOW	G patch domain and KOW motifs-containing protein
PIN1;PIN1P1	Peptidyl-prolyl cis-trans isomerase NIMA-interacting 1;Putative PIN1-like protein
MINA	Bifunctional lysine-specific demethylase and histidyl-hydroxylase MINA

B

Most upregulated GlyGly peptides (potentially direct substrates) in USP11 knockout cells after 4 h EBSS treatment

HSP90AB1	Heat shock protein HSP 90-beta
PSIP1	PC4 and SFRS1-interacting protein
TMEM30A	Cell cycle control protein 50A
FAM199X	Protein FAM199X
HNRNPDL	Heterogeneous nuclear ribonucleoprotein D-like
SSSCA1	Sjoegren syndrome/scleroderma autoantigen 1
DHX9	ATP-dependent RNA helicase A
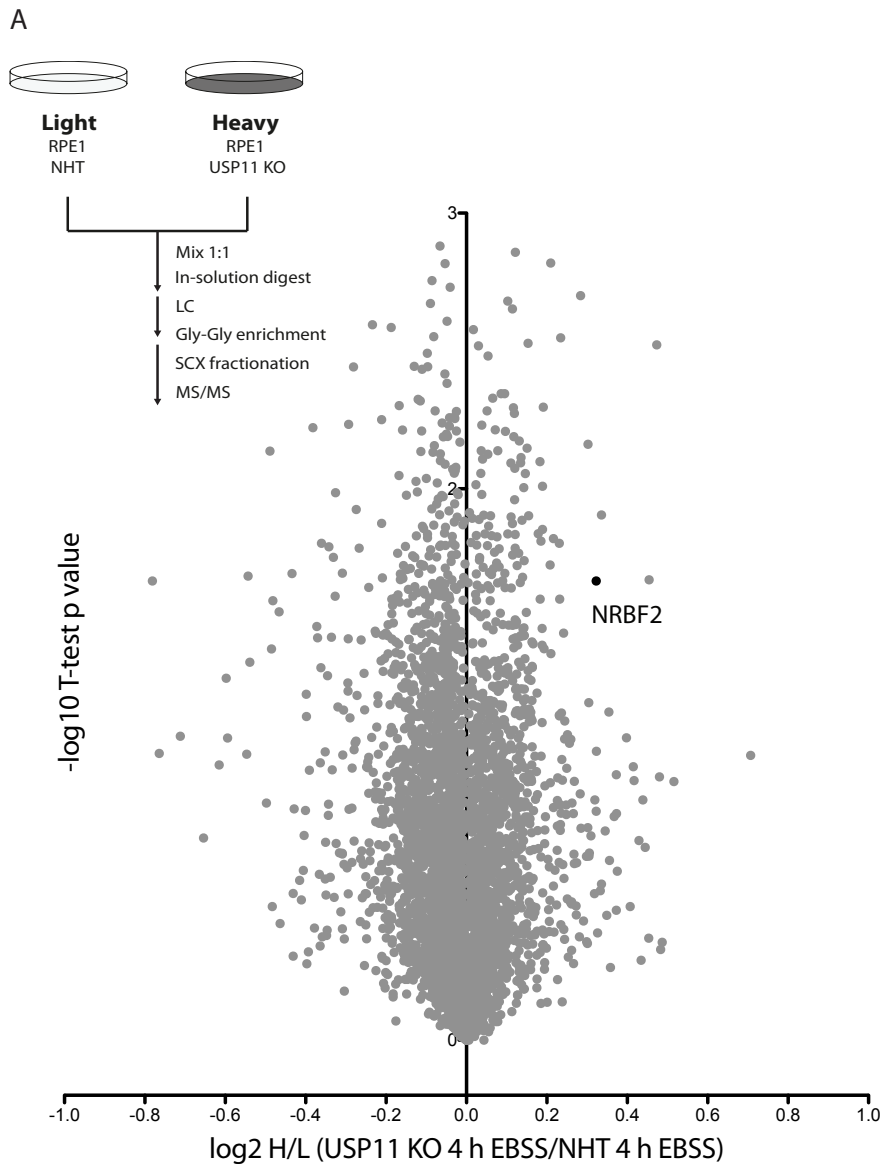
Figure 24: SILAC-based mass spectrometry approach to identify USP11 substrates after 4 hour EBSS treatment. A A volcano plot showing protein enrichment. On the left side are the proteins that were more abundant in the NHT control, and on the right, the ones more enriched in the USP11 knockouts. Schematic representation of the workflow is included in the figure.

Table 4: SILAC-based mass spectrometry approach to identify USP11 substrates led to insights into proteome changes in USP11 knockout cells after 4 hour EBSS treatment compared to NHT control. A List of the most downregulated proteins in the USP11 knockout cells compared to the NHT control after 4 hour EBSS treatment. All labeled hits are significant (FDR<5 %). **B** List of the most upregulated proteins in the USP11 knockout cells compared to the NHT control after 4 hour EBSS treatment. NRBF2 was one of the top hits. All labeled hits are significant (FDR<5 %).

A

Most downregulated proteins in USP11 knockout cells after 4 h EBSS treatment

ZNF185	Zinc finger protein 185
ACAA2	3-ketoacyl-CoA thiolase. mitochondrial
PLA2G4A	Cytosolic phospholipase A2;PhospholipaseA2;Lysophospholipase
LAMTOR2	Ragulator complex protein LAMTOR2
FAM175B	BRISC complex subunit Abro1
LXN	Latexin
VCAN	Versican core protein
MAN2A2	Alpha-mannosidase 2x
FBN1	Fibrillin-1
CDK13	Cyclin-dependent kinase 13
CAMK4	Calcium/calmodulin-dependent protein kinase type IV
ITGA2	Integrin alpha-2
SORBS2	Sorbin and SH3 domain-containing protein 2
LIPA	Lysosomal acid lipase/cholesteryl ester hydrolase

B

Most upregulated proteins in USP11 knockout cells after 4 h EBSS treatment

PGM5	Phosphoglucomutase-like protein 5
PKP2	Plakophilin-2
AK5	Adenylate kinase isoenzyme 5
NRBF2	Nuclear receptor-binding factor 2
ANO6	Anoctamin-6
CD63	CD63 antigen
KRAS	GTPase KRas;GTPase KRas. N-terminally processed
CORO1C	Coronin-1C;Coronin
C9orf78	Uncharacterized protein C9orf78
DDX55	ATP-dependent RNA helicase DDX55
YBX3	Y-box-binding protein 3
AURKA	Aurora kinase A
TMSB4X	Thymosin beta-4;Hematopoietic system regulatory peptide
PUM2	Pumilio homolog 2

Combining mass spectrometry and GlyGly enrichment to identify USP11 substrates and investigate the changes in the proteome is generally one of

the most efficient ways to gather a broad understanding of the effect of a deubiquitinating enzyme under a defined condition. Unfortunately, here, the quality of the data was not satisfactory, although it gave one interesting protein as a hit, NRBF2, which will become more important with further experiments and will be discussed in the further chapters.

2.4.1 USP11 interactome after 4 hour autophagy induction with Torin1

The substrate identification under autophagy induction resulted in a very few identified proteins in general, both in the proteome dataset, as well as in the GlyGly enriched peptides. Alternative approaches were necessary. To expand the understanding of USP11 involvement in autophagy regulation, a secondary mass spectrometry approach was utilized in collaboration with Florian Bonn (former Goethe University). Generally, overexpression of tagged proteins followed by immunoprecipitation (IP) under mild lysis condition leads to the identification of potential interaction partners of the protein of interest. They may be stable interactors or transient interactors, such as substrates. The latter is harder to identify using this approach. However, to increase the chances such proteins are captured, the catalytic inactive version of USP11 was overexpressed. Catalytic cysteine of USP11 is located at position 318. When mutated, the DUB is inactive. Most often, the catalytic cysteine is mutated to an alanine (e.g. USP11 (C318A)) or a serine (e.g. USP11 (C318S)). In the case of mutated catalytic cysteine, USP11 is unable to release its substrate, thereby acting as a "trapping mutant" (Morrow et al. 2018). Cysteine mutation should not compromise stable USP11 interactions, but increase the chances of capturing transient interactions it has with substrates. The GFP only control or GFP-tagged USP11 (C318S) was overexpressed in Hek293 cells and autophagy was induced with 250 nM Torin1 treatment for 4 hours. Lysates were incubated with GFP-Trap® Agarose beads to enrich GFP or USP11 (C318S)-GFP together with the proteins they bind. GFP control is necessary to minimize the identification of false positive USP11 interactors due to their specific interaction with the tag

only. The sample preparation was done label-free followed by LC-MS/MS. With this approach, many known autophagy proteins were found significantly enriched with the catalytic inactive USP11 (C318S) compared to GFP control (Figure 25 A). Importantly, USP11 was the highest enriched protein, as expected. Strikingly, two major autophagy kinases were found in the USP11 (C318S) IP sample, mTOR and PRKAA1 (catalytic subunit of the AMPK). Furthermore, many proteins described to regulate the PI3KC3 complex were found, such as USP19, RNF2, DDB1, TRIM28 (KAP1), and GNB2L1 (RACK1) (Table 5) (Jin et al. 2016; Cui, Jin, and Wang 2016; Xia et al. 2014; Antonioli et al. 2014; Yang et al. 2013; Zhao et al. 2015). Moreover, a core subunit of the PI3KC3 complex itself, VPS15, was identified, too.
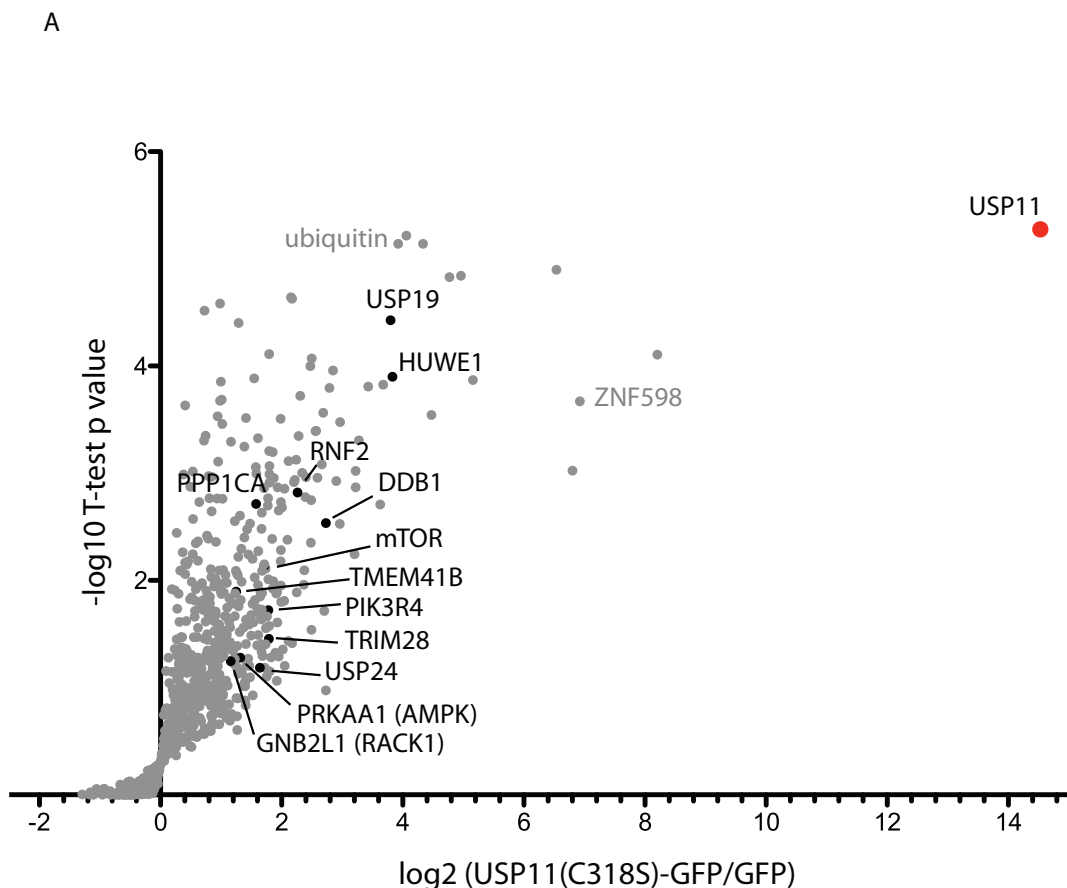
A

Figure 25: Label-free mass spectrometry led to the identification of multiple autophagy-linked USP11 interactors and reported USP11 interactors or substrates after 4 hour 250 nM Torin1 treatment. A A volcano plot depicting results of the label-free catalytic inactive USP11 interactome. USP11 is the most enriched protein. Black dots represent autophagy-linked proteins. Grey dots represent ubiquitin and ZNF598, which

together with HUWE1, was used to verify the quality of the data. All labeled hits are significant (FDR<5 %).

Table 5: Label-free mass spectrometry led to the identification of autophagy-linked USP11 interactors after 4 hour 250 nM Torin1 treatment. A Table listing autophagy-linked USP11 interactors or substrates, values plotted in the volcano plot, and published references. All the hits are significant (FDR<5 %).

Protein name	Log2 enrichment USP11 (C318S) over GFP	-Log Student's T-test p-value USP11 (C318S) over GFP	Published link to autophagy
USP11 (bait)	**14,53**	**5,27**	**Bait**
HUWE1	3,83	3,9	E3 ligase targeting WIPI2 in mTORC1-dependent manner (Wan et al. 2018), induces AMBRA1 activity (Di Rita et al. 2018)
USP19	3,80	4,42	Beclin-1 DUB (Jin et al. 2016; Cui, Jin, and Wang 2016)
DDB1	2,73	2,53	Cul4 adaptor targeting AMBRA1 for degradation (Antonioli et al. 2014)
RNF2	2,26	2,82	E3 ligase targeting AMBRA1 for degradation (Xia et al. 2014)
TRIM28 (KAP1)	1,79	1,45	Dual role in autophagy: Ubiquitinates and degrades AMPK (Pineda and Potts 2015), and SUMOylates PIK3C3 (VPS34) (Yang et al. 2013)

PIK3R4 (VPS15)	1,78	1,72	PI3KC3 complex subunit
mTOR	1,71	2,13	Master regulator of metabolism, phosphotylates NRBF2 (X. Ma et al. 2017)
USP24	1,64	1,18	Regulates ULK1 stability, negative regulator of autophagy (Thayer et al. 2020)
PPP1CC;PPP1CA;PPP1CB	1,57	2,71	USP11 substrate (Sun et al. 2019), CSNK2-meidated phosphorylation of ATG16L1 (Song et al. 2015)
PRKAA1 (AMPK cat. subunit)	1,31	1,27	AMPK phosphorylates VPS34 (Kim et al. 2013)
TMEM41B	1,25	1,89	Autophagosome maturation (Moretti et al. 2018)
GNB2L1 (RACK1)	1,15	1,24	Interaction partner of ATG5 (Erbil et al. 2016), AMPK substrate; promotes PI3KC3 complex assembly (Zhao et al. 2015)

To verify the relevance of these findings, a GFP control or GFP-tagged catalytic active and inactive USP11 were overexpressed together with two suspected interactors, E3 ligases HUWE1 and ZNF598, under basal conditions and 4 hour 250 nM Torin1 treatment, and immunoprecipitated from Hek293 cells. Both tested proteins were successfully found co-immunprecipitating with USP11, as mass spectrometry data suggested, implying reliability of the data (Figure 26 A, B). Moreover, both of these proteins were found in SILAC-based mass spectrometry experiment aimed to

determine USP11 (C318S) interactome under basal conditions (data not shown).
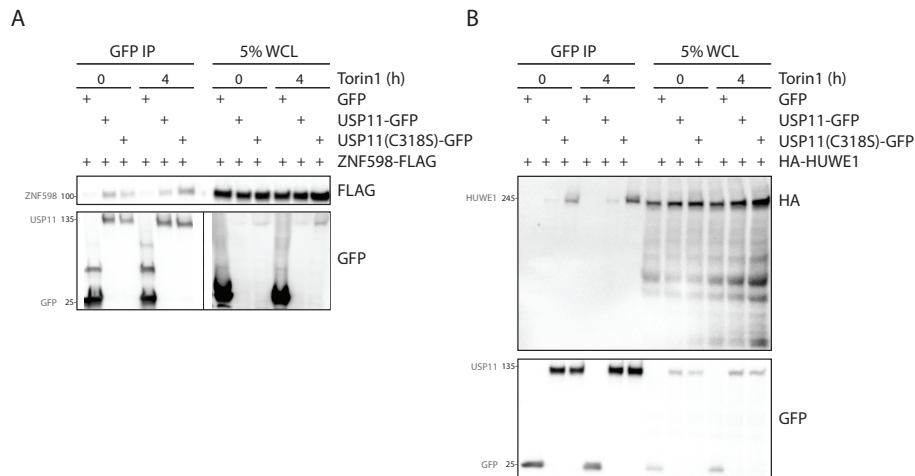
Figure 26: Validation of label-free mass spectrometry of the USP11 (C318S) interactome after 4 hour 250 nM Torin1 treatment. A Verification of the mass spectrometry data using a high confident binding E3 ligase ZNF598, previously not reported to play a role in autophagy, by co-immunoprecipitation with USP11, or USP11 (C318S) under basal conditions, and after 4 hour Torin1 treatment. **B** The verification of the data using HUWE1 E3 ligase, previously reported to play a role in autophagy, with the same conditions as ZNF598.

Identification of the USP11 (C318S) interactors and substrates led to the discovery of a surprisingly large number of autophagy-related proteins. Further experiments focused on the potential autophagy regulation via the PI3KC3 complex and mTOR. Importantly, this data suggested that USP11 does not play a single, unique role in autophagy regulation. Rather, it appeared it could be found in different complexes, important for different stages of autophagy, once again emphasizing the important role for USP11 in autophagy regulation.

2.5 USP11-dependant autophagy regulation via interacting with the PI3KC3 complex I

2.5.1 Loss of USP11 stabilizes NRBF2

Analysis of the USP11 (C318S) interactome under autophagy induction gave strong evidence pointing to the regulation via the PI3KC3 complex (Figure 25 A). As a deubiquitinase, USP11 can regulate a proteasomal and a non-proteasomal ubiquitination status of its substrates. A proteasomal signal is reflected by modulation of the substrate stability and a non-proteasomal can determine the substrate interactome, localization, or activity (Komander and Rape 2012; Yau and Rape 2016). To follow up on that lead, levels of PI3KC3 complex were looked into. Surprisingly, NRBF2, a dimer-inducing subunit, had elevated levels in the RPE1 USP11 knockout cells compared to the NHT control cells when autophagy was induced with EBSS for shorter time points of 30 minutes and 1 hour (Figure 27 A). No obvious difference was observed under physiological conditions between the cell lines. Elevated NRBF2 levels could not be explained by USP11 rescuing NRBF2 from the proteasomal degradation as the opposite would be the case. Rather, NRBF2 could be targeted by an E3 ligase that is a direct USP11 substrate. Meaning, loss of USP11 leads to a loss of an E3 ligase or its impaired activity leading to stable NRBF2 levels. It could also be that USP11 regulates a non-proteasomal signal on NRBF2 regulating its association with the complex. Upon loss of USP11, this hypothesized ubiquitination leads to a stronger complex association and is protecting NRBF2 from proteasomal degradation. Third possibility is that the loss of USP11 leads to an increase in NRBF2 mRNA levels, subsequently resulting in increased NRBF2 protein levels. To differentiate these hypotheses, autophagy was induced with EBSS for longer time points: 2, 4, and 6 h, and the medium supplemented with CHX to inhibit new protein synthesis. A striking NRBF2 stability was observed in USP11 knockout cells, as opposed to steady protein loss in NHT control (Figure 27 B). Considering CHX was used to eliminate the contribution of newly synthesized protein, USP11-mediated transcriptional regulation is not a likely explanation, although it cannot be completely excluded. Meaning, this result favored the first two hypotheses; USP11 regulates NRBF2 directly or indirectly on a post-translational level. The steady decrease of NRBF2 levels in the NHT control could be a result of a negative feedback loop to restrict autophagy upon prolonged induction. Notably, the LC3-II accumulation upon

BafA1 treatment was observed as expected, and was more prominent in the USP11 knockout cells, as expected (Figure 27 B).
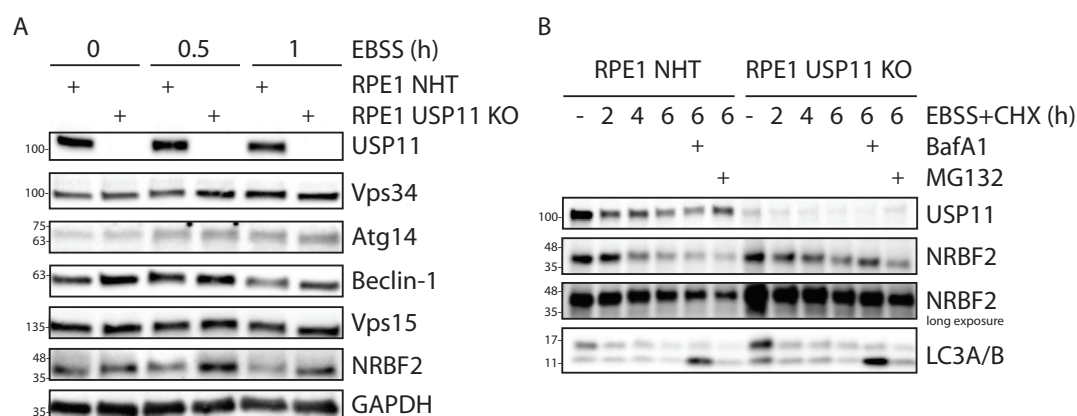
Figure 27: A striking NRBF2 stabilization, the PI3KC3 complex dimer-inducing subunit, was observed upon autophagy induction in RPE1 USP11 knockout cells, compared to NHT control. A A representative western blot determining protein stability of the PI3KC3 complex upon autophagy induction demonstrated increased NRBF2 stability in the USP11 knockout cells (N=2). **B** A CHX chase confirming striking NRBF2 stability in the USP11 knockout cells compared to the control cells upon longer autophagy induction. The LC3-II levels accumulated under BafA1 treatment were higher in the USP11 knockout cells compared to the NHT control, as expected (N=3).

In conclusion, the loss of USP11 results in increased stability of NRBF2. This observation was also made in the proteome analysis of the USP11 knockout cells after 4 h of EBSS treatment. Most likely this is due to an USP11-dependant post-translational regulation of NRBF2. Regulation of the NRBF2 mRNA levels by USP11 cannot be excluded, however, it is unlikely to be a significant contribution.

2.5.2 USP11 regulates the post-translational modification status of the PI3KC3 complex I subunits

As discussed in the previous section, an increased stability of proteins can be achieved by increased transcription and translation or by regulation of post-translational modifications (PTMs): by decreased degradation targeting or by

increased removal of the degradation signal. Here, the transcriptional and translational contributions were not investigated in details; however, PTMs were, considering acquired data suggested regulation of NRBF2 stability via PTMs. Both proteasomal and non-proteasomal ubiquitination of the PI3KC3 complex components has been reported (extensively discussed in chapter 1.2.3.), however, NRBF2 in this context was not investigated in depth. To investigate a potential USP11-dependent ubiquitination of NRBF2, co-immunoprecipitation experiments between USP11 and NRBF2 were performed in the presence of overexpressed ubiquitin. Moreover, the two USP11 versions were used, GFP-tagged catalytically active WT USP11, and catalytic inactive USP11 (C318S). The western blot showed a smeared band with the HA antibody in the sample with the catalytic inactive USP11, but not with the WT USP11 (Figure 28 A). This strongly suggested that NRBF2 is post-translationally modified in a USP11 activity-dependent manner. Surprisingly, this modification seems to exclusively depend on the activity of USP11, but not on the autophagy status of the cells, as the appearance of the band does not change between the physiological and the autophagy induction conditions (4 hour treatment with 250 nM Torin1) (Figure 28 A). Strikingly, when the catalytic subunit of the complex was looked at, the lipid kinase VPS34, a similar, another striking observation was made. An additional, higher molecular weight band was observed to co-IP with the catalytic inactive USP11 and not with the WT USP11 under physiological condition (Figure 28 B). This observation was further investigated in a time course-dependent manner to determine how autophagy may influence the modification, and similarly to NRBF2, no autophagy-dependence was observed, only USP11 activity-dependence (Figure 28 C). Further investigation in the PTM status of the complex components revealed there are two species of Beclin-1 found in the co-IP with the USP11 (C318S) compared to one found with the WT USP11 (Figure 28 D). As well as for VPS34, this modification seemed unaltered in the course of autophagy induction. ATG14, a pro-autophagic signature complex component, did not appear to be modified in USP11-, or autophagy-dependent manner (Figure 28 E). Interestingly, only VPS15 as a PI3KC3 complex component was identified in the mass spectrometry interactome analysis, in addition to many

proteins known to regulate the complex. Similarly to NRBF2, VPS15 also displayed a smeared band appearance with the catalytic inactive USP11 on a western blot (Figure 28 F).
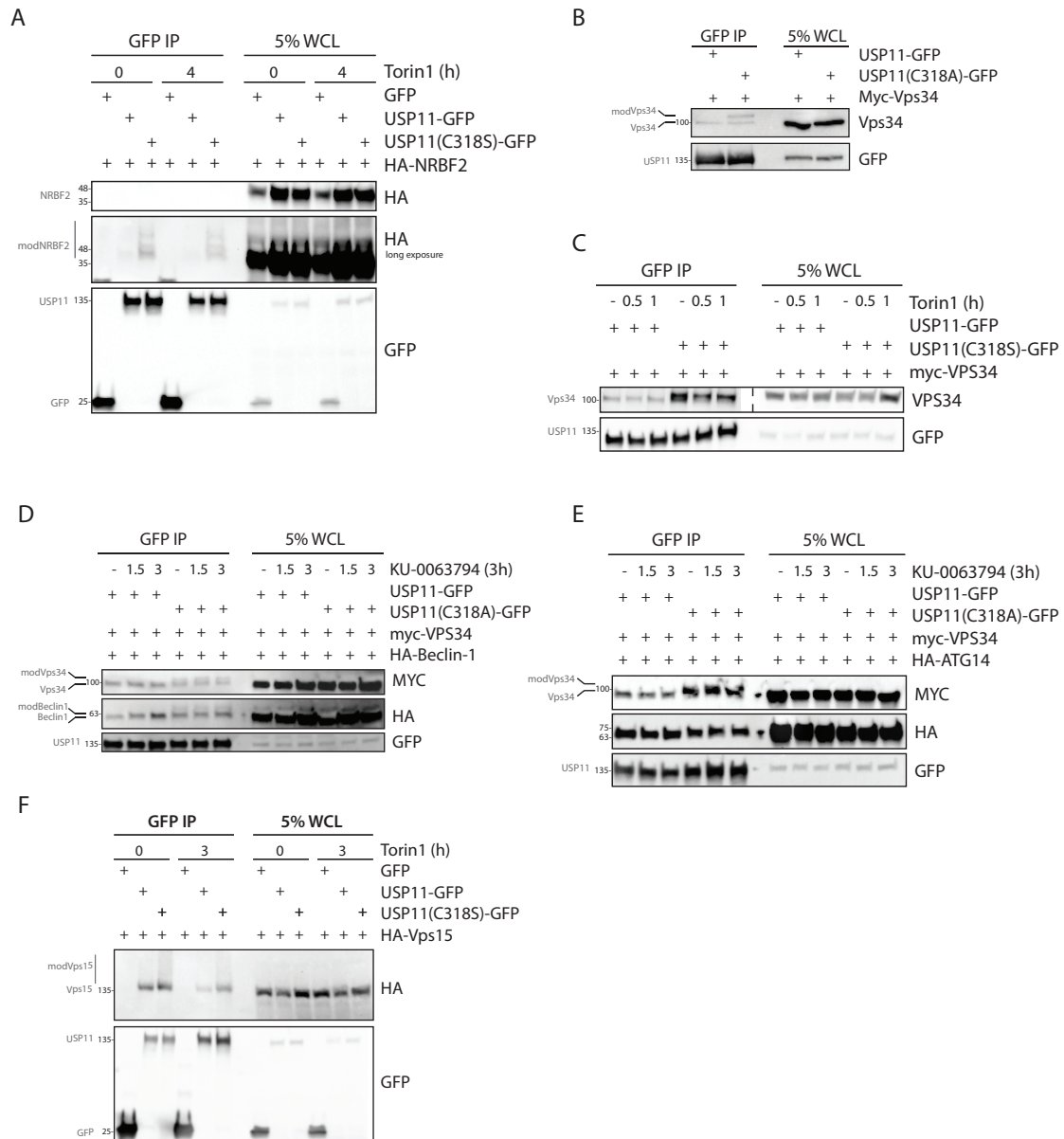
Figure 28: USP11 activity affects the post-translational modification status of NRBF2, VPS34, and Beclin-1, but not of ATG14. A A western blot of a co-IP of the WT USP11, or the catalytic inactive USP11 (C318S), and NRBF2 suggests an USP11 activity-dependent modification, but not autophagy-dependent (N=2). **B** A western blot of a co-IP of the USP11, or the catalytic inactive USP11 (C318A), and VPS34 under physiological conditions revealed a higher molecular weight modified specie of VPS34 interacting with the inactive USP11 (N>5). **C** A western blot of a co-IP of USP11, or catalytic inactive USP11, and VPS34 suggests an USP11 activity-dependent modification, but not autophagy-dependent (N>5). **D**

A western blot of a co-IP of USP11, or catalytic inactive USP11, and VPS34 together with Beclin-1 suggests an USP11 activity-dependent modification, but not autophagy-dependent (N=2). **E** Western blot of co-IP of USP11, or catalytic inactive USP11, and VPS34 together with ATG14 implied no USP11- or autophagy-dependent modification on ATG14 (N=2). **E** Western blot of a co-IP of USP11, or catalytic inactive USP11, and VPS15 showed a smeared VPS15 band with the catalytic inactive USP11 (N=2).

Taken together, the mass spectrometry interactome data and the reproducibility of this data in the form of co-IPs, as well as the band appearances of the immunoprecipitated proteins, strongly suggest USP11 indeed interacts and regulates the PI3KC3 complex.

2.5.3 VPS34 modification analysis

As VPS34 is the lipid kinase component of the PI3KC3 complex, further investigations focused on this protein. The PTMs on VPS34 were addressed via mass spectrometry thus far without success (data not shown), however further indirect approaches were employed to shed light on the modified sites, or on the type of the modification. In the first approach, publicly available mass spectrometry databases (source: iPTMnet and PhosphoSitePlus®) were screened for the reported ubiquitination and SUMOylation sites on VPS34. At the time, five ubiquitination sites were reported and one SUMO-site. All the reported modified lysines were mutated by site-directed mutagenesis into arginines (K to R) and co-IP experiments were repeated. If any of the sites was responsible for the modification observed on the western blots, a mutation should cause the loss of the upper band. The results of repeated co-IPs did not lead to the identification of the site (Figure 29 A, B). The reason for this could be that the modified site was not among the reported five. Indeed, currently the number of reported sites has risen to 21 (source: iPTMnet, April 2020). Furthermore, it may be that there were more sites simultaneously modified and mutating individual residues is insufficient to detect on a western blot. In the second approach to elucidate the VPS34 modification, more focus was brought onto identifying the type of the modification and away from the exact site. All PTMs can be enzymatically

counteracted. Ubiquitination is removed by deubiquitinases (DUBs), SUMOylation by deSUMOylating enzymes (SENPs), phosphorylation by phosphatases etc. If a modification can be counteracted by presence of any of these enzymes, it would lead to its identification. To this end, co-IP experiments were repeated and recombinantly expressed catalytic domains of USP2 (an unspecific DUB) was incubated with the immunoprecipitated, modified VPS34. Similarly to the mutagenesis, if any of the enzymes would reverse the modification, it would result in a "collapse" of the upper band in favor of the lower, unmodified one. The results of this approach were ambiguous. Addition of the catalytic domain of USP2 slightly increased the intensity of the lower band, however, it did not eliminate the upper band completely (Figure 29 C). Several possible explanations for this ambiguity can be discussed. First, catalytic domain of USP2 may not be able to efficiently remove the "last" ubiquitin, most proximal to the substrate. Second, if the catalytically inactive USP11 trapped VPS34 as a substrate, it may block the access of USP2 to remove the ubiquitin on VPS34. Third, the mild effect observed on the western blot may indicate there is both SUMOylation and ubiquitination on VPS34, and that both modifications contribute to the upper band. Hence, slight reduction may reflect the collapse of the ubiquitinated fraction, and the rest remaining is in fact the SUMOylated fraction. The latter could be addressed by repeating the experiment with adding catalytic domain of SENP2 together with USP2. This approach did not clarify the question (Figure 29 E), as we did not have the positive control for the activity of the recombinant SENP2 catalytic domain used in the experiments. Unlike for the SENP2, the recombinant USP2 catalytic activity was tested using propargylated ubiquitin (PA-ubiquitin) and the activity of USP2 was confirmed (Figure 29 D). PA-ubiquitin is a "suicide probe" (Ekkebus et al. 2013), meaning in the presence of a catalytically active DUB it forms a covalent bond with the catalytic cysteine. This bond formation can be detected by Coomassie staining of the *in vitro* reaction, as an increase in molecular weight equivalent to binding the ubiquitin probe by the DUB. As previously described, VPS34 is also phosphorylated (Ohashi, Tremel, and Williams 2019). Protein phosphorylation is reversed by phosphatases, so the experiment was repeated with the addition of a commercially available

lambda phosphatase. The lambda phosphatase is reported to dephosphorylate threonines, serines and tyrosines (Zhuo et al. 1993). The preliminary result suggested a minor reduction in the upper band in favor of the lower band (Figure 29 F); however, the conclusion cannot be reached beyond the point of phosphorylation being a minor contributor to the higher molecular weight specie. Within the scope of this project, further VPS34 PTMs, such as acetylation, were not addressed.

Figure 29: An indirect investigation of the USP11-dependent modification on VPS34. A A western blot of a co-IP of the catalytic inactive USP11 (C318A), and VPS34 lysine to arginine mutants did not reveal a single ubiquitination (modification) site on VPS34. The K630R mutant was not successfully cloned at first, hence the experiment was repeated (in Figure B) (N=2). **B** Western blot of a co-IP of the catalytic inactive USP11 (C318A), and a

correct VPS34 K630R mutant, as well as the reported SUMOylation site mutant K840R did not provide further insight in site location (N=1). **C** A western blot of a co-IP of the GFP control, WT USP11, or catalytic inactive USP11 (C318A), and VPS34. Additional sample of the catalytic inactive USP11 (C318A) was included that contained recombinantly expressed catalytic domain of USP2. If the modification of VPS34 were ubiquitination, the addition of USP2 would collapse the upper band. This was observed, albeit to a limited degree (N=2). **D** A Coomassie staining of the USP2 activity test using PA-ubiquitin. The USP2 activity was confirmed by the increase in molecular weight gained by formation of the covalent bond between USP2 and PA-ubiquitin. **D** Western blot of a co-IP of the WT USP11, or the catalytic inactive USP11 (C318A), and VPS34. Additional samples of the catalytic inactive USP11 with VPS34 included the recombinantly expressed catalytic domain of USP2, the catalytic domain of SENP2, or both (N=2). **F** A western blot of a co-IP of the WT USP11, or the catalytic inactive USP11 (C318A), and VPS34. Additional sample of the catalytic inactive USP11 with VPS34 included the lambda phosphatase. Addition of the lambda phosphatase mildly reduced the appearance of the upper band (N=1).

In summary, all the indirect approaches to address the question of the modification on the catalytic subunit of the PI3KC3 complex did not result in a univocal answer. In fact, all the enzymes used to counteract known modifications from the literature showed a mild effect, however, did not fully collapse the detected band. Further experiments will be necessary to elucidate this question.

2.5.4 USP11 affects the activity of the PI3KC3 complex I, likely by increasing the complex stability, leading to the increased activity

PTMs are known to regulate the activity of the complex (Ohashi, Tremel, and Williams 2019). The activity is directly connected to the complex composition defined by above-mentioned PTMs. Considering the abundant evidence of the USP11-dependent regulation of post-transitional modifications on almost all of the complex components; stability and activity of the complex as a whole were assessed. As mentioned, the pro-autophagic PI3KC3 complex I is defined by containing ATG14 (Kihara et al. 2001). This was taken advantage of in an endogenous IP of ATG14 and checking for its interaction with the other complex components. The data showed a surprising increase in the co-immunoprecipitation of endogenous VPS34, Beclin-1, and to a lesser extent NRBF2, with the endogenous ATG14 from the USP11 knockout cells

compared to the NHT control cells (Figure 30 A). This increase in complex formation may be responsible for the increase in the autophagic flux observed upon loss of USP11. Strikingly, when the same experiment was performed in 293 cells, but with overexpressing GFP control or GFP-tagged USP11, the opposite was observed (Figure 30 B). There is a significant reduction in NRBF2 co-immunoprecipitating with endogenous ATG14. It appeared that overexpression did not alter the stability of NRBF2 like absence of USP11 does, but the association with the complex was dramatically decreased (figure 30 B). This result suggests that USP11 is regulating a PTM on NRBF2, likely a ubiquitin signal that leads to a stronger complex association. The fact that USP11 depletion and overexpression do not have the opposite phenotype, indicates two interconnected things: USP11 may work with accessory proteins and USP11 regulates the complex components in a different way, and for some it may be that its function is exerted by acting as a scaffold protein and recruits actual effectors. In both cases, the complex is more tightly bound in the absence of USP11. And if that were the case, it could be reflected in a higher complex activity, so this was addressed next. One way to directly address the lipid kinase activity is by using *in vitro* kinase assays. In short, VPS34 lipid kinase is immunoprecipitated from cells in which autophagy was induced and provided with lipid substrates *in vitro*. In this case, the substrates are phosphatidylinositols (PIs). Phosphorylated lipids, phosphatidylinositol 3-phosphates (PI(3)P), produced by the kinase activity are then measured. The readout depends on the individual assay. Here, commercially available competitive enzyme-linked immunosorbent assays (ELISA) were used. These assays comprise of plates coated with PI(3)Ps and detector proteins that bind them. In the first step, the *in vitro* kinase assay was performed with the VPS34 immunoprecipitated from the NHT control and the USP11 knockout cells in the autophagy time-dependent manner. PI(3)Ps generated in these reactions were then extracted and added to PI(3)P coated plates with the detector protein for competitive binding. The more externally added PI(3)Ps generated by immunoprecipitated VPS34, the less binding of the detector protein can be measured as it is sequestered by washing away. Meaning, the signal from the detector protein is inversely proportional to the added PI(3)Ps. The readout is a colorimetric-based reaction. Up to now, *in*

vitro kinase assays using endogenous VPS34 from the NHT control and the USP11 knockout cells were not successful (data not shown) as even with a large number of the cells used to isolate VPS34, the final quantity of purified protein was not sufficient to produce enough phosphorylated lipids that were in the range of the detection of the available ELISA assays, despite the manufacturer's recommendations. To bypass this, an image-based readout was used. Phosphorylated lipids produced by the PI3KC3 complex I serve as a recruitment signal for downstream effector proteins involved in the autophagosome growth and maturation, such as the WIPI2 proteins (Proikas-Cezanne et al. 2015). Upon autophagy induction, WIPI2 proteins form distinct dots that can be visualized using an antibody for the endogenous WIPI2 proteins and quantified (Proikas-Cezanne et al. 2007). Surprisingly, upon autophagy induction with EBSS for 1 hour, more dots per cell were observed and quantified in USP11 knockout cells compared to the NHT control indicative of more phosphorylated lipids responsible for the dot formation (Figure 30 C, D) (p-value < 0.05, unpaired t-test). More phosphorylated lipids can be attributed to a more active PI3KC3 complex I and could be a likely reason for a higher autophagic flux observed upon loss of USP11.
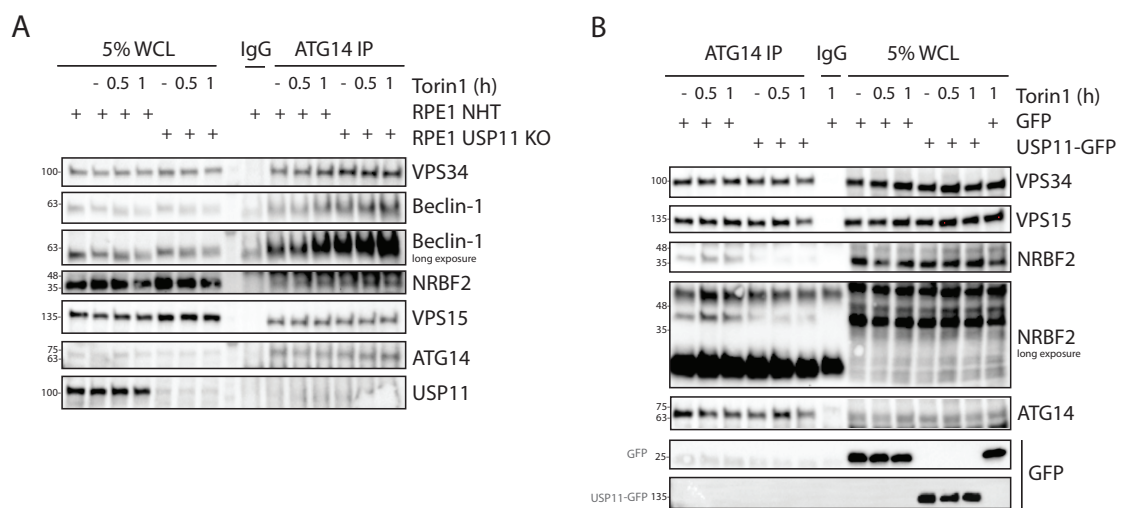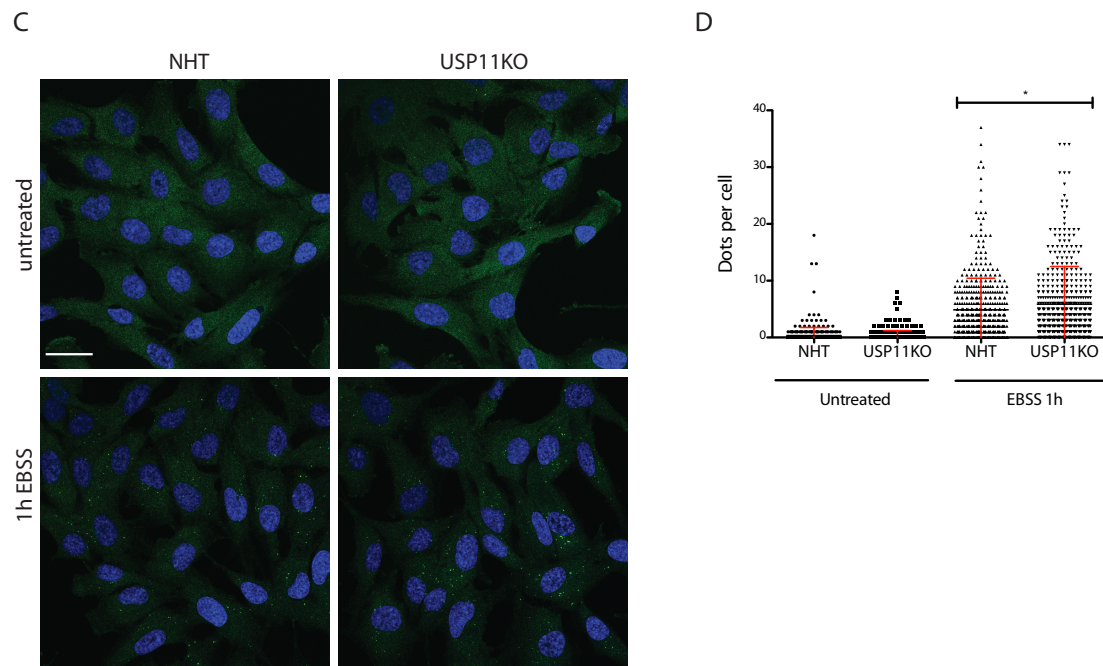
Figure 30: USP11 affects the PI3KC3 complex stability and the increased complex I formation is reflected by a higher lipid kinase activity. A A western blot of the endogenous ATG14 IP demonstrated more VPS34, Beclin-1, and to lesser extent NRBF2, binding in the USP11 KO cells compared to the NHT control (N=2). **B** A western blot of the endogenous ATG14 IP from the Hek293 cells with overexpressed USP11 demonstrated less NRBF2 binding in the USP11 overexpressed cells compared to the GFP control (N=2).
C Immunofluorescence of the endogenous WIPI2 showed an increased dot formation in the USP11 knockout cells, compared to the NHT control cells after 1 hour EBSS treatment. WIPI2 dots are formed upon binding to PI(3)Ps produced by the PI3KC3 complex I. Therefore, higher number of dots is an indirect readout of the increased activity of the complex I. **D** Quantification of the immunofluorescence images showed the difference in dot formation is statistically significant (p-value < 0.05, unpaired t-test, ≈450 cells per sample, per condition, N=3).

2.6 USP11-dependant autophagy regulation via mTOR stability

2.6.1 mTOR is a USP11 substrate and USP11 regulates mTOR stability

Serine/threonine kinase mTOR was one of the identified proteins in the USP11 (C318S) interactome under 4 hour 250 nM Torin1 treatment. As it is considered a master regulator of cell metabolism regulating everything from protein translation to autophagy induction (Liu and Sabatini 2020), it was looked into in more detail. First, the potential interaction was confirmed with a co-IP of overexpressed WT USP11 or catalytic inactive USP11 (C318S),

together with mTOR under physiological condition, as well as upon autophagy induction with 250 nM Torin1 for 4 hours. As expected based on the interactome data, mTOR was found in the co-IP with the catalytic inactive USP11 and to a significantly lesser amount with the WT USP11 (Figure 31 A). Even more surprising, no difference in interaction was observed when autophagy was induced. Notably, a smear band observed for mTOR prompted further experiments in the direction of determining potential USP11-dependent ubiquitination. To this end, cells were transfected with His-tagged ubiquitin, and treated with Torin1, BafA1, and Mg132 for 6 hours. In addition, the cells were transfected either with the WT or the catalytic inactive USP11 (C318S) that were subsequently immunoprecipitated. Remarkably, an ubiquitin-specific antibody suggested significantly more modified mTOR in the co-IP with the catalytic inactive USP11, as opposed to the wild type USP11 (Figure 31 B). Same observation was made with only Torin1 treatment, without additional BafA1 or Mg132 treatment (data not shown). These results were obtained when the co-immunoprecipitation was done under mild lysis conditions to preserve the protein interactions. The ubiquitin antibody used in this context calls for caution when interpreting the data. The smeared appearance is likely due to mTOR modification, however, there is certainly a contribution of other ubiquitinated proteins in the respective immunoprecipitations contributing to the signal.
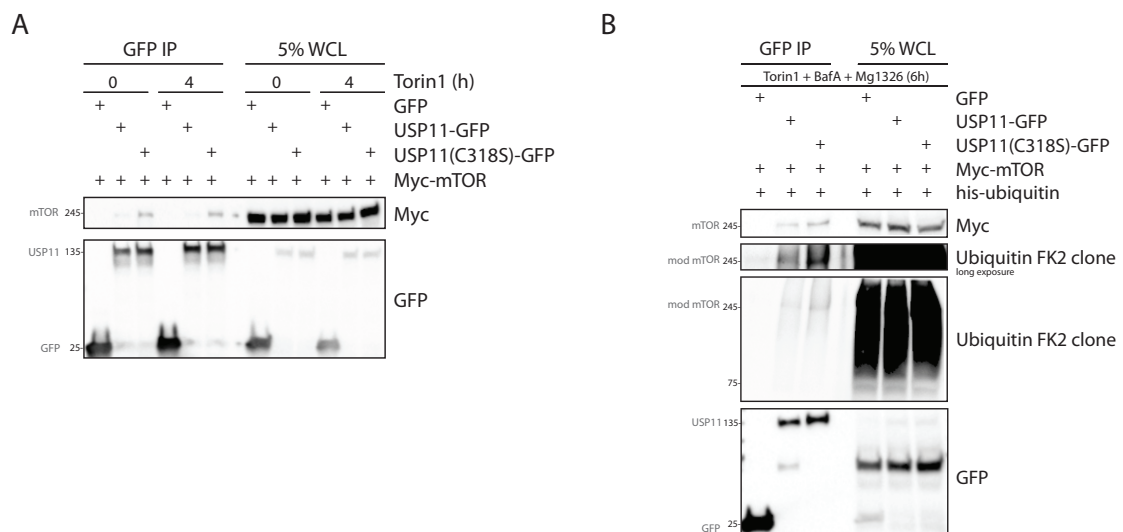
Figure 31: Catalytic inactive USP11 co-immunoprecipitated modified mTOR, the wild type USP11 to a lesser degree. A A western blot of USP11, catalytic inactive USP11 and mTOR co-IP under physiological conditions, or after 4 hour 250 nM Torin1 treatment showing more mTOR in the co-IP with the catalytic inactive USP11, as opposed to the WT USP11. **B** A western blot of WT USP11, catalytic inactive USP11 and mTOR co-IP, with additional his-ubiquitin overexpression, from cells treated for 6 hours with Torin1, BafA1, and Mg132 showed increased levels of modified mTOR in the catalytic inactive USP11 IP.

The mass spectrometry results, as well as the western blot band appearance from the co-IP experiments suggest mTOR is a substrate of USP11 and not a stable interactor. To test if this suspected ubiquitin signal is a proteolytic or a non-proteolytic signal, a CHX chase was performed. The NHT control and the USP11 knockout cells were treated with EBSS supplemented with CHX for 2, 4, and 6 hours, and the levels of mTOR were monitored. Strikingly, the mTOR levels gradually decreased in the USP11 knockout cells, but remained stable in the NHT control (Figure 32 A). Furthermore, the decrease of mTOR level was rescued by the supplementation with Mg132, suggesting that USP11 is rescuing mTOR from proteasomal degradation.
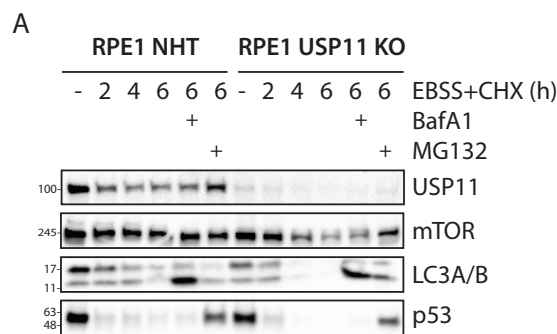
Figure 32: Loss of USP11 resulted in reduced mTOR protein levels, indicative of mTOR being a USP11 substrate, and USP11 rescuing mTOR from proteolytic degradation upon autophagy induction. A A western blot of a CHX chase showing loss of USP11 led to a decrease in mTOR levels upon autophagy induction. The levels of mTOR were rescued with Mg132 treatment, suggesting that USP11 is rescuing mTOR from proteasomal degradation (N=3).

Considering the importance of mTOR in regulating metabolism, further experiments are need to elucidate the extent to which the observed USP11-

dependent stability regulation is reflected in regulating autophagy, as opposed to other known mTOR functions. Nonetheless, if loss of mTOR, or a faster mTOR turnover is reflected on the impaired downstream signaling via its substrates on autophagy in an USP11-dependent manner, it would be in agreement with the hypothesis that USP11 is a negative regulator of autophagy via multiple angles.

3   Discussion

3.1   USP11 as a novel negative regulator of autophagy

USP11 has many described roles, both in the nucleus and in the cytoplasm. Depending on the cellular context, it has assigned both tumor promoting and tumor suppressing roles. However, to this date, none reporting the USP11 involvement in autophagy regulation. Here, it was demonstrated that USP11 is a novel, negative regulator or autophagy.

To study USP11 in the context of autophagy, NHT and USP11 single clone cell lines were created harboring the GFP-LC3-RFP-LC3ΔG probe. This probe is processed by the endogenous ATG4, as is the endogenous LC3. GFP-LC3 can be utilized by the autophagy machinery and degraded in the course of autophagy which can be monitored by flow cytometry as a loss of the GFP fluorescent signal, while the RFP-LC3ΔG remains in the cytoplasm serving as an internal control. Using fluorescently tagged proteins in cells for this purpose has many advantages. To name a few: specificity, low toxicity, low artifact probability etc. The single clones were carefully selected based on their physical properties, approximate 1:1 ratio of the GFP/RFP signal under physiological conditions, and homogenous behavior of the entire population upon autophagy induction indicative of monoclonality of the cell line. A striking loss of the GFP signal in USP11 knockout cells compared to NHT control cells, suggested USP11 has a negative effect on autophagy. This finding was verified in another single clone cell line harboring the GFP-LC3-RFP probe that works in the same way as the above-mentioned probe. Here, USP11 was depleted using two different siRNA, and a scrambled siRNA was used as a control. After each experiment repetition, the leftover cells were lysed to confirm the efficacy of the knockdown. Similarly to the USP11 SC2 cell line, a significant loss of the GFP signal was observed upon transient loss of USP11. Most significant advantage of flow cytometry is that it allows accurate monitoring of the behavior of an entire, yet precisely defined cell population. Hence, unforeseen interference of any potential artifacts with the readout is minimized. Moreover, in these experiments USP11 was depleted in

two fundamentally different ways and the results pointed to the same conclusion. The advantage of a transient depletion of a protein with siRNA is that the cells have no time to adapt and compensate for the depleted protein, although often it is pointed out that siRNAs have significant off-target effects. To overcome this drawback, two USP11-specific target sequences were used. Another drawback of this technology is that each experiment requires transfection with reagents that are damaging to the cells. To account for this, scrambled sequences are used as a transfection control. Interestingly, the exact contribution of the transfection as a cell stressor was quantified in our experiments and we identified transfection a contributing factor to the cumulative effect on autophagy. On the other hand, the advantage of using CRISPR/Cas9 method to deplete a protein is the reliability of the permanent protein depletion and avoidance of any additional stressors. The drawback of stable protein depletion is that it allows the cells to adapt, often leading to the absence of, or an attenuated phenotype. Therefore, using distinct depletion methods, as well as sufficient and appropriate controls is essential to obtaining meaningful results. Despite the described advantages of using flow cytometry, the drawback is that it mirrors the population behavior only at a specific time point. To this end, we employed long-term live cell imaging. Long-term live cell imaging provides a remarkable insight in studying dynamic processes, such as autophagy. However, considering it automatically records images and calculates the GFP/RFP ratio, it is prone to record potential artifacts, and it does not account for different proliferation rates of different cell lines. This, of course, is the reason for having an internal control, RFP. However, the denser the cell population gets over longer periods of time, the more secondary effects on cell signaling on the molecular level can be accumulated. Meaning, it may affect the fluorescent readout. Considering the first drawback, flow cytometry is a superior method, as it allows to precisely define the cell population of interest. Thereby, it excludes doublets, dead cells, or any outlying cell population. These factors should be considered when analyzing automatically acquired and calculated data, which is the case here. To account for the latter drawback, the fluorescent ratio was normalized to 1 at time point 1 hour. Nonetheless, both may be one of the reasons to account for differences in the autophagic flux assessed by the same readout,

namely, the GFP/RFP ratio, by flow cytometry and live cell imaging. Although importantly, the trend of the difference in the fluorescence ratio between the NHT SC1 and the USP11 KO SC2 cell line at time point 4 hour is visible in live cell imaging as well, it becomes statistically significantly different only at the later time points. Another important factor to consider is the mean of the autophagy induction; EBSS used in flow cytometry experiments compared to mTOR inhibition by Torin1 in long-term live cell imaging. EBSS induces autophagy via mTOR, however, it is expected to have a more broad effect on cellular signaling compared to a direct, chemical mTOR inhibition, and this has to be taken into consideration when comparing the data, and potentially the reason why live cell data shows slightly attenuated effect compared to the flow cytometry data obtained with EBSS treatment. Of interest to keep in mind is that Torin1 inhibits both mTORC1 complexes, not just autophagy-relevant mTORC1. Importantly, the long-term live cell imaging confirmed there is no difference between the NHT SC1 cell line, and the monoclonal cell line used for knockdown experiments, justifying its use as a control in relations to the USP11 knockout cell line. In general, the advantage of live cell imaging is providing more reliable and relevant insights in biological processes compared to "snapshots" fixed samples are providing, or any samples collected at a certain time point. In addition, cells are studied in their optimal conditions, without any additional stress, such as trypsinization that flow cytometry requires. However, the disadvantage of the fluorescent live cell imaging is autofluorescent background that can interfere with the readout, photobleaching that occurs over a longer period of time, and some others discussed above. Hence, combining both flow cytometry, and long-term live cell imaging well compensates for drawbacks of each described method, and importantly, here both collectively identify USP11 as a negative regulator of autophagy. The third approach to determine the effect of loss, or overexpression of USP11 on autophagy is by monitoring the LC3 lipidation by western blot. First, LC3 lipidation was monitored by western blot in a CHX chase in NHT and USP11 polyclonal knockout cell lines. CHX was added to the medium to limit the cells to use only their existent, cytoplasmic LC3 pool, and eliminate the potential contribution of newly synthesized LC3. After 6 hours of autophagy induction with EBSS and BafA1 treatment to block the

autolysosomal degradation, significantly more lipidated LC3 (LC3-II) was accumulated in USP11 knockout cells compared to NHT control cells. This suggested an accelerated autophagy rate upon loss of USP11. Importantly, qPCR analysis of LC3B mRNA levels showed no difference between control NHT and USP11 KO cells. Although this data requires further repetition, it suggested there is no effect on the LC3 transcription level. However, an additional effect of USP11 on the transcription or translation cannot be excluded. USP11 was shown to regulate IKKα transcription upon TNFα stimulation (Yamaguchi et al. 2007). Moreover, USP11 was shown to regulate transcription factors p53 (Ke et al. 2014) and E2F1 (Wang et al. 2017), transcription co-factor VGLL4 (Zhang et al. 2016), chromatin remodelers ARID1A (Luo et al. 2020) and EZH2 (Yang et al. 2017), histone modifications (Maertens et al. 2010; Ting et al. 2019), as well as the translation initiation factor eIF4B (Kapadia et al. 2018), all of which have effects on gene expression and mRNA translation. In particular, p53 was shown to have both positive and negative effect on autophagy induction (Feng et al. 2005; Tasdemir et al. 2008; Crighton et al. 2006). It is therefore not unlikely that USP11 might play a role in regulating autophagy on transcriptional or translational levels via p53, or via any other described substrate and interactor. To address this question, transcriptomics analysis can be conducted to determine how exactly the expression profile of cells changes depending on USP11 under autophagy induction. However, this was beyond the scope of this project. The controls needed for the experiments conducted here did not suggest transcriptional regulation, but overall it cannot be excluded completely. Considering the loss of USP11 led to an increase in the autophagic flux, the question was if overexpression of USP11 led to a decrease in the flux. Indeed, as evaluated by monitoring the LC3 lipidation by western blot, overexpression of USP11 led to a striking reduction in the LC3-II levels compared to both untransfected control and the tag-only control. Again, both controls were necessary to gain reliable data, as overexpression itself induced autophagy. The reduction of LC3-II levels in the USP11 knockout cells is even more striking considering that a polyclonal cell line was used. Using polyclonal cell lines has obvious advantages, as it excludes reliability on the potential monoclonal defects. However, the polyclonal cell lines often

have different protein depletion efficiency, different random off-target effects amplified over time etc. leaving a lot of room for a minor subpopulation to mask a potential phenotype reflecting the rest of the population. Hence, when using a polyclonal cell line, and a readout that in an unbiased manner reflects the entire population, like western blots, shows a convincing reduction on a protein level, it is a striking observation. Unanimously, the data presented here identified USP11 as a negative regulator of autophagy. What would be interesting to further investigate is the contribution of the activity of USP11 in autophagy regulation. In the context of USP11 as a negative regulator of NF-κB signaling, shown to regulate IκBα stability (Sun et al. 2010), overexpression of catalytic inactive USP11 partially rescued the phenotype suggesting USP11 has a scaffolding role, too. To investigate this aspect, the catalytic inactive USP11 can be overexpressed or an USP11 inhibitor can be used. Interestingly, mitoxantrone (MTX) was described as a USP11 inhibitor (Burkhart et al. 2013), despite originally being identified as a topoisomerase inhibitor (Crespi et al. 1986; Bellosillo et al. 1998), suggesting severe off-target effects. In our hands, MTX was toxic, even at lower concentrations (data not shown) and induced cell death. Considering the former, overexpressing catalytic inactive USP11 comes with different challenges. The RPE1 cells, where stable USP11 knockout was established, have poor transfection efficiency, therefore requiring more potent and more toxic reagents to achieve near-endogenous USP11 expression level, which affects autophagy per se. Moreover, Cas9 in these cells can efficiently attenuate the exogenous USP11 expression (data not shown) and creating the guide-resistant USP11 construct requires multiple mutagenesis steps. To bypass this, the overexpression of the catalytic inactive USP11 in cells with the endogenous USP11 present is an alternative, however, may not demonstrate the dominant negative effect over the active, endogenous USP11. These described challenges well reflect the issues encountered while trying to rescue the autophagy phenotype by overexpressing the WT USP11 in knockout cell lines. Therefore, generation of a guide-resistant USP11 construct will be crucial for further research. Furthermore, the development of the specific and potent USP11 inhibitors would be a helpful tool. One important step in this direction is the discovered USP11-specific targeting

peptide (Spiliotopoulos et al. 2019), however, it is targeting the non-catalytic domain of USP11, and has only been investigated in the context of homologous recombination–mediated DNA repair, so the potential to be used in the context of autophagy, and as an inhibitor, is yet to be established.

3.2 The USP11-dependant autophagy regulation is mechanistically conserved in *Caenorhabditis elegans*

Remarkably, the USP11-dependent autophagy regulation is mechanistically conserved, as the results obtained from the human cell culture were reproducible in the model organism *Caenorhabditis elegans (C. elegans)*. To establish the USP11 effect on autophagy in *C.elegans*, the USP11 ortholog, H34C03.2, was depleted using siRNA in a worm strain expressing GFP-tagged LGG-1 (GFP::LGG-1). The empty vector was used as control, and H34C03.2 depletion was confirmed after each experiment by qPCR. Both by evaluating GFP-LGG-1 lipidation, as well as using confocal microscopy to evaluate GFP-LGG-1 punctae formation, it was confirmed that the loss of H34C03.2 led to increased GFP-LGG-1-II levels, and increased punctae formation, both indicating a higher autophagy rate. Importantly, these experiments reflect increased basal autophagy rate, as the worms were only treated with BafA1. Although monitoring the LGG-1 lipidation is not as straightforward as monitoring the LC3 lipidation in human cells, the quantification of the western blots and normalization to a loading control, as well as to the LGG-1-I, increases reliability of the data. The greatest advantage of using a model organism is the availability of engineered strains that serve as disease models. They allow investigation of a protein function in a disease context that affects a whole organism, and in the case of *C. elegans*, in a fast, reproducible, and inexpensive way. One such strain expresses the human β-amyloid protein 1-42 (hAβ42) specifically in the muscle cells. Similarly to what happens to neurons with high aggregation-prone protein expression leading to the neuronal cell death and disease, these worms become paralyzed over time. Mechanistically, it is due to a proteasome- and autophagy-mediated degradation system being

overwhelmed by the aggregation. This phenotype can be recorded and quantified. Strikingly, the loss of H34C03.2 led to a delayed phenotype in adult worms compared to the EV control. This data implies a therapeutic potential in restricting USP11 and unleashing the autophagic potential. Hence, as already discussed, it would be important to dissociate the contribution of the protein presence and its catalytic activity, and to establish if inhibiting the activity of USP11 results in the same phenotype as knocking it down, or out. In the context of *C. elegans*, it is important to note that H34C03.2 is the human USP4 ortholog, however, human USP4, USP11 and USP15 are paralogues, containing high domain architecture similarity, and high sequence similarity. Phylogenetic and syntenic reconstruction methods revealed USP11 is a result of small-scale USP4 duplication (Vlasschaert et al. 2015). Therefore, H34C03.2 is an ortholog of all three DUBs: USP4, USP11, and USP15.

3.3 USP11 likely regulates autophagy via multiple interactions

USP11 was first linked to autophagy regulation by mass spectrometry interactome analysis of 32 autophagy-related proteins in 293T cells (Behrends et al. 2010). It was identified as a high confident interaction partner of the ubiquitin-like conjugation machinery, as well as the lipid kinase complex. Precisely, USP11 was found in the ATG4B, ATG12, and ATG10 immunoprecipitations, as well as VPS34, Beclin-1 and AMBRA1. Moreover, it was found to co-immunoprecipitate with LC3A, LC3B and LC3C, as well as GABARAPL1 and L2. Additionally, as a validation of the found results, USP11 was knocked down with 4 siRNAs in U2OS under basal conditions and after 6 hour Rapamycin treatment, and the LC3B punctctae were quantified. This experiment revealed that the loss of USP11 resulted in an increase in the LC3B-positive punctae. As discussed, this could be due to an increase of the flux, or due to the inability to efficiently degrade autophagosomes in the late stages of autophagy. Here, multiple proteomics approaches were employed to elucidate the precise molecular mechanisms of the USP11-dependent

autophagy regulation. Our interactome data after 4 h Torin1 treatment confirmed USP11 involvement with various autophagy complexes. In other words, USP11 being a novel negative regulator of autophagy could be defined as the total summary of all USP11 autophagy-related interactions that result in autophagy restriction. We verified the quality of the acquired interactome data by performing co-immunoprecipitation experiments with two candidate E3 ligases, HUWE1 and ZNF598. Both of them were identified as USP11 interactors by mass spectrometry under basal conditions (data not shown), and after 4 h Torin1 treatment. A smeared HUWE1 band appearance in the USP11 (C318S) IP suggested that HUWE1 is likely a USP11 substrate. Interestingly, recently, HUWE1 was reported to regulate autophagy by regulating WIPI2 levels in an mTOR-dependent manner (Wan et al. 2018). Our preliminary data on HUWE1-dependent autophagy regulation was not conclusive (data not shown). On the other hand, ZNF598 appeared to be a more stable interactor of USP11 based on the band appearance on the western blot. Further confirmation of the reliability of the data was the identification of multiple proteins with published links to USP11 listed in Table 6.

Table 6: Label-free mass spectrometry led to the identification of reported USP11 interactors or substrates after 4 hours of Torin1 treatment. A A table listing reported USP11 interactors or substrates, values plotted in the volcano plot, and published references. All the hits are significant (FDR<5 %)

Protein name	Log2 enrichment USP11 (C318S) over GFP	-Log Student's T-test p-value USP11 (C318S) over GFP	Published link to USP11
USP7	6,80	3,02	USP11 interactor ((Maertens et al. 2010; Shah et al. 2017) and more)
RAE1	2,04	1,81	Substrate, non-proteolytic signal (Stockum et al. 2018)
PEG10	1,77	2,69	E2F1 TF (USP11 substrate) regulates

			peg10 mRNA (Wang et al. 2017)
PPP1CC;PPP1CA;PPP1CB	1,57	2,71	Substrate (Sun et al. 2019)

Regarding the autophagy-related proteins, two key kinases necessary for autophagy induction, mTOR and PRKAA1 (AMPK catalytic subunit) were identified. Furthermore, a striking number of proteins with published link to PI3KC3 complex were identified, as well. Moreover, TMEM41B, important for the autophagosome maturation is found, too. Interestingly, a genome-wide, high-throughput siRNA screen identified USP19 and USP24 as proteins knockdown of which increases autophagic flux under basal conditions and both of them were found in our dataset (Lipinski et al. 2010).

A comprehensive list of most prominent overall autophagy-related USP11 interactors can be found listed in Table 5 with references and in table below without references, however, in chronological order of their activity in autophagy. This implies USP11 involvement not only in different complexes, but also at different stages of autophagy. This makes investigating the role of USP11 in the context of autophagy challenging, as it requires molecularly dissecting each stage of autophagy, to try to dissociate contributions of different interactions on the autophagic flux, assessed by LC3 lipidation.

Table 7: Label-free mass spectrometry led to the identification of multiple autophagy-related proteins after 4 hours of Torin1 treatment. A table listing reported autophagy-related proteins in chronological order of their activity in the process.

Induction	PI3KC3 complex (membrane initiation)	PI(3)P effector proteins	LC3 conjugation machinery, autophagosome maturation
mTOR	HUWE1	HUWE1	PPP1CC;PPP1CA;PPP1CB
PRKAA1 (AMPK catalytic subunit)	USP19		TMEM41B
TRIM28	DDB1		GNBL1 (RACK1)

USP24	RNF2
	TRIM28
	VPS15
	GNBL1 (RACK1)

In the following section, individual protein complexes investigated in this project will be discussed in more detail. However, there are many interesting autophagy-related proteins found in our proteome-wide and interactome screens that were not investigated here, yet likely also contribute to the observed phenotypes.

3.4   USP11 regulates autophagy via the PI3KC3 complex I

We could identify VPS15, a PI3KC3 complex component, in the USP11 interactome analyzed from the cells after 4 hour Torin1 treatment. Moreover, we identified the regulators of PI3KC3 complex in the interactome, too, listed above in Table 7. Considering the strong evidence pointing in the direction of PI3KC3 complex, we went on to investigate the connection between USP11 and the lipid kinase complex. Indeed, we could co-IP USP11 with all components of the PI3KC3 complex, both under basal conditions, and after autophagy induction. Importantly, the aforementioned co-IPs were done under mild lysis conditions, thus the complexes were preserved, meaning any of the suspected interactors could be interactors of a close USP11 interactor, but not interact with it directly. This is especially important in the case of triple overexpression experiments, specifically for Beclin-1 and ATG14 co-IPs. Given that the placement of USP11 within the complex is consistent with published data (Behrends et al. 2010), it is indeed highly likely that USP11 interacts with the complex directly. However, how the protein bands appeared on the western blot with the catalytically inactive USP11 was protein-dependent. VPS34 and Beclin-1 showed two distinct bands suggesting a mono-modification, whereas NRBF2 appeared to be heavily modified. ATG14 and VPS15 seemed to interact with USP11 irrespectively of activity of USP11, as well as irrespectively of autophagy status of the cells. Importantly,

in the context of NRBF2, we found that the protein is stabilized in USP11 knockout cells, as opposed to other complex components that had unchanged levels in the USP11 knockout cells. Based on our CHX chase, it seems unlikely this is due to the increased NRBF2 transcription and translation, however, this cannot be fully excluded, as discussed in the context of LC3. Moreover, the presented evidence of USP11-dependent modification implies a regulation via PTMs. It is unclear if the modification is the cause of the stabilization, in the case where this modification leads to a stronger complex formation, and the protection from degradation, or if this modification is a result of stabilization, in case where it is leading to a stronger complex formation, preventing access for an E3 ligase to target NRBF2 for degradation. The complexity of this question is emphasized by the fact that loss of USP11 does not have the reciprocal effect on stability as USP11 overexpression, but it does in terms of complex formation. To our knowledge, this is the first time that NRBF2 is reported as a protein with increased turnover rate in autophagy. It is likely that this is a mechanism of a negative feedback loop restricting formation of the autophagosomal membranes after prolonged starvation. We hypothesized that one of the initial steps to restrict the activity of the complex upon prolonged starvation is to eliminate the dimerizing subunit. It was shown that in monomeric form, the complex is still active, however, not to a degree as the dimeric form (Araki et al. 2013). Concerning the modification on NRBF2, this also raises the question of the E3 ligase responsible for the deposition of this modification. This hypothetical E3 ligase is the likely USP11 substrate. In the absence of USP11, it is either degraded, as USP11 is not present to deubiquitinate and stabilize it, or it is regulating a non-degradation signal on the E3 ligase impairing its activity to efficiently target NRBF2. In our interactome screen, we identified several E3 ligases, including HUWE1, that has a reported role in autophagy regulation (Di Rita et al. 2018; Wan et al. 2018). Our preliminary data did not confirm that the modulation of HUWE1 levels affects autophagy (data not shown). It would be interesting to take a look at other E3 ligases identified in our interactome. Regardless, our observation is that the PI3KC3 complex I is more stable in the USP11 knockout cells, and this is reflected in a higher complex activity. It is still unclear what is the exact cause of this increased

activity. All complex components seem to be modified in an USP11-dependent way, except for ATG14. Furthermore, the band appearances imply different nature of these modifications further increasing the complexity of USP11 role in the complex. As VPS34 is the lipid kinase component, it was investigated in more detail. VPS34 has been reported to be ubiquitinated, SUMOylated, acetylated, and phosphorylated (Ohashi, Tremel, and Williams 2019). The band appearance could be caused by any of them. Regarding the published data, a similar band appearance confirming existence of a double band was observed and attributed to both phosphorylation and SUMOylation (Yuan, Russell, and Guan 2013; Yang et al. 2013). In the former publication in Figure 2 A, the upper band of VPS34 is absent in the presence of mutant Rag GTPases that inhibit mTOR, however the phenomena is not discussed. In the latter, the majority of the figures depict modified and unmodified VPS34. We also undertook significant efforts to identify the modification type and site on VPS34, thus far without success (data not shown). The alternative strategy that involved mutating the reported sites or using the enzymes to catalytically reserve the modification only implied it might be ubiquitination. However, both in our interactome, as well as in the GlyGly mass spectrometry experiment, we identified TRIM28 (KAP1), previously reported to SUMOylate VPS34 at Lys840 enhancing its association with the complex (Yang et al. 2013). We mutated the site, but did not observe the loss of the upper band co-immunoprecipitating with USP11 (C318S). However, this may be due to the contribution of other sites or modifications. Moreover, in the aforementioned publication, the authors similarly used a recombinant SENP5 to reverse the modification, and while successfully collapsing high molecular weight SUMO1 chains made in an *in vitro* reaction on VPS34, a single band remained. Therefore, the best way to identify the modification is by mass spectrometry analysis. One challenge that we encountered whilst addressing the VPS34 modification by mass spectrometry, is that the fraction of intracellular VPS34 that interacts with USP11 is small, as seen by ratio of input and co-immunoprecipitated VPS34 with USP11 (C318S). Within this small fraction, and even smaller fraction is found in the modified form, as seen by the ratio of the upper to the lower band. To overcome this, a large starting amount of cell material was needed, however, this was still

insufficient to detect the modified peptide. Having established that USP11 interacts with the VPS34 complex, regulates the PTM status on several subunits (VPS34, Beclin-1, and NRBF2), and that the loss of USP11 led to increased levels of NRBF2, we asked next if this results in increased complex formation, and more importantly, increased complex activity. To address the former, we performed endogenous co-immunoprecipitation of ATG14, and evaluated how presence or absence of USP11 favors the pro-autophagic complex formation. We found that the loss of USP11 led to an increase in complex formation as seen by increased co-immunoprecipitation of both endogenous VPS34, and Beclin-1 with ATG14 both after 30 min and 1 hour EBSS treatment. To address the latter, if increased complex formation translates into increased complex formation, we performed a kinase assay with a commercially available ELISA-based kit. To account for the overall USP11 effect on the complex, we aimed to co-immunoprecipitate the endogenous VPS34 under mild conditions to preserve the complex, from NHT or USP11 knockout cells in an autophagy time-dependent manner. Despite extensive optimization efforts, and a high amount of starting cell material, we could not achieve the predicted PI(3)P concentration range. To circumvent this, we decided to use an indirect, image-based approach, by quantifying WIPI2 punctae formation. The VPS34 lipid kinase produces PI(3)P of the autophagosome. Consequently, WIPI2 is recruited by binding to the PI(3)P, forming distinct punctae. We found that in the absence of USP11 more WIPI2 punctae are formed, indicative of higher kinase activity leading to the production of a higher amount of the PI(3)Ps. Taken together, we presented strong evidence of USP11-dependent regulation of the PI3KC3 complex, however the exact molecular mechanism remains elusive. Future research should aim to identify the distinct modifications on the complex components and the contribution of each of them to the complex stability and/or activity. Moreover, the identification of the mediator(s) responsible for these modifications, the likely direct USP11 substrate, would provide a more complete insight in this complex and the multilayered USP11-dependent autophagy regulation. Considering we demonstrated this regulation is conserved in *C. elegans*, it is worth noting that all complex components have identified orthologs, except for NRBF2, to the best of our knowledge

(Meléndez and Levine 2009; Tian et al. 2010; Yang and Zhang 2011; Cheng et al. 2013). Moreover, it has been shown that *C. elegans* VPS34 is K63 ubiquitinated by UBC-13–UEV-1–CHN-1 and that this promotes the stability of VPS34, implying that the non-proteolytical ubiquitination plays an important role in the complex regulation also in *C. elegans* (Liu et al. 2018).

3.5 USP11 regulates the stability of mTOR

When aiming to identify USP11 interactors that could elucidate the mechanism of USP11 autophagy regulation, we found mTOR to be a high confident hit. The serine/threonine kinase mTOR is one of the key metabolic regulators involved in almost any signaling pathway from lysosomal biogenesis via TFEB in mTORC1 to cytoskeleton rearrangement via PKCα in mTORC2 (Liu and Sabatini 2020). For autophagy regulation, only the mTORC1 is relevant and it is defined by its accessory proteins mLST8 and RAPTOR. In mTORC2, RAPTOR is replaced by RICTOR. Interestingly, in our interactome analysis we found RICTOR as a high confident USP11 interactor (log2 enrichment USP11 (C318S)/GFP 2,36, and –log student T-test p value 1,95). In the future, it would be interesting to determine which mTOR complex USP11 is associating with, and to which degree. We hypothesize it could be both, or that the preference for the complex is determined by cell type. The fact that mTOR was identified upon autophagy induction, but not under basal conditions as a USP11 (C318S) interactor via mass spectrometry (the second mass spectrometry dataset not shown), favors the association with the mTORC1 as it implies autophagy-dependent interaction, however, the identification of RICTOR under the same conditions challenges this hypothesis. It is worth noting again that the experiment was performed under mild lysis conditions, and any identified hit might not be a direct interactor of USP11, rather co-immunoprecipitated by a "bystander" principle. Moreover, the mTORC1 and mTORC2 signaling is highly interconnected, thereby cannot be considered strictly distinct. The published data implies USP11 links

to both mTORC1 and mTORC2 signaling pathways, however not to mTOR directly.

An active mTORC1 regulates protein translation by phosphorylating S6K, subsequently activated further by PDK1 (Alessi et al. 1998) leading to S6K-mediated phosphorylation of the members of the translation initiation complex, among which is eIF4B (Holz et al. 2005). Upon S6K-mediated phosphorylation, eIF4B dissociates from both S6K and mTOR leading to translation initiation. Interestingly, S6K was shown to phosphorylate USP11 at S453 leading to USP11 and eIF4B interaction and the stabilization of eIF4B by USP11 deubiquitination, thereby driving translation initiation (Kapadia et al. 2018). This publication directly links USP11 and mTORC1-mediated translation regulation placing USP11 on the same signaling axis as the active mTORC1, which indicates conditions under which autophagy is suppressed.

However, USP11 was also shown to deubiquitinate and stabilize PTEN in the nucleus, a negative regulator of PI3K/AKT pathway (Park et al. 2019). Furthermore, the same publication shows PTEN drives USP11 expression in a FOXO1/SIRT1 dependent-pathway leading to increased levels of USP11 and further stabilization of PTEN in a feed-forward mechanism. PTEN has been shown to positively regulate autophagy (Ueno et al. 2008; Errafiy et al. 2013; Arico et al. 2001), and as a known negative regulator of IGF-1-AKT-mTOR pathway, the extent to which USP11 stimulates autophagy via PTEN remains unclear. Considering AKT, one of the regulators of FOXO localization and thereby activity (Webb and Brunet 2014) is predominantly under mTORC2 regulation (Hay 2011), USP11 may have complex-specific roles with different outcomes for autophagy.

Here, we presented data implying mTOR could be a direct substrate of USP11. We confirmed USP11 interaction with mTOR in a co-immunoprecipitation experiment with the WT and the catalytic inactive USP11, with and without Torin1 treatment. We found that mTOR poorly interacts with the WT USP11, but well with USP11 (C318S). Moreover, mTOR seems to be heavily modified in the USP11 (C318S) sample, indicating it is likely a USP11 substrate. To determine if USP11 regulates mTOR stability, we performed a CHX chase experiment that revealed that in the absence of USP11, the levels of mTOR are significantly reduced

compared to the NHT cells where the levels are stable. Moreover, these reduced levels can be rescued by adding MG132, a proteasome inhibitor. This indicates that mTOR is a USP11 substrate, and that USP11 regulates a proteolytic signal on mTOR. Furthermore, when the co-immunoprecipitation with USP11, or USP11 (C318S) mutant was done after BafA1 and MG132 treatment, the smeared mTOR band was significantly more prominent with the catalytic inactive USP11.

What remains unexplored is what the USP11-dependent mTOR regulation means in the context of cell metabolism and autophagy. We observed the increased mTOR turnover in the USP11 knockout cells, however this is observed only after prolonged starvation, and with CHX blocking new protein synthesis. Yet, there seems to be a more acute effect on autophagy in the absence of USP11 as already after 30 min EBSS treatment we could observe upregulated NRBF2 levels, and after 1 h EBSS treatment we see increased WIPI2 punctae formation. However, it is unclear if additionally to the regulation of stability of mTOR, USP11 can affect the activity of mTOR at earlier autophagy time points. There are several approaches to address the activity of mTOR. The most straightforward is evaluating phosphorylation status of mTOR substrates by western blotting using phospho-site specific antibodies. Such proteins are downstream substrates like S6K and ULK1 that have available antibodies for the T389 and S757 sites, respectively. These signals need to be normalized to the signal of the total protein amount. Due to the involvement of S6K in both USP11 regulation (Kapadia et al. 2018), as well as contradictory findings with respect to regulation of autophagy (Klionsky et al. 2005), we concluded it is not a suitable substrate to use here. However, ULK1 is. Nonetheless, we found contradictory results (data not shown); while inhibitory ULK1 site S757 mediated by mTOR was more phosphorylated in the USP11 knockout cells suggesting higher mTOR activity and autophagy supression compared to the NHT at time points 15 min, 30 min and 1h of EBSS treatment, we observed the same increase for the activating site S555 mediated by AMPK, indicative of a higher ULK1 activity and an increased autophagy activation (Egan et al. 2011). A better approach, and a more global one, would be to do a phosphoproteomics analysis after autophagy induction in NHT and USP11 knockout cells. This would also allow

a more global view of all mTOR substrates, both mTORC1- and mTORC2-related ones. It may reveal a difference in a specific pathway branch, for which antibodies are not available, moreover, screening each substrate individually is time consuming and expensive. This approach would also elucidate the contradictory ULK1 phosphorylation observation. ULK1 has many known downstream autophagy-related substrates and they would be identified to confirm if indeed ULK1 is more active in USP11 knockout cells and the activating S555 site overrides the inhibiting site at S757. Interestingly, the activating S555 site on ULK1 is AMPK-dependent, and AMPK was identified in our USP11 interactome screen. It may be that the two events are decoupled, that the mTOR activity is unrelated to the increased AMPK activity activating ULK1. It is also a possibility that the time points we have chosen are reflecting intermediate period in which ULK1 is dissociating from mTOR and associating with AMPK. Importantly, AMPK is not regarded important in the starvation-induced autophagy, only glucose depletion. Within this project, we mostly focused on starvation-induced autophagy, however, Torin1 was used that targets the mTOR kinase directly and induces autophagy even in presence of amino acids, hence, may have led to AMPK-related observations.

Considering the importance and the wide effect both of these kinases have on cell metabolism, broad, mass spectrometry-based proteomic approaches, such as phosphoproteomic profile of the USP11 depleted cells would allow a complete overview of the pathways affected and the identification of the contribution to autophagy regulation.

4 Materials and methods

4.1 Materials

4.1.1 Equipment

Machine	Company
Avanti J-26 XP	Beckman Coulter
Automated cell counter TC20	Bio-Rad
BioSpectrometer basic + µcuvette G1.0	Eppendorf
Flow Cytometer BD FACS Diva	BD Biosciences
ChemiDoc MP imaging system	Bio-Rad
Centrifuge MicroStar 17	VWR
Centrifuge MicroStar 17R	VWR
Fusion express	witec
Heracell 150i, CO_2 incubator	Thermo Scientific
Incubator Heratherm Compact	Fisher Scientific
Incubator/Shaker Ecotron	Infors HAT
Incubator Heratherm Compact	Fisher Scientific
Light Cycler 480 II	Roche Life Sciences
MacBook Pro	Apple
Magnetic stirrer w. heating	VWR
Mastercycler Nexus X2	Eppendorf
Megafuge 16R + Rotor TX-400	VWR
Microwave	Siemens
Mini centrifuge Sprout	Heathrow Scientific
Mini-Sub Cell GT Cell	Bio-Rad
Mini-Protean Tetra Cells	Bio-Rad
Mini Trans-Blot Cells	Bio-Rad
NanoDrop One	Thermo Scientific
PH meter	Mettler-Toledo
Pipetman Neo P2, P10, P20, P200, P1000	Gilson
Pipetboy 2	Integra
PowerPac Basic Power Supplies	Bio-Rad
PowerPac HC High-Current Power Supply	Bio-Rad
Roller	A. Hartenstein
Scale M-Pact AX623	Sartorius
See-saw rocker SSL4	Stuart
TCS SP8 Confocal microscope	Leica
Thermoblock	Grant QBD2

Thermomix (from AR)	Eppendorf
Thermomix F1.5	Eppendorf
Vacusip aspirator	Integra Biosciences
Vacuum pump VP820	VWR
Vortex Genie 2	Scientific Industries
Water bath Aqualine AL5	Lauda

4.1.2 Software

Software	Company	Application
Adobe Illustrator CS5	Adobe Systems Inc.	Figure design
Biomath Calculators	Promega	Cloning vector:insert calculation
BLAST	NIH, USA	Sequence alignment, sequencing result analysis
FlowJo V9	FlowJo LLc	Flow cytometry analysis, figure design
ImageJ 1.48	NIH, USA	Western blot analysis, IF analysis
Image Lab 5.2.1	Bio-Rad	Gel electrophoresis imaging and analysis, western blot imaging and analysis
In-Fusion Tool	TaKaRa	Cloning primer design
Office for Mac 2011	Microsoft Corp.	Word, Excel, PowerPoint
Prism for Mac OS X 5.0b	GraphPad Software Inc.	Statistical analysis, figure design
QuickChange Primer Design	Agilent	Site directed mutagenesis primer design
Serial Cloner 2-6-1	Serial Basics	Cloning, primer design

4.1.3 Chemicals and reagents

Item	Cat. number	Company
10× PBS Dulbecco w/o Ca/Mg	D1408	Sigma-Aldrich
2-Propanol	20.842.323	VWR
Acetic acid	BP1185-500	Thermo Fisher Scientific
Acetic acid 100 %	A3686.0500	Applichem

Acetone	32201R	Sigma-Aldrich
Acetonitrile	AE70.1	Roth
Acrylamide-solution (40 %)	A4989,0500	Applichem
Agarose LE GeneticPure	850070	Biozym Scientific
Albumin Frakt. V >98 % Prot./IgG-free	T844.2	Carl Roth
Ammonium bicarbonate (ABC)	S2454	Sigma-Aldrich
Ammonia solution 25 % for LC-MS	5.33003.0050	Merck
Ammonium peroxidisulphate (APS)	9592.3	Carl Roth
Ampicillin sodium salt	K029.1	Carl Roth
Antarctic phosphatase	M0289	NEB
Aprotinin	A2132	Applichem
Bafilomycin A1	B-1080	LC Laboratories
Benzonase (25.000U)	71205-3	Merck Chemicals
Blasticidin	ant-bl-1	InvivoGen
BradfordUltra	BFU1L	Expedeon
Bromphenolblue	A2331	Applichem
Calcium chloride dihydrate	A3587	Applichem
Chloramphenicol	A7495	Applichem
Chloroacetamide	22790	Sigma-Aldrich
Chloroform	32211	Sigma-Aldrich
Chloroquine		
Complete EDTA-free	4693132001	Roche
Cycloheximide solution	C4859	Sigma-Aldrich
Dimethyl sulfoxide (DMSO) for cell culture	A3672	Applichem
Dimethyl sulfoxide (DMSO)	A3006	Applichem
Dithiotreitol (DTT)	6908.2	Carl Roth
DMEM 4,5 g/l Gluc. M.Glutamaxl/o. Pyr.	61965-059	Life Technologies/ Invitrogen
DMEM/F-12, GlutaMAX™ Supplement	31331-093	Life Technologies/ Invitrogen
DMEM/F-12 for SILAC	88370	Thermo Fisher Scientific
DNA Ladder 1 kb	N3232	NEB
DNA MW Ladder 2-log (0,1-10 kb)	N3200L	NEB
Dializyed FBS for SILAC medium	26400044	Thermo Fisher Scientific
dNTP Set 4×25 umol in 4×250 µl (100 mM)	DNTP100-1KT	Sigma-Aldrich
Doxycycline hydrochloride	D9891	Sigma-Aldrich
EBSS (+Ca/Mg, +phenol red)	24010-043	Gibco/ Thermo Fisher
ECL Prime Western Blot Det. Reagent	RPN2232P	VWR

EDTA	A5097	Applichem
Ethanol 70 % distilled	T913.7	Carl Roth
Ethanol abs. distilled	K928.4	Carl Roth
Ethanol abs.	32205	Sigma-Aldrich
FBS South American	10270106	Thermo Fisher Scientific
Fe(II)-sulphate heptahydrate	215422	Sigma-Aldrich
Formic acid 98-100 %	1.11670.0250	Merck
Glucose (D+) monohydrate	A3730	Applichem
Glycine	A1067	Applichem
HEPES 99,5 %	A1069	Applichem
Hexadimethrine bromide (polybrene)	H9268	Sigma-Aldrich
Hydrochloric acid 37 %	X942.1	Carl Roth
Hygromycin B (50 mg/mL)	10687-010	Thermo Fisher Scientific/ Life Technologies
InstantBue	ISB1L	Expedeon
INTERFERIN siRNA transfection reagent	409-10	VWR
jetPRIME®	114-15	Polyplus Transfection
Kanamycin sulphate for cell culture	T832.1	Carl Roth
Ku-0063794	Cay13597-5	Biomol
L-arginine (R0)	A8094	Sigma
L-lysine (K0)	L8662	Sigma
L-arginine-U-13C6-15N4 99 % (R10)	CNLM-539	Cambridge Isotope Laboratories
L-lysine-U-13C6-15N2 99 (Lys8)	CNLM-291	Cambridge Isotope Laboratories
Leupeptin hemisulfate	A2183	Applichem
Lipofectamine 2000	11668019	Invitrogen
Lipofectamine RNAiMAX	13778075	Invitrogen
Lysyl endopeptidase (LysC)	4987481427648	Wako Chemicals
Luria Agar (Millers LB Agar)	X969.3	Carl Roth
Luria Broth Base (Millers LB Br.B.)	X968.3	Carl Roth
Magnesium chloride hexahydrate	A4425	Applichem
Magnesium sulphate heptahydrate	A1037	Applichem
Mangan(II)chloride × 4H_2O	T881.1	Carl Roth
Methanol HPLC	20864.290	VWR
Methanol	32213	Sigma-Aldrich
MG132 (Z-Leu-Leu-Leu-CHO)	C2211	Sigma-Aldrich Chemie
Mycoplasma-Off	OAD-1000 (W15-1000)	Biochrom AG

MOPS	102370	MP Biochemicals
N-Ethylmaleimide (NEM)	E3876	Sigma-Aldrich
Nonidet p-40/Igepal Ca-630	A1694	Applichem
nuPAGE LDS Sample Buffer (4×)	NP0007	Life Technologies
Opti-MEM, serum-depleted	31985-062	Life Technologies/ Invitrogen
Paraformaldehyde 4 % in PBS pH>6.5	sc-281692	Santa Cruz
PBS Dulbecco with Ca/Mg	D8662	Sigma-Aldrich
PBS Dulbecco w/o Ca/Mg	14190-169	Life Technologies/ Invitrogen
Phenylmethansulfonyl fluoride (PMSF)	6367.1	Carl Roth
Phosphoric acid	345245	Sigma-Aldrich
PhosSTOP Inhibitor Tablets	4906845001	Roche
Polyethylenimine, linear (MW 25000)	23966-2	Polysciences Europe
Potassium chloride	31248	Sigma-Aldrich
ProLong Gold Antifade Reagent with DAPI	P36941	Thermo Fisher Scientific/ Life Technologies
Propanol-2	A3928	Applichem
Protein MW Marker (10-245 kD) prest.	A8889	Applichem
Puromycin dihydrochloride	P8833	Sigma-Aldrich
Rnase AWAY spray bottle	A998.4 (7002-MBP)	Carl Roth
Roti-Safe Gel Stain	3865.1	Carl Roth
SDS Buffer (20×), sterile filtered	1057.1	Carl Roth
SDS solution 20 %	A0675	Applichem
Sequencing grade Trypsin (0.5 µg/µl in 50 mM acetic acid)	11 418 475 001	Sigma-Aldrich
Sodiumazide	A1430	Applichem
Sodium dihydrogen phosphate monohydrate	28015.261	VWR
Sodium chloride	31434R	Sigma-Aldrich
Sodium deoxycholate	A1531	Applichem
Sodium fluoride	A3904	Applichem
Sodium orthovanadate 99,98 %	450243	Sigma-Aldrich
Sodium phosphate	342483	Sigma-Aldrich
Sodium pyruvate	11360-039	Life Technologies/ Invitrogen
TEMED	2367.3	Carl Roth
Torin1	4247	Tocris Bioscience
Trichloroacetic acid	T6399	Sigma-Aldrich
Trifluoroacetic acid (TFA)	302031	Sigma-Aldrich

TRIS	AE15.3	Carl Roth
(Tris(2-carboxyethyl)phosphine) (TCEP)	646547	Sigma-Aldrich
Triton-X 100	3051	Carl Roth
Trypsin/EDTA (1×) HBSS with phenolred	25300-054	Life Technologies/ Invitrogen
Tween®20	P9416	Sigma-Aldrich
Tween®20	A4974	Applichem
Ubiquitin-Propargylamide (Ub-PA)	UbiQ-057	UbiQ
UltraPure™ DNase/RNase-free distilled water	10977035	Thermo Fisher Scientific
UltraPure™ DNase/RNase-Free distilled water	10977035	Life Technologies/ Invitrogen
Urea	A1049	Applichem
Venor GeM 100T #VGM-100	11-1100	Minerva Biolabs

4.1.4 Cloning enzymes

Item	Cat. number	Company
Alkaline Phosphatase	M0290S	NEB
BamHI	R3136S	NEB
BsmbI	R0739	NEB
DpnI	R0176S	NEB
MB TAQ DNA Polymerase	53-0100	Minerva Biolabs
NotI	R3189S	NEB
PfuUltra II Fusion HS DNA Polymerase	600672	Agilent
Phusion High-Fidelity DNA Polymerase	M0530S	NEB

4.1.5 Bacteria, cloning kits, qPCR kits

Item	Cat. number	Company
NovaBlue Singles Competent Cells	70181-4	Merck Millipore
Stellar Competent Cells	636766	TaKaRa/Clontech

In-Fusion® HD Cloning Kit	638917	TaKaRa/Clontech
EZNA Gel Extraction Kit, Classic	12-2501-02	Peqlab
Gel Extraction Kit	20021	QIAGEN
QIAquick Gel Extraction Kit	28706	QIAGEN
EZNA Plasmid Miniprep I Classic	12-6942-02	Peqlab
PureYield Plasmid Maxiprep System	A2393	Promega
PeqGOLD Total RNA Kit	12-6834/12-6634	Peqlab
cDNA Reverse Transcription Kit (High capacity)	4368814	Life Technologies
LightCycler 480 SYBR Green I Master	04707516001	Roche

4.1.6 Buffers and solutions

Cell lysis/co-immunoprecipitation

Buffer	Composition
RIPA lysis buffer	50 mM TRIS-HCl pH 7.5, 150 mM NaCl, 1 % NP-40, 0.5 % Na-deoxycholate, 0.1 % SDS, 0.5 µL/mL Benzonase, Aprotinin 1.5 µM, Leupeptin 100 µM, PMSF 1 mM, 10 mM
GFP-Trap® bead Immunoprecipitiation (IP) lysis buffer	20 mM TRIS-HCl pH 7.5, 150 mM NaCl, 1 % NP-40, 0.5 % Triton-X, Aprotinin 1.5 µM, Leupeptin 100 µM, PMSF 1 mM, 10 mM NaF
GlyGly modified RIPA buffer	50 mM TRIS-HCl pH 7.5, 150 mM NaCl, 1 mM EDTA, 1 % NP-40, 0.1 % Na-deoxycholate (+phosphatase inhibitor tablet, +protease inhibitor tablet, +NEM)
Endogenous ATG14 IP lysis buffer / wash buffer	20 mM TRIS-HCl pH 7.5, 150 mM NaCl, 0.05 % NP-40 (+protease inhibitor tablet)
GFP-Trap® bead Immunoprecipitiation (IP) wash buffer	20 mM TRIS pH 7.5, 150 mM NaCl
DUB buffer	500 mM NaCl, 500 mM TRIS-HC- pH 7.5, DTT 50 mM

SDS-PAGE, western blotting

Buffer	Composition
SDS-PAGE unning buffer	25 mM TRIS, 1.92 M Glycine, pH 8.3, 1 % SDS
Transfer buffer	25 mM TRIS, 1.92 M Glycine, pH 8.3, autoclave
TBS	50 mM TRIS, 150 mM NaCl, pH 7.5, autoclave
TBS-T	TBS, 0.1 % Tween®20
Blocking solution	2.5 % BSA in TBS-T
Antibody solution	2 % BSA, 0.05 % NaN_3 in TBS-T

Fluorescent western blotting

Buffer	Composition
Blocking solution	0.2 % I-Block™, 0.1 % Tween®20 in PBS
Antibody solution	0.2 % I-Block/PBS-T

Mass spectrometry

Buffer	Composition
GlyGly denaturation buffer	6 M urea / 2 M urea in 10 mM HEPES pH 8
GlyGly digestion buffer	50 mM ammonium bicarbonate in H_2O pH 8
GlyGly reduction buffer	1 M Dithiothreitol
GlyGly alkylation buffer	550 mM CAA
GlyGly digestion buffer	0.5 µg/µL LysC / 0.5 µg/µL Trypsin in GlyGly digestion buffer
GlyGly SepPak washing buffer	0.1 % TFA
GlyGly SepPak elution buffer	50 % Acetonitrile, 0.1 % TFA
GlyGly x10 IAP buffer	500 mM MOPS pH 7.2, 100 mM Na_3PO_4, 500 mM NaCl
GlyGly IP wash buffer 1	×1 IAP buffer, 150mM NaCl, 0.5 % NP-40
GlyGly IP wash buffer 2	×1 IAP buffer

GlyGly Micro SCX extraction disk wash buffer	40 % Acetonitrile, 0.1 % TFA in H_2O
GlyGly Micro SCX extraction disk elution buffer concentrate	40 mM Acetic acid, 40 mM Boric acid, 40 mM Phosphoric acid
GlyGly Micro SCX extraction disk elution buffer	Acetonitrile:contentrate (above) 2:3
GlyGly Buffer A'	2 % Acetonitrile, 1 % TFA
C18 buffer A (wash buffer)	0.1 % Formic acid in water
C18 buffer B (elution buffer)	80 % Acetonitrile, 0.1 % Formic acid
GFP-Trap® on-bead digest elution buffer	50 mM ABC, 2 % Na-deoxycholate, 5 mM TCEP, 20 mM Chloroacetamide (CAA)
GFP-Trap® on-bead digest dilution buffer	50 mM ABC
GFP-Trap® on-bead digest digestion buffer	0.5 µg/µL LysC / 0.5 µg/µL Trypsin in GlyGly digestion buffer
StageTip wash 1	0.1 % TFA in isopropanol
StageTip wash 2	0.1 % TFA in H_2O
StageTip elution	5 % Ammoniumhydroxide in 80 % Acetonitrile

4.1.7 Cloning

Buffer	Composition
LB medium for bacterial growth	25 g in 1 L H_2O, autoclave
LB-agar	40 g in 1 L H_2O, autoclave
dNTPs	2.5 mM each dNTP
TAE	40 mM TRIS, 20 mM Acetic acid, 1 mM EDTA, pH 8.4, autoclave

4.1.8 Plasmids

Plasmid	Source
pEGFP-N1	Clonetech (gift from Ivan Dikic Lab)
pEGFP-N1-USP11	Custom made Bremm Lab
pEGFP-N1-USP11 (C318S)	Custom made Bremm Lab
pEGFP-N1-USP11 (C318A)	Custom made Bremm Lab
pcDNA3-Myc-PIK3C3	Gift from Ivan Dikic Lab
pcDNA3-Myc-PIK3C3 (K96R)	Custom made Bremm Lab
pcDNA3-Myc-PIK3C3 (K158R)	Custom made Bremm Lab

pcDNA3-Myc-PIK3C3 (K209R)	Custom made Bremm Lab
pcDNA3-Myc-PIK3C3 (K346R)	Custom made Bremm Lab
pcDNA3-Myc-PIK3C3 (K630R)	Custom made Bremm Lab
pcDNA3-Myc-PIK3C3 (K840R)	Custom made Bremm Lab
pIREpuro2-HA-C1-ATG14	Custom made Bremm Lab
pIREpuro2-HA-C1-Beclin-1	Custom made Bremm Lab
pIREpuro2-HA-C1-NRBF2	Custom made Bremm Lab
pIREpuro2-HA-C1-VPS15	Custom made Bremm Lab
pCMV-HA-HUWE1 (511-4374)	Gift from Sonja Lorenz
pcDNA3.1-ZNF598-TEV-3xFLAG	Addgene
RK5-myc-mTOR	Gift from Ivan Dikic Lab
BSSK-8×his-ubiquitin	Gift from Stefan Müller Lab
pMRX-IP-GFP-LC3-RFP-LC3ΔG	Addgene
PCG Pol and SVG plasmids for viral transduction of the autophagy probe	Gift from Ivan Dikic Lab
PAX2 and pMD2.G plasmids for viral transduction for generation of CRISPR/Cas9 cells	Addgene

4.1.9 Primers and oligos

Oligos used to generate CRISPR/Cas9 knockout cell lines

Gene	Direction	Sequence
Non-human targeting (NHT) 1	5´-3'	Gaaaaagcttccgcctgatgg
Non-human targeting (NHT) 2	5´-3'	Gaaaacaggacgatgtgcggc
Non-human targeting (NHT) 3	5´-3'	Gaaaacatcgaccgaaagcgt
USP11 knockout 1	5´-3'	CACCggtctccatgatgatcaact
USP11 knockout 2	5´-3'	CACCgtgggcgagaacgtccactg
USP11 knockout 3	5´-3'	CACCGtgataggcagtggaacactg

4.1.10 siRNA

Target	Sequence	Cat. number	Company
siCtrl (non-targeting) AllStars Neg Control	n.a.	1027281	Qiagen
USP11	GCGCACAGCUGCAUGUCAU	J-006063-05	GE Healthcare/ Dharmacon
USP11	GAGAAGCACUGGUAUAAGC	J-006063-06	GE Healthcare/ Dharmacon
USP11	GGACCGUGAUGAUAUCUUC	J-006063-07	GE Healthcare/ Dharmacon
USP11	GAAGAAGCGUUACUAUGAC	J-006063-08	GE Healthcare/ Dharmacon

4.1.11 Antibodies

Primary antibodies	Cat. number	Company
ATG14	5504	Cell Signaling
Beclin-1 (D40C5)	3495	Cell Signaling
GAPDH (14C10)	2118	Cell Signaling
GFP (B-2)	sc-9996	Santa Cruz
HA-Tag (6E2)	2367	Cell Signaling
LC3A/B (D3U4C) XP	12741	Cell Signaling
mTor (7C10)	2983	Cell Signaling
Multiubiquitin chain (Clone FK2)	14220	Cayman Chemical
Myc-Tag (9B11)	2276	Cell Signaling
NRBF-2 (D8G1)	8633	Cell Signaling
p-Ulk1 (S757)	6888	Cell Signaling
p53 (1C12)	2524	Cell Signaling
Phospho-ULK1 (Ser555) (D1H4)	5869	Cell Signaling
PI3K Class III (D4E2)	3358	Cell Signaling
Tubulin	2125	Cell Signaling
ULK1 (D8H5)	8054	Cell Signaling
USP11	HPA003103	Sigma
Vinculin	V4505	Sigma
Vps15	A302-571A-M	BETHYL (Biomol)
WIPI2 (2A2)	ab105459	Abcam

Secondary antibodies	Cat. number	Company
Anti-mouse IgG-HRP	sc-2096	Santa Cruz
Anti-rabbit IgG-HRP	sc-2054	Santa Cruz
Anti-mouse IgG-HRP	7076	Cell Signaling
Anti-rabbit IgG-HRP	7074	Cell Signaling
Anti-mouse IgG (H+L) Cross-Adsorbed DyLight 755	SA5-10171	ThermoFisher
Anti-Rabbit IgG light chain (HRP)	99697	Abcam

Immunoprecipitation antibodies	Cat. number	Company
GFP-Trap® beads	gta	Chromotek
GlyGly enrichement antibody (PTM Scan ubiquitin branch motif IAP beads)	1990	Cell Signalling
Anti-Atg14 pAb	PD026	MBL
SureBeads Protein A Magnetic beads	161-4013	Bio-Rad

Immunofluorescence antibodies	Cat. number	Company
WIPI2 (2A2)	ab105459	Abcam
Anti-mouse-Alexa 488	A-11029	ThermoFisher

4.1.12 Cell lines

Cell line	Source
U2OS	German Collection of Microorganisms and Cell Culture (DSMZ)
RPE1	Gift from Manuel Kaulich Lab
RPE1 NHT	Custom made Bremm Lab
RPE1 USP11 KO	Custom made Bremm Lab
U2OS USP11 KO	Custom made Bremm Lab
RPE1 NHT + GFP-LC3-RFP-LC3ΔG	Custom made Bremm Lab
RPE1 USP11 KO + GFP-LC3-RFP-LC3ΔG	Custom made Bremm Lab
Hek293	German Collection of Microorganisms and Cell Culture (DSMZ)
Hek293T	Gift from Ernst Stelzer Lab

4.2 Methods

4.2.1 Cell culture

4.2.1.1 Cell maintenance

The Hek293 and the U2OS cell lines were cultured in DMEM, RPE1 in DMEM/F-12 supplemented with 10 % fetal bovine serum (FBS) and 1 % penicillin-streptomycin solution at 37 ^{o}C and 5 % CO_2. In addition, the medium of RPE-1 cell was supplemented with 200 µg/mL Hygromycin B. For the SILAC labeling, the RPE1 cells were cultured in the media containing K0 and R0 (light), or K8 and R10 (heavy), and dialyzed FBS for a total of 5 splitting cycles after which the amino acid incorporation was tested. The cells were split every 2-3 days in 1:6, or 1:12 ratios, respectively, by washing with PBS, adding 0.05 % Trypsin-EDTA, collecting in fresh media and seeding in a new dish.

4.2.1.2 Cryopreserving and thawing cells

Following the protocol for cell splitting, the collected cells were spun down at 800 × g for 5 min and the supernatant containing 0.05 % Trypsin-EDTA aspirated. The cells were resuspended in DMEM, or DMEM/F-12, supplemented with 10% DMSO and distributed in the cryotubes. The cryotubes were placed in isopropanol isolation container, and placed at -80 ^{o}C. Alternatively, for a long-term storage, the tubes were transferred to -150 ^{o}C. To thaw the cells, the contents of cryotubes were resuspended in the appropriate medium; DMEM, or DMEM-F12, and spun down for 2 min at 800 × g. The medium containing DMSO was aspirated and replaced by maintenance medium and cells were seeded in a new dish.

4.2.1.3 Cell transfection

Experiment in Figure 19 was done using jetPRIME following the manufacturer's protocol. For 1 μg DNA, 2 μl reagent was used, in 100 μl prewarmed Opti-MEM per well of a 6-well plate. Alternatively, cell transfection was performed using polyethylenimine (PEI) using 1/3 ratio of the DNA μg/PEI μl in 300 μl prewarmed Opti-MEM per 10 cm dish, and in 100 μl per well of a 6-well plate.

The knockdowns in the RPE1 cells were performed by reverse transfecting 2 μl of 20 μM siRNA diluted in 200 μl prewarmed Opti-MEM per well of a 6-well plate.

For all the above experiments, DNA or siRNA was pipetted directly into prewarmed Opti-MEM. Afterwards, the reagent was added. The mixture was vortexed for 10 s and quickly spun down. The mixure was left to incubate for 10 min at RT before being drop-wise added to the cells grown to 60-80 % confluency.

4.2.1.4 Stable cell line generation

Stably expressing GFP-LC3-RFP-LC3ΔG cells were generated by seeding 0.5×10^5 NHT and USP11 knockout cells, transducing 24 h later by replacing the medium with one containing 8 μg/ml Polybrene and 200 μl thawed lentiviral supernatant per well. 48 h later the cells were put under selection with a total of 14 days, after which they were sorted by FACS into single clones, in the 96-well plates and expanded.

Stable CRISPR/Cas9 knockout cells were generated by Verena Bittl (Goethe University), by seeding 0.5×10^5 RPE1 cells, transducing 24 h later by replacing medium with one containing 8 μg/ml Polybrene and 200 μl of the thawed lentiviral supernatant per well. Stably transduced cells were selected with 10 μg/ml puromycin and efficiency of USP11 knockout was confirmed by immunoblotting using antibody against USP11 (Figure 12).

4.2.1.5 Generation of high-titer lentivirus

To generate stably expressing GFP-LC3-RFP-LC3ΔG NHT and USP11 RPE1 knockout cells, 8×10^5 Hek293T cells were seeded into a 6-well plate, and cultivated in DMEM without antibiotics 24 h prior to transfection. The cells were transfected with 200 µl prewarmed Opti-MEM containing 9 µl Lipofectamine2000 and plasmids in ratio 1:1:3 PCG Pol:SVG:GFP-LC3-RFP-LC3ΔG plasmid for a total of 3 µg DNA. Medium was changed 12 h later and the viral supernatant was collected 24 h and 48 h subsequently, pooled, aliquoted, and stored at -80 °C.

The generation of the stable NHT and USP11 RPE1 knockout cells was done with Verena Bittl (Goethe University). 7.5×10^5 Hek293T cells were seeded into a 6-well plate and cultivated in DMEM without antibiotics 24 h prior to transfection. The cells were transfected with 200 µl prewarmed Opti-MEM and 3.3 µg transfer vector containing the gRNAs (pLentiCRISPRv2), 2.7 µg PAX2, and 1 µg pMD2.G. The medium was changed 12 h later, and the viral supernatant was collected 24 h and 48 h subsequently, pooled, aliquoted, and stored at -80 °C.

4.2.1.6 Flow cytometry

Cells were grown in 6-well plates, washed with PBS, and trypsinized in 100 µl 0.05 % Trypsin-EDTA, same as for cell splitting. The cells were collected in 1 ml PBS supplemented with 1 % FBS and passed through the cap filter of the FACS tubes. The cells were kept on ice until measurement.

4.2.1.7 Cell culture treatments with EBSS and various inhibitors

To induce autophagy with EBSS, cells were washed 2 × with EBSS and then EBSS was added.

To treat the cells with cycloheximide, a master mix was generated containing either CHX in EBSS, CHX and Mg132 in EBSS, or CHX and BafA1 in EBSS. The cells were washed 2 × with EBSS before adding the medium with the inhibitor(s).

The experiments in the Hek293 cells were done by adding the inhibitors directly into the medium to an appropariate concentration. All concentrations are listed below.

Inhibitor	Final concentration
Bafilomycin A1	200 mM
Choloroquine	50 µM
Cycloheximide	100 µg/ml
Bafilomycin A1	200 mM
MG132 (Z-Leu-Leu-Leu-al)	10 µM
Torin1	250 nM
KU-0063794	10 µM

4.2.1.8 Immunofluorescence

The WIPI2 immunofluorescence protocol was established by Alexandra Kalb (Goethe University). The cells were grown on the coverslips in 6-well plates until 70-80 % confluency, washed with PBS w Mg/Ca and fixed in 4 % PFA in PBS for 15 min at RT. Afterwards, coverslips were washed 2 × with PBS and cells permeabilized with 1 % Triton-X 100 in PBS for 15 min at RT. Coverslips were washed 2 × with PBS, followed by a final wash with PBS/0.05 % Tween 20. Coverslips were blocked with 2.5 % BSA in PBS/0.05 % Tween 20 by flipping them upside down on the parafilm where the blocking solution was previously carefully pipetted in a shape of a drop and incubated for 15-30 min at RT. After blocking, the coverslips were incubated in the primary antibody solution (WIPI2 1:250) in the same fashion as for blocking for 1 h at RT. The coverslips were then washed 3 × 5 min with PBS to remove the residual primary antibody solution by rocking them on the see-saw shaker. Subsequently, the coverslips were incubated in secondary antibody solution

(anti-mouse-Alexa 488 1:200) again in the same fashion for 1 h at RT shielded from the light. After the secondary antibody solution, the coverslips were washed with PBS for 3 × 5 min by rocking. To mount the slides, a drop of RT ProLong Gold Antifade Reagent with DAPI was placed on the slide, and the coverslips placed on top upside down avoiding generating air bubbles.

4.2.1.9 IncuCyte® live-cell imaging

The IncuCyte® live-cell imaging protocol was established by Mariana Tellechea and Alexandra Stolz (Goethe University). 7×10^4 RPE1 cells stably expressing the GFP-LC3-RFP probe, or the RPE1 NHT and the USP11 KO cells expressing the GFP-LC3-RFP-LC3ΔG probe were seeded in a 96-well plate (165305, Thermo) and grown o/n for 18 h. The cells were treated with 0.1 % DMSO control or 250 nM Torin1. The plate was subsequently placed and monitored in the IncuCyte® (Sartorius) for 20 h. The cells were scanned at indicated times for phase contrast and green/red fluorescence to obtain the information about the confluency and the autophagic flux, respectively.

4.2.2 Caenorhabditis elegans methods

All *C. elegans* experiments were done in collaboration with Andreas Kern and Christian Behl (Mainz University).

4.2.2.1 *Caenorhabditis elegans* knockdown and qPCR verification

According to standard procedures, *C. elegans* were maintained at 20 °C on the nematode growth medium plates seeded with HB101 *E. coli*. RNAi was induced by feeding dsRNA as described previously (Kern et al. 2010). The

knockdown efficiency was quantified by qPCR, analyzing mRNA levels of H34C03.2.

4.2.2.2 *Caenorhabditis elegans* autophagic flux analysis

The autophagic activity was investigated employing age-synchronized nematodes that express the GFP::LGG1 (ex[Plgg-1::GFP::lgg-1/pRF4], kind gift of Beth Levine). The worms were cultivated under RNAi conditions at 20 °C and at first day of adulthood treated with DMSO or bafilomycin A1 for 6 h. Thereafter, the worms were lysed and the GFP::LGG1 as well as the tubulin protein levels were evaluated by immunoblotting using NuPAGE 4-12 % Bis-Tris gels (Invitrogen) for protein separation and antibodies directed against GFP (Biolegend, BLD 902602) and tubulin (Sigma Aldrich, T9026) for detection. Alternatively, these worms were imaged by confocal fluorescence microscopy employing the laser-scanning microscope LSM710 (Zeiss, Oberkochen).

4.2.2.3 *Caenorhabditis elegans* paralysis assay

For the paralysis analysis, age-synchronized CL2006 (dvIs [Punc-54::hAß42/pRF4]) nematodes (Link 1995) were cultivated at 15 °C on RNAi plates. Starting at the first day of adulthood the worms were transferred onto fresh RNAi plates daily and were tested for paralysis by tapping their nose with a platinum wire. The worms that moved their head, but failed to move their body were scored as paralyzed. Dead nematodes or those that showed other phenotypes were not included into the statistics.

4.2.3 Molecular biology

4.2.3.1 Plasmid generation, cloning, and site directed mutagenesis

A PCR amplification mix was prepared according to the manufacturer's protocol for MB TAQ DNA Polymerase, PfuUltra II Fusion HS DNA Polymerase, or Phusion High-Fidelity DNA Polymerase by preparing a 50 µl mix per reaction, using a 40 ng DNA template, and 5 % DMSO. PCR reactions were ran according to the program stated below. The elongation time was calculated following the formula: 1 min/kbp of expected PCR product. For site-directed mutagenesis, elongation time was set to 10 min regardless of the template size, and 30 ng of template DNA was used. This protocol included additional incubation with DpnI for 2 h at 37 °C to digest the template DNA.

	Initial denaturation	Denaturation	Annealing	Elongation	Final extension	Storage
Temp.	95 °C	95 °C	60 °C	72 °C	72 °C	4 °C
Time	5 min	40 s	1 min	1 min/kbp	10 min	∞

The PCR primers for fragment amplification were designed with Online In-Fusion Tool and for site-directed mutagenesis using QuickChange Primer design. Primers used in this thesis are listed in tables below for PCR and site-directed mutagenesis, respectively.

Primers used for plasmid generation

Plasmid	Restriction site	Forward primer	Reverse primer
pEGFP-N1	BamHI	CGCGGGCCCGGGATCaccATG	GGCGACCGGTGGATC(stop)
pIRESpuro2-HA-C1	NotI	GGAGGATCCGCGGCCaccATG	GTTATCTATGCggccTTA

Primers used for site-directed mutagenesis

Gene	Direction	Amino acid change	Sequence
USP11	5´-3'	C318A	CTCACCAATCTGGGCAACACGGCCTTCATGAACTCGGCCCTGCAG
USP11	5´-3'	C318S	CTCACCAATCTGGGCAACACGTCCTTCATGAACTCGGCCCTGCAG
VPS34	5´-3'	K96R	tgaatggctgaaactaccagtaagataccctgacctg
VPS34	5´-3'	K158R	ctgccaggagttcttgtgggttctgatccatctgc
VPS34	5´-3'	K209R	acatttagagaaatagaaatgataaatgagagtgaaagacgaagt tctaatttcatg
VPS34	5´-3'	K346R	tctacctcaagaggccagacaggccttggaac
VPS34	5´-3'	K630R	gatggaggcagatatccagttatatttaagcatgGAGATGATTTA CGTCAAGATCAA
VPS34	5´-3'	K840R	gcggaatttatcctgaacctttctcacagttttatctggttcaag

To digest the vector backbones for cloning, the same protocol was followed for pEGFP-N1 and pIRESpuro2-HA-C1, except using different restriction enzymes: BamHI and NotI, respectively, and respective buffers provided by the manufacturer. 3 µg of a vector was digested in the total of 50 µl reaction volume for 3 h at 37 °C. Afterwards, 6 µl of phosphatase buffer, and 1 µl of the phosphatase were added for additional 20 min.

PCR products and digested vector backbones were ran on a 0.5-1 % agarose gel, depending on the size in TAE buffer and ran for 40 min at 90 V. Under the UV light bands at the correct size were excised and purified with EZNA Gel Extraction Kit, Classic, Gel Extraction Kit, or QIAquick Gel Extraction Kit from Qiagen, according to the manufacturer's protocol. Elution was done in 50 µl water and concentration measured on the BioSpectrometer basic.

To generate plasmids, In-Fusion HD cloning kit was used according to the manufacturer's protocol. Molar ratios of insert:vector were calculated using the Biomath calculators. Each cloning reaction was filled up to 5 µl, and incubated for 15 min at 50 °C. 2.5 µl was transformed into competent cells and plated on selection plate o/n.

For the site-directed mutagenesis, the reaction was purified without running it on a gel using the same listed kits. Elution was also done in 50 µl. 100 ng was transformed into competent cells and plated on selection plate o/n.

4.2.3.2 Bacterial transformation, plasmid amplification

To transform bacteria with cloning or site-directed mutagenesis products, 50 µl competent bacteria were incubated with DNA on ice for 20 min followed by a heat shock for 45 s at 42 $^\circ$C. The bacteria were cooled down on ice for 30 s and LB-media without antibiotics added to the tube for 1 h recovery by shaking at 800 rpm at 37 °C. Afterwards, the bacteria were spun down at 800 × g for 1 min, resuspended in a small amount of remaining supernatant and plated out on selection plates o/n at 37 °C. The following day, single clones were picked for sequence verification or for plasmid amplification. For sequence verification, single clones were inoculated in 5 ml LB-media with antibiotics with shaking o/n at 37 °C. The following day, mini-preparation was done and plasmid DNA sent for sequencing.

For plasmid amplification, a scoop of clones from the plate was inoculated in 250 ml LB-media with antibiotics shaken o/n at 37 °C. The following day, maxi-preparation was done and plasmid DNA sent for sequencing if necessary.

4.2.3.3 Plasmid preparation, and sequence verification

Single clones grown in 5 ml cultures were prepared using Plasmid Miniprep Kit, according to the manufacturer's protocol. Elution was done in 50 µl water, and the concentration was measured at BioSpectrometer basic.

Clones grown in 250 ml cultures for plasmid amplification were prepared using PureYield Plasmid Maxiprep System, according to the manufacturer's protocol. Elution was done in 3 rounds of 250 µl water and the concentration was measured at BioSpectrometer basic, or NanoDrop.

An appropriate amount of DNA was sent for sequencing according to service providers Eurofins, or Seq_Lab according to their requirements using primers from their database, depending on the backbone. In case of site directed mutagenesis, custom-made primers were used if the site was distant from the plasmid backbone.

Plasmid	Primer	Sequence
pEGFP-N1 (Seq_Lab)	EGFPN1-for	CAACGGGACTTTCCAAAATG
pIRESpuro2-HA-C1 (Seq_Lab)	CMV-for	CGCAAATGGGCGGTAGGCGTG
pEGFP-N1-USP11	USP11_seq primer	GCCAAGAACTCAGAAGGCTC
pcDNA3-Myc-PIK3C3	VPS34_nt900	GAGTTATCCACCAACCAAGC
pcDNA3-Myc-PIK3C3	VPS34_nt1701	GAAAAAGAATGAGAGACTAC

4.2.3.4 Quantitative real time PCR (qPCR)

The qPCR protocol was established by Verena Bittl (Goethe University). Pre-designed primers (Predesigned SYBR Green Primers) were ordered from Sigma-Aldrich. The RNA was extracted from the NHT and the USP11 RPE1 knockout cells, according to the manufacturer's protocol using the Total RNA Kit from PeqLab. The RNA was eluted in 70 µl H_2O and the RNA concentration determined by absorbance measurements using the NanoDrop. Subsequently, 1 µg RNA in a total volume of 10 µl was reverse transcribed into cDNA using the High-Capacity cDNA Reverse Transcription Kit, according to the manufacturer's protocol. To later serve as a negative control, an additional reaction was included lacking the reverse transcriptase, referred to as non-amplification control (NAC). The resulting cDNA was diluted 1:25 to 2 ng/µl and was subsequently used as a template for qPCR. Master mix for specific primer set was prepared containing 5 µl SYBR green, 1 µl of each of the forward and reverse primer dissolved to 10 µM, and 1 µl H_2O per reaction. 8 µl of the master mix was pipetted into a well of a 384-well plate. 2 µl of the diluted cDNA, NAC, or H_2O control, were added to respective wells in duplicates. The plate was quickly spun down, sealed with a foil, and the qPCR reaction was performed using the following cycling conditions. An initial denaturing step was followed by 50 amplification cycles each starting with a short denaturing step at 95 °C for 10 s, a subsequent 10 s annealing phase at 55 °C and 20 s of extension at 72 °C. Comparative quantification of the obtained values was achieved using the ΔΔCt method. Raw data was first normalized to the housekeeping gene, before values were

normalized to untreated RPE1 NHT control cells. The obtained ΔΔCt values were incorporated in order to determine fold difference in gene expression.

Oligos used for qPCR

Gene	Direction	Sequence
MAP1LC3B	5′-3'	ATAGAACGATACAAGGGTGAG
GAPDH	5′-3'	ACAGTTGCCATGTAGACC

4.2.4 Biochemistry

4.2.4.1 Cell lysis

The cells were washed with ice-cold PBS and lysed in 100 µl RIPA buffer per well of a 6-well plate or in 300 µl per 10 cm cell culture plate. The lysates were collected in 1.5 ml tubes and incubated on ice for 20 min. The lysates were spun down at 12,000 rpm at 4 °C, and the supernatant or the input mixed in a clean tube with 4 × LDS and boiled at 95 °C for 3 min. The cells for the GFP-Trap® bead immunoprecipitation were lysed in GFP-Trap® bead lysis buffer. The same buffer was used for the interactome analysis. For the endogenous ATG14 IP, ATG14 IP lysis buffer was used. Additionally, lysates were incubated for 30 min with rotation. For GlyGly IP, a modified RIPA buffer was used. In all the above IP experiments, after centrifugation, the rest of the supernatant that was not used for input was used for the IP.

4.2.4.2 Co-immunoprecipitation

GFP-Trap® beads co-immunoprecipitation

The cells were lysed as described above. GFP-Trap® beads were washed 3 × in GFP-Trap® beads wash buffer. To each lysate, 10 µl of the slurry GFP-Trap® beads were added. The immunoprecipitation (IP) samples were incubated for 1 h at 4 °C with rotation. The beads were washed 3× with 500 µl

IP wash buffer by spinning at 3.5 × g at 4 $^{\circ}$C, in between letting beads settle on ice for 2 min. After the last wash, 20 µl elution buffer was added directly to the beads and samples were boiled for 10 min at 95 $^{\circ}$C.

To co-IP experiments with recombinantly expressed SENP2, USP2, or commercially available Antarctic phosphatase included, several steps were added. After 1 h incubation with GFP-Trap® beads and washing, the enzymes were added to the IPs. For SENP2 and USP2, the proteins were resuspended in 50 µl DUB buffer per sample and added to IPs. The Antarctic phosphatase was incubated in the buffer provided with the enzyme. All reactions were incubated for 1h at 37 $^{\circ}$C. Afterwards, samples were boiled for 10 min at 95 $^{\circ}$C.

The test for USP2 activity involving propargylated ubiquitin, 2 µg of recombinantly expressed USP2 was incubated with 2 µg of PA-ubiquitin, or without (volume compensation with PBS) in DUB buffer. The reactions were incubated with shaking for 30 min at 37 $^{\circ}$C, then briefly spun down, mixed with 4 × LDS with DTT and ran on a 8 % acrylamide gel. The gel was stained with InstantBlue.

4.2.4.3 The endogenous ATG14 co-immunoprecipitation

The cells were lysed as described above. To each lysate, 5 µl of ATG14 pAb was added, and to the control, 5 µl normal rabbit IgG Ab. IPs were incubated for 1 h with rotation at 4 $^{\circ}$C. SureBeads Protein A Beads (20 µl per sample) were washed 3 × in PBS-T using the magnetic rack, and added to the IPs. The IPs were incubated additionally for 1 h at RT. The magnetic beads were washed with ATG14 IP lysis buffer and boiled at 95 $^{\circ}$C for 10 min.

4.2.4.4 SDS-PAGE

Boiled protein lysates were kept either at -20 $^{\circ}$C, or cooled down on ice before being separated by SDS-PAGE. Samples were loaded on a self-cast acrylamide gels of 8 % (VPS34 modification IP experiments) or 15 % (experiment Figure OE USP11 and CQ). All other samples were ran on pre-cast 4-15 % gradient gels from Bio-Rad. The gels were ran in TRIS-Glycine running buffer. The self-cast gels were ran at 90 V for 10 min, then at 120 V for about 45 min. The pre-cast gels were ran at 120-230 V.

Self-cast gel recipe

Gel	Acrylamide	TRIS-HCl	SDS	APS (m/v)	TEMED (v/v)
Stacking	5 %	125 mM pH 6.8	0.1 %	0.1 %	0.1 %
8 % separating	8 %	370 mM pH 8.8	0.1 %	0.1 %	0.1 %
15 % separating	15 %	370 mM pH 8.8	0.1 %	0.1 %	0.1 %

4.2.4.5 Western blotting

After separating the proteins by SDS-PAGE, the proteins were transferred to methanol-activated Immobilon-IP, 0.45 µm polyvinylidene fluoride (PVDF) membranes (Millipore) using the Bio-Rad system. The transfer buffer was supplemented with 10 % methanol. Transfer conditions were set to constant 200 mA for 90 min or to constant 55 V for 75 min. After the transfer, the membranes were briefly washed in TBS-T and then blocked in 2.5 % BSA in TBS-T for 1 h at RT on the see-saw shaker. The membranes were again briefly washed in TBS-T and incubated in the primary antibody solution (1:1,000) in 50 ml Falcon tubes o/n at 4 $^{\circ}$C with rotation. The next day, the membranes were washed 3 × 5 min with TBS-T followed by the secondary antibody incubation (1:10,000 for Santa Cruz AB, 1:2,500 for Cell Signaling AB) for 1 h at RT on the see-saw shaker. To visualize the HRP-conjugated secondary antibodies, ECL Prime Western Blot Det. Reagent was used and

chemiluminescence detected with ChemiDoc MP Imaging system. Fluorescent western blot was done following the same protocol with minor exceptions. Blocking and antibody solutions were based on I-block and PBS-T. The secondary antibody solution was 1:2,000, and protected from light. The fluorescence was measured on Fusion express.

4.2.5 Mass Spectrometry

4.2.5.1 GlyGly remnant immunoprecipitation

The GlyGly IP protocol was established by Petra Beli Lab.

Acetone precipitation

After cell lysis in a modified RIPA buffer (1 ml per 245 × 245 cell dish), and incubation on ice for 15 min, 1/10 of the total cell lysis volume in NaCl was added and sonicated (3 × 30 s, output=1, kept on ice in between). The lysates were spun down at 16,000 × g for 15 min at 4 °C. 50 μl was taken from the supernatant as the input sample (combined with 4× LDS and boiled for 3 min at 95 °C). The protein concentration of the samples was measure using a Bradford assay, and combined in a way to take 1:1 and a maximum amount of all the samples. 50 μg of the pooled sample was used for the whole cell proteome analysis (combined with 4 × LDS, heated for 10 min at 70 °C, cooled down, and combined with CAA to a concentration of 55 mM, and incubated for 30 min at RT in the dark). Meanwhile, ice-cold acetone was added to the combined lysate sample to an 80 % concentration and precipitated o/n at -20°C.

In-solution digest

Acetone precipitate was pelleted by centrifugation at 2,000 rpm for 5 min. The supernatant was poured out and pellet briefly dried on air. Subsequently, the pellet was dissolved in GlyGly denaturation buffer and resuspended in the

shaker at 1,000 rpm for 30 min at RT. The GlyGly reduction buffer was added to a final concentration of 1 mM DTT and shaked at 300 rpm for additional 45 min at RT. The protein concentration was again measured using a Bradford assay. The GlyGly alkylation buffer was added to a final concentration of 5 mM CAA and incubated for 30 min in the dark. 1 μg of LysC was added for every 200 μg of protein in the sample and digested with shaking at 300 rpm for 3 h at RT. The sample was then diluted with water 1:4, and 1 μg of trypsin was added for every 200 μg of protein in the sample with shaking at 300 rpm o/n at RT. The next day, the digest was stopped with TFA for a final concentration of 0.5 %, and precipitation induced by incubating the sample for 30 min at 4 °C.

C18 SepPak purification of peptides

SepPak column was inserted into a 10 ml syringe, and 5 ml of ACN was added. The column was then washed 3 × with 5 ml 0.1 % TFA. Acidified peptides were spun down at 4,000 rpm for 10 min. The column was loaded with clarified peptide mixture then washed 3 × with 10 ml water.

GlyGly enrichement

Peptides were eluted from the column with 4 ml GlyGly elution buffer. Peptide concentration was approximately evaluated by NanoDrop (50 % ACN was used as blank). 100 μl of 10 × IAP buffer was added and sample split into 4× 1 ml (2 ml tubes). The samples were dried by a SpeedVac for 1 h at 45 °C to a total volume of 1 ml for a combined total sample. 80 μl of PTM Scan beads were washed with GlyGly wash buffer II, spun down at 1 000 × g for 45 s at 4 °C. The supernatant liquid was removed, and the wash was repeated for 2 more times. The peptides were spun down at 13,000 rpm for 10 min. The supernatant was added to washed beads, and incubated with rotation for 4 h at 4 °C. The beads were spun down and washed with GlyGly wash buffer I for a total of two washes, followed by washing with GlyGly wash buffer II for a total of two washes. The beads were washed two more times with ddH$_2$O. The beads were dried with a syringe and eluted with 100 μl 0.15 % TFA.

Eluted peptides were shaken at 1,000 rpm for 5 min at RT, briefly spun down, and supernatant collected in a new tube. Elution was repeated two more times for a total of 4 washes. Eluates were spun down to remove any remaining beads, and then fractionated by micro-SCX into 6 fractions.

Micro-SCX

The StageTips were prepared by cutting out 6 SCX filter discs and placing them into 200 µl pipet tips. The StageTips were washed with 50 µl methanol, followed by 2 more buffer washes (first with the lowest, then the highest pH). The StageTips were then washed with 100 µl GlyGly wash buffer. The samples were loaded on the StageTips, eluted with 100 µl buffers (first with the lowest, then the highest pH). The eluates were dried by a SpeedVac for 12 min at 45 °C. The acidification was done with Buffer A', followed by C18 Stage tipping.

C18 Stage tipping

C18 StageTips were cut out in 2 discs per StageTip and placed into 200 µl pipet tips. They were activated with 30 µl methanol, then spun down at 4,000 rpm for 2 min, followed by buffer B wash and spin, with a final buffer A wash and spin that was repeated one additional time. C18 StageTips should not dry out in the process. The samples were then loaded on the tips, and bound by spinning at 4,000 rpm for 4 min. The StageTips were washed with 30 µl buffer, spun down at 4,000rpm for 2 min, and dried out with a syringe and kept at 4 °C until measurement. Elution prior to measurement was done with 30 µl buffer B by allowing elution buffer to enter the StageTip with a syringe. The elution buffer was incubated for 15 min at RT. After 15 min, the elution was done in a fresh tube by a syringe, dried out with a SpeedVac until a 2-3 µl volume (cca 10 min at 30 °C), and filled up with 8 µl buffer A, then shot.

4.2.5.2 Label-free interactome of USP11(C318S)-GFP after 4 h 250 mM Torin1

In-solution digest

The Hek293 cells were maintained, transfected, and treated as described above. The immunoprecipitation was done as described and washed 5x with 500 µl IP wash buffer. After the last wash, 20 µl elution buffer was added directly to the beads and samples were boiled for 10 min at 95 $^{\circ}$C. The cooled down samples were incubated with 0.5 µg LysC with shaking at 850 rpm for 3 h at 37 $^{\circ}$C. 20 µl of ABC together with 0.5 µg trypsin were added and incubated with shaking o/n at 850 rpm at 37 $^{\circ}$C.

SDB-RPS Stage tipping

SDB-RPS StageTip were cut out in 2 discs per StageTip and placed into 200 µl pipet tips. The digested samples were mixed with 80 µl isopropanol and 12 µl 10 % TFA to stop the digest and directly loaded on SDB-RPS StageTip by centrifugation for 5 min at 1,200 × g. The StageTips were washed with 50 µl StageTip wash buffer 1, and 50 µl StageTip wash buffer 2, eluted with 30 µl StageTip elution buffer in a clean tube, and evaporated to dryness in a SpeedVac for 30-45 min at 45-60 $^{\circ}$C. The dried samples were rehydrated with 10 µl 1 % Formic acid, and 2 % ACN, then shot.

4.2.6 Data analysis, and statistics

To determine the significance of acquired data, several statistical tests were used. In instances with more than two variables, e.g. cell line and time, 2way ANOVA test was employed. In examples where a comparison between two samples was analyzed, but with only one variable, e.g. a *C. elegans* strain, one sample t-test was performed and compared to a hypothetical value of 1. In the WIPI2 quantification experiment, unpaired t-test was employed. Aforementioned statistical analysis was done using GraphPad Prism.

For each experiment, number of replicates is indicated in figure legend as "N=n". In some experiments there were no biological replicates, rather technical and they are indicated in figure legend as "tN=n".

5   References

Acevo-Rodríguez, Pilar Sarah, Giovanna Maldonado, Susana Castro-Obregón, and Greco Hernández. 2020. "Autophagy Regulation by the Translation Machinery and Its Implications in Cancer." *Frontiers in Oncology*. https://doi.org/10.3389/fonc.2020.00322.

Al-Salihi, M A, L Herhaus, T Macartney, and G P Sapkota. 2012. "USP11 Augments TGFβ Signalling by Deubiquitylating ALK5." *Open Biol* 2. https://doi.org/10.1098/rsob.120063.

Alessi, Dario, Mark T. Kozlowski, Qing Ping Weng, Nick Morrice, and Joseph Avruch. 1998. "3-Phosphoinositide-Dependent Protein Kinase 1 (PDK1) Phosphorylates and Activates the P70 S6 Kinase in Vivo and in Vitro." *Current Biology*. https://doi.org/10.1016/S0960-9822(98)70037-5.

Antonioli, Manuela, Federica Albiero, Francesca Nazio, Tiziana Vescovo, Ariel Basulto Perdomo, Marco Corazzari, Claudia Marsella, et al. 2014. "AMBRA1 Interplay with Cullin E3 Ubiquitin Ligases Regulates Autophagy Dynamics." *Developmental Cell* 31 (6): 734–46. https://doi.org/https://doi.org/10.1016/j.devcel.2014.11.013.

Araki, Yasuhiro, Wei-Chi Ku, Manami Akioka, Alexander I May, Yu Hayashi, Fumio Arisaka, Yasushi Ishihama, and Yoshinori Ohsumi. 2013. "Atg38 Is Required for Autophagy-Specific Phosphatidylinositol 3-Kinase Complex Integrity." *The Journal of Cell Biology* 203 (2): 299 LP – 313. https://doi.org/10.1083/jcb.201304123.

Arico, Sébastien, Anne Petiot, Chantal Bauvy, Peter F Dubbelhuis, Alfred J Meijer, Patrice Codogno, and Eric Ogier-Denis. 2001. "The Tumor Suppressor PTEN Positively Regulates Macroautophagy by Inhibiting the Phosphatidylinositol 3-Kinase/Protein Kinase B Pathway." *Journal of Biological Chemistry* 276 (38): 35243–46. https://doi.org/10.1074/jbc.C100319200.

Axe, Elizabeth L, Simon A Walker, Maria Manifava, Priya Chandra, H Llewelyn Roderick, Anja Habermann, Gareth Griffiths, and Nicholas T Ktistakis. 2008. "Autophagosome Formation from Membrane Compartments Enriched in Phosphatidylinositol 3-Phosphate and Dynamically Connected to the Endoplasmic Reticulum." *Journal of Cell Biology* 182 (4): 685–701. https://doi.org/10.1083/jcb.200803137.

Backer, Jonathan M. 2016. "The Intricate Regulation and Complex Functions of the Class III Phosphoinositide 3-Kinase Vps34." *The Biochemical Journal* 473 (15): 2251–71. https://doi.org/10.1042/BCJ20160170.

Bartolomeo, Sabrina Di, Marco Corazzari, Francesca Nazio, Serafina Oliverio, Gaia Lisi, Manuela Antonioli, Vittoria Pagliarini, et al. 2010. "The Dynamic Interaction of AMBRA1 with the Dynein Motor Complex Regulates Mammalian Autophagy." *The Journal of Cell Biology* 191 (1): 155–68. https://doi.org/10.1083/jcb.201002100.

Baskaran, Sulochanadevi, Lars Anders Carlson, Goran Stjepanovic, Lindsey N. Young, Do J.in Kim, Patricia Grob, Robin E. Stanley, Eva Nogales, and James H. Hurley. 2014. "Architecture and Dynamics of the Autophagic Phosphatidylinositol 3-Kinase Complex." *ELife*. https://doi.org/10.7554/eLife.05115.

Behrends, Christian, Mathew E Sowa, Steven P Gygi, and J Wade Harper. 2010. "Network Organization of the Human Autophagy System." *Nature* 466 (7302): 68–76. https://doi.org/10.1038/nature09204.

Bellosillo, Beatriz, Dolors Colomer, Gabriel Pons, and Joan Gil. 1998. "Mitoxantrone, a Topoisomerase II Inhibitor, Induces Apoptosis of B-Chronic Lymphocytic Leukaemia Cells." *British Journal of Haematology* 100 (1): 142–46. https://doi.org/10.1046/j.1365-2141.1998.00520.x.

Berndsen, Christopher E., and Cynthia Wolberger. 2014. "New Insights into Ubiquitin E3 Ligase Mechanism." *Nature Structural and Molecular Biology*. https://doi.org/10.1038/nsmb.2780.

Bhalla, K., A. M. Ibrado, E. Tourkina, C. Tang, S. Grant, G. Bullock, Y. Huang, V. Ponnathpur, and M. E. Mahoney. 1993. "High-Dose Mitoxantrone Induces Programmed Cell Death or Apoptosis in Human Myeloid Leukemia Cells." *Blood*. https://doi.org/10.1182/blood.v82.10.3133.bloodjournal82103133.

Birgisdottir, Åsa Birna, Trond Lamark, and Terje Johansen. 2013. "The LIR Motif - Crucial for Selective Autophagy." *Journal of Cell Science*. https://doi.org/10.1242/jcs.126128.

Burkhart, Richard A, Yu Peng, Zoë A Norris, Renée M Tholey, Vanessa A Talbott, Qin Liang, Yongxing Ai, et al. 2013. "Mitoxantrone Targets Human Ubiquitin-Specific Peptidase 11 (USP11) and Is a Potent Inhibitor of Pancreatic Cancer Cell Survival." *Molecular Cancer*

Research 11 (8): 901 LP – 911. https://doi.org/10.1158/1541-7786.MCR-12-0699.

Cao, Yanyan, Yichen Wang, Widian F Abi Saab, Fajun Yang, Jeffrey E Pessin, and Jonathan M Backer. 2014. "NRBF2 Regulates Macroautophagy as a Component of Vps34 Complex I." *The Biochemical Journal* 461 (2): 315–22. https://doi.org/10.1042/BJ20140515.

Cheng, Shiya, Yanwei Wu, Qun Lu, Jiacong Yan, Hong Zhang, and Xiaochen Wang. 2013. "Autophagy Genes Coordinate with the Class II PI/PtdIns 3-Kinase PIKI-1 to Regulate Apoptotic Cell Clearance in C. Elegans." *Autophagy*. https://doi.org/10.4161/auto.26323.

Choi, Augustine M.K., Stefan W. Ryter, and Beth Levine. 2013. "Autophagy in Human Health and Disease." *New England Journal of Medicine*. https://doi.org/10.1056/nejmra1205406.

Ciechanover, A., H. Heller, S. Elias, A. L. Haas, and A. Hershko. 1980. "ATP-Dependent Conjugation of Reticulocyte Proteins with the Polypeptide Required for Protein Degradation." *Proceedings of the National Academy of Sciences of the United States of America*. https://doi.org/10.1073/pnas.77.3.1365.

Ciechanover, Aaron, Daniel Finley, and Alexander Varshavsky. 1984. "The Ubiquitin-mediated Proteolytic Pathway and Mechanisms of Energy-dependent Intracellular Protein Degradation." *Journal of Cellular Biochemistry*. https://doi.org/10.1002/jcb.240240104.

Ciehanover, Aharon, Yaacov Hod, and Avram Hershko. 1978. "A Heat-Stable Polypeptide Component of an ATP-Dependent Proteolytic System from Reticulocytes." *Biochemical and Biophysical Research Communications*. https://doi.org/10.1016/0006-291X(78)91249-4.

Clague, Michael J., Igor Barsukov, Judy M. Coulson, Han Liu, Daniel J. Rigden, and Sylvie Urbé. 2013. "Deubiquitylases from Genes to Organism." *Physiological Reviews*. https://doi.org/10.1152/physrev.00002.2013.

Clague, Michael J., Sylvie Urbé, and David Komander. 2019. "Breaking the Chains: Deubiquitylating Enzyme Specificity Begets Function." *Nature Reviews Molecular Cell Biology*. https://doi.org/10.1038/s41580-019-0099-1.

Crespi, Martin D, Sofia E Ivanier, Jorge Genovese, and Alberto Baldi. 1986. "Mitoxantrone Affects Topoisomerase Activities in Human Breast Cancer Cells." *Biochemical and Biophysical Research Communications* 136 (2): 521–28. https://doi.org/https://doi.org/10.1016/0006-291X(86)90471-7.

Crighton, Diane, Simon Wilkinson, Jim O'Prey, Nelofer Syed, Paul Smith, Paul R Harrison, Milena Gasco, Ornella Garrone, Tim Crook, and Kevin M Ryan. 2006. "DRAM, a P53-Induced Modulator of Autophagy, Is Critical for Apoptosis." *Cell* 126 (1): 121–34. https://doi.org/https://doi.org/10.1016/j.cell.2006.05.034.

Cuervo, Ana Maria, and Esther Wong. 2014. "Chaperone-Mediated Autophagy: Roles in Disease and Aging." *Cell Research* 24 (1): 92–104. https://doi.org/10.1038/cr.2013.153.

Cui, Jun, Shouheng Jin, and Rong-Fu Wang. 2016. "The BECN1-USP19 Axis Plays a Role in the Crosstalk between Autophagy and Antiviral Immune Responses." *Autophagy* 12 (7): 1210–11. https://doi.org/10.1080/15548627.2016.1173801.

Cummins, Jordan M, Carlo Rago, Manu Kohli, Kenneth W Kinzler, Christoph Lengauer, and Bert Vogelstein. 2004. "Disruption of HAUSP Gene Stabilizes P53." *Nature* 428 (6982): 1–2. https://doi.org/10.1038/nature02501.

Deng, Tanggang, Guobei Yan, Xin Song, Lin Xie, Yu Zhou, Jianglin Li, Xiaoxiao Hu, et al. 2018. "Deubiquitylation and Stabilization of P21 by USP11 Is Critical for Cell-Cycle Progression and DNA Damage Responses." *Proceedings of the National Academy of Sciences* 115 (18): 4678 LP – 4683. https://doi.org/10.1073/pnas.1714938115.

Deshaies, Raymond J., and Claudio A.P. Joazeiro. 2009. "RING Domain E3 Ubiquitin Ligases." *Annual Review of Biochemistry*. https://doi.org/10.1146/annurev.biochem.78.101807.093809.

Dooley, Hannah C, Minoo Razi, Hannah E J Polson, Stephen E Girardin, Michael I Wilson, and Sharon A Tooze. 2014. "WIPI2 Links LC3 Conjugation with PI3P, Autophagosome Formation, and Pathogen Clearance by Recruiting Atg12-5-16L1." *Molecular Cell* 55 (2): 238–52. https://doi.org/10.1016/j.molcel.2014.05.021.

Dostal, Vishantie, and Christopher D Link. 2010. "Assaying β-Amyloid Toxicity Using a Transgenic C. Elegans Model." *JoVE*, no. 44: e2252. https://doi.org/doi:10.3791/2252.

Egan, Dan, Joungmok Kim, Reuben J Shaw, and Kun-Liang Guan. 2011. "The Autophagy

Initiating Kinase ULK1 Is Regulated via Opposing Phosphorylation by AMPK and MTOR." *Autophagy* 7 (6): 643–44. https://doi.org/10.4161/auto.7.6.15123.

Egan, Daniel F., Matthew G.H. Chun, Mitchell Vamos, Haixia Zou, Juan Rong, Chad J. Miller, Hua Jane Lou, et al. 2015. "Small Molecule Inhibition of the Autophagy Kinase ULK1 and Identification of ULK1 Substrates." *Molecular Cell*. https://doi.org/10.1016/j.molcel.2015.05.031.

Egan, Daniel F, David B Shackelford, Maria M Mihaylova, Sara Gelino, Rebecca A Kohnz, William Mair, Debbie S Vasquez, et al. 2011. "Phosphorylation of ULK1 (HATG1) by AMP-Activated Protein Kinase Connects Energy Sensing to Mitophagy." *Science* 331 (6016): 456 LP – 461. https://doi.org/10.1126/science.1196371.

Ekkebus, Reggy, Sander I van Kasteren, Yogesh Kulathu, Arjen Scholten, Ilana Berlin, Paul P Geurink, Annemieke de Jong, et al. 2013. "On Terminal Alkynes That Can React with Active-Site Cysteine Nucleophiles in Proteases." *Journal of the American Chemical Society* 135 (8): 2867–70. https://doi.org/10.1021/ja309802n.

Erbil, Secil, Ozlem Oral, Geraldine Mitou, Cenk Kig, Emel Durmaz-Timucin, Emine Guven-Maiorov, Ferah Gulacti, et al. 2016. "RACK1 Is an Interaction Partner of ATG5 and a Novel Regulator of Autophagy." *Journal of Biological Chemistry* 291 (32): 16753–65. https://doi.org/10.1074/jbc.M115.708081.

Errafiy, Rajaa, Carmen Aguado, Ghita Ghislat, Juan M Esteve, Anabel Gil, Mohammed Loutfi, and Erwin Knecht. 2013. "PTEN Increases Autophagy and Inhibits the Ubiquitin-Proteasome Pathway in Glioma Cells Independently of Its Lipid Phosphatase Activity." *PloS One* 8 (12): e83318. https://doi.org/10.1371/journal.pone.0083318.

Faesen, Alex C., Mark P.A. Luna-Vargas, Paul P. Geurink, Marcello Clerici, Remco Merkx, Willem J. van Dijk, Dharjath S. Hameed, Farid El Oualid, Huib Ovaa, and Titia K. Sixma. 2011. "The Differential Modulation of USP Activity by Internal Regulatory Domains, Interactors and Eight Ubiquitin Chain Types." *Chemistry & Biology* 18 (12): 1550–61. https://doi.org/https://doi.org/10.1016/j.chembiol.2011.10.017.

Falquet, Laurent, Nicole Paquet, Séverine Frutiger, Graham J. Hughes, Khan Hoang-Van, and J. C. Jaton. 1995. "A Human De-Ubiquitinating Enzyme with Both Isopeptidase and Peptidase Activities in Vitro." *FEBS Letters*. https://doi.org/10.1016/0014-5793(94)01451-6.

Fan, Weiliang, Ashley Nassiri, and Qing Zhong. 2011. "Autophagosome Targeting and Membrane Curvature Sensing by Barkor/Atg14(L)." *Proceedings of the National Academy of Sciences* 108 (19): 7769 LP – 7774. https://doi.org/10.1073/pnas.1016472108.

Feng, Zhaohui, Haiyan Zhang, Arnold J Levine, and Shengkan Jin. 2005. "The Coordinate Regulation of the P53 and MTOR Pathways in Cells." *Proceedings of the National Academy of Sciences of the United States of America* 102 (23): 8204 LP – 8209. https://doi.org/10.1073/pnas.0502857102.

Fujioka, Yuko, Nobuo N. Noda, Hitoshi Nakatogawa, Yoshinori Ohsumi, and Fuyuhiko Inagaki. 2010. "Dimeric Coiled-Coil Structure of Saccharomyces Cerevisiae Atg16 and Its Functional Significance in Autophagy." *Journal of Biological Chemistry*. https://doi.org/10.1074/jbc.M109.053520.

Fujita, Naonobu, Mitsuko Hayashi-Nishino, Hiromi Fukumoto, Hiroko Omori, Akitsugu Yamamoto, Takeshi Noda, and Tamotsu Yoshimori. 2008. "An Atg4B Mutant Hampers the Lipidation of LC3 Paralogues and Causes Defects in Autophagosome Closure." *Molecular Biology of the Cell*. https://doi.org/10.1091/mbc.E08-03-0312.

Fujita, Naonobu, Takashi Itoh, Hiroko Omori, Mitsunori Fukuda, Takeshi Noda, and Tamotsu Yoshimori. 2008. "The Atg16L Complex Specifies the Site of LC3 Lipidation for Membrane Biogenesis in Autophagy." *Molecular Biology of the Cell*. https://doi.org/10.1091/mbc.E07-12-1257.

Fujita, Naonobu, Eiji Morita, Takashi Itoh, Atsushi Tanaka, Megumi Nakaoka, Yuki Osada, Tetsuo Umemoto, et al. 2013. "Recruitment of the Autophagic Machinery to Endosomes during Infection Is Mediated by Ubiquitin." *Journal of Cell Biology*. https://doi.org/10.1083/jcb.201304188.

Furuya, Tsuyoshi, Minsu Kim, Marta Lipinski, Juying Li, Dohoon Kim, Tao Lu, Yong Shen, et al. 2010. "Negative Regulation of Vps34 by Cdk Mediated Phosphorylation." *Molecular Cell*. https://doi.org/10.1016/j.molcel.2010.05.009.

Gammoh, Noor, Oliver Florey, Michael Overholtzer, and Xuejun Jiang. 2013. "Interaction between FIP200 and ATG16L1 Distinguishes ULK1 Complex-Dependent and -

Independent Autophagy." *Nature Structural & Molecular Biology* 20 (2): 144–49. https://doi.org/10.1038/nsmb.2475.

Garcia, Daniel A, Christina Baek, M Valeria Estrada, Tiffani Tysl, Eric J Bennett, Jing Yang, and John T Chang. 2018. "USP11 Enhances TGFβ-Induced Epithelial–Mesenchymal Plasticity and Human Breast Cancer Metastasis." *Molecular Cancer Research* 16 (7): 1172 LP – 1184. https://doi.org/10.1158/1541-7786.MCR-17-0723.

Goldknopf, I. L., and H. Busch. 1977. "Isopeptide Linkage between Nonhistone and Histone 2A Polypeptides of Chromosomal Conjugate Protein A24." *Proceedings of the National Academy of Sciences of the United States of America*. https://doi.org/10.1073/pnas.74.3.864.

Goldknopf, I. L., M. F. French, R. Musso, and H. Busch. 1977. "Presence of Protein A24 in Rat Liver Nucleosomes." *Proceedings of the National Academy of Sciences of the United States of America*. https://doi.org/10.1073/pnas.74.12.5492.

Goldstein, G., M. Scheid, U. Hammerling, D. H. Schlesinger, H. D. Niall, and E. A. Boyse. 1975. "Isolation of a Polypeptide That Has Lymphocyte Differentiating Properties and Is Probably Represented Universally in Living Cells." *Proceedings of the National Academy of Sciences of the United States of America*. https://doi.org/10.1073/pnas.72.1.11.

Gómez-Sánchez, Rubén, Jaqueline Rose, Rodrigo Guimarães, Muriel Mari, Daniel Papinski, Ester Rieter, Willie J Geerts, et al. 2018. "Atg9 Establishes Atg2-Dependent Contact Sites between the Endoplasmic Reticulum and Phagophores." *Journal of Cell Biology* 217 (8): 2743–63. https://doi.org/10.1083/jcb.201710116.

Grou, Claudia P., Manuel P. Pinto, Andreia V. Mendes, Pedro Domingues, and Jorge E. Azevedo. 2015. "The de Novo Synthesis of Ubiquitin: Identification of Deubiquitinases Acting on Ubiquitin Precursors." *Scientific Reports*. https://doi.org/10.1038/srep12836.

Gwinn, Dana M, David B Shackelford, Daniel F Egan, Maria M Mihaylova, Annabelle Mery, Debbie S Vasquez, Benjamin E Turk, and Reuben J Shaw. 2008. "AMPK Phosphorylation of Raptor Mediates a Metabolic Checkpoint." *Molecular Cell* 30 (2): 214–26. https://doi.org/10.1016/j.molcel.2008.03.003.

Haahr, Peter, Nikoline Borgermann, Xiaohu Guo, Dimitris Typas, Divya Achuthankutty, Saskia Hoffmann, Robert Shearer, Titia K. Sixma, and Niels Mailand. 2018. "ZUFSP Deubiquitylates K63-Linked Polyubiquitin Chains to Promote Genome Stability." *Molecular Cell*. https://doi.org/10.1016/j.molcel.2018.02.024.

Han, Tianyu, Meng Guo, Mingxi Gan, Bentong Yu, Xiaoli Tian, and Jian Bin Wang. 2018. "TRIM59 Regulates Autophagy through Modulating Both the Transcription and the Ubiquitination of BECN1." *Autophagy*. https://doi.org/10.1080/15548627.2018.1491493.

Hanada, Takao, Nobuo N. Noda, Yoshinori Satomi, Yoshinobu Ichimura, Yuko Fujioka, Toshifumi Takao, Fuyuhiko Inagaki, and Yoshinori Ohsumi. 2007. "The Atg12-Atg5 Conjugate Has a Novel E3-like Activity for Protein Lipidation in Autophagy." *Journal of Biological Chemistry*. https://doi.org/10.1074/jbc.C700195200.

Hara, Kenta, Yoshiko Maruki, Xiaomeng Long, Ken-ichi Yoshino, Noriko Oshiro, Sujuti Hidayat, Chiharu Tokunaga, Joseph Avruch, and Kazuyoshi Yonezawa. 2002. "Raptor, a Binding Partner of Target of Rapamycin (TOR), Mediates TOR Action." *Cell* 110 (2): 177–89. https://doi.org/10.1016/S0092-8674(02)00833-4.

Hay, Nissim. 2011. "Interplay between FOXO, TOR, and Akt." *Biochimica et Biophysica Acta (BBA) - Molecular Cell Research* 1813 (11): 1965–70. https://doi.org/https://doi.org/10.1016/j.bbamcr.2011.03.013.

Hayashi-Nishino, Mitsuko, Naonobu Fujita, Takeshi Noda, Akihito Yamaguchi, Tamotsu Yoshimori, and Akitsugu Yamamoto. 2009. "A Subdomain of the Endoplasmic Reticulum Forms a Cradle for Autophagosome Formation." *Nature Cell Biology* 11 (12): 1433–37. https://doi.org/10.1038/ncb1991.

He, Jinshan, Qianzheng Zhu, Gulzar Wani, Nidhi Sharma, Chunhua Han, Jiang Qian, Kyle Pentz, Qi-en Wang, and Altaf A Wani. 2014. "Ubiquitin-Specific Protease 7 Regulates Nucleotide Excision Repair through Deubiquitinating XPC Protein and Preventing XPC Protein from Undergoing Ultraviolet Light-Induced and VCP/P97 Protein-Regulated Proteolysis." *Journal of Biological Chemistry* 289 (39): 27278–89. https://doi.org/10.1074/jbc.M114.589812.

Hendriks, Ivo A, Joost Schimmel, Karolin Eifler, Jesper V Olsen, and Alfred C O Vertegaal. 2015. "Ubiquitin-Specific Protease 11 (USP11) Deubiquitinates Hybrid Small Ubiquitin-like Modifier (SUMO)-Ubiquitin Chains to Counteract RING Finger Protein 4 (RNF4)."

Journal of Biological Chemistry 290 (25): 15526–37. https://doi.org/10.1074/jbc.M114.618132.

Herman, P K, and S D Emr. 1990. "Characterization of VPS34, a Gene Required for Vacuolar Protein Sorting and Vacuole Segregation in Saccharomyces Cerevisiae." *Molecular and Cellular Biology*. https://doi.org/10.1128/mcb.10.12.6742.

Hermanns, Thomas, Christian Pichlo, Ilka Woiwode, Karsten Klopffleisch, Katharina F. Witting, Huib Ovaa, Ulrich Baumann, and Kay Hofmann. 2018. "A Family of Unconventional Deubiquitinases with Modular Chain Specificity Determinants." *Nature Communications*. https://doi.org/10.1038/s41467-018-03148-5.

Hershko, A., A. Ciechanover, H. Heller, A. L. Haas, and I. A. Rose. 1980. "Proposed Role of ATP in Protein Breakdown: Conjugation of Protein with Multiple Chains of the Polypeptide of ATP-Dependent Proteolysis." *Proceedings of the National Academy of Sciences of the United States of America*. https://doi.org/10.1073/pnas.77.4.1783.

Hershko, A, and A Ciechanover. 1982. "Mechanisms of Intracellular Protein Breakdown." *Annual Review of Biochemistry*. https://doi.org/10.1146/annurev.bi.51.070182.002003.

Hiles, Ian D., Masayuki Otsu, Stefano Volinia, Michael J. Fry, Ivan Gout, Ritu Dhand, George Panayotou, et al. 1992. "Phosphatidylinositol 3-Kinase: Structure and Expression of the 110 Kd Catalytic Subunit." *Cell*. https://doi.org/10.1016/0092-8674(92)90166-A.

Holz, Marina K, Bryan A Ballif, Steven P Gygi, and John Blenis. 2005. "MTOR and S6K1 Mediate Assembly of the Translation Preinitiation Complex through Dynamic Protein Interchange and Ordered Phosphorylation Events." *Cell* 123 (4): 569–80. https://doi.org/10.1016/j.cell.2005.10.024.

Hosokawa, Nao, Taichi Hara, Takeshi Kaizuka, Chieko Kishi, Akito Takamura, Yutaka Miura, Shun-ichiro Iemura, et al. 2009. "Nutrient-Dependent MTORC1 Association with the ULK1-Atg13-FIP200 Complex Required for Autophagy." *Molecular Biology of the Cell* 20 (7): 1981–91. https://doi.org/10.1091/mbc.e08-12-1248.

Hu, Min, Pingwei Li, Muyang Li, Wenyu Li, Tingting Yao, Jia Wei Wu, Wei Gu, Robert E. Cohen, and Yigong Shi. 2002. "Crystal Structure of a UBP-Family Deubiquitinating Enzyme in Isolation and in Complex with Ubiquitin Aldehyde." *Cell*. https://doi.org/10.1016/S0092-8674(02)01199-6.

Ichimura, Yoshinobu, Takayoshi Kirisako, Toshifumi Takao, Yoshinori Satomi, Yasutsugu Shimonishi, Naotada Ishihara, Noboru Mizushima, et al. 2000. "A Ubiquitin-like System Mediates Protein Lipidation." *Nature*. https://doi.org/10.1038/35044114.

Ideguchi, Haruko, Atsuhisa Ueda, Masatsugu Tanaka, Jun Yang, Takashi Tsuji, Shigeru Ohno, Eri Hagiwara, Akiko Aoki, and Yoshiaki Ishigatsubo. 2002. "Structural and Functional Characterization of the USP11 Deubiquitinating Enzyme, Which Interacts with the RanGTP-Associated Protein RanBPM." *Biochemical Journal* 367 (1): 87–95. https://doi.org/10.1042/bj20011851.

Inoki, Ken, Yong Li, Tianquan Zhu, Jun Wu, and Kun-Liang Guan. 2002. "TSC2 Is Phosphorylated and Inhibited by Akt and Suppresses MTOR Signalling." *Nature Cell Biology* 4 (9): 648–57. https://doi.org/10.1038/ncb839.

Inoki, Ken, Tianqing Zhu, and Kun-Liang Guan. 2003. "TSC2 Mediates Cellular Energy Response to Control Cell Growth and Survival." *Cell* 115 (5): 577–90. https://doi.org/10.1016/S0092-8674(03)00929-2.

Istomine, Roman, Fernando Alvarez, Yasser Almadani, Anie Philip, and Ciriaco A Piccirillo. 2019. "The Deubiquitinating Enzyme Ubiquitin-Specific Peptidase 11 Potentiates TGF-β Signaling in CD4<Sup>+</Sup> T Cells to Facilitate Foxp3<Sup>+</Sup> Regulatory T and T<Sub>H</Sub>17 Cell Differentiation." *The Journal of Immunology* 203 (9): 2388 LP – 2400. https://doi.org/10.4049/jimmunol.1801689.

Itakura, Eisuke, Chieko Kishi, Kinji Inoue, and Noboru Mizushima. 2008. "Beclin 1 Forms Two Distinct Phosphatidylinositol 3-Kinase Complexes with Mammalian Atg14 and UVRAG." *Molecular Biology of the Cell* 19 (12): 5360–72. https://doi.org/10.1091/mbc.e08-01-0080.

Jacko, A M, L Nan, S Li, J Tan, J Zhao, D J Kass, and Y Zhao. 2016. "De-Ubiquitinating Enzyme, USP11, Promotes Transforming Growth Factor β-1 Signaling through Stabilization of Transforming Growth Factor β Receptor II." *Cell Death & Disease* 7 (11): e2474–e2474. https://doi.org/10.1038/cddis.2016.371.

Jeon, Sang-Min. 2016. "Regulation and Function of AMPK in Physiology and Diseases." *Experimental & Molecular Medicine* 48 (7): e245–e245.

https://doi.org/10.1038/emm.2016.81.

Jin, Shouheng, Shuo Tian, Yamei Chen, Chuanxia Zhang, Weihong Xie, Xiaojun Xia, Jun Cui, and Rong-Fu Wang. 2016. "USP 19 Modulates Autophagy and Antiviral Immune Responses by Deubiquitinating Beclin-1." *The EMBO Journal*. https://doi.org/10.15252/embj.201593596.

Johansen, Terje, and Trond Lamark. 2011. "Selective Autophagy Mediated by Autophagic Adapter Proteins." *Autophagy* 7 (3): 279–96. https://doi.org/10.4161/auto.7.3.14487.

Judith, Delphine, Harold B.J. Jefferies, Stefan Boeing, David Frith, Ambrosius P. Snijders, and Sharon A. Tooze. 2019. "ATG9A Shapes the Forming Autophagosome through Arfaptin 2 and Phosphatidylinositol 4-Kinase IIIβ." *Journal of Cell Biology*. https://doi.org/10.1083/jcb.201901115.

Jung, Chang Hwa, Chang Bong Jun, Seung-Hyun Ro, Young-Mi Kim, Neil Michael Otto, Jing Cao, Mondira Kundu, and Do-Hyung Kim. 2009. "ULK-Atg13-FIP200 Complexes Mediate MTOR Signaling to the Autophagy Machinery." *Molecular Biology of the Cell* 20 (7): 1992–2003. https://doi.org/10.1091/mbc.e08-12-1249.

Kabeya, Y. 2000. "LC3, a Mammalian Homologue of Yeast Apg8p, Is Localized in Autophagosome Membranes after Processing." *The EMBO Journal*. https://doi.org/10.1093/emboj/19.21.5720.

Kaizuka, Takeshi, Hideaki Morishita, Yutaro Hama, Satoshi Tsukamoto, Takahide Matsui, Yuichiro Toyota, Akihiko Kodama, Tomoaki Ishihara, Tohru Mizushima, and Noboru Mizushima. 2016. "An Autophagic Flux Probe That Releases an Internal Control." *Molecular Cell* 64 (4): 835–49. https://doi.org/10.1016/j.molcel.2016.09.037.

Kametaka, Satoshi, Takafumi Okano, Mariko Ohsumi, and Yoshinori Ohsumi. 1998. "Apg14p and Apg6/Vps30p Form a Protein Complex Essential for Autophagy in the Yeast, Saccharomyces Cerevisiae." *Journal of Biological Chemistry*. https://doi.org/10.1074/jbc.273.35.22284.

Kapadia, Bandish, Nahid M Nanaji, Kavita Bhalla, Binny Bhandary, Rena Lapidus, Afshin Beheshti, Andrew M Evens, and Ronald B Gartenhaus. 2018. "Fatty Acid Synthase Induced S6Kinase Facilitates USP11-EIF4B Complex Formation for Sustained Oncogenic Translation in DLBCL." *Nature Communications* 9 (1): 829. https://doi.org/10.1038/s41467-018-03028-y.

Karanasios, Eleftherios, Simon A. Walker, Hanneke Okkenhaug, Maria Manifava, Eric Hummel, Hans Zimmermann, Qashif Ahmed, Marie Charlotte Domart, Lucy Collinson, and Nicholas T. Ktistakis. 2016. "Autophagy Initiation by ULK Complex Assembly on ER Tubulovesicular Regions Marked by ATG9 Vesicles." *Nature Communications*. https://doi.org/10.1038/ncomms12420.

Ke, Jia ying, Cong jie Dai, Wen lin Wu, Jin hua Gao, Ai juan Xia, Guang ping Liu, Kao sheng Lv, and Chun lin Wu. 2014. "USP11 Regulates P53 Stability by Deubiquitinating P53." *Journal of Zhejiang University: Science B* 15 (12): 1032–38. https://doi.org/10.1631/jzus.B1400180.

Kern, Andreas, Bianca Ackermann, Albrecht M. Clement, Heike Duerk, and Christian Behl. 2010. "HSF1-Controlled and Age-Associated Chaperone Capacity in Neurons and Muscle Cells of C. Elegans." *PLoS ONE*. https://doi.org/10.1371/journal.pone.0008568.

Kihara, A, T Noda, N Ishihara, and Y Ohsumi. 2001. "Two Distinct Vps34 Phosphatidylinositol 3-Kinase Complexes Function in Autophagy and Carboxypeptidase Y Sorting in Saccharomyces Cerevisiae." *The Journal of Cell Biology* 152 (3): 519–30. https://doi.org/10.1083/jcb.152.3.519.

Kihara, Akio, Takeshi Noda, Naotada Ishihara, and Yoshinori Ohsumi. 2001. "Two Distinct Vps34 Phosphatidylinositol 3–Kinase Complexes Function in Autophagy and Carboxypeptidase Y Sorting InSaccharomyces Cerevisiae." *The Journal of Cell Biology* 152 (3): 519–30. https://doi.org/10.1083/jcb.152.3.519.

Kim, John, Valerie M Dalton, Kimberly P Eggerton, Sidney V Scott, and Daniel J Klionsky. 1999. "Apg7p/Cvt2p Is Required for the Cytoplasm-to-Vacuole Targeting, Macroautophagy, and Peroxisome Degradation Pathways." *Molecular Biology of the Cell* 10 (5): 1337–51. https://doi.org/10.1091/mbc.10.5.1337.

Kim, Joungmok, Young Chul Kim, Chong Fang, Ryan C Russell, Jeong Hee Kim, Weiliang Fan, Rong Liu, Qing Zhong, and Kun-Liang Guan. 2013. "Differential Regulation of Distinct Vps34 Complexes by AMPK in Nutrient Stress and Autophagy." *Cell* 152 (1–2): 290–303. https://doi.org/10.1016/j.cell.2012.12.016.

Kim, Joungmok, Mondira Kundu, Benoit Viollet, and Kun-Liang Guan. 2011. "AMPK and

MTOR Regulate Autophagy through Direct Phosphorylation of Ulk1." *Nature Cell Biology* 13 (2): 132–41. https://doi.org/10.1038/ncb2152.

Kim, Woong, Eric J. Bennett, Edward L. Huttlin, Ailan Guo, Jing Li, Anthony Possemato, Mathew E. Sowa, et al. 2011. "Systematic and Quantitative Assessment of the Ubiquitin-Modified Proteome." *Molecular Cell*. https://doi.org/10.1016/j.molcel.2011.08.025.

Kim, Young-Mi, Chang Hwa Jung, Minchul Seo, Eun Kyoung Kim, Ji-Man Park, Sun Sik Bae, and Do-Hyung Kim. 2015. "MTORC1 Phosphorylates UVRAG to Negatively Regulate Autophagosome and Endosome Maturation." *Molecular Cell* 57 (2): 207–18. https://doi.org/https://doi.org/10.1016/j.molcel.2014.11.013.

Kirisako, T, Y Ichimura, H Okada, Y Kabeya, N Mizushima, T Yoshimori, M Ohsumi, T Takao, T Noda, and Y Ohsumi. 2000. "The Reversible Modification Regulates the Membrane-Binding State of Apg8/Aut7 Essential for Autophagy and the Cytoplasm to Vacuole Targeting Pathway." *The Journal of Cell Biology* 151 (2): 263–76. https://doi.org/10.1083/jcb.151.2.263.

Kirisako, Takayoshi, Kiyoko Kamei, Shigeo Murata, Michiko Kato, Hiromi Fukumoto, Masato Kanie, Soichi Sano, Fuminori Tokunaga, Keiji Tanaka, and Kazuhiro Iwai. 2006. "A Ubiquitin Ligase Complex Assembles Linear Polyubiquitin Chains." *EMBO Journal*. https://doi.org/10.1038/sj.emboj.7601360.

Kirkin, Vladimir, David G. McEwan, Ivana Novak, and Ivan Dikic. 2009. "A Role for Ubiquitin in Selective Autophagy." *Molecular Cell*. https://doi.org/10.1016/j.molcel.2009.04.026.

Klann, Kevin, Georg Tascher, and Christian Münch. 2020. "Functional Translatome Proteomics Reveal Converging and Dose-Dependent Regulation by MTORC1 and EIF2α." *Molecular Cell*. https://doi.org/10.1016/j.molcel.2019.11.010.

Klionsky, Daniel J., Kotb Abdelmohsen, Akihisa Abe, Md Joynal Abedin, Hagai Abeliovich, Abraham Acevedo Arozena, Hiroaki Adachi, et al. 2016. "Guidelines for the Use and Interpretation of Assays for Monitoring Autophagy (3rd Edition)." *Autophagy*. https://doi.org/10.1080/15548627.2015.1100356.

Klionsky, Daniel J., James M. Cregg, William A. Dunn, Scott D. Emr, Yasuyoshi Sakai, Ignacio V. Sandoval, Andrei Sibirny, et al. 2003. "A Unified Nomenclature for Yeast Autophagy-Related Genes." *Developmental Cell*. https://doi.org/10.1016/S1534-5807(03)00296-X.

Klionsky, Daniel J, Alfred J Meijer, Patrice Codogno, Thomas P Neufeld, and Ryan C Scott. 2005. "Autophagy and P70S6 Kinase." *Autophagy* 1 (1): 59–61. https://doi.org/10.4161/auto.1.1.1536.

Komander, David, Michael J. Clague, and Sylvie Urbé. 2009. "Breaking the Chains: Structure and Function of the Deubiquitinases." *Nature Reviews Molecular Cell Biology*. https://doi.org/10.1038/nrm2731.

Komander, David, and Michael Rape. 2012. "The Ubiquitin Code." *Annual Review of Biochemistry* 81 (1): 203–29. https://doi.org/10.1146/annurev-biochem-060310-170328.

Komatsu, Masaaki, Satoshi Waguri, Masato Koike, Yu shin Sou, Takashi Ueno, Taichi Hara, Noboru Mizushima, et al. 2007. "Homeostatic Levels of P62 Control Cytoplasmic Inclusion Body Formation in Autophagy-Deficient Mice." *Cell*. https://doi.org/10.1016/j.cell.2007.10.035.

Koyama-Honda, Ikuko, Eisuke Itakura, Takahiro K Fujiwara, and Noboru Mizushima. 2013. "Temporal Analysis of Recruitment of Mammalian ATG Proteins to the Autophagosome Formation Site." *Autophagy* 9 (10): 1491–99. https://doi.org/10.4161/auto.25529.

Kwasna, Dominika, Syed Arif Abdul Rehman, Jayaprakash Natarajan, Stephen Matthews, Ross Madden, Virginia De Cesare, Simone Weidlich, et al. 2018. "Discovery and Characterization of ZUFSP/ZUP1, a Distinct Deubiquitinase Class Important for Genome Stability." *Molecular Cell*. https://doi.org/10.1016/j.molcel.2018.02.023.

Larsen, Christopher N., Bryan A. Krantz, and Keith D. Wilkinson. 1998. "Substrate Specificity of Deubiquitinating Enzymes: Ubiquitin C-Terminal Hydrolases." *Biochemistry*. https://doi.org/10.1021/bi972274d.

Lee, E-W, D Seong, J Seo, M Jeong, H-K Lee, and J Song. 2015. "USP11-Dependent Selective CIAP2 Deubiquitylation and Stabilization Determine Sensitivity to Smac Mimetics." *Cell Death & Differentiation* 22 (9): 1463–76. https://doi.org/10.1038/cdd.2014.234.

Lee, Jong Woo, Sungman Park, Yoshinori Takahashi, and Hong-Gang Wang. 2010. "The Association of AMPK with ULK1 Regulates Autophagy." *PloS One* 5 (11): e15394.

https://doi.org/10.1371/journal.pone.0015394.

Legesse-Miller, Aster, Yuval Sagiv, Rina Glozman, and Zvulun Elazar. 2000. "Aut7p, a Soluble Autophagic Factor, Participates in Multiple Membrane Trafficking Processes." *Journal of Biological Chemistry* 275 (42): 32966–73. https://doi.org/10.1074/jbc.M000917200.

Levine, Beth, and Guido Kroemer. 2008. "Autophagy in the Pathogenesis of Disease." *Cell* 132 (1): 27–42. https://doi.org/https://doi.org/10.1016/j.cell.2007.12.018.

Li, Muyang, Christopher L Brooks, Ning Kon, and Wei Gu. 2004. "A Dynamic Role of HAUSP in the P53-Mdm2 Pathway." *Molecular Cell* 13 (6): 879–86. https://doi.org/https://doi.org/10.1016/S1097-2765(04)00157-1.

Li, Muyang, Delin Chen, Ariel Shiloh, Jianyuan Luo, Anatoly Y Nikolaev, Jun Qin, and Wei Gu. 2002. "Deubiquitination of P53 by HAUSP Is an Important Pathway for P53 Stabilization." *Nature* 416 (6881): 648–53. https://doi.org/10.1038/nature737.

Liang, Xiao Huan, Saadiya Jackson, Matthew Seaman, Kristy Brown, Bettina Kempkes, Hanina Hibshoosh, and Beth Levine. 1999. "Induction of Autophagy and Inhibition of Tumorigenesis by Beclin 1." *Nature* 402 (6762): 672–76. https://doi.org/10.1038/45257.

Lim, Key-Hwan, Bharathi Suresh, Jung-Hyun Park, Young-Soo Kim, Suresh Ramakrishna, and Kwang-Hyun Baek. 2016. "Ubiquitin-Specific Protease 11 Functions as a Tumor Suppressor by Modulating Mgl-1 Protein to Regulate Cancer Cell Growth." *Oncotarget* 7 (12): 14441–57. https://doi.org/10.18632/oncotarget.7581.

Lin, Ching-Hui, Hung-Shu Chang, and Winston C Y Yu. 2008. "USP11 Stabilizes HPV-16E7 and Further Modulates the E7 Biological Activity." *Journal of Biological Chemistry* 283 (23): 15681–88. https://doi.org/10.1074/jbc.M708278200.

Link, Christopher D. 1995. "Expression of Human β-Amyloid Peptide in Transgenic Caenorhabditis Elegans." *Proceedings of the National Academy of Sciences of the United States of America*. https://doi.org/10.1073/pnas.92.20.9368.

Linke, S P, K C Clarkin, A Di Leonardo, A Tsou, and G M Wahl. 1996. "A Reversible, P53-Dependent G0/G1 Cell Cycle Arrest Induced by Ribonucleotide Depletion in the Absence of Detectable DNA Damage." *Genes & Development* 10 (8): 934–47. https://doi.org/10.1101/gad.10.8.934.

Lipinski, Marta M., Greg Hoffman, Aylwin Ng, Wen Zhou, Bénédicte F. Py, Emily Hsu, Xuxin Liu, et al. 2010. "A Genome-Wide SiRNA Screen Reveals Multiple MTORC1 Independent Signaling Pathways Regulating Autophagy under Normal Nutritional Conditions." *Developmental Cell*. https://doi.org/10.1016/j.devcel.2010.05.005.

Liu, Chin Chih, Yu Ching Lin, Yu Hsuan Chen, Chun Ming Chen, Liang Yu Pang, Hsuan An Chen, Pei Rung Wu, et al. 2016. "Cul3-KLHL20 Ubiquitin Ligase Governs the Turnover of ULK1 and VPS34 Complexes to Control Autophagy Termination." *Molecular Cell*. https://doi.org/10.1016/j.molcel.2015.11.001.

Liu, Grace Y, and David M Sabatini. 2020. "MTOR at the Nexus of Nutrition, Growth, Ageing and Disease." *Nature Reviews Molecular Cell Biology* 21 (4): 183–203. https://doi.org/10.1038/s41580-019-0199-y.

Liu, Jinchao, Meijiao Li, Lin Li, She Chen, and Xiaochen Wang. 2018. "Ubiquitination of the PI3-Kinase VPS-34 Promotes VPS-34 Stability and Phagosome Maturation." *Journal of Cell Biology*. https://doi.org/10.1083/jcb.201705116.

Liu, Junli, Hongguang Xia, Minsu Kim, Lihua Xu, Ying Li, Lihong Zhang, Yu Cai, et al. 2011. "Beclin1 Controls the Levels of P53 by Regulating the Deubiquitination Activity of USP10 and USP13." *Cell* 147 (1): 223–34. https://doi.org/https://doi.org/10.1016/j.cell.2011.08.037.

Liu, Qingsong, Jae Won Chang, Jinhua Wang, Seong A. Kang, Carson C. Thoreen, Andrew Markhard, Wooyoung Hur, et al. 2010. "Discovery of 1-(4-(4-Propionylpiperazin-1-Yl)-3-(Trifluoromethyl)Phenyl)-9- (Quinolin-3-Yl)Benzo[h][1,6]Naphthyridin-2(1 H)-One as a Highly Potent, Selective Mammalian Target of Rapamycin (MTOR) Inhibitor for the Treatment of Cancer." *Journal of Medicinal Chemistry*. https://doi.org/10.1021/jm101144f.

Löffler, Antje S., Sebastian Alers, Alexandra M. Dieterle, Hildegard Keppeler, Mirita Franz-Wachtel, Mondira Kundu, David G. Campbell, Sebastian Wesselborg, Dario R. Alessi, and Björn Stork. 2011. "Ulk1-Mediated Phosphorylation of AMPK Constitutes a Negative Regulatory Feedback Loop." *Autophagy*. https://doi.org/10.4161/auto.7.7.15451.

Long, Xiaomeng, Sara Ortiz-Vega, Yenshou Lin, and Joseph Avruch. 2005. "Rheb Binding to

Mammalian Target of Rapamycin (MTOR) Is Regulated by Amino Acid Sufficiency." *The Journal of Biological Chemistry* 280 (25): 23433–36. https://doi.org/10.1074/jbc.C500169200.

Lu, Jiahong, Liqiang He, Christian Behrends, Masatake Araki, Kimi Araki, Qing Jun Wang, Joseph M Catanzaro, et al. 2014. "NRBF2 Regulates Autophagy and Prevents Liver Injury by Modulating Atg14L-Linked Phosphatidylinositol-3 Kinase III Activity." *Nature Communications* 5 (1): 3920. https://doi.org/10.1038/ncomms4920.

Lund, P. K., B. M. Moats-Staats, J. G. Simmons, E. Hoyt, A. J. D'Ercole, F. Martin, and J. J. Van Wyk. 1985. "Nucleotide Sequence Analysis of a CDNA Encoding Human Ubiquitin Reveals That Ubiquitin Is Synthesized as a Precursor." *Journal of Biological Chemistry*.

Luo, Qingyu, Xiaowei Wu, Yabing Nan, Wan Chang, Pengfei Zhao, Yiping Zhang, Dan Su, and Zhihua Liu. 2020. "TRIM32/USP11 Balances ARID1A Stability and the Oncogenic/Tumor-Suppressive Status of Squamous Cell Carcinoma." *Cell Reports* 30 (1): 98-111.e5. https://doi.org/https://doi.org/10.1016/j.celrep.2019.12.017.

Ma, Meisheng, Jun-Jie Liu, Yan Li, Yuwei Huang, Na Ta, Yang Chen, Hua Fu, et al. 2017. "Cryo-EM Structure and Biochemical Analysis Reveal the Basis of the Functional Difference between Human PI3KC3-C1 and -C2." *Cell Research* 27 (8): 989–1001. https://doi.org/10.1038/cr.2017.94.

Ma, Xi, Shen Zhang, Long He, Yueguang Rong, Livia Wilz Brier, Qiming Sun, Rong Liu, et al. 2017. "MTORC1-Mediated NRBF2 Phosphorylation Functions as a Switch for the Class III PtdIns3K and Autophagy." *Autophagy* 13 (3): 592–607. https://doi.org/10.1080/15548627.2016.1269988.

Maertens, Goedele N, Selma El Messaoudi-Aubert, Sarah Elderkin, Kevin Hiom, and Gordon Peters. 2010. "Ubiquitin-Specific Proteases 7 and 11 Modulate Polycomb Regulation of the INK4a Tumour Suppressor." *The EMBO Journal* 29 (15): 2553–65. https://doi.org/10.1038/emboj.2010.129.

Maria Fimia, Gian, Anastassia Stoykova, Alessandra Romagnoli, Luigi Giunta, Sabrina Di Bartolomeo, Roberta Nardacci, Marco Corazzari, et al. 2007. "Ambra1 Regulates Autophagy and Development of the Nervous System." *Nature* 447 (7148): 1121–25. https://doi.org/10.1038/nature05925.

Martina, Jose A, Yong Chen, Marjan Gucek, and Rosa Puertollano. 2012. "MTORC1 Functions as a Transcriptional Regulator of Autophagy by Preventing Nuclear Transport of TFEB." *Autophagy* 8 (6): 903–14. https://doi.org/10.4161/auto.19653.

Matsunaga, Kohichi, Eiji Morita, Tatsuya Saitoh, Shizuo Akira, Nicholas T. Ktistakis, Tetsuro Izumi, Takeshi Noda, and Tamotsu Yoshimori. 2010. "Autophagy Requires Endoplasmic Reticulum Targeting of the PI3-Kinase Complex via Atg14L." *Journal of Cell Biology*. https://doi.org/10.1083/jcb.200911141.

Matsunaga, Kohichi, Tatsuya Saitoh, Keisuke Tabata, Hiroko Omori, Takashi Satoh, Naoki Kurotori, Ikuko Maejima, et al. 2009. "Two Beclin 1-Binding Proteins, Atg14L and Rubicon, Reciprocally Regulate Autophagy at Different Stages." *Nature Cell Biology* 11 (4): 385–96. https://doi.org/10.1038/ncb1846.

Mauthe, Mario, Idil Orhon, Cecilia Rocchi, Xingdong Zhou, Morten Luhr, Kerst-Jan Hijlkema, Robert P Coppes, Nikolai Engedal, Muriel Mari, and Fulvio Reggiori. 2018. "Chloroquine Inhibits Autophagic Flux by Decreasing Autophagosome-Lysosome Fusion." *Autophagy* 14 (8): 1435–55. https://doi.org/10.1080/15548627.2018.1474314.

Meléndez, Alicia, and Beth Levine. 2009. "Autophagy in C. Elegans." *WormBook : The Online Review of C. Elegans Biology*. https://doi.org/10.1895/wormbook.1.147.1.

Mevissen, Tycho E.T., and David Komander. 2017. "Mechanisms of Deubiquitinase Specificity and Regulation." *Annual Review of Biochemistry*. https://doi.org/10.1146/annurev-biochem-061516-044916.

Mijaljica, Dalibor, Mark Prescott, and Rodney J Devenish. 2011. "Microautophagy in Mammalian Cells: Revisiting a 40-Year-Old Conundrum." *Autophagy* 7 (7): 673–82. https://doi.org/10.4161/auto.7.7.14733.

Mizushima, Noboru. 2007. "Autophagy: Process and Function." *Genes & Development* 21 (22): 2861–73. https://doi.org/10.1101/gad.1599207.

Mizushima, Noboru, Akiko Kuma, Yoshinori Kobayashi, Akitsugu Yamamoto, Masami Matsubae, Toshifumi Takao, Tohru Natsume, Yoshinori Ohsumi, and Tamotsu Yoshimori. 2003. "Mouse Apg16L, a Novel WD-Repeat Protein, Targets to the Autophagic Isolation Membrane with the Apg12-Apg5 Conjugate." *Journal of Cell Science*. https://doi.org/10.1242/jcs.00381.

Mizushima, Noboru, Takeshi Noda, and Yoshinori Ohsumi. 1999. "Apg16p Is Required for the Function of the Apg12p-Apg5p Conjugate in the Yeast Autophagy Pathway." *EMBO Journal*. https://doi.org/10.1093/emboj/18.14.3888.

Mizushima, Noboru, Takeshi Noda, Tamotsu Yoshimori, Yae Tanaka, Tomoko Ishii, Michael D George, Daniel J Klionsky, Mariko Ohsumi, and Yoshinori Ohsumi. 1998. "A Protein Conjugation System Essential for Autophagy." *Nature* 395 (6700): 395–98. https://doi.org/10.1038/26506.

Mizushima, Noboru, Akitsugu Yamamoto, Masahiko Hatano, Yoshinori Kobayashi, Yukiko Kabey, Kuninori Suzuki, Takeshi Tokuhis, Yoshinori Ohsumi, and Tamotsu Yoshimori. 2001. "Dissection of Autophagosome Formation Using Apg5-Deficient Mouse Embryonic Stem Cells." *Journal of Cell Biology*. https://doi.org/10.1083/jcb.152.4.657.

Mizushima, Noboru, Tamotsu Yoshimori, and Yoshinori Ohsumi. 2002. "Mouse Apg10 as an Apg12-Conjugating Enzyme: Analysis by the Conjugation-Mediated Yeast Two-Hybrid Method." *FEBS Letters*. https://doi.org/10.1016/S0014-5793(02)03739-0.

Moretti, Francesca, Phil Bergman, Stacie Dodgson, David Marcellin, Isabelle Claerr, Jonathan M Goodwin, Rowena DeJesus, et al. 2018. "TMEM41B Is a Novel Regulator of Autophagy and Lipid Mobilization." *EMBO Reports* 19 (9): e45889. https://doi.org/10.15252/embr.201845889.

Morrow, Marie E, Michael T Morgan, Marcello Clerici, Katerina Growkova, Ming Yan, David Komander, Titia K Sixma, Michal Simicek, and Cynthia Wolberger. 2018. "Active Site Alanine Mutations Convert Deubiquitinases into High-Affinity Ubiquitin-Binding Proteins." *EMBO Reports* 19 (10): e45680. https://doi.org/10.15252/embr.201745680.

Nakamura, Shuhei, and Tamotsu Yoshimori. 2017. "New Insights into Autophagosome-Lysosome Fusion." *Journal of Cell Science*. https://doi.org/10.1242/jcs.196352.

Nakao, Atsuhito, Mozhgan Afrakhte, Anita Morn, Takuya Nakayama, Jan L Christian, Rainer Heuchel, Susumu Itoh, et al. 1997. "Identification of Smad7, a TGFβ-Inducible Antagonist of TGF-β Signalling." *Nature* 389 (6651): 631–35. https://doi.org/10.1038/39369.

Nakatogawa, Hitoshi, Junko Ishii, Eri Asai, and Yoshinori Ohsumi. 2012. "Atg4 Recycles Inappropriately Lipidated Atg8 to Promote Autophagosome Biogenesis." *Autophagy*. https://doi.org/10.4161/auto.8.2.18373.

Nazio, Francesca, Flavie Strappazzon, Manuela Antonioli, Pamela Bielli, Valentina Cianfanelli, Matteo Bordi, Christine Gretzmeier, et al. 2013. "MTOR Inhibits Autophagy by Controlling ULK1 Ubiquitylation, Self-Association and Function through AMBRA1 and TRAF6." *Nature Cell Biology* 15 (4): 406–16. https://doi.org/10.1038/ncb2708.

Nemoto, Takahiro, Isei Tanida, Emiko Tanida-Miyake, Naoko Minematsu-Ikeguchi, Masahiro Yokota, Mariko Ohsumi, Takashi Ueno, and Eiki Kominami. 2003. "The Mouse APG10 Homologue, an E2-like Enzyme for Apg12p Conjugation, Facilitates MAP-LC3 Modification." *Journal of Biological Chemistry*. https://doi.org/10.1074/jbc.M300550200.

Nguyen, Thanh Ngoc, Benjamin Scott Padman, Joanne Usher, Viola Oorschot, Georg Ramm, and Michael Lazarou. 2016. "Atg8 Family LC3/GAB ARAP Proteins Are Crucial for Autophagosome-Lysosome Fusion but Not Autophagosome Formation during PINK1/Parkin Mitophagy and Starvation." *Journal of Cell Biology*. https://doi.org/10.1083/jcb.201607039.

Nishimura, Taki, Takeshi Kaizuka, Ken Cadwell, Mayurbhai H. Sahani, Tatsuya Saitoh, Shizuo Akira, Herbert W. Virgin, and Noboru Mizushima. 2013. "FIP200 Regulates Targeting of Atg16L1 to the Isolation Membrane." *EMBO Reports*. https://doi.org/10.1038/embor.2013.6.

Noda, Nobuo N., Yoshinori Ohsumi, and Fuyuhiko Inagaki. 2010. "Atg8-Family Interacting Motif Crucial for Selective Autophagy." *FEBS Letters*. https://doi.org/10.1016/j.febslet.2010.01.018.

Noda, Nobuo N, and Yuko Fujioka. 2015. "Atg1 Family Kinases in Autophagy Initiation." *Cellular and Molecular Life Sciences* 72 (16): 3083–96. https://doi.org/10.1007/s00018-015-1917-z.

Noda, Takeshi, and Yoshinori Ohsumi. 1998. "Tor, a Phosphatidylinositol Kinase Homologue, Controls Autophagy in Yeast." *Journal of Biological Chemistry* 273 (7): 3963–66. https://doi.org/10.1074/jbc.273.7.3963.

Novak, Ivana, Vladimir Kirkin, David G. McEwan, Ji Zhang, Philipp Wild, Alexis Rozenknop, Vladimir Rogov, et al. 2010. "Nix Is a Selective Autophagy Receptor for Mitochondrial Clearance." *EMBO Reports*. https://doi.org/10.1038/embor.2009.256.

Obara, Keisuke, Takayuki Sekito, Kaori Niimi, and Yoshinori Ohsumi. 2008. "The Atg18-Atg2 Complex Is Recruited to Autophagic Membranes via Phosphatidylinositol 3-Phosphate and Exerts an Essential Function." *Journal of Biological Chemistry* 283 (35): 23972–80. https://doi.org/10.1074/jbc.M803180200.

Oh, Eugene, David Akopian, and Michael Rape. 2018. "Principles of Ubiquitin-Dependent Signaling." *Annual Review of Cell and Developmental Biology*. https://doi.org/10.1146/annurev-cellbio-100617-062802.

Ohashi, Yohei, Nicolas Soler, Miguel García Ortegón, Lufei Zhang, Marie L Kirsten, Olga Perisic, Glenn R Masson, et al. 2016. "Characterization of Atg38 and NRBF2, a Fifth Subunit of the Autophagic Vps34/PIK3C3 Complex." *Autophagy* 12 (11): 2129–44. https://doi.org/10.1080/15548627.2016.1226736.

Ohashi, Yohei, Shirley Tremel, and Roger L. Williams. 2019. "VPS34 Complexes from a Structural Perspective." *Journal of Lipid Research*. https://doi.org/10.1194/jlr.R089490.

Orsi, A, M Razi, H C Dooley, D Robinson, A E Weston, L M Collinson, and S A Tooze. 2012. "Dynamic and Transient Interactions of Atg9 with Autophagosomes, but Not Membrane Integration, Are Required for Autophagy." *Molecular Biology of the Cell* 23 (10): 1860–73. https://doi.org/10.1091/mbc.E11-09-0746.

Park, Ji Man, Chang Hwa Jung, Minchul Seo, Neil Michael Otto, Douglas Grunwald, Kwan Hyun Kim, Branden Moriarity, et al. 2016. "The ULK1 Complex Mediates MTORC1 Signaling to the Autophagy Initiation Machinery via Binding and Phosphorylating ATG14." *Autophagy*. https://doi.org/10.1080/15548627.2016.1140293.

Park, Mi Kyung, Yixin Yao, Weiya Xia, Stephanie Rebecca Setijono, Jae Hwan Kim, Isabelle K Vila, Hui-Hsuan Chiu, et al. 2019. "PTEN Self-Regulates through USP11 via the PI3K-FOXO Pathway to Stabilize Tumor Suppression." *Nature Communications* 10 (1): 636. https://doi.org/10.1038/s41467-019-08481-x.

Peng, Junmin, Daniel Schwartz, Joshua E. Elias, Carson C. Thoreen, Dongmei Cheng, Gerald Marsischky, Jeroen Roelofs, Daniel Finley, and Steven P. Gygi. 2003. "A Proteomics Approach to Understanding Protein Ubiquitination." *Nature Biotechnology*. https://doi.org/10.1038/nbt849.

Pengo, N., A. Agrotis, K. Prak, J. Jones, and R. Ketteler. 2017. "A Reversible Phospho-Switch Mediated by ULK1 Regulates the Activity of Autophagy Protease ATG4B." *Nature Communications*. https://doi.org/10.1038/s41467-017-00303-2.

Pickart, C. M., and I. A. Rose. 1985. "Ubiquitin Carboxyl-Terminal Hydrolase Acts on Ubiquitin Carboxyl-Terminal Amides." *Journal of Biological Chemistry*.

Pineda, Carlos T, and Patrick Ryan Potts. 2015. "Oncogenic MAGEA-TRIM28 Ubiquitin Ligase Downregulates Autophagy by Ubiquitinating and Degrading AMPK in Cancer." *Autophagy* 11 (5): 844–46. https://doi.org/10.1080/15548627.2015.1034420.

Platta, Harald W., Hilde Abrahamsen, Sigrid B. Thoresen, and Harald Stenmark. 2012. "Nedd4-Dependent Lysine-11-Linked Polyubiquitination of the Tumour Suppressor Beclin 1." *Biochemical Journal*. https://doi.org/10.1042/BJ20111424.

Polson, Hannah E J, Jane de Lartigue, Daniel J Rigden, Marco Reedijk, Sylvie Urbé, Michael J Clague, and Sharon A Tooze. 2010. "Mammalian Atg18 (WIPI2) Localizes to Omegasome-Anchored Phagophores and Positively Regulates LC3 Lipidation." *Autophagy* 6 (4): 506–22. https://doi.org/10.4161/auto.6.4.11863.

Proikas-Cezanne, Tassula, Sabine Ruckerbauer, York Dieter Stierhof, Carolin Berg, and Alfred Nordheim. 2007. "Human WIPI-1 Puncta-Formation: A Novel Assay to Assess Mammalian Autophagy." *FEBS Letters*. https://doi.org/10.1016/j.febslet.2007.06.040.

Proikas-Cezanne, Tassula, Zsuzsanna Takacs, Pierre Dönnes, and Oliver Kohlbacher. 2015. "WIPI Proteins: Essential PtdIns3P Effectors at the Nascent Autophagosome." *Journal of Cell Science* 128 (2): 207–17. https://doi.org/10.1242/jcs.146258.

Qian, Xu, Xinjian Li, Qingsong Cai, Chuanbao Zhang, Qiujing Yu, Yuhui Jiang, Jong Ho Lee, et al. 2017. "Phosphoglycerate Kinase 1 Phosphorylates Beclin1 to Induce Autophagy." *Molecular Cell*. https://doi.org/10.1016/j.molcel.2017.01.027.

Rabinowitz, Joshua D, and Eileen White. 2010. "Autophagy and Metabolism." *Science* 330 (6009): 1344 LP – 1348. https://doi.org/10.1126/science.1193497.

Reggiori, Fulvio, Katherine A. Tucker, Per E. Stromhaug, and Daniel J. Klionsky. 2004. "The Atg1-Atg13 Complex Regulates Atg9 and Atg23 Retrieval Transport from the Pre-Autophagosomal Structure." *Developmental Cell*. https://doi.org/10.1016/S1534-5807(03)00402-7.

Reggiori, Fulvio, and Christian Ungermann. 2017. "Autophagosome Maturation and Fusion."

Journal of Molecular Biology. https://doi.org/10.1016/j.jmb.2017.01.002.

Rita, Anthea Di, Angelo Peschiaroli, Pasquale D'Acunzo, Daniela Strobbe, Zehan Hu, Jens Gruber, Mads Nygaard, et al. 2018. "HUWE1 E3 Ligase Promotes PINK1/PARKIN-Independent Mitophagy by Regulating AMBRA1 Activation via IKKα." *Nature Communications* 9 (1): 3755. https://doi.org/10.1038/s41467-018-05722-3.

Roccio, M, J L Bos, and F J T Zwartkruis. 2006. "Regulation of the Small GTPase Rheb by Amino Acids." *Oncogene* 25 (5): 657–64. https://doi.org/10.1038/sj.onc.1209106.

Roczniak-Ferguson, Agnes, Constance S Petit, Florian Froehlich, Sharon Qian, Jennifer Ky, Brittany Angarola, Tobias C Walther, and Shawn M Ferguson. 2012. "The Transcription Factor TFEB Links MTORC1 Signaling to Transcriptional Control of Lysosome Homeostasis." *Science Signaling* 5 (228): ra42 LP-ra42. https://doi.org/10.1126/scisignal.2002790.

Rostislavleva, Ksenia, Nicolas Soler, Yohei Ohashi, Lufei Zhang, Els Pardon, John E Burke, Glenn R Masson, et al. 2015. "Structure and Flexibility of the Endosomal Vps34 Complex Reveals the Basis of Its Function on Membranes." *Science* 350 (6257): aac7365. https://doi.org/10.1126/science.aac7365.

Rotin, Daniela, and Sharad Kumar. 2009. "Physiological Functions of the HECT Family of Ubiquitin Ligases." *Nature Reviews Molecular Cell Biology.* https://doi.org/10.1038/nrm2690.

Russell, Ryan C, Ye Tian, Haixin Yuan, Hyun Woo Park, Yu-Yun Chang, Joungmok Kim, Haerin Kim, Thomas P Neufeld, Andrew Dillin, and Kun-Liang Guan. 2013. "ULK1 Induces Autophagy by Phosphorylating Beclin-1 and Activating VPS34 Lipid Kinase." *Nature Cell Biology* 15 (7): 741–50. https://doi.org/10.1038/ncb2757.

Sagiv, Y, A Legesse-Miller, A Porat, and Z Elazar. 2000. "GATE-16, a Membrane Transport Modulator, Interacts with NSF and the Golgi v-SNARE GOS-28." *The EMBO Journal* 19 (7): 1494–1504. https://doi.org/10.1093/emboj/19.7.1494.

Sahtoe, Danny D., and Titia K. Sixma. 2015. "Layers of DUB Regulation." *Trends in Biochemical Sciences.* https://doi.org/10.1016/j.tibs.2015.05.002.

Sancak, Yasemin, Liron Bar-Peled, Roberto Zoncu, Andrew L Markhard, Shigeyuki Nada, and David M Sabatini. 2010. "Ragulator-Rag Complex Targets MTORC1 to the Lysosomal Surface and Is Necessary for Its Activation by Amino Acids." *Cell* 141 (2): 290–303. https://doi.org/10.1016/j.cell.2010.02.024.

Sancak, Yasemin, Timothy R Peterson, Yoav D Shaul, Robert A Lindquist, Carson C Thoreen, Liron Bar-Peled, and David M Sabatini. 2008. "The Rag GTPases Bind Raptor and Mediate Amino Acid Signaling to MTORC1." *Science* 320 (5882): 1496 LP – 1501. https://doi.org/10.1126/science.1157535.

Sanchez-Wandelmer, Jana, Nicholas T Ktistakis, and Fulvio Reggiori. 2015. "ERES: Sites for Autophagosome Biogenesis and Maturation?" *Journal of Cell Science* 128 (2): 185–92. https://doi.org/10.1242/jcs.158758.

Schoenfeld, Alan R, Sarah Apgar, Georgia Dolios, Rong Wang, and Stuart A Aaronson. 2004. "BRCA2 Is Ubiquitinated In Vivo and Interacts with USP11, a Deubiquitinating Enzyme That Exhibits Prosurvival Function in the Cellular Response to DNA Damage." *Molecular and Cellular Biology* 24 (17): 7444 LP – 7455. https://doi.org/10.1128/MCB.24.17.7444-7455.2004.

Schulman, Brenda A., and J. Wade Harper. 2009. "Ubiquitin-like Protein Activation by E1 Enzymes: The Apex for Downstream Signalling Pathways." *Nature Reviews Molecular Cell Biology.* https://doi.org/10.1038/nrm2673.

Settembre, Carmine, Chiara Di Malta, Vinicia Assunta Polito, Moises Garcia Arencibia, Francesco Vetrini, Serkan Erdin, Serpil Uckac Erdin, et al. 2011. "TFEB Links Autophagy to Lysosomal Biogenesis." *Science (New York, N.Y.)* 332 (6036): 1429–33. https://doi.org/10.1126/science.1204592.

Settembre, Carmine, Roberto Zoncu, Diego L Medina, Francesco Vetrini, Serkan Erdin, SerpilUckac Erdin, Tuong Huynh, et al. 2012. "A Lysosome-to-Nucleus Signalling Mechanism Senses and Regulates the Lysosome via MTOR and TFEB." *The EMBO Journal* 31 (5): 1095–1108. https://doi.org/10.1038/emboj.2012.32.

Shah, Palak, Lei Qiang, Seungwon Yang, Keyoumars Soltani, and Yu-Ying He. 2017. "Regulation of XPC Deubiquitination by USP11 in Repair of UV-Induced DNA Damage." *Oncotarget* 8 (57): 96522–35. https://doi.org/10.18632/oncotarget.22105.

Shi, Chong Shan, and John H. Kehrl. 2010. "TRAF6 and A20 Regulate Lysine 63-Linked Ubiquitination of Beclin-1 to Control TLR4-Induced Autophagy." *Science Signaling.*

https://doi.org/10.1126/scisignal.2000751.

Shintani, Takahiro, and Daniel J Klionsky. 2004. "Autophagy in Health and Disease: A Double-Edged Sword." *Science* 306 (5698): 990 LP – 995. https://doi.org/10.1126/science.1099993.

Shintani, Takahiro, Noboru Mizushima, Yoko Ogawa, Akira Matsuura, Takeshi Noda, and Yoshinori Ohsumi. 1999. "Apg10p, a Novel Protein-Conjugating Enzyme Essential for Autophagy in Yeast." *EMBO Journal*. https://doi.org/10.1093/emboj/18.19.5234.

Smit, Judith J., and Titia K. Sixma. 2014. "RBR E3-Ligases at Work." *EMBO Reports*. https://doi.org/10.1002/embr.201338166.

Smith, Ewan M, Stephen G Finn, Andrew R Tee, Gareth J Browne, and Christopher G Proud. 2005. "The Tuberous Sclerosis Protein TSC2 Is Not Required for the Regulation of the Mammalian Target of Rapamycin by Amino Acids and Certain Cellular Stresses." *Journal of Biological Chemistry* 280 (19): 18717–27. https://doi.org/10.1074/jbc.M414499200.

Song, Huiwen, Jun Pu, Lin Wang, Lihua Wu, Jianmin Xiao, Qigong Liu, Jun Chen, et al. 2015. "ATG16L1 Phosphorylation Is Oppositely Regulated by CSNK2/Casein Kinase 2 and PPP1/Protein Phosphatase 1 Which Determines the Fate of Cardiomyocytes during Hypoxia/Reoxygenation." *Autophagy* 11 (8): 1308–25. https://doi.org/10.1080/15548627.2015.1060386.

Spiliotopoulos, Anastasios, Lia Blokpoel Ferreras, Ruth M. Densham, Simon G. Caulton, Ben C. Maddison, Joanna R. Morris, James E. Dixon, Kevin C. Gough, and Ingrid Dreveny. 2019. "Discovery of Peptide Ligands Targeting a Specific Ubiquitin-like Domain–Binding Site in the Deubiquitinase USP11." *Journal of Biological Chemistry*. https://doi.org/10.1074/jbc.RA118.004469.

Stack, J H, P K Herman, P V Schu, and S D Emr. 1993. "A Membrane-Associated Complex Containing the Vps15 Protein Kinase and the Vps34 PI 3-Kinase Is Essential for Protein Sorting to the Yeast Lysosome-like Vacuole." *The EMBO Journal* 12 (5): 2195–2204. https://doi.org/10.1002/j.1460-2075.1993.tb05867.x.

Stockum, Anna, Ambrosius P Snijders, and Goedele N Maertens. 2018. "USP11 Deubiquitinates RAE1 and Plays a Key Role in Bipolar Spindle Formation." *PLOS ONE* 13 (1): e0190513. https://doi.org/10.1371/journal.pone.0190513.

Stolz, Alexandra, Andreas Ernst, and Ivan Dikic. 2014. "Cargo Recognition and Trafficking in Selective Autophagy." *Nature Cell Biology* 16 (6): 495–501. https://doi.org/10.1038/ncb2979.

Sun, Hongze, Baochi Ou, Senlin Zhao, Xueni Liu, Liwei Song, Xisheng Liu, Rangrang Wang, and Zhihai Peng. 2019. "USP11 Promotes Growth and Metastasis of Colorectal Cancer via PPP1CA-Mediated Activation of ERK/MAPK Signaling Pathway." *EBioMedicine* 48: 236–47. https://doi.org/https://doi.org/10.1016/j.ebiom.2019.08.061.

Sun, Qiming, Weiliang Fan, Keling Chen, Xiaojun Ding, She Chen, and Qing Zhong. 2008. "Identification of Barkor as a Mammalian Autophagy-Specific Factor for Beclin 1 and Class III Phosphatidylinositol 3-Kinase." *Proceedings of the National Academy of Sciences of the United States of America* 105 (49): 19211–16. https://doi.org/10.1073/pnas.0810452105.

Sun, Wenjing, Xiaojie Tan, Yi Shi, Gufeng Xu, Renfang Mao, Xue Gu, Yihui Fan, et al. 2010. "USP11 Negatively Regulates TNFα-Induced NF-KB Activation by Targeting on IκBα." *Cellular Signalling* 22 (3): 386–94. https://doi.org/https://doi.org/10.1016/j.cellsig.2009.10.008.

Swanson, Deborah A, Carol L Freund, Lynda Ploder, Roderick R McInnes, and David Valle. 1996. "A Ubiquitin C-Terminal Hydrolase Gene on the Proximal Short Arm of the X Chromosome: Implications for X-Linked Retinal Disorders." *Human Molecular Genetics* 5 (4): 533–38. https://doi.org/10.1093/hmg/5.4.533.

Swatek, Kirby N., and David Komander. 2016. "Ubiquitin Modifications." *Cell Research*. https://doi.org/10.1038/cr.2016.39.

Takahashi, Yoshinori, Domenico Coppola, Norimasa Matsushita, Hernani D Cualing, Mei Sun, Yuya Sato, Chengyu Liang, et al. 2007. "Bif-1 Interacts with Beclin 1 through UVRAG and Regulates Autophagy and Tumorigenesis." *Nature Cell Biology* 9 (10): 1142–51. https://doi.org/10.1038/ncb1634.

Tanida, Isei, Noboru Mizushima, Miho Kiyooka, Mariko Ohsumi, Takashi Ueno, Yoshinori Ohsumi, and Eiki Kominami. 1999. "Apg7p/Cvt2p: A Novel Protein-Activating Enzyme Essential for Autophagy." *Molecular Biology of the Cell*.

https://doi.org/10.1091/mbc.10.5.1367.

Tasdemir, Ezgi, M Chiara Maiuri, Lorenzo Galluzzi, Ilio Vitale, Mojgan Djavaheri-Mergny, Marcello D'Amelio, Alfredo Criollo, et al. 2008. "Regulation of Autophagy by Cytoplasmic P53." *Nature Cell Biology* 10 (6): 676–87. https://doi.org/10.1038/ncb1730.

Thayer, Julia A, Ola Awad, Nivedita Hegdekar, Chinmoy Sarkar, Henok Tesfay, Cameran Burt, Xianmin Zeng, Ricardo A Feldman, and Marta M Lipinski. 2020. "The PARK10 Gene USP24 Is a Negative Regulator of Autophagy and ULK1 Protein Stability." *Autophagy* 16 (1): 140–53. https://doi.org/10.1080/15548627.2019.1598754.

Tian, Ye, Zhipeng Li, Wanqiu Hu, Haiyan Ren, E. Tian, Yu Zhao, Qun Lu, et al. 2010. "C. Elegans Screen Identifies Autophagy Genes Specific to Multicellular Organisms." *Cell*. https://doi.org/10.1016/j.cell.2010.04.034.

Ting, Xia, Lu Xia, Jianguo Yang, Lin He, Wenzhe Si, Yongfeng Shang, and Luyang Sun. 2019. "USP11 Acts as a Histone Deubiquitinase Functioning in Chromatin Reorganization during DNA Repair." *Nucleic Acids Research* 47 (18): 9721–40. https://doi.org/10.1093/nar/gkz726.

Tsukada, Miki, and Yoshinori Ohsumi. 1993. "Isolation and Characterization of Autophagy-Defective Mutants of Saccharomyces Cerevisiae." *FEBS Letters* 333 (1–2): 169–74. https://doi.org/10.1016/0014-5793(93)80398-E.

Ueno, Takashi, Wataru Sato, Yasuo Horie, Masaaki Komatsu, Isei Tanida, Mitsutaka Yoshida, Shigetoshi Ohshima, Tak Wah Mak, Sumio Watanabe, and Eiki Kominami. 2008. "Loss of Pten, a Tumor Suppressor, Causes the Strong Inhibition of Autophagy without Affecting LC3 Lipidation." *Autophagy*. https://doi.org/10.4161/auto.6085.

Vijay-kumar, Senadhi, Charles E. Bugg, and William J. Cook. 1987. "Structure of Ubiquitin Refined at 1.8 Å Resolution." *Journal of Molecular Biology*. https://doi.org/10.1016/0022-2836(87)90679-6.

Vlasschaert, Caitlyn, Xuhua Xia, Josée Coulombe, and Douglas A Gray. 2015. "Evolution of the Highly Networked Deubiquitinating Enzymes USP4, USP15, and USP11." *BMC Evolutionary Biology* 15 (1): 230. https://doi.org/10.1186/s12862-015-0511-1.

Vousden, Karen H., and David P. Lane. 2007. "P53 in Health and Disease." *Nature Reviews Molecular Cell Biology*. https://doi.org/10.1038/nrm2147.

Wagner, Sebastian A., Petra Beli, Brian T. Weinert, Michael L. Nielsen, Jürgen Cox, Matthias Mann, and Chunaram Choudhary. 2011. "A Proteome-Wide, Quantitative Survey of In Vivo Ubiquitylation Sites Reveals Widespread Regulatory Roles." *Molecular & Cellular Proteomics*. https://doi.org/10.1074/mcp.m111.013284.

Walczak, Marta, and Sascha Martens. 2013. "Dissecting the Role of the Atg12-Atg5-Atg16 Complex during Autophagosome Formation." *Autophagy*. https://doi.org/10.4161/auto.22931.

Wan, Wei, Zhiyuan You, Li Zhou, Yinfeng Xu, Chao Peng, Tianhua Zhou, Cong Yi, Yin Shi, and Wei Liu. 2018. "MTORC1-Regulated and HUWE1-Mediated WIPI2 Degradation Controls Autophagy Flux." *Molecular Cell* 72 (2): 303-315.e6. https://doi.org/https://doi.org/10.1016/j.molcel.2018.09.017.

Wang, Chao-Wen, John Kim, Wei-Pang Huang, Hagai Abeliovich, Per E Stromhaug, William A Dunn, and Daniel J Klionsky. 2001. "Apg2 Is a Novel Protein Required for the Cytoplasm to Vacuole Targeting, Autophagy, and Pexophagy Pathways." *Journal of Biological Chemistry* 276 (32): 30442–51. https://doi.org/10.1074/jbc.M102342200.

Wang, Dan, Jing Zhao, Shuang Li, Jianxin Wei, Ling Nan, Rama K Mallampalli, Nathaniel M Weathington, Haichun Ma, and Yutong Zhao. 2017. "Phosphorylated E2F1 Is Stabilized by Nuclear USP11 to Drive Peg10 Gene Expression and Activate Lung Epithelial Cells." *Journal of Molecular Cell Biology* 10 (1): 60–73. https://doi.org/10.1093/jmcb/mjx034.

Wang, H, F K Bedford, N J Brandon, S J Moss, and R W Olsen. 1999. "GABA(A)-Receptor-Associated Protein Links GABA(A) Receptors and the Cytoskeleton." *Nature* 397 (6714): 69–72. https://doi.org/10.1038/16264.

Wang, Richard C., Yongjie Wei, Zhenyi An, Zhongju Zou, Guanghua Xiao, Govind Bhagat, Michael White, Julia Reichelt, and Beth Levine. 2012. "Akt-Mediated Regulation of Autophagy and Tumorigenesis through Beclin 1 Phosphorylation." *Science*. https://doi.org/10.1126/science.1225967.

Wang, Weiwei, Jing Wang, Hua Yan, Kai Zhang, and Yang Liu. 2019. "Upregulation of USP11 Promotes Epithelial‑to‑mesenchymal Transition by Deubiquitinating Snail in Ovarian Cancer." *Oncology Reports*. https://doi.org/10.3892/or.2018.6924.

Waters, Sarah, Katie Marchbank, Ellen Solomon, Caroline Whitehouse, and Mathias Gautel.

2009. "Interactions with LC3 and Polyubiquitin Chains Link Nbr1 to Autophagic Protein Turnover." *FEBS Letters*. https://doi.org/10.1016/j.febslet.2009.04.049.

Webb, Ashley E, and Anne Brunet. 2014. "FOXO Transcription Factors: Key Regulators of Cellular Quality Control." *Trends in Biochemical Sciences* 39 (4): 159–69. https://doi.org/10.1016/j.tibs.2014.02.003.

Wei, Yongjie, Zhongju Zou, Nils Becker, Matthew Anderson, Rhea Sumpter, Guanghua Xiao, Lisa Kinch, et al. 2013. "EGFR-Mediated Beclin 1 Phosphorylation in Autophagy Suppression, Tumor Progression, and Tumor Chemoresistance." *Cell*. https://doi.org/10.1016/j.cell.2013.08.015.

Wiborg, O., M.S. Pedersen, A. Wind, L.E. Berglund, K.A. Marcker, and J. Vuust. 1985. "The Human Ubiquitin Multigene Family: Some Genes Contain Multiple Directly Repeated Ubiquitin Coding Sequences." *The EMBO Journal*. https://doi.org/10.1002/j.1460-2075.1985.tb03693.x.

Wilkinson, K. D., M. K. Urban, and A. L. Haas. 1980. "Ubiquitin Is the ATP-Dependent Proteolysis Factor I of Rabbit Reticulocytes." *Journal of Biological Chemistry*.

Wiltshire, Timothy D, Courtney A Lovejoy, Tong Wang, Fen Xia, Mark J O'Connor, and David Cortez. 2010. "Sensitivity to Poly(ADP-Ribose) Polymerase (PARP) Inhibition Identifies Ubiquitin-Specific Peptidase 11 (USP11) as a Regulator of DNA Double-Strand Break Repair." *Journal of Biological Chemistry* 285 (19): 14565–71. https://doi.org/10.1074/jbc.M110.104745.

Wu, Hsin-Chieh, Yu-Ching Lin, Cheng-Hsin Liu, Hsiang-Ching Chung, Ya-Ting Wang, Ya-Wen Lin, Hsin-I. Ma, Pang-Hsien Tu, Sean E Lawler, and Ruey-Hwa Chen. 2014. "USP11 Regulates PML Stability to Control Notch-Induced Malignancy in Brain Tumours." *Nature Communications* 5 (1): 3214. https://doi.org/10.1038/ncomms4214.

Xia, Pengyan, Shuo Wang, Ying Du, Zhenao Zhao, Lei Shi, Lei Sun, Guanling Huang, et al. 2013. "WASH Inhibits Autophagy through Suppression of Beclin 1 Ubiquitination." *EMBO Journal*. https://doi.org/10.1038/emboj.2013.189.

Xia, Pengyan, Shuo Wang, Guanling Huang, Ying Du, Pingping Zhu, Man Li, and Zusen Fan. 2014. "RNF2 Is Recruited by WASH to Ubiquitinate AMBRA1 Leading to Downregulation of Autophagy." *Cell Research* 24 (8): 943–58. https://doi.org/10.1038/cr.2014.85.

Xie, Weihong, Shouheng Jin, and Jun Cui. 2020. "The NEDD4-USP13 Axis Facilitates Autophagy via Deubiquitinating PIK3C3." *Autophagy*. https://doi.org/10.1080/15548627.2020.1743071.

Xie, Zhiping, and Daniel J Klionsky. 2007. "Autophagosome Formation: Core Machinery and Adaptations." *Nature Cell Biology* 9 (10): 1102–9. https://doi.org/10.1038/ncb1007-1102.

Xu, Congfeng, Kuan Feng, Xiaonan Zhao, Shiqian Huang, Yiji Cheng, Liu Qian, Yanan Wang, et al. 2014. "Regulation of Autophagy by E3 Ubiquitin Ligase RNF216 through BECN1 Ubiquitination." *Autophagy* 10 (12): 2239–50. https://doi.org/10.4161/15548627.2014.981792.

Xu, Zhiwei, Xiaohong Li, Jianping Chen, Jianmei Zhao, Jun Wang, Yuhong Ji, Yifen Shen, Lijian Han, Jiansheng Shi, and Dongmei Zhang. 2016. "USP11, Deubiquitinating Enzyme, Associated with Neuronal Apoptosis Following Intracerebral Hemorrhage." *Journal of Molecular Neuroscience* 58 (1): 16–27. https://doi.org/10.1007/s12031-015-0644-0.

Yamaguchi, Tomoko, Junko Kimura, Yoshio Miki, and Kiyotsugu Yoshida. 2007. "The Deubiquitinating Enzyme USP11 Controls an IκB Kinase α (IKKα)-P53 Signaling Pathway in Response to Tumor Necrosis Factor α (TNFα)." *Journal of Biological Chemistry* 282 (47): 33943–48. https://doi.org/10.1074/jbc.M706282200.

Yamamoto, Hayashi, Soichiro Kakuta, Tomonobu M. Watanabe, Akira Kitamura, Takayuki Sekito, Chika Kondo-Kakuta, Rie Ichikawa, Masataka Kinjo, and Yoshinori Ohsumi. 2012. "Atg9 Vesicles Are an Important Membrane Source during Early Steps of Autophagosome Formation." *Journal of Cell Biology*. https://doi.org/10.1083/jcb.201202061.

Yan, Ying, Rory J. Flinn, Haiyan Wu, Rachel S. Schnur, and Jonathan M. Backer. 2009. "HVps15, but Not Ca2+/CaM, Is Required for the Activity and Regulation of HVps34 in Mammalian Cells." *Biochemical Journal* 417 (3): 747–55. https://doi.org/10.1042/BJ20081865.

Yang, Ling, Mo Zhu, Xinxing Ma, and Chunhong Hu. 2017. "USP11 Promotes Tumorigenesis

and Enhances MRI Detection in Breast Cancer." *Translational Cancer Research; Vol 6, No 1 (February 2017): Translational Cancer Research (Focused Issue: Advances on Clinical Immunotherapy)*. http://tcr.amegroups.com/article/view/11961.

Yang, Peiguo, and Hong Zhang. 2011. "The Coiled-Coil Domain Protein EPG-8 Plays an Essential Role in the Autophagy Pathway in C. Elegans." *Autophagy*. https://doi.org/10.4161/auto.7.2.14223.

Yang, Yonghua, Warren Fiskus, Bao Yong, Peter Atadja, Yoshinori Takahashi, Tej K Pandita, Hong-Gang Wang, and Kapil N Bhalla. 2013. "Acetylated Hsp70 and KAP1-Mediated Vps34 SUMOylation Is Required for Autophagosome Creation in Autophagy." *Proceedings of the National Academy of Sciences* 110 (17): 6841 LP – 6846. https://doi.org/10.1073/pnas.1217692110.

Yau, Richard, and Michael Rape. 2016. "The Increasing Complexity of the Ubiquitin Code." *Nature Cell Biology* 18 (6): 579–86. https://doi.org/10.1038/ncb3358.

Ye, Yihong, and Michael Rape. 2009. "Building Ubiquitin Chains: E2 Enzymes at Work." *Nature Reviews Molecular Cell Biology*. https://doi.org/10.1038/nrm2780.

Yoshimori, T, A Yamamoto, Y Moriyama, M Futai, and Y Tashiro. 1991. "Bafilomycin A1, a Specific Inhibitor of Vacuolar-Type H(+)-ATPase, Inhibits Acidification and Protein Degradation in Lysosomes of Cultured Cells." *Journal of Biological Chemistry* 266 (26): 17707–12. http://www.jbc.org/content/266/26/17707.abstract.

Young, Andrew R J, Edmond Y W Chan, Xiao Wen Hu, Robert Köchl, Samuel G Crawshaw, Stephen High, Dale W Hailey, Jennifer Lippincott-Schwartz, and Sharon A Tooze. 2006. "Starvation and ULK1-Dependent Cycling of Mammalian Atg9 between the TGN and Endosomes." *Journal of Cell Science* 119 (18): 3888 LP – 3900. https://doi.org/10.1242/jcs.03172.

Young, Lindsey N, Kelvin Cho, Rosalie Lawrence, Roberto Zoncu, and James H Hurley. 2016. "Dynamics and Architecture of the NRBF2-Containing Phosphatidylinositol 3-Kinase Complex I of Autophagy." *Proceedings of the National Academy of Sciences* 113 (29): 8224 LP – 8229. https://doi.org/10.1073/pnas.1603650113.

Yu, Miao, Kun Liu, Zebin Mao, Jianyuan Luo, Wei Gu, and Wenhui Zhao. 2016. "USP11 Is a Negative Regulator to ΓH2AX Ubiquitylation by RNF8/RNF168." *Journal of Biological Chemistry* 291 (2): 959–67. https://doi.org/10.1074/jbc.M114.624478.

Yu, Xinlei, Yun Chau Long, and Han-Ming Shen. 2015. "Differential Regulatory Functions of Three Classes of Phosphatidylinositol and Phosphoinositide 3-Kinases in Autophagy." *Autophagy* 11 (10): 1711–28. https://doi.org/10.1080/15548627.2015.1043076.

Yuan, Hai-Xin, Ryan C Russell, and Kun-Liang Guan. 2013. "Regulation of PIK3C3/VPS34 Complexes by MTOR in Nutrient Stress-Induced Autophagy." *Autophagy* 9 (12): 1983–95. https://doi.org/10.4161/auto.26058.

Zalckvar, Einat, Hanna Berissi, Miriam Eisenstein, and Adi Kimchi. 2009. "Phosphorylation of Beclin 1 by DAP-Kinase Promotes Autophagy by Weakening Its Interactions with Bcl-2 and Bcl-XL." *Autophagy*. https://doi.org/10.4161/auto.5.5.8625.

Zhang, Encheng, Bing Shen, Xingyu Mu, Yan Qin, Fang Zhang, Yong Liu, Jiantao Xiao, et al. 2016. "Ubiquitin-Specific Protease 11 (USP11) Functions as a Tumor Suppressor through Deubiquitinating and Stabilizing VGLL4 Protein." *American Journal of Cancer Research* 6 (12): 2901–9. https://www.ncbi.nlm.nih.gov/pubmed/28042509.

Zhang, Sheng, Chengrong Xie, Honghe Li, Kang Zhang, Jie Li, Xiaomin Wang, and Zhenyu Yin. 2018. "Ubiquitin-Specific Protease 11 Serves as a Marker of Poor Prognosis and Promotes Metastasis in Hepatocellular Carcinoma." *Laboratory Investigation* 98 (7): 883–94. https://doi.org/10.1038/s41374-018-0050-7.

Zhao, Jing, Jianxin Wei, Su Dong, Rachel K Bowser, Lina Zhang, Anastasia M Jacko, and Yutong Zhao. 2016. "Destabilization of Lysophosphatidic Acid Receptor 1 Reduces Cytokine Release and Protects Against Lung Injury." *EBioMedicine* 10 (August): 195–203. https://doi.org/10.1016/j.ebiom.2016.07.020.

Zhao, Yawei, Qingyang Wang, Guihua Qiu, Silei Zhou, Zhaofei Jing, Jingyang Wang, Wendie Wang, et al. 2015. "RACK1 Promotes Autophagy by Enhancing the Atg14L-Beclin 1-Vps34-Vps15 Complex Formation upon Phosphorylation by AMPK." *Cell Reports* 13 (7): 1407–17. https://doi.org/https://doi.org/10.1016/j.celrep.2015.10.011.

Zhong, Yu, Deanna H Morris, Lin Jin, Mittul S Patel, Senthil K Karunakaran, You-Jun Fu, Emily A Matuszak, Heidi L Weiss, Brian T Chait, and Qing Jun Wang. 2014. "Nrbf2 Protein Suppresses Autophagy by Modulating Atg14L Protein-Containing Beclin 1-Vps34 Complex Architecture and Reducing Intracellular Phosphatidylinositol-3

Phosphate Levels." *Journal of Biological Chemistry* 289 (38): 26021–37. https://doi.org/10.1074/jbc.M114.561134.

Zhong, Yun, Qing Jun Wang, Xianting Li, Ying Yan, Jonathan M Backer, Brian T Chait, Nathaniel Heintz, and Zhenyu Yue. 2009. "Distinct Regulation of Autophagic Activity by Atg14L and Rubicon Associated with Beclin 1–Phosphatidylinositol-3-Kinase Complex." *Nature Cell Biology* 11 (4): 468–76. https://doi.org/10.1038/ncb1854.

Zhou, Zhuan, Aiping Luo, Indira Shrivastava, Mingjing He, Yi Huang, Ivet Bahar, Zhihua Liu, and Yong Wan. 2017. "Regulation of XIAP Turnover Reveals a Role for USP11 in Promotion of Tumorigenesis." *EBioMedicine* 15 (February): 48–61. https://doi.org/10.1016/J.EBIOM.2016.12.014.

Zhuo, S, J C Clemens, D J Hakes, D Barford, and J E Dixon. 1993. "Expression, Purification, Crystallization, and Biochemical Characterization of a Recombinant Protein Phosphatase." *The Journal of Biological Chemistry* 268 (24): 17754–61.

6   Acknowledgements

First and foremost, I would like to thank my supervisor, Anja Bremm. Thank you for having trust in me to be your first student, together with Julia. We started everything together; it was exciting, it was an adventure, sometimes it was challenging, but it made me who I am today, both as a scientist, and as a person. I can undoubtedly say I learnt a lot from you, our joint experience shaped my presence, and steered my future. There is a lot to be grateful for and remember going forward.

In this manner, I would thank my collaborators Christian Behl and Andreas Kern. Your contribution to this project brought a lot both in terms of science, as well as motivation to pursue the project when doubts arose.

Florian with whom I have likely performed the best interactome experiment of my life, Georg with whom I spend unforgettable time troubleshooting the experiments that did not end up in the thesis, and Paolo who besides providing the cells I used that solved a lot of issues at the time, I also had endless project discussions. We all shared some great moments on our bicycles, travelled, had wine and dined together, and I am so grateful IBC2 brought us together.

Which brings me to a special thanks to Ivan. I admire your work both in science, as well as outside of the lab. Regardless of your schedule, you found time for science and life/career discussions with me, and this I will never forget. IBC2 is an amazing institute to work in, and I am so, so proud I was a part of it. Many thanks to everyone who make it what it is. Sharing reagents, ideas, constructs… A big thank you especially to the members of Ivan's lab, but also everyone who brought a smile on my face passing down the corridor.

However, one of things I will be most grateful for is that I had amazing lab mates accompanying me along this journey, Alexandra, Julia, and Verena. I could not wish for better colleagues, and I know the path to completing this thesis would be a lot harder without you, if not impossible.

Julia, I could not have wished for a better colleague to have by my side when we started together in 2014. Your determination and resilience inspired me when it was hard, and the organized chaos of the way in which you work made every day with you fun and full of laughter. Needless to say, we became true friends beyond sharing lab space, and I am excited to see what the future brings us.

Verena, words cannot express the gratitude I feel for you joining the lab in 2016. The ease at which you take things, yet responsibly fulfill all your tasks calmed me in times of chaos and stress, and helped me see things differently. I cannot think of many experiences in Frankfurt that marked this time that I do not associate with you. You have become and essential part of who I am, I am so grateful for you, and I will take you wherever I go.

There are so many other colleagues I wish to express my gratitude to, as well.

Koraljka, you are the best unofficial lab member I can imagine. Having you around the lab, especially when work extended to late hours are some of my favorite "ordinary moments", exactly because they are anything but. I look up to you; your courage and strength became a

part of me, too. We spent fun time in the company of Andrea and Ines, and together, they were welcome moments of a "home away from home" feeling. Thank you for that.

I would also want to mention my colleagues Hannah, Jonas, and Süleyman. Hannah, your positive energy is felt in the institute halls, and I am grateful for the countless time you offered me coffee and sweets in times of need. Jonas and I worked together at both BMLS and IBC2, and we have known each other much longer and became good friends, however, Süleyman swiftly became a good friend, too, a lab mate, and a positive presence at the institute. Thank you all for lifting my spirits at times, and for the unforgettable times outside the lab as well. The endless corridor laughs with Adriana and Alexis lifted my days regularly, outside the lab as well. Maybe especially then.

My Frankfurt life and experience would not nearly be the same without my friend Jowita. You are my family, and as such you been there through all sorts of situations with me, and have always been there for me without hesitation, and without a second thought. For this, I cannot thank you enough.

There are so many ways in which I was supported in the lab and outside during my time in Frankfurt, some of which are my gym companions, Marc, my former flatmate, people who's work makes mine much easier, like Tata and Andrea, and Annette with whom I spent a lot of time sitting at the FACS machine, it was such a pleasure working with you.

There are many childhood friends to thank, but mostly, I would thank Ines. Our friendship is essential to me, and it has never stopped evolving. One thing was constant, your energy and loyalty I was blessed with by knowing you.

And last, but not least, I dedicate this thesis to my family. Each step of the way I knew you always had my back and I knew I was never alone. Mom, dad, and Grga: I love you more than I can phrase in words. I love our family and I am eternally grateful for the love and support I am surrounded with. Without your encouragement, your belief in me, without all the fun times we spent together, which are all of them, even the hard ones, I would not be where I am today. Hvala.

Baka i dida, vama na svemu što ste za mene napravili od najmanjih nogu, od brige i ljubavi koju ste mi dali, do znatiželje koju ste u mene usadili. Vjerujem da je veliki dio razloga zašto sam postala znanstvenica to što sam toliko puno vremena provela s vama učeći, promatrajući, i popravljajući stvari.

With completing this thesis, I am overwhelmed with joy and pride I share with all of you, and many more important people in my life who I could not mention now in order to avoid having the acknowledgment part longer than some essential parts of the thesis. This in no way means I am not thinking of you, sharing the excitement for our future and the fondness for our past.

7 Curriculum Vitae

Mila Basic

Date of birth: 12/May/1989
Nationality: Croatian
E-mail: milabasic@gmx.de

Education

Apr/2014-Jun/2020	Institute of Biochemistry II, Goethe University Frankfurt, Germany PhD, Biochemistry
Oct/2011-Sep/2013	Biotechnology Center (BIOTEC), Technical University Dresden, Germany MSc, Molecular bioengineering
Oct/2008-Sep/2011	Faculty of Science, University of Zagreb, Croatia BSc, Molecular biology

Working experience

Jun/2018-Jun2020 Apr/2014-Jun/2018	Institute of Biochemistry II, Goethe University Frankfurt, Germany Buchmann Institute for Molecular Life Sciences, Goethe University Frankfurt, Germany PhD thesis: Versatile regulation of autophagy by the deubiquitinase USP11 Molecular cell biology lab of Dr. Anja Bremm
Apr/2013-Dec/2013	Biotechnology Center (BIOTEC), Technical University Dresden, Germany HiWi Master thesis: Generation of a reversible gene-expression system to analyze MLL2 activity and dynamics in knockout cells Genomics lab of Prof. Dr. Francis Stewart
Mar/2011-Jul/2011	Faculty of Science, University of Zagreb, Croatia HiWi Practical course assistant Histology lab of Prof. Dr. Gordana Lackovic-Venturin

Related working experience (voluntary activities)

Jan/2019-present	preLights, The Company of Biologists Voluntary contributions, preprint selection and highlighting

May/2014-Jun/2018	PhD Student representative, Buchmann Institute for Molecular Life Sciences

Memberships and Associations

Nov/2016-Jun/2020	Goethe Research Academy for Early Career Researchers (GRADE)
Jun/2015- Jun/2020	Integrative Research Graduate Program (IRTG) of SFB1177 on Autophagy

Posters and publications

2020 Publication	*Ubiquitin-specific protease 11 (USP11) regulates autophagy via the PI3KC3 complex I (Manuscript in preparation)* Mila Basic, Alexandra Kalb, Florian Bonn, Ivan Dikic, Andreas Kern, Christian Behl, Anja Bremm
2019 GBM/DGZ Fall Conference on Age-related human diseases, Special focus: Autophagy Tübingen, Germany	*Autophagy is restricted by the ubiquitin-specific protease 11 (USP11)* Mila Basic, Alexandra Kalb, Florian Bonn, Ivan Dikic, Andreas Kern, Christian Behl, Anja Bremm
2019 CSHL conference on Ubiquitins, Autophagy and Disease Cold Spring Harbor, USA	*Autophagy is restricted by the ubiquitin-specific protease 11 (USP11)* Mila Basic, Alexandra Kalb, Florian Bonn, Ivan Dikic, Andreas Kern, Christian Behl, Anja Bremm
2018 2nd Frankfurt Conference on Quality Control in Life Processes Frankfurt, Germany	*Autophagy is restricted by the ubiquitin-specific protease 11 (USP11)* Mila Basic, Alexandra Kalb, Florian Bonn, Andreas Kern, Ivan Dikic, Christian Behl, Anja Bremm
2017 EMBO Autophagy Conference Cavtat, Croatia	*USP11 – a novel regulator of autophagy* Mila Basic, Alexandra Kalb, Anja Bremm
2016 Frankfurt Conference on Quality Control Frankfurt, Germany	*USP11 – a novel regulator of autophagy* Mila Basic, Alexandra Kalb, Anja Bremm
2015 EMBO Conference on Ubiquitin and ubiquitin-like modifiers: From molecular mechanisms to human diseases Cavtat, Croatia	